STATICS AND DYNAMICS OF A TENSION LEG PLATFORM IN INTACT AND TETHER DAMAGE CONDITIONS

MANAS KUMAR DEB

STATICS AND DYNAMICS OF A TENSION LEG PLATFORM IN INTACT AND TETHER DAMAGE CONDITIONS

by

© Manas Kumar Deb, B.Tech.(Hons.)

A Thesis submitted to the School of Graduate Studies
in partial fulfilment of the requirements
for the degree of
Master of Engineering

Faculty of Engineering and Applied Science
Memorial University of Newfoundland

November, 1986

St. John's Newfoundland Canada

ISBN 0-315-36976-0

Abstract

The aim of the present investigation is to study the static and dynamic behaviour of a tension leg platform in the intact condition and after partial or total loss of tether at any corner. The exercise involves formulating the statics and dynamics of column stabilised structures with taut moorings and implementing the same in appropriate computer softwares. Formulations are also made to calculate the equilibrium tensions after a loss of tether.

The computer program for hydrostatics is capable of generating the standard hydrostatic information as well as locating the equilibrium configuration of the floating body under a given set of external static loads. This is used to assess the statical stability of the tension leg platform in damaged cases and compare the same with its various other configurations.

Under the category of hydrodynamic analysis, two major types of approaches, namely 'frequency domain' and 'time domain' are employed. In the frequency domain approach, wave amplitudes and all displacements are assumed to be small.

Also, integration of the hydrodynamic forces is carried out over the mean wetted surface of the body. The wave excitation forces are calculated via a 'Morison type' formula and an iterative scheme is adopted to handle the nonlinear drag term. This analysis is used to compute the 'response amplitude operators' (RAOs) in intact and damaged conditions. Significant responses are also computed using these RAOs and Pierson-Moskowitz wave spectra for chosen wind speeds. In the time domain analysis, though assumptions similar to frequency domain analysis are made regarding the incident wave. However, no restriction is put on the motion of the body. The excitation and the reactive forces are calculated over the instantaneous wetted surface and at the displaced position. Nonlinear equations of motion are integrated using Adam's method. This analysis is used to obtain time-series data of motion and tension responses in order to study the variation of steady state amplitudes in intact and damaged conditions as well as transients following a loss of tether.

A special study of the occurrence of Mathieu type dynamic instabilty in tension leg platforms is also undertaken. A formulation to calculate unstable combinations of wave height and frequency is developed based on Floquet theory for periodic systems. The effect of various pertinent

parameters including loss of tether on instability is also investigated.

Furthermore, a 1:100 scale model of a representative tension leg platform is designed and fabricated. Experiments are conducted in regular and irregular waves in both intact and damaged configurations and the experimental observations are compared with those predicted by the theoretical models.

It is seen that a complete loss of tether at any corner can reduce the statical stability of a tension leg platform drastically. A loss of tether, in general, is found to increase the platform motions in vertical planes as well as the static and dynamic tensions in the remaining intact tethers. Total loss of tether at one corner induces snap loads in one or more corners. Depending on the wave height and frequency, these snap loads could be high enough to trigger further tether failures. With regard to Mathieu type dynamic instability, even a 25% loss of total axial stiffness of the tethers is seen to have insignificant effect on the occurrence of such instability.

ACKNOWLEDGEMENT

The author wishes to express his heart-felt gratitude to Dr. M. Booton for his supervision, support and encouragement during the entire course of the present work. The author is also obligated to Dr. J.S. Pawlowski for his valuable suggestions and helpful discussions in connection with this thesis work.

The author is indebted to Dr. F.A. Aldrich, Dean of Graduate Studies for awarding a university fellowship for the duration of this work. Sincere thanks are due to Dr. G.R. Peters, Dean of Engineering and Applied Science and to Dr. T.R. Chari, Associate Dean of Engineering and Applied Science for their encouragement.

The author wishes to extend his deep appreciation to the staff of model fabrication shop, machine shop, welding shop, structures laboratory and fluids laboratory for their help and suggestions during the fabrication and instrumentation of the model tension leg platform and to MSRL for the underwater work during the installation of the model in the wave tank. Special thanks are due to Mr. H.

Mesh, Mr. B. Wilkie, Mr. M. Sullivan and Mr. A. Kuczora for their help in conducting the experiments and in analysing the experimental data and to Mrs. M. Brown in typing this thesis. Fellow graduate students are also remembered for their help and companionship.

Finally, the author wishes to sincerely thank his parents and wife for their love and encouragement, to whom this work is dedicated.

CONTENTS

LIST OF TABLES

LIST OF FIGURES

Chapter 1

INTRODUCTION

The escalation in the size of conventional drilling platforms for deeper waters and more severe environments could make much of the oil discovered in such areas remain unrecovered. Many innovative designs that have evolved in the last two decades aim to provide economically viable solutions to this problem.

Among the conventional oil production facilities, steel jacket or concrete gravity type in fixed structures and floating platforms such as semi-submersibles are the most popular. Fixed structures offer the best working conditions since they provide a stable platform from which to work. Unfortunately, the natural periods of oscillation for these structures increase with water depth and get into the 'high energy content zone' of the sea energy spectrum, making the structures vulnerable to high dynamic stresses due to environmental loads. This may be avoided by providing extra stiffening and thus keeping the natural periods down, but this solution makes the structure very heavy and

uneconomical. Floating units with soft moorings, on the other hand, are economically viable for greater water depths but fail to remain adequately stable during heavy weather conditions. Therefore, a lot of down-time becomes unavoidable.

'Compliant platforms' emerged as suitable alternatives for deep water applications where the platform natural periods are outside the high energy zone of the sea energy spectrum. These have options of restricting motions in certain desired degrees of freedom while moving 'compliantly' with the external loads in the others. A 'tension leg platform' (TLP), alternatively known as 'tethered buoyant platform' (TBP) is one such compliant structure that, in recent years, has received a great deal of attention from oil companies and researchers. Its suitablility in deep water applications in terms of cost against fixed jacket structures is demonstrated in Fig. 1.1 (Dunn, 1979). Fig. 1.2 shows the typical TLP natural periods as compared to typical sea energy spectrums.

A TLP is a positively buoyant unit that is kept in position at a location by the help of a set of taut moorings. The tension in these moorings balance the difference in buoyancy and weight. The static pretension may

typically be in the order of 25 to 30 per cent of the total displacement of the platform. The mooring elements have very high axial stiffness due to which motions in the vertical planes i.e. heave, roll and pitch are severely suppressed. The platform, however, would exhibit large excursions in the horizontal plane i.e. in surge, sway and yaw modes, thus absorbing the wave energy through the gained momentum.

The first design of such a structure was produced by the pioneering English engineer, A.F. Daniel, some twenty five years ago; his platform was named 'Triton' shown in Fig. 1.3. In order to obtain better performances, the TLP configuration has undergone a lot of modifications since the time of Triton. The present day TLP is a column stabilised structure appearing somewhat like the familiar semi-submersible rig with much bigger columns pulled down to the sea bed by vertical taut moorings. To date the only TLP in operation is the one in Hutton field in North Sea. As a concept, a TLP is intended to be used at water depths greater than 600 feet, but the Hutton TLP is deployed in a water depth of only about 485 feet since the sponsors felt that the cost of the TLP for that location would not be higher than conventional jacket structure and also a better knowledge about TLP behaviours was necessary before it could be selected for deeper waters. Table 1.1 (Ellers, 1982)

offers a brief comparison of certain relevant aspects between the Hutton TLP and a few other types of offshore production facilities.

The superior performance and elegance of TLPs depend largely on the performance of the taut moorings or the so called 'tethers' (alternatively known as 'tension legs' or 'tendons'). Thus, quite justifiably; tethers themselves have received a good share of the total research work devoted to TLPs. Damage to one or more tethers may have rather undesirable effects on the overall performance of TLP and to the well being of the rest of the tethers. The main thrust of this thesis is to investigate these effects through theoretical and experimental means since not much is reported in the published literature on this particular topic.

Chapter 2 offers a description of a tension leg platform. Thesis objectives and research plan are given in Chapter 3. A brief review of relevant published literature is provided in Chapter 4. Details of model scale simulation of a TLP at Memorial University of Newfoundland, St. John's, Canada, given in Chapter 5, include development of modelling laws, description of the model, experimental arrangements and instrumentations, test program and data analysis etc. A

procedure to calculate the equilibrium tensions after a loss of tether is developed and illustrated in Chapter 6. Hydrostatic and hydrodynamic analyses are described in Chapter 7 and Chapter 8, respectively. Both frequency domain and time domain approaches are discussed under hydrodynamic analysis. Chapter 9 gives the details of the investigations on Mathieu type dynamic instability of TLPs.

In accordance with the convention followed in this thesis, theoretical and experimental results are discussed in every chapter, as applicable. A summary of observations, however, is presented in Chapter 10. Additionally, general comments on the present study, recommendations for future research etc., as realized by the author, are also included in this chapter. The text of the thesis is followed by a list of references, and tables and figures. Four appendices are also provided which give the source listings of some of the computer codes developed during this thesis work. All the input variables required to create the input files and the computed output variables are described in the header information of each program. Additionally, the input data are also reproduced on the output in a convenient form.

Chapter 2

THE TENSION LEG PLATFORM

A tension leg platform is a floating production unit where buoyancy exceeds its weight. It is held down by means of a few clusters of tethers. The tension that balances the difference in buoyancy and the weight keeps these tethers taut at all times.

The main buoyant unit of the structure is the 'hull', which, unlike semi-submersibles has larger vertical columns and relatively smaller horizontal pontoons. This hull, on the upper side, bears the production facilities and on the lower side is connected to the tethers. The platform is constrained to move in vertical planes by providing very high axial stiffness to the tethers. It is, of course, compliant in the horizontal modes.

Since the TLP is a relatively new concept, a brief description of its various components and their functions may be of help for the reader to appreciate the complexieties and the problems associated with such a structure. This will probably be best achieved by choosing

the Hutton TLP as a representative TLP. Fig. 2.1 shows a perspective view of this TLP while the main particulars are given in Table 2.1.

The Hutton TLP has a six-column configuration. The column tops are connected by a box deck structure which is essentially a grillage of deep plate girders. The bottom of the column is connected by rectangular pontoons thus increasing the overall rigidity of the platform. The columns and the pontoons are of stiffened plate construction.

A mooring compartment is housed in each corner column where the top ends of the tethers are secured. The mooring equipment, including the load block, is placed on the mooring flat. The tension load on the load block is passed onto the mooring flat and the body of the hull through the locking collar of the tension adjustment assembly and a cross load bearing (CLB). The mooring compartments are located in the 'double-wall' portion of the columns. The double-wall construction extends over the splash zone and thus, besides protecting the mooring equipments, helps improve 'flooding damage control'.

The lower ends of the tethers are fixed to the anchor templates which are in turn piled onto the sea floor. The

bottom end of each tether has an anchor connector for attaching itself to the template. This connector is activated by the force of gravity. It can be disconnected by hydraulic devices remotely operated from the deck.

Both ends of the tethers have elastomeric flex-joints which allow free rotation upto 18.5 degrees.

The hull and the decks are fabricated separately and mated in shallow water. The assembled hull is towed to the offshore site and installed with the help of the mooring system.

The tether system installation is carried out in calm weather. The platform is temporarily moored with the help of an eight-point catenary mooring. High strength steel tubulars, which make up the tether elements, are stored in the mooring compartment. First, a single tether in each column is assembled and lowered to be 'stabbed' into the already installed anchor templates on the sea floor. Once the locking of the bottom ends is achieved, the platform is pulled down by hydraulic jacks. The remaining tethers are now installed and the platform brought to its operating draught by combined deballasting and pulling down on the tethers by hydraulic jacks. The platform is now in the 'TLP

mode'. The load cells in each corner continuously monitor the tether tensions and these values are used to adjust on-board load distribution.

TLPs are regarded as better performing platforms than many other designs for a number of reasons. It can be very suitably deployed in deep water. Since it can be moved from one location to the other fairly easily, it is expected to be useful in developing marginal fields. For use in deeper water (within a certain range) only the extra lengths of tethers would be necessary thus keeping the deployment cost low.

While the TLPs are expected to be one of the most popular offshore structures in the near future, concern regarding their operation has been expressed by industry and researchers. TLPs are highly sensitive to the weight on-board and its distribution. Because of the presence of tethers, coupled dynamic anlysis is often required. In order to bear the extra loads arising out of the tether tensions, the structural arrangements tend to become more complicated. Tethers are very critical structural members subjected to high stresses and fatigue loads. Additionally, various nonlinear phenomena are of relevance in case of TLPs. In

particular, response to second order forces and dynamic instability may be mentioned.

Although a considerable amount of knowledge has been gained regarding the behaviour of TLPs, much is yet left to be understood so that efficient and reliable design philosophies may be established so that the operability and safety of the structure may be assured.

Chapter 3

THESIS OBJECTIVES AND RESEARCH PLAN

It must be appreciated at this point that the presence of highly tensioned tethers with large axial stifness in a TLP is the major reason why it behaves so differently than other floating structures. It is therefore imperative that attention is given to analyses of situations with total or partial loss of tethers at one or more corners. Such losses may occur due to failure of anchors, failure of locking arrangements, breakage of tether tubulars or similar reasons. It would then become necessary to remove the damaged tethers for repair or replacement. Damage to columns also deserve adequate attention but provided that the safety of the water-tight hull is not at stake, such damages may be much less fatal than a sizeable loss of tethers. Tether loss is likely to affect the stability and the responses of the platform and may induce higher loads in the remaining active tethers as well as the riser strings. Sudden loss of tethers may initiate high transient loadings that may trigger progressive damage of the rest of the tethers.

It may be mentioned here that no detailed and comprehensive study of TLP behaviour following a sizeable tether loss is yet reported in published literature. The primary objective of this thesis is to study the changes in static and dynamic behaviour of an example TLP in 'intact' and 'loss-of-tether' (hereafter also referred to as 'damaged') conditions through both theoretical and experimental investigations. In brief, the scope of the present thesis work may be described as :

1. Develop/adopt formulations necessary for hydrostatic and hydrodynamic investigations.

2. Develop computer software for hydrostatic and hydrodynamic computations.

3. Analyze the chosen TLP for evaluation of stability characteristics and motion and tension responses in intact and tether damage conditions.

4. Design and conduct model-scale experiments to obtain data for comparison with the theoretical findings.

In addition, a special study is also undertaken to analyse the Mathieu type dynamic instability peculiar to

structures such as TLPs. Table 3.1 lays out the key plan of the major research activities.

Chapter 4

LITERATURE REVIEW

The two major systems that interact closely to portray the overall behaviour of a TLP are namely its main buoyancy unit (the hull) and its moorings (the tethers). To obtain a complete information on the responses of one of these systems, knowledge of responses of the other becomes a pre-requisite. Thus the response analysis becomes nonlinear and iterative in nature although depending on the type of information sought, simplifications compatible to current engineering practice are often made to obtain practical solution to the problem. Previous experiences with analysis of floating bodies, semi-submersibles and other compliant structures have provided the required basis for much of the techniques being employed for analysis of TLPs.

In most analytical models for evaluation of overall response of TLP, the hull is regarded as a rigid body while the tethers are modelled as elastic members. The hull and the tethers may be excited by waves and currents. Additionally, the above water portion of the hull would also experience wind loads. In order to obtain the responses, standard form of equations of

motion are used which are essentially the generalised force balance equations.

Three main approaches, all amenable to only numerical schemes of solution for real life applications, may be identified in connection with computation of the hydrodynamic loading. The first approach requires the fluid flow to be solved on the boundary of interest in order that the pressure distribution can be calculated. The forces and moments are then found by proper integration of this pressure. This is done by obtaining solution to the classical Laplace Equation in 'ideal fluid' domain, subject to the prevailing boundary conditions. The theory is classical but the computational difficulties that arise when a practical structure has to be considered have been circumvented only in recent years. A particular scheme of solution called the 'three-dimensional source-sink distribution technique' has been suggested, amongst others, by Faltinsen and Michelson (1974).

The above approach, though mathematically rigorous, has many disadvantages. The formulation is quite involved and the typical computation time is very long, particularly in cases where iterative methods are to be used. Often handling of very large matrices becomes necessary thus imposing limitations on the size and/or shape of the body to be analysed. Also the effect of viscous drag cannot be taken into account thus leading to

inaccurate estimation of forces on relatively slender bodies. An alternate approach which relies on semi-emperical relations or simpler strip theory formulations is often employed to evaluate the hydrodynamic loadings on three dimensional bodies. This approach is particularly advantageous in handling structures as space frames but also introduces errors due to the simplistic assumptions used.

Estimation of hydrodynamic forces on a slender pile by semi-emperical relation was first proposed by Morison et al. (1951). Under the second category, the present day formulations for estimation of forces on tubulars of floating structures are essentially derived or intuitively extended from the original Morison equation. The work of Burke (1970), Paulling and Horton (1970), Hooft (1971), Kim and Chou (1973) are typical examples of the use of this approach. In order that the total force on a structure may be computed from the forces calculated on its component members, the hydrodynamic interactions among them is ignored. The forces on individual members thus may be added vectorially to yield the total force on the structure. This assembly is what has been termed as 'hydrodynamic synthesis' (Paulling, 1985). It may be noted that in this approach the viscous drag effects are also included via semi-empirical relations while diffraction effects are neglected. Discussion on

the use and applicability of this method may be found in Sarpkaya, 1981.

The third approach aims to combine both the above approaches by applying the first one to larger members and the second one to the relatively slender members. This is expected to yield improved results, see for example Standing (1979), Garrison (1983) etc. As the merits of both the approaches are merged into one, the inherent demerits of each one of them also become a part of the combined method. A comparison of results obtained via various approaches is given by Paulling (1981).

The tethers provide restoring forces to the platform and thus are included in the equations of motion. The earliest work on TLP responses reported by Paulling and Horton (1970) provided a linearized model for frequency domain analysis. In this work, the tethers are taken as linear springs with only axial stiffness. Computed results matched fairly well with some experimental data.

A time domain analysis was used by Paulling (1977) to evaluate responses of a TLP where a few nonlinear effects such as (i) nonlinear terms in the rotational equations of motion, (ii) nonlinear drag force, (iii) integration of the hydrodynamic forces over the instantaneous wetted surface and (iv) position

dependent tether tensions for calculation of restoring forces were included. This model is capable of providing both steady state and transient solutions.

Effect of various other related phenomena such as 'inertia relief', 'draw-down forces', etc. on TLP responses are studied in the analysis by Kirk and Etok (1979). TLPs are treated as coupled systems by implicitly including the tether dynamics in the response analysis by Patel and Lynch (1983). Amongst the second order loadings, the effect of drift has been calculated by authors such as Burns (1983). Kareem and Dalton (1982) and Haritos (1985) have computed the typical loads due to constant and time-varying wind flows and have shown the importance of the inclusion of such effects in the overall TLP dynamics.

The general motion and tension responses have also been evaluated by experimental means and correlated with the theoretical predictions. Some of this work is described by Faltinsen et al. (1974), Rowe et al. (1979), Lyons et al. (1983), Dunsire and Owen (1984), Dillingham (1984).

Rainey (1977) has demonstrated the possible occurrence of Mathieu type dynamic instability in TLP response at critical wave frequencies. In this work a 'feed back system' analogy has been used. Analytical methods for determination of such critical

regimes of wave loading have been suggested by Richardson (1979), Patel and Jefferys (1981), Yoneya and Yoshida (1982), Paulling (1982), Conceicao and Neves (1983) etc. A numerical method based on Floquet theory readily adaptible to computer applications has been described by Deb and Booton (1986a) and Deb and Booton (1986b). A report by Rowe and Jackson (1980) describes experiments conducted to observe unstable TLP responses in model scale.

In normal situations a TLP has an equal amount of tether stiffness at all corners. Loss of stiffness and equilibrium tension redistribution would take place if any of these tethers were to fail, and would influence the responses of a TLP. In spite of its indisputable significance, detailed analysis of TLPs in tether-loss conditions is rare in published literature. Static tension redistribution after a complete loss of tethers at one corner was noted during an experiment by Sebastini et al. (1981). The effect of small losses of tether stiffness on the overall characteristics has been described by Booton et al. (1986). The impact of a sudden loss of all the tethers at one corner on the tensions in rest of the tethers is briefly reported by Sekita and Sakai (1984). Indication of simulations carried out by CONOCO to obtain similar information for the Hutton TLP are given in a short state-of-the-art report by Schamaun and Sannum (1985).

The complex and often contradicting design requirements of a TLP have demanded ongoing attention by researchers. Investigations related to design and development and applications of various analysis to guide the design procedures of a TLP are found in the research of Godfrey (1976), Roren et al. (1977), Capanoglu (1979), Perrett and Webb (1980), Chou et al. (1980), Tien et al. (1981), Ellers (1982), Ellis (1982), Karsan et al. (1982), Mercier et al. (1982), Chou et al. (1983), Faulkner et al. (1983), Patel and Witz (1985) etc. For general references on dynamic analysis of the TLP and its tether system, the work of Albrecht et al. (1978), Asford and Wood (1978), Denise and Heaf (1979), Gie and de Boom (1981), Stiatnsen and Chen (1981), Hudspeth and Leonard (1982), Yoneya and Yoshida (1982), Jefferys and Patel (1982), Agarwal and Spanos (1983), de Boom et al. (1983), Teigen (1983), Paulling (1986) etc. may be mentioned.

Chapter 5

MODEL SCALE SIMULATION OF TLP

5.1 General :

The tension leg platform is a relatively new concept and, as a system, highly complex. In spite of efforts made by various researchers, quite a few aspects regarding its response to environmental loads are not completely understood. Quite often the analytical methods have to sacrifice rigor in order to be computationally efficient and thus bear the possibility of yielding inaccurate results. Some times enough is not known to adequately describe a phenomenon by analytical means. Hence, in an effort to gain confidence in theoretical predictions made or to better understand some of the complex phenomena involved, a number of TLP model tests have already been undertaken. In the present research, model scale tests are primarily designed to provide the following :

(i) experimental data from statical stability and steady state motion response tests to cross check computer

codes developed for hydrostatic and hydrodynamic calculations.

(ii) observations of certain types of behaviour of a TLP such as transient and steady state responses following loss of tether, and dynamic instability phenomenon at critical wave frequencies.

The above can be achieved by a 'dynamically similar' scaled model of a representative TLP prototype.

5.2 Development of Modelling Laws :

In order to be able to reproduce prototype phenomena in a model scale simulation or to project back the findings from the model tests to prototype size, the design of the model and the experimental conditions must conform to a set of mathematical relations which may be termed as 'modelling laws'. For the purpose of delineating the key parameters, the TLP system under investigation may be broken up as :

$$TLP_{system} = TLP_{hull} + Tethers + Waves$$

The relevant parameters have been identified and listed in Table 5.1. The dimensionless numbers are derived from

this list by using the 'matrix method' described by Deb and Deb (1986) and are given at the bottom of Table 5.1. Since, for proper modelling these ratios must be kept constant for both model and prototype, these can also be used to form mathematical relations between prototype and model parameters. Scaling relations that evolved out of such an exercise are presented in Table 5.2.

The design of the model and the test environment are now accomplished using the scaling guidelines already derived. It may be noted that since both Froude Number and Reynolds Number similarities cannot be maintained simultaneously if water is used in the wave tank (see for example Sharp, 1981), the latter is omitted on the grounds that the flow around the model would be turbulent and that the inaccuracies in the reproduction of the viscous effects would not significantly alter the experimental results. Even though serious concerns regarding this dissimilarity have been raised, such a practice, due to lack of any suitable alternative, appears to be the only practical solution to the problem.

5.3. Fabrication of the Physical Model :

The main aim of this research being a study of certain overall behaviours of TLP, the prototype particulars are chosen such that they are representative of a feasible TLP and not necessarily correspond to any particular TLP design. Fig. 5.1a and Fig. 5.1b show the main dimensions of the chosen TLP in elevation and plan; main particulars are given in Table 5.3. This platform hereafter is also referred to as the 'example TLP'.

It is a well known fact that matching of various parameters in a scaled model becomes progressively more difficult as the size of the model gets smaller. However, the upper limit of the size of the model may be limited by the available testing facilities and the cost involved. Due to such restrictions the model scale simulation in this study has been done at 1:100 scale. The model dimensions are calculated from the prototype using the relations in Table 5.2.

The task of modelling the integrated TLP system is divided into two major groups, namely the hull and the mooring systems.

The rigid hull of the model TLP is made out of clear perspex ('plexiglass'). The geometry could be easily scaled

down as far as the outer dimensions are concerned. Fixed lead ballasts are used to scale mass and inertia properties. Fig. 5.2 offers a view of the model after assembly. The columns are made out of 6" and 4" dia tubes, the larger ones being at the corners. 4" dia tubes are used to form the pontoons. The cross deck and the derrick are made of 1/8" perspex sheets. Flat bar stiffners are provided between decks on the diagonals and on the sides to achieve high rigidity. The joints are glued togather using chloroform. Perspex plugs with 'O'-rings are used to close the bottom ends of the corner columns. A 1/4" dia steel threaded rod runs through each corner column whose bottom end is screwed down to the plug. These rods pierce through the upper deck of the model and through a steel 'handling frame' placed on top of the upper deck. The handling frame is held down in place by means of locking nuts on the threaded rods. The model hull is watertight up to the bottom of the upper deck and all its members are interconnected. Watertightness is checked by filling the model with water. The lead ballast weights are casted in the form of annular disks and held in place around the threaded rods by means of nuts and washer plates.

In the present study, platform behaviour and representative tension response are seen as the topics of

major interest. For the sake of simplicity, only the axial stiffness and equilibrium tension similarity for the tethers are modelled since these, among all the tether properties, have the maximum influence on the overall TLP behaviour. While scaling the stiffness and the tension, the combined effect of the tether cluster at each corner is considered. One 'equivalent' tether per corner with scaled properties is provided except for corner # 1 where two identical model tethers equally share the scaled tether at that corner. The reason for putting two tethers at corner # 1 is to make the simulations of different amount of tether loss (viz. 50% and 100% loss at # 1) possible. The tether is modelled by using a nylon coated high strength steel cable in combination with a spring at one end. The steel cable has very high axial stiffness and it is the spring that provides the required tether stiffness in the axial direction. The active tether length is maintained in accordance with the scaling laws.

5.4 Experimental Determination of Model Characteristics :

Although the key properties of the model such as mass, vertical centre of gravity (VCG), mass moments of inertia etc. are calculated from the dimensions and the weight of each component member of the model, experimental

verification of some of these properties is deemed necessary.

The gross weight of the model is confirmed by weighing it on a balance at an accuracy level of 10 grams. To check the VCG, an inclining experiment is done with the model in free-float condition. An external heeling moment (M_h) is applied by shifting a known weight on the deck of the model. The resulting inclination (ϕ) is measured using a 'Spectron L210 Two Axis Electrolytic Level Sensor' and a 'Bruel and Kjaer 1526 Digital Display'. At small angles of inclination, the metacentric height (GM) is found from :

$$GM = M_h / W \sin(\phi) \qquad (5.1)$$

where,

W = weight of the model

The VCG is now determined from :

$$VCG = VCB + BM - GM \qquad (5.2)$$

where,

VCB = vertical centre of buoyancy

BM = metacentric radius

Both VCB and BM are calculated from the hydrostatic information of the model generated by the computer program 'HYDROSTATICS' (described in section 7.4).

To establish the radii of gyration, a 'tilting platform' shown in Fig. 5.3 is used. First the adjustable distance between the knife edges and the table is set equal to the model VCG. The heights of the counter weights are adjusted such that the VCG of the tilting platform is brought in line with the line of the knife edges. The assembled model is placed at the centre of the table. The model radius of gyration about any axis is found by measuring the time periods of oscillation of the empty platform and the model and the platform togather about the axis of interest using (McDuff and Curreri, 1958) :

$$k^2 = I/m = (I_{p+m} - I_p)/m$$
$$= \sum K_i d_i^2 \ (T_{p+m}^2 - T_p^2)/4\pi^2 m \qquad (5.3)$$

where,

k = radius of gyration

I = mass moment of inertia of the model

I_{p+m} = mass momment of inertia of the platform and the model

I_p = mass moment of inertia of the platform

m = mass of the model

K_i = spring constant of the ith spring

d_i = distance of the ith spring from the centre of the platform

T_{p+m} = time period of oscillation of platform and model

T_p = time period of oscillation of platform

The time periods are found from the central period of the power spectrum of analog output of a 'Bruel and Kjaer 8306 Accelerometer' placed on the platform. This power spectrum is obtained after Fourier analysis of the accelerometer output by an 'HP 5420B Digital Signal Analyser'.

Attempts were made to verify the natural periods of oscillation of the model after it is placed in the wave tank in tethered configuration. The model was given an initial push such that it oscillates in the desired degree of freedom. The period of oscillation can be then found from a similar Fourier analysis of the motion record. With the available accuracy levels of the equipments being used, only the natural periods in surge, sway and yaw modes could be measured.

5.5 Experimental Arrangement :

The TLP experiments are carried out in a 58.27 m (length) x 4.57 m (width) x 3.04 m (depth) wave tank facility at Memorial University, St. John's, Canada (see Muggeridge and Murray, 1981 for details of the tank). The waves are generated by an MTS servo-hydraulic piston type wave board. Schematic plan and cross section of the tank are shown in Fig. 5.4.

The model with the correct amount of ballast is placed in the wave tank with its orientation coinciding with the desired wave heading. The model is held in place by its mooring system. Fig. 5.5 shows a schematic of this arrangement. The tethers are connected to the bottom of the corner columns of the model by means of eye bolts. The tethers run vertically downwards to the 'A' pulleys which are bolted to a steel frame rigidly fixed on the tank floor. Tethers are taken around these pulleys and passed through the 'B' pulleys and then continued vertically upwards to connect them to the 'load cell - turn-buckle - spring' unit of the mooring system located above water level. Detail 'X' of Fig. 5.5 shows a schematic of this arrangement. The 'ring type' load cell is used to read out the line tension, the

turn-buckle to make small tension adjustments and the spring to provide the required axial stiffness of the tether. The tethers are continued beyond the springs and passed over the 'C' pulleys. Known weights are hung from the free ends of the tethers. This arrangement helps set the line tensions close to the desired values. Finer adjustments are carried out with turn-buckles, once the tops of the tethers are clamped. Fig. 5.6 shows the the above-water portion of the mooring system and Fig. 5.7 displays the some of the items used in it. Fig. 5.8 shows the TLP model in waves. Underwater installations needed to set up the experiments were accomplished with the help of surface divers.

5.6 Instrumentation and Data Acquisition :

Data acquired during experiments are of three major types viz. (i) wave data, (ii) platform motion data and (iii) tether tension data. A block diagram of the instrumentation and data recording scheme is given in Fig. 5.9.

For measurement of the wave profiles, the 'primary wave probe', a standard twin wire linear resistance type probe is placed about 1.5 metres upstream of the model on the tank centre line. Another probe of similar specifications is

placed by the side of the model at a distance of about 1.5 metres from the tank centre line. This 'secondary' probe is used for back up and special reference purposes. The probes are calibrated prior to start of experiments after any reasonably long break to eliminate error due to water temperature differential. The output from the probes are recorded as analog signals on an eight channel, six speed 'HP 3968A Instrumentation Tape Recorder' capable of FM recording over a bandwidth of 0 to 5 KHz and/or direct recording of signals upto 64 KHz.

The platform motion data are acquired through a SELSPOT (SELective SPOT recognition) system manufactured by Selective Electronic Company (SELCOM) of Sweden. This optical-electronic device is capable of three dimensional position measurement of 30 points defined by infrared Light Emitting Diodes (LEDs). The LEDs are pulsed sequentially which are recorded via two mutually orthogonal electronic cameras. A pulse rate of one per every 3.2 ms allows a maximum sample rate of 312.5 frames a second. The cameras provide digitized output of the angular displacements of each LED from its focal plane. This information, and the known positions of the cameras (obtained by survey with respect to the tank coordinates) and the LEDs (obtained by survey and cross checked by SELSPOT output), enables one to

compute the motions in six degrees of freedom of a given point on the model by means of suitable software. A minimum of three non-collinear LEDs are necessary for such analysis. The SELSPOT sytem is capable of yielding translation and rotational accuracies in the order of 0.2 cm and 0.2 degrees, respectively.

The measurement of tension in each line is carried out using previously calibrated strain gauge outputs of the load cell in that line. The strain gauge outputs are amplified through a ten channel 'Vishay Instruments 2100 Strain Gauge Conditioner and Amplifier System' before they are recorded on the previously mentioned FM recorder. The load cells are taken out of the mooring system from time to time to check the calibration. On line monitoring of the tensions is done with the help of digital multimeters connected to the strain gauge amplifier.

All runs of the test are video recorded for reference at a later date.

5.7 Test Summary :

The entire test program may be divided under two major heads e.g. (i) statics and (ii) dynamics.

In statics, the experiments carried out are :

- inclining experiments in free-float condition to determine the VCG.

- statical stability experiments in tethered condition with complete loss of tether at corner # 1 to obtain righting moments as a function of heel angle.

Under dynamics category two types of observations are made e.g. (i) steady state response and (ii) transient response.

Steady state motion and tension responses are measured for three distinct cases namely (i) intact, (ii) 50% loss of stiffness at corner # 1 i.e. one model tether inactive at #1 and (iii) 100% loss of stiffness at corner # 1 i.e. both the model tethers inactive at # 1. For tests in regular waves, prototype wave period is varied from 8.0 sec to 24.0 sec at an increment of 2.0 sec; for each frequency prototype wave height is varied from 5.0 m to 20.0 m at increments of 5.0 m each. Tests have also been conducted in irregular waves for the intact and damaged cases. Pierson-Moskowitz spectra for fully developed sea corresponding to prototype wind speeds of 30.0 m/sec and 20.0 m/sec are used to generate the wave profiles.

It may be mentioned here that the water depth, the wave periods and the wave heights are set to their scaled values (as may be found from Table 5.2) during the tests.

Transients in motion and tension responses are observed after sudden loss of 50% and 100% tether stiffness at # 1. These are simulated by releasing the top clamp of one or two tether(s) simultaneously with the help of an electromagnetic device that could be triggered remotely and at a predetermined time. Output from the secondary wave probe is viewed on an oscilloscope and a trigger is set after a desired length of time. This oscilloscope is connected to a 'relay circuit' which activates the electro-magnetic release mechanism. Thus the failures could be simulated at different parts of the wave form. Since it is found difficult to perform such runs at various combinations of wave period and height it is decided that only one combination be chosen and that experimental observation be compared with theoretical predictions for that case. Accordingly such tests are done at a prototype wave period of 21.9 sec and wave height of 20.0 m.

Dynamic instabilities are another kind of transient response. Few runs are devoted to verification of predicted

occurrence of Mathieu type unstable motion of a TLP. At a critical combination of wave period and wave height the model is pushed by hand to induce some motion in the unstable degree of freedom under investigation. If this motion grows with time, the model is regarded to be exhibiting unstable motion at the test wave period and wave height combination.

5.8 Data Analysis :

As mentioned in section 5.6, motion data are recorded in digitized form while wave and tensions measurements are recorded as analog signals. Over a selected 'time window', common for all the records for a particular run, average double amplitudes, maximums, minimums etc. are computed using in-house software (Little, 1985) with the help of an IBM PC (XT) for motion data and a HP 86 computer in conjunction with a HP 5420B Digital Signal Analyser for wave and tension data. Typically a time interval of 0 to 20 seconds is used for such computations. 'Response Amplitude Operators' (RAOs) are found by dividing the double amplitude of a particular response by the corresponding double amplitude of wave. A wave height of 10 m is used for the RAO computations.

While data recording by SELSPOT system is found to be satisfactory for horizontal translations such as surge and sway, motions in vertical planes i.e. heave, pitch and roll are found to be small to be recorded with sufficient reliability owing to the accuracy levels of the measuring system. These data, therefore, are not used for any further analysis.

Standard Fourier analysis is done on the wave and tension records from the irregular sea tests to compute response spectra and transfer functions (i.e. the RAOs). Analog data from the FM Recorder is digitized using a HP 5466B Analog to Digital Converter at a sampling frequency of 50 Hz. The digitized data is then transferred to a VAX 8800 computer for further analysis. In an attempt to reduce the noise content of the signals, they are passed through a 'low-pass pulse type' filter of 4 Hz upper cutoff. The wave and tension spectra are then obtained from Fourier transformation of the filtered time records. The transfer functions are obtained from the standard 'cross-spectral' analysis. Although experiments are conducted using PM spectra for wind speeds 20 m/sec and 30 m/sec, records obtained for the latter spectrum are dropped from all frequency domain analysis because of frequent occurrence of breaking waves and under-deck slamming.

It may be mentioned here that unless otherwise indicated, all the experimental data presented are to be regarded as those corresponding to the 'example TLP' scaled to prototype size.

Chapter 6

STATIC EQUILIBRIUM AFTER LOSS OF TETHER

If a certain number of tethers are damaged at any corner of TLP such that they are rendered inactive, we may say that the platform has suffered a tether loss at that corner. A 'loss of stiffness' at that corner is a direct consequence of tether loss. This would cause the platform to move into a new equilibrium configuration causing a redistribution of the resulting total pretension. To find the static equilibrium tension at each corner the new displacements at the corners must be determined. It may be readily seen that the problem is statically indeterminate since the number of unknowns are in excess of the number of independent force/moment equilibrium equations. A method is developed here to compute the equilibrium displacements (and therefore, the tensions) and is described in the following.

Fig. 6.1 shows a skeleton diagram of a TLP with linear springs at the corners to represent the axial stiffnesses (K_1, K_2 etc.) of the tethers. Let d_1, d_2 etc. be the new equilibrium displacements corresponding to the springs K_1, K_2 etc. and let Z_d be the Z-distance of a datum from which

these displacements are measured. Now the static equilibrium equations are written as :

$$\sum F_z = 0, \text{ i.e.}$$

$$K_1d_1 + K_2d_2 + K_3d_3 + K_4d_4 = T_P + \Delta B$$

$$\sum M_X = 0, \quad \text{i.e.}$$

$$K_1d_1Y_1 + K_2d_2Y_2 - K_3d_3Y_3 - K_4d_4Y_4 = \Delta M_x \qquad (6.1)$$

$$\sum M_Y = 0, \quad \text{i.e.}$$

$$K_1d_1X_1 - K_2d_2X_2 - K_3d_3X_3 + K_4d_4X_4 = -\Delta M_y$$

where,

T_P = total pretension

ΔB = change in buoyancy

ΔM_x, ΔM_y = resultant hydrostatic moments about X and Y axes

X_1, Y_1 etc. = X and Y coordinates of the tether tops at corners # 1 etc.

It may be pointed out that the hydrostatic stiffness in the vertical direction arising out of the waterplane area of the columns is typically a small percentage (about 2 to 4) of the total axial stiffness of the tethers. Thus, even if there is a large change in tension at any corner, the resulting vertical movement would cause insignificant change in buoyancy. Also these displacements would be so small

compared to the lengthwise dimensions of TLP hull that they would only cause very small inclinations (typically a complete loss of tether at one corner would tilt the hull by about 0.1 degrees) thus making the resulting hydrostatic moments to be insignificant. There is, however, a marked redistribution of the total pretension.

According to the reasonings given in the preceeding, ΔB, ΔM_x and ΔM_y may be assumed to be zero. Also if the platform weight remains unchanged, the total pretension would remain unaltered after the tether loss. Now if we assume that the springs are attached to a rigid frame we can write the follwing identity from the Z coordinate of the crossing point of the diagonals #1-#3 and #2-#4 :

$$(Z_d + d_1 + Z_d + d_3)/2 = (Z_d + d_2 + Z_d + d_4)/2$$

$$\text{or,} \quad d_1 + d_3 = d_2 + d_4$$

$$\text{or,} \quad d_4 = d_1 - d_2 + d_3 \qquad (6.2)$$

Letting ΔB, ΔM_x and ΔM_y to zero and substituting for d_4 from equation (6.2) in equation (6.1) and rewriting in matrix form, we obtain :

$$\begin{bmatrix} K_1+K_4, & K_2-K_4, & K_3+K_4 \\ K_1Y_1-K_4Y_4, & K_2Y_2+K_4Y_4, & -K_3Y_3-K_4Y_4 \\ K_1X_1+K_4X_4, & -K_2X_2-K_4X_4, & -K_3X_3+K_4X_4 \end{bmatrix} \begin{Bmatrix} d_1 \\ d_2 \\ d_3 \end{Bmatrix} = \begin{Bmatrix} T_p \\ 0 \\ 0 \end{Bmatrix} \qquad (6.3)$$

Now, for any given pretension and stiffness values, the equilibrium displacements d_1, d_2 etc. can be easily calculated by multiplying the r.h.s. with the inverse of the coefficient matrix. Once these are known, d_4 can be calculated from equation (6.2). The various equilibrium tensions T_1, T_2 etc. would then be found as :

$$T_1 = K_1 d_1$$
$$T_2 = K_2 d_2 \quad \text{etc.} \qquad (6.4)$$

For illustration purposes a TLP with $T_p = 1.44 \times 10^8$ N and intact axial stiffness/corner = 7.6×10^7 N/m is chosen. The stiffness at corner # 1 is reduced in steps. The resulting tension redistribution, keeping T_p constant, is calculated via a computer program 'EQUILIB' (listed in Appendix 'A') based on the above-mentioned method and graphically represented in Fig. 6.2. It may be noticed that as the platform tips towards corner # 3 due to tether loss at # 1, the tension decreases at both the corners; at # 1 due to reduced stiffness and at # 3 due to reduced displacement. The tension lost from # 1 and # 3 is picked up

by the tethers on the opposite diagonal i.e. #2-#4 where an increase in tension takes place. If T_p, ΔM_x and ΔM_y are to be taken as nonzero values, an iterative scheme would have to be employed where for every trial solution of the equilibrium displacements, these quantities would have to be evaluated by hydrostatics software and fed back as inputs till desired ~~level~~ of convergence is achieved. In such a case, the equlibrium tensions at #1 and #3 would cease to be equal (as seen in Fig. 6.2), but the difference would still be very small.

A TLP is very weight sensitive and the distribution of loads on-board is carefully matched with the current tension distribution. Knowledge of equilibrium tensions with any given combination of stiffnesses is, therefore, of much relevance. Besides, these values are also needed to assure safety of the tethers, as input data for various dynamic analyses etc.

Chapter 7

HYDROSTATIC ANALYSIS

7.1 General :

A floating body (also referred to as 'vessel') must be 'hydrostatically stable' to be sea worthy. The ability of a vessel to counteract the resultant external force or moment is its measure of stability, and when these loads are applied statically the body responds according to its hydrostatic properties. Referring to Fig. 7.1 we can see that when the body tilts about any particular axis, the centre of gravity (C.G.) and the centre of buoyancy (C.B.) cease to remain on the same vertical line thus generating a resultant moment in the plane that contains these two points. The component of this resultant moment that opposes the external moment is what is known as the 'righting moment'. A floating body would keep on listing untill the righting moment equals the external one. Statical stability analysis essentially aims to quantify the ability of a vessel to generate this righting moment.

7.2 Statical Stability of TLPs :

For a free floating body, the stability characteristics at any given inclination of the body with respect to the water plane depends on the geometry of the buoyant volume and the distribution of weight or in other words on the relative disposition of C.G. and C.B. A TLP in free-float modes displays stability characteristics similar to semi-submersibles. In operational mode, however, it derives high restoring moments from its tethers due to their high axial stiffness. The restoring moments due to tethers are in fact so high that if the tethers were to remain intact and the major hull were to remain watertight, the statical stabilty of TLP would be well in excess of what may be regarded as safe. In what follows, attempts are made to investigate the effect of tether loss on the statical stability of TLP. Fig. 7.2 gives a schematic representation of the major TLP configurations that may be of interest in the context of stabilty assessment. The first three are examples from free-float configurations where buoyancy equals the weight always. The fourth one shows the TLP in operational draught with complete loss of tethers at one corner, say # 1. It may be immediately realised that the high rigidity of TLP in intact operational condition is now lost and the platform would easily tilt towards corner # 3 if an external moment

such as that caused by wind load is applied in the vertical plane containing # 1 and # 3. Tethers at # 3 would also lose tension and go slack as the TLP stoops towards # 3. Tether stifnesses being very high, vertical movement of the hull would be very small. Thus the platform would virtually rotate about a space fixed axis passing through the top of tethers at # 2 and # 4. Any change in buoyancy will cause proportional change in the tensions in # 2 and # 4. Should there be such an emergency (possibly caused by blow-outs etc.) such that it has to switch to free-float mode at once, the tethers would have to be suddenly disconnected before any change in ballast/on-board weights could be brought about. This 'emergency disconnect' configuration, which can be viewed as a case of 100% tether loss at all corners or as a special free-floating case, is what is depicted in the fifth schematic. In the present chapter, configuration with operational draught and 100% loss of tether at # 1 will be studied in greater detail and its statical stability status will be compared with some of the other configurations.

For brevity only three out of the five configurations shown in Fig. 7.2 will be analysed. Out of the first three configurations, a careful inspection of some pertinent parameters such as draught, displacement, location of the vertical centre of gravity (VCG) etc. would indicate that

the third one should be analysed most critically. Hence, the cases that would be considered here are (i) TLP at operational draught with complete loss of tether at corner # 1 (Case 1), (ii) TLP immediately after 'emergency disconnect' (Case 2) and (iii) TLP in 'post-mating' draught (Case 3). Information regarding the exact displacements, weight, VCG etc. of most of these configurations is not adequate in published literature since such data are regarded as 'proprietory'. Judicious estimations are, therefore, done to make the analysis realistic. The geometry of the hull considered here is the same as that described in Chapter 5 (also see Table 5.3 and Figs. 5.1A and 5.1B). Other pertinent parameters for the three cases are listed in Table 7.1.

7.3 Assessment of Stability :

In the usual methods of assessment of stability, the initial metacentric height is required to be positive. Some classification societies also provide a stipulated value for the minimum initial metacentric height. The righting moment as a function of heel angle (usually about the axis where the righting moments are the least) is another yard stick. The external moment due to wind etc. is superimposed on a plot of righting moment and heel angle (see Fig. 7.3). The

resulting plot is the well known 'stability diagram'. The 'first intercept' is the angle where the external moment equals the righting moment and the 'down-flooding angle' is the angle beyond which the vessel would experience progressive flooding and is likely to capsize. For the vessel to successfully resist the external load, the first intercept must have to be smaller than the down-flooding angle. If we take a ratio of the areas under the righting moment curve and the external heeling moment curve upto the 'down-flooding angle', the higher the ratio the higher is the ablity of the vessel to work against the external moment. Most maritime authorities require that this ratio be at least equal to 1.3. This is also refered to as the 'dynamic stability criterion'. This reserve, as indicated by the 30% extra area is expected to take care of the dynamic effects of the external loads.

The above-mentioned procedures are commonly used in practice, although they are perhaps not the best way of assessing statical stability. The usefulness and applicabilty of such nominal rules, particularly to non-ship-shape floating structures, have been reviewed and questioned (see Pawlowski and Deb, 1986, Martinovich and Praught, 1986). These rules always refer to the the upright configuration of the vessel, whereas quite often a shift of

weight on-board may have significant effect on the righting moment. Besides, such methods do not provide any basis for comparison of statical stabilities of different vessels or the same vessel at different configurations. Also, no clear guidance is available as to how such rules may be applied to TLPs. A new method of assessment of stability of floating structures, proposed by Pawlowski (1985) and Pawlowski and Deb (1986), aims to circumvent such drawbacks of the existing methods. The vulnerability of a given floating body to exceed the desired limit of one or a combination of few pertinent parameters influencing the stability of the vessel is taken as the rationale in this approach. At a given displacement and VCG, the maximum allowable lateral shift of C.G. is taken as a measure of the degree of such vulnerability.

The new approach can also be applied to statical stability evaluation purposes by setting the pertinent parameters such that they relate to the stabilty diagram. This may be easily done by chosing the already described area ratio as the pertinent parameter and a value of this ratio may be chosen as the limit. The allowable lateral shifts of C.G. may now be evaluated over a range of VCG such that any further shift of C.G. would make the vessel incapable of meeting the specified area ratio. The

magnitudes of these 'shifts' can be used to ensure safety or to make comparisons.

7.4 The Hydrostatic Formulation :

Refering to Fig. 7.1 we see that if the weight and the CG is known then the total buoyancy force and the CB have to be known ih order to calculate the righting moment from :

$$\text{Righting Moment} = M_B - M_W \qquad (7.1)$$

where, M_B and M_W are the moments due to buoyancy and weight forces about a common point of reference.

In case the tethers are active, moments due to tensions about the same point, with proper signs, must be included in equation (7.1) to obtain the effective righting moment.

Let P be the centroid of an elemental patch of area dA on the surface of the floating body shown in Fig. 7.1. Let $\bar{R} = (R_1, R_2, R_3)^T$ be the position vector of P, and $\bar{n} = (n_1, n_2, n_3)^T$ be the outwardly normal vector to the surface at P with respect to a global frame of reference O123. The elemental hydrostatic force $d\bar{F}$ is then calculated as :

$$d\bar{F} = - \rho_w g h \, dA \, \bar{n} \qquad (7.2)$$

where,

ρ_w = mass density of water

g = acceleration due to gravity

h = depth of P below water surface.

Integration of $d\bar{F}$ over the entire immersed surface would yield the total hydrostatic force $\bar{F} = (F_1, F_2, F_3)^T$. For a free floating body F_3 is the only non-zero component of $\bar{F}$ which is the total buoyancy force. F_3 can also be found as :

$$F_3 = \int_S dF_3 = - \int_S \rho_w g h \, \bar{n} \cdot \bar{e}_3 \, dA \qquad (7.3)$$

where, S is the immersed surface and $\bar{e}_3$ is the unit vector corresponding to 0-3 axis.

The coordinates of CB i.e. CB_1, CB_2 and CB_3 can be found as :

$$\begin{aligned} CB_1 &= -\int_S R_1 dF_3 \; / \; F_3 \\ CB_2 &= -\int_S R_2 dF_3 \; / \; F_3 \\ CB_3 &= -\int_S h dF_3 \; / \; 2F_3 \end{aligned} \qquad (7.4)$$

It may be necessary to compute the righting moments for heel angles about an axis that is coplanar to O1-O2 plane but makes an angle (θ) with O1-axis. As the body is heeled about this 'heel axis' (O1'-axis), there may arise unbalanced moment about a 'trim axis' (O2'-axis), perpendicular to the heel axis. This would lead to a natural hydrostatic equilibrium 'trim angle'. In order to compute the force or moments in the global system, vectors in the primed system must be first converted to their corresponding representations in O123. This can be done as follows.

Let $\bar{a}$ be a vector in O123 which undergoes rotations ϕ (heel angle) and ξ (trim angle) measured in the primed system (θ being the angle between O-1 and O-1' axis) and attains a new vector configuration $\bar{a}'$, then the representations of $\bar{a}'$ in the non-primed system can be found from (see Pawlowski, 1985) :

$$(\bar{a}') = [\underset{\sim}{R}](\bar{a}) \tag{7.5}$$

where, $\underset{\sim}{R}$ is the resultant tensor of rotation and is given as :

$$\underset{\sim}{R} = \underset{\sim}{R}_2 \cdot \underset{\sim}{R}_1 \tag{7.6}$$

The components of the tensor R_1 are :

$$R_1(1,1) = e_1^2 + (1 - e_1^2)\, C$$

$$R_1(1,2) = e_1\, e_2 - e_1\, e_2\, C$$

$$R_1(1,3) = e_2\, S$$

$$R_1(2,1) = e_2\, e_1 - e_2\, e_1\, C$$

$$R_1(2,2) = e_2^2 + (1 - e_2^2)\, C$$

$$R_1(2,3) = - e_1\, S$$

$$R_1(3,1) = - e_2\, S$$

$$R_1(3,2) = e_1\, S$$

$$R_1(3,3) = C$$

where,

$e_1 = \cos \theta$

$e_2 = \sin \theta$

$C = \cos \phi$

$S = \sin \phi$

In order to obtain the components of $\underset{\sim}{R}_2$, same expressions as in case of $\underset{\sim}{R}_1$ are used with θ and ϕ replaced by $\theta+90°$ and ξ, respectively.

The choice of global system and the heel axis may vary from problem to problem.

Based on the above-mentioned theory, a computer program 'HYDROSTATICS' is developed (listed in appendix 'B') to generate righting moment as a function of given heel angle. The output of this program is used for the stability assessments. Fig. 7.4 presents a flow chart for 'HYDROSTATICS'.

7.5 Hydrostatic Experiments :

A typical output of 'HYDROSTATIC' for a GVA-4000 semisubmersible has been compared with values determined from model tests (Stone, 1986) and the agreement is found to be satisfactory.

Righting moments are also measured by shifting weight on deck and noting the resulting heel angle for the present TLP model for Case 1. The experimental values, plotted in Fig. 7.5 show good agreement with the calculated values.

7.6 Results :

'HYDROSTATICS' is used to compute the righting moments of the example TLP for the three cases already described (see section 7.3 and Table 7.1 for details). The wind speed is taken equal to 100 knots in all cases. Calculations are

repeated for heel axis rotated by 0 and 45 degrees with respect to the O1-axis (i.e. about the centre line and about the diagonal, #2 - #4, if #1 is taken as the damaged corner). In all three cases the heel axis at 45 degrees to the O1-axis is found to yield a smaller area under the righting moment curve. This axis is, therefore, used for statical stability assessment. The corresponding stability diagrams showing the righting moment and wind heeling moment curves for these three cases are given in Fig. 7.5 through Fig. 7.7. The righting moment curves correspond the VCGs given in Table 7.1.

It is seen from the stability diagrams that all the cases satisfy the usual stability criteria, that is, the initial GM is positive since the righting moment curves have positive slopes at 0 degree heel and also the area ratios are greater than 1.3. The new procedure already described is now employed to indicate the vulnerability of each case to loss of adequate stability. In order to do so, for each case, righting moment data are generated over a range of VCGs (from 30.0 m to 40.0 m) for different amount of lateral shifts of the CG in the direction of list at these VCGs. The ratio of the areas under the righting moment curve and the wind moment is calculated for each combination of VCG and lateral shift. Limiting values of shift at every VCG are

found by setting the minimum area ratio to a value of 1.3. The limiting values, termed as 'admissible shifts', are plotted in Fig. 7.8. As mentioned before, at a given VCG any further lateral shift of CG than what is admissible, would result in inadequate reserve of statical stability. Consequently, the vessel would be susceptible to loss of stability and capsize.

It may be readily seen from Fig. 7.8 that at the assumed operating levels of VCGs, all three cases, including the tethered configuration with tether loss at # 1, appear more or less comparable in terms of their vulnerabilty to loss of adequate stability. In general, small values of admissible shifts indicate that great caution must be exercised while shifting any weight on-board. The worst of these cases, however, is Case 2 where at operating VCG even a shift of CG as small as 0.4m may render the platform unsafe. Case 1, however, may appear to be marginally safer than the others, increase in tension in the active tethers (i.e. #2 and #4) due to the combined effect of loss of tensions in #1 and #3 and increase in buoyancy with heel angle may be of harmful consequence. For case 1, typical increase in tensions at the active corners are also shown in Fig. 7.5.

Chapter 8

HYDRODYNAMIC ANALYSIS

8.1 General :

Evaluation of the hydrodynamic force field and computation of motion response of the body exposed to this force field constitute the essentials of the problem of hydrodynamic analysis. Typically the total force field would include (i) fluid excitation forces i.e. those due to wave, current etc., (ii) restoring forces i.e. hydrostatic and mooring forces, (iii) damping forces and (iv) inertia forces. With regard to response evaluation, elastic responses of the body surface are assumed to be sufficiently small so that the immersed portion of the body may be taken as rigid. The equations of motion then are essentially the generalised force balance equations in Newtonian mechanics. These equations may be solved in time or frequency domain to obtain the various respones and their time derivatives. In time domain analysis, motion of the body is described by the instantaneous equilibrium configuration while in frequency domain analysis, amplitudes and phases of the three

translational (viz. surge, sway and heave) and the three rotational (viz. roll, pitch and yaw) displacements are used to define the body motion. Frequency domain analysis is inexpensive with respect to computation time but requires the equations of motion to be linear. Spectral analyses, therefore, are often handled via frequency domain approach. Time domain solution schemes, although consume remarkably high computation time, are capable of admitting nonlinear phenomena relatively easily.

8.2 Time Domain Simulation of a TLP :

The problem of the time domain simulation of a TLP is quite similar to that of a free floating body except for the inclusion of restoring forces due its taut tethers. In general terms, the task involves (i) formulation of the kinematics of the rigid body i.e. transformations of displacements and their derivatives between a fixed and a moving frame of reference, (ii) computation of the excitation and the reactive forces and (iii) solution of the equations of motion. Examples of such formulations as applied to TLPs can be found in the work of Paulling (1986), Paulling (1975), Paulling (1971), Natvig and Pendered (1979), Faltinsen et al. (1982) etc. The basic equations used here to describe the rigid body motion, given in

Pawlowski, 1985 are outlined as follows.

The definition diagram in Fig 8.1a shows the space fixed axis system $OX_1X_2X_3$ attached to the waterline (for the sake of convenience) and the body fixed axis system $OX_1'X_2'X_3'$ with its origin coinciding with the centre of gravity of the body. The translations and the successive rotations of the primed reference with respect to the non-primed reference are given by X_i (i=1,2,3) and η_i (i=1,2,3), respectively. Rotational motions about the centre of gravity of the body are described by the angular velocities ω_i (i=1,2.3) about the axes OX_i' (i=1,2,3). The equations of motion are then written as :

$$[M]\,\ddot{X}_G = F \tag{8.1}$$

$$[J]\,\dot{\omega} + \omega \wedge [J]\,\omega = \Gamma' \tag{8.2}$$

where,

[M] = Mass matrix for the platform

[J] = Inertia matrix for the platform about C.G. with respect to primed axes

F = Force vector in non-primed axes

Γ' = Moment vector about C.G. in primed system

X_G = Position vector of centre of gravity with respect to non-primed axes

$\dot{}$ = Denotes a time derivative (i.e. d/dt of)

Λ = Denotes a cross product

The rotation of the primed axes relative to the non-primed axes is given by :

$$[\dot{R}] = [R][\underline{\omega} \Lambda \underline{I}] \tag{8.3}$$

where,

$$\underline{\omega} \Lambda \underline{I} = \begin{bmatrix} 0 & -\omega_3 & \omega_2 \\ \omega_2 & 0 & -\omega_1 \\ -\omega_2 & \omega_1 & 0 \end{bmatrix}$$

If $\underline{a}$ in the non-primed system represents an arbitary vector $\underline{a}'$ in the primed system, then they are related by the rotation matrix [R] as :

$$\underline{a} = [R]\,\underline{a}' \tag{8.4}$$

Also, the various kinematic relations for an arbitary point P on the body (ref Fig. 8.1a) are given by the following vector equations :

$$\begin{aligned} X_P &= X_G + [R]\,\underline{a}_P \\ \dot{X}_P &= \dot{X}_G + \underline{\omega} \Lambda (X_P - X_G) \end{aligned} \tag{8.5}$$

$$\underline{X}_P = \underline{X}_G + \underline{\omega} \wedge (\underline{X}_P - \underline{X}_G) + \underline{\omega} \wedge (\underline{\omega} \wedge (\underline{X}_P - \underline{X}_G))$$

where,

$\underline{X}_P$ = Insntatneous position vector of P

$\underline{a}_P$ = Radius vector of P (see Fig. 8.1a)

The angles η_i are found from the equation :

$$\underline{\omega} = [B]\,\dot{\underline{\eta}} \tag{8.6}$$

where,

$$[B] = \begin{bmatrix} C_2 & 0 & -C_1S_2 \\ 0 & 1 & S_1 \\ S_2 & 0 & C_1C_2 \end{bmatrix}$$

and $C_i = \cos\eta_i$, $S_i = \sin\eta_i$

The above equations are now rewritten as a system of 21 first order differential equations as :

$$\begin{aligned}
\dot{\underline{X}} &= \underline{V} && \text{(3 equations)} \\
\dot{\underline{V}} &= [M]^{-1}\,\underline{F} && \text{(3 equations)} \\
\dot{\underline{\omega}} &= [J]^{-1}\,(\underline{\Gamma}' - \underline{\omega} \wedge [J]\,\underline{\omega}) && \text{(3 equations)} \qquad (8.7) \\
\dot{[R]} &= [R][\underline{\omega} \wedge \underline{I}] && \text{(9 equations)} \\
\dot{\underline{\eta}} &= [B]^{-1}\,\underline{\omega} && \text{(3 equations)}
\end{aligned}$$

The system of equations in (8.7) may now be solved by a suitable predictor-corrector type 'differential equation solver' based on techniques such as Adam's method, Runge-Kutta etc. (see Paulling, 1971). Several iterations at any time step may be necessary in order to achieve convergence of the state variables when nonlinearities are present. In the present analysis, a standard IMSL (1984) routine called 'DGEAR' has been used to integrate equations (8.7).

Fig. 8.1b shows the commonly referred six degrees of freedom of a floating body.

Having established the equations of motion, the force field needs to be calculated from a suitable method. For the sake of computational efficiency, the philosophy of 'hydrodynamic synthesis' is adopted in the present analysis. Morison's equation (Morison et al., 1950) is applied to calculate the hydrodynamic loading, with the assumption that the platform may be represented as a space-frame assembly of slender cylindrical members which are 'hydrodynamically isolated' from each other. According to this formulation, the total fluid force on any member consists of (i) pressure in the undisturbed flow field, to be integrated over the wetted surface, (ii) inertial force proportional to relative acceleration between fluid and the cylinder, to be

integrated over the length of the members and (iii) drag force proportional to the square of the relative velocity also to be integrated over the length of the members. The pressure force is given as a sum of two components i.e. p_s, the static part and p_d, the dynamic part. If the members are regarded as slender then the total force on the structure may be expressed in the form (Hooft, 1971) :

$$F_h = \int p_s \, \underline{n} \, ds + \int p_d \, \underline{n} \, ds_1 + \rho_w A_m \int [C_m \, \underline{a}_{fn} - C_m \, \underline{x}_n] \, dl + 0.5 D_m \rho_w C_d \int \underline{v}_{rn} \, |\underline{v}_{rn}| \, dl \qquad (8.8)$$

where,

$\underline{n}$ = Normal vector in the inward direction on the member surface

ρ_w = Mass density of water

D_m = Member diameter

$A_m = \pi D_m^2 / 4$

C_m = Added mass coefficient

C_d = Quadratic drag coefficient

$\underline{a}_{fn}$ = Fluid acceleration normal to the member

$\underline{x}_n$ = Component of body acceleration normal to the member

$\underline{v}_{rn}$ = Component of the local relative velocity between the fluid and the member ($\underline{v}_{fn} - \underline{x}_n$), normal to the member.

ds = Elemental member surface

d_{s1} = Elemental flat surface such as bottom of cylinders etc.

dl = Elemental member length

The assumptions inherent in the above formulation also require that the members are slender in comparison with the incident wave length such that the fluid flow is not disturbed and also that diffraction effects are insignificant. Also, since the hydrodynamic interaction bewteen members is ignored, the total force on the structure can be found by summing the forces on all the component members.

The surface elevation and the basic fluid flow parameters such as particle velocity and accelerations and the pressure are calculated from the incident wave potential, Φ, which in accordance with Airy's small amplitude wave theory may be written as (Sarpkaya and Issacson, 1981) :

$$\Phi = (\omega H \cosh(ks) \sin(k\xi - \omega t)) / (2k \cosh(kd)) \qquad (8.9)$$

where,

ω = Wave angular frequency

H = Wave height

k = Wave number

d = Water depth

s = d + z; 'z' is the vertical distance of a point in fluid from the mean water level, z is measured positive from the waterline upwards

ξ = Wave coordinate

= $X_1 \cos\theta + X_2 \sin\theta$; θ is the wave heading angle

t = Time

The wave number is given by the 'dispersion relation' as :

$$\omega^2 = gk \tanh (kd) \qquad (8.10)$$

where,

g = Acceleration due to gravity.

The relations given in (8.9) and (8.10), for the case of deep water (i.e. $kd > \pi$), take the forms :

$$\Phi = \omega H e^{kz} \sin (k\xi - \omega t) / 2k \qquad (8.11)$$

$$\omega^2 = gk \qquad (8.12)$$

The instantaneous surface elevation of the wave, ζ

corresponding to the above potential is :

$$\zeta = H \cos (k\xi - \omega t) / 2 \qquad (8.13)$$

The required fluid flow parameters are found from :

$$v_i = \partial\Phi/\partial X_i$$

$$a_i = \partial v_i/\partial t$$

$$p_s = - \rho_w g z \qquad (8.14)$$

$$p_d = - \rho_w \partial\Phi/\partial t \quad \text{(from linearized Bernoulli's equation)}$$

To find the component of velocity $\underline{v}$ normal to a member (denoted by $\underline{v}_n$), the following relation is used (Chakraverti et al., 1975) :

$$\underline{v}_n = \underline{n} \wedge (\underline{v} \wedge \underline{n}) \qquad (8.15)$$

where,

$\underline{n}$ = Unit vector of the centre line of the member.

The normal component of acceleration or any other vector can also be found by a relation similar to equation 8.15.

The static pressure 'p_s' in equation (8.14) i.e. ρgz, on integration yields the hydrostatic reactive force. In the case of a TLP, additional restoring forces arise out of the reactions from the tethers. In the present analysis, the tethers are represented by linear springs with a 'spring constant' equal to the axial stiffness of the tethers. If δ_{Ti} is the instantaneous elongation of the jth tether top, jth the tether reaction, $\underline{F}_{Tj}$, is then given as :

$$\underline{F}_{Tj} = K_{Tj}\delta_{Tj}\,\underline{n}_{Tj} \qquad (8.16)$$

where,

K_{Tj} = Spring constant of the jth tether

$\underline{n}_{Tj}$ = Unit vector of the jth tether (ref Fig. 8.1a)

Thus the total force $\underline{F}$ in the non-primed system can be written as :

$$\underline{F} = \underline{F}_h + \underline{F}_T \qquad (8.17)$$

The moment $\underline{L}'$ in the body fixed system can be found from :

$$\underline{L}' = \int \underline{r}' \wedge d\underline{F}' \qquad (8.18)$$

where,

$\underline{r}'$ = Position vector of a point

$d\underline{F}'$ = Differential force at the above point.

The forces calculated as above include the following nonlinearities :

(i) nonlinearity arising due to integration over instantaneous wetted surface

(ii) inclusion of the nonlinear terms in the rotational equations of motion

(iii) quadratic drag force

(iv) position dependent restoring forces.

$\underline{F}$ is evaluated at every time step, more than once if iterations are required for convergence, and equations (8.7) are solved to obtain the state variables at that step. A computer program named 'TIME_DOMAIN' (listed in Appendix C) has been developed based on the formulation described in the preceeding, which has been used to generate various response time histories for the example TLP. In order to minimize the initial transients a 'half cosine' function is multiplied to the wave amplitude. The form of this ramp function is given as (Paulling, 1977) :

$$(1 - \cos\pi t/T_0) / 2; \quad t < T_0 \tag{8.19}$$

where,

T_0 = Time length over which the function is applied.

8.3 Frequency Domain Analysis :

In frequency domain analysis an approach very similar to that described in the preceeding section is utilized. In such an analysis the equations to be solved must be linear. Therefore, additional assumptions are made which are listed below :

(i) The displacements and the angles are assumed to be small.

(ii) The nonlinear term in the rotational equation of motion is considered to be small and hence dropped.

(iii) The integration of the forces are carried out over the mean wetted surface.

(iv) Linear hydrostatic stiffnesses are assumed.

(v) The mooring stiffness matrix is constructed on the basis of mean pretension of the tethers corresponding to the static equilibrium configuration and small displacement assumptions.

The presence of the quadratic drag term poses an obstacle in frequency domain analysis because of its nonlinear nature. This term may be linearized by the 'equivalent drag' concept (Paulling, 1985) as follows :

$$C_{dl}\underline{v}_{rn} = 8C_d|V_{rn}|\underline{v}_{rn} / 3\pi \qquad (8.19)$$

where,

C_{dl} = Equivalent linear drag coefficient

V_{rn} = Amplitude of $\underline{v}_{rn}$

The forces are calculated by the Morison equation approach already discussed in the previous section.

Collecting all the response dependent terms on the left hand side and the wave excitation terms on the right hand side, the equations (8.1) and (8.2) are combined and rewritten in a matrix form as :

$$[[M]+[M_a]](\delta) + [C](\delta) + [[K_h]+[K_T]](\delta) = (F_w) \qquad (8.20)$$

where,

[M] = Generalised physical mass matrix

$[M_a]$ = Generalised added mass matrix

[C] = Damping matrix

$[K_h]$ = Hydrostatic stiffness matrix

$[K_T]$ = Mooring stifness matrix

$\{F_W\}$ = Generalised wave excitation force vector

$\{\delta\}$ = Generalised displacement vector of the centre of gravity.

The hydrostatic and mooring stiffness matrices are constructed according to formulations described in Chou et al. (1983).

The solution of equation (8.20) yields the required amplitudes and the relative phases of the motion in six degrees of freedom. In this case, the equation is written in a complex form (see Hooft, 1971). Accordingly, excitation force vector can be written in the complex form as :

$$\{F_W\} = \{F_{waj}\, e^{i\omega t + i\sigma j}\}; \quad j = 1,2,\ldots,6 \qquad (8.21)$$

where,

F_{waj} = Amplitude of the excitation force

$= (F_{WRj}^2 + F_{WIj}^2)^{1/2}$

F_{WRj} = Force term proportional to cos(ωt) (real part)

F_{WIj} = Force term proprtional to sin(ωt) (imaginary part)

σ_j = Phase difference = $\tan^{-1}\ (F_{WIj}/F_{WRj})$

$i = \sqrt{-1}$.

If a steady state solution (δ_j) of equation (8.20) is assumed which is written in complex form with obvious notations as :

$$(\delta_j) = (\delta_{aj}\, e^{i\omega t + i\epsilon_j}) \qquad (8.22)$$

where,

ϵ_j = Phase difference

then the complex equations of motion can be written as :

$$[-\omega^2[[M]+[M_a]] + [[K_h]+[K_T]] + i\omega[C]](\delta) = (F_w) \qquad (8.23)$$

In the present analysis, equation (8.23) is solved by a standard IMSL routine, 'LEQ2C', capable of obtaining solution of a general system of complex linear equations to find the amplitudes and the phases of the various displacements. Since, the amplitude of the normal component the local relative velocity, V_{rn}, is not known before the solution is found, iterative computations are necessary to solve equation (8.23). A computer program named 'FREQ_DOMAIN' Has been developed (listed in Appendix D) and

used to calculate responses of the example TLP.

Once the responses of the centre of gravity are known, the tether tension amplitudes T_{aj} are calculated as follows (ref. Chou et al., 1983) :

$$T_{aj} = K_j(|\delta_{G1} + \delta_{G2} \wedge (X_{T1j} - X_G) + X_{T1j} - X_{T2j}| - |X_{T1j} - X_{T2j}|) \qquad (8.24)$$

where,

K_j = Axial stiffness of the jth tether

δ_{G1} = Translational displacement vector of the CG

δ_{G2} = Rotational displacement vector of the CG

X_G = Position vector of the CG

X_{T1j} = Position vector of tether top end of jth tether

X_{T2j} = Position vector of tether bottom end of jth tether

8.4. Spectral Analysis :

In an actual seaway, the waves do not occur at an isolated frequency and height combination; instead, a realistic sea has irregular elevation with no set pattern of wave length, height or period. Irregular sea behaviour, however, is often defined by its direction and energy

content over a range of frequency band. One such popularly practised concept is to employ an irregular sea in a two-dimensional seaway, a long crested sea that can be produced in a wave tank.

Significant motion response calculations in irregular seas are based on spectral theory which describes how regular wave elements combine to produce irregular sea pattern and how each component affects the behaviour of the floating body (ref. Bhattacharya, 1978). The underlying principle, of course, rests on the validity of linear superposition of the body responses to harmonic (sinusoidal) components of the irregular sea.

Frequency domain approach is usually used for spectral analysis. Significant response is calculated from :

$$R_{j1/3} = 4.0 \left(\left(\int_0^\infty S_{Rj}(\omega) \, d\omega \right)^{1/2} \right. \qquad (8.25)$$

where,

$R_{j1/3}$ = Significant amplitude (1/3 rd highest) of the jth response

$S_{Rj}(\omega)$ = Spectrum of the jth response

The response spectrum is found from the relation :

$$S_{Rj}(\omega) = RAO_j(\omega)^2 \; S(\omega) \qquad (8.26)$$

where,

$RAO_j(\omega)$ = Response Amplitude Operator (RAO) of the jth response i.e. response to wave of unit amplitude

$S(\omega)$ = Sea wave energy density spectrum defining the sea state.

The RAOs are computed by the program 'FREQ_DOMAIN'. It may be noted here that the equations (8.25) and (8.26) are also applied to tension responses.

8.5 Results :

In the context of of dynamics of an offshore structure, the type of responses commonly calculated are those caused by regular and irregular wave excitations. In the case of regular waves, steady state amplitudes are computed as a function of wave frequency while, for irregular waves, significant response amplitudes corresponding a given sea energy spectrum are of relevance. Transient responses are also of interest when a sudden change of a pertinent system parameter occurs.

For systems that possess input-output linearity, frequency domain analysis may be considered as an efficient tool for the prediction of steady state response amplitudes. A frequency domain analysis is faster with regard to computation time and thus very convenient for parametric studies. Since linearity is assumed, the response amplitudes are usually presented in the form of 'Response Amplitude Operators' or RAOs which are essentially the responses caused by a wave of unit amplitude at a given frequency. In the case of TLPs, even though significant nonlinearities exist, RAOs are often calculated in the hope of obtaining some idea of the responses due to small amplitude waves.

C_d depends on Reynolds number and Keulegan Carpenter number and C_m varies with frequency. But often for computational ease, constant values of C_d and C_m are used. In the present study, for the calculation of wave loading, C_d and C_m have been taken as 1.0 and 1.0, respectively. Surge and tension RAOs are computed via the program 'FREQ_DOMAIN' for a TLP described by Lyons et al. (1983) and compared with the published results in Figs. 8.4a and 8.4b. For the example TLP, motion and tension RAOs are presented in Fig. 8.5 through Fig. 8.9 for 0 degree heading and in Fig. 8.10 through Fig. 8.15 for 45 degree heading. Only intact (shown in full line) and 50% tether loss at # 1

(shown in broken line) are presented since a 100% loss of tether at any corner is found to cause significant nonlinear responses thus introducing obvious contradiction to the basic assumptions of frequency domain analysis.

Following the same logic of calculation of RAOs from the experimentally obtained time series data, RAOs are also calculated from the time series data generated by the program 'TIME_DOMAIN'. Once again, consistent with the experimental data analysis, a wave height of 10 m is used for such calculations.

In the case of surge and sway, tether loss appears to have insignificant effect on the response amplitude. Results from time domain analysis and regular sea experiments, plotted in Fig. 8.5 and Fig. 8.10 support this observation. This may be expected as the total pretension, which has the largest influence on surge/sway motion, remains practically unchanged in the tether damaged configurations. Calculated surge and sway RAOs, which are known to be quite insensitive to the choice of hydrodynamic coefficients (see Lyons et al., 1983), are found to be in good agreement with the experimental observations.

As far as motions in vertical planes are concerned,

increase in RAOs is always noted (also see Booton et al. for similar observations). In the case of a 0° heading, asymmetric distribution of tether stiffness and static equilibrium tensions is expected to introduce cross motions in sway, roll and yaw modes. Such cross motions are also reflected in frequency domain analysis; for 50% loss of stiffness at # 1 an insignificant sway as compared to surge amplitudes is predicted while the roll motion, as shown in Fig. 8.7, is found to be quite substantial.

Tension RAOs from regular and irregular sea experiments and from 'TIME_DOMAIN' are plotted for corner # 1 in Fig. 8.8 and Fig. 8.13. Such variations may be regarded as typical. Due to the scatter observed, experimental and 'TIME_DOMAIN' data are presented only for the intact cases. It is seen that the tether RAOs computed by 'FREQ_DOMAIN' do not match very well with those found from experiments or 'TIME_DOMAIN'. Correlation is particularly poor for wave frequencies greater than 0.8 rad/sec or so. RAOs from 'TIME_DOMAIN', on the other hand, portray a trend closer to what is observed from the experiments but still the numerical values are not always very close. Besides experimental errors, the difference may be attributed to the inability to correctly estimate the hydrodynamic forces by Morison type formula (ref. Lyons et al., 1983, Paulling,

1981) resulting in erroneous estimation of motions, particularly those in vertical planes which in turn affect the tension calculations. Additionally, in the case of frequency domain analysis, assumptions regarding linearity are likely to cause further errors in the computed results.

Inspecting the frequency domain results, it may be inferred that for 0° heading, following a tether loss at # 1, the tension RAOs at # 1, # 2 and # 4 increase while those at # 3 decrease. The difference is significant for both # 1 and # 4 while # 2 and # 3 experience only a mild variation in magnitudes. For 45° heading, tension RAOs increase at all the corners. It may clarified here that, for # 1, although tension RAOs in damaged cases appear to be less than those for intact cases in the diagrams presented, the tension is borne only by the remaining 50% of the initial tether cluster at that corner; and these tethers, in effect, suffer an increased variation in tension.

Fig. 8.16 through Fig. 8.21 present the time records of waves and tensions from the irregular tests. The waves correspond to a Pierson-Moskowitz spectrum with wind speed equal to 20 m/sec. A typical wave energy spectrum from the experimental data is shown in Fig. 8.22. In Figs. 8.23 through 8.26 tension spectra obtained from Fourier

transformation of the experimental time series data (shown in full line) are presented along with the corresponding theoretical spectra (shown in broken line) superimposed on them. The theoretical spectra are derived by multiplying the wave spectrum by the square of the RAOs obtained from 'FREQ_DOMAIN'. Once again mismatch between experimentally observed and theoretically calculated values is prominent, particularly at higher frequencies. Significant tension double amplitudes (1/3 rd highest) calculated from the areas under the spectra and the actual time records are compared in Table 8.1. Inspite of the mismatch, significant tension amplitudes are predicted reasonably close by the theoretical calculations which is due to a cancellation of error effect i.e. the extra spectral density predicted by theory at lower frequencies gets nullified by the absence of the same at higher frequencies. Such spectral analysis necessarily employs the linearity assumptions. The cases corresponding to 100% loss of tether are, therefore, not analysed by such a technique since prominent snap loads are evident from the time records.

Apart from being able to accomodate nonlinearities and large displacement kinematics, time domain domain simulations are also capable of reproducing certain transient responses of relevant interest. In the present

context, transient responses following a sudden loss of tether are simulated by the program 'TIME_DOMAIN' by simply proportionally reducing the axial stiffness at the designated corner from a desired time step onwards. In general, transient responses are influenced by the magnitudes of the state variables immediately preceeding the initiation of such phenomena. While attempting to study the transients following a tether loss, an obvious question that would arise is regarding the instant at which the tether breakage should be simulated so that the transients are the highest. To tackle this problem, tether breakage simulation experiments are repeated such that the breakage points are spread over one cycle of the tension wave-form at the affected corner (as indicated in Fig. 8.27a). A variation not exceeding 10% in transient tension amplitudes is noted due to choice of breakage instant while the highest values occured when the damage took place at the peak of the tension response at the affected corner. This may be attributed to the fact that under such a circumstance, the amount of tension released from the tethers at the affected corner, into the system is the highest, causing the maximum increase of tension in the remaining intact tethers. Time series data from 'TIME_DOMAIN' and experiments corresponding to highest transients are presented in Figs. 8.29a through 8.35 for 50% and 100% loss of tether at # 1 for 0 degree and

45 degree heading. A regular wave of 21.9 sec period and 20.0. m height is chosen for these case studies. For each combination, theoretically predicted motion and tension responses are presented followed by tension responses from the experiments.

Once again, increase in motion responses except for surge/sway is noted. Cross motions due to asymmetric stiffness distribution resulting from the damage can be seen for 0 degree heading. It may noted here that a small amount of yaw developed due to such asymmetry was not predicted in the frequency domain analysis. Tension responses also increase except for a slight reduction at # 3 for 0 degree heading case.

Steady state tensions, before and after the loss as well as transient tensions immediately following the loss are found from theoretical and experimental time records and compared in Tables 8.2a and 8.2b. The quantities compared are defined in Fig. 8.27b. For intact and 50% loss cases, steady state tension responses calculated from 'FREQ_DOMAIN' are also included in these tables. It can be seen that between time domain analysis and the experiments, a better match exists for transient responses than the steady state amplitudes. This may be due to the fact that the transient

responses take place fast enough not to be largely influenced by the hydrodynamic forces. Discrepancies in steady state amplitudes are due to inaccuracies in estimation of hydrodynamic forces, exclusion of various nonlinear effects such as wave ride-up on columns, second order effects, experimental error etc.

Similar calculations are also performed with a wave of 12 sec period and 20.0 m height and the tensions are tabulated in Table 8.3 for a 100% loss case. It may noted that at this frequency, complete loss of tether introduces snap loads (with magnitudes about 4 to 5 times that of the static pretension) at all corners.

From the above case studies, a quartering sea (i.e. 45° heading) appears to cause higher tension loads as compared to head sea (i.e. 0° heading).

Chapter 9

UNSTABLE MOTIONS OF TLP

9.1 General :

In the case of a compliant floating structure such as a TLP, motion in a particular mode can influence the motion in another mode through time varying changes in the stifness of the system. Most often, the motions in the vertical planes significantly affect the motions in the horizontal plane. This may lead to unstable motions of the structure, resulting in large response amplitudes at certain combinations of wave frequency and wave height. During the design stage, these unstable zones should be estimated to ensure that they do not coincide with the design wave parameters. Fig. 9.1 shows the zone of unstable time periods as compared to typical wave spectrum.

In this chapter, a brief review of previous work relating to the investigation of such instabilities of TLPs is presented. A procedure to establish the stability boundary for a given TLP, based on Floquet Theory

(Leipholtz, 1970) for periodic systems, is developed. This procedure is first illustrated using a simplified tension leg structure. Only the effect of heave on sway motion is considered in this case and the stability boundaries are established. Furtermore, the approach is extended to the general coupled equations of motion of a TLP.

9.2 Equations of Motion and Instability Phenomena :

Let us consider the simplified model of a tension leg structure shown in Fig. 9.2 where a positively buoyant unit is anchored to the sea-bed by means of a taut mooring cable. Let us assume that the structure is subjected to the action of a regular planar wave progressing in the positive OX_1 (surge) direction so that there is no wave excitation in the OX_2 (sway) direction. Under first order approximations, the equations of motion in heave and sway, respectively, can be written as :

$$M_3\ddot{\delta}_3 + C_{d3}|\dot{\delta}_3|\dot{\delta}_3 + K_3\delta_3 = F_3(t) \qquad (9.1)$$

$$M_2\ddot{\delta}_2 + C_{d2}|\dot{\delta}_2|\dot{\delta}_2 + K_2\delta_2 = 0 \qquad (9.2)$$

where,

M_3, M_2 = Virtual masses in heave and sway, respectively

C_{d3}, C_{d2} = Nonlinear drag coefficients in heave and sway, respectively

K_3 = Stiffness coeff. in heave = $(g\rho_w A_{wp} + EA/L)$ (9.3)

K_2 = Stiffness coeff. in sway (first order approx.)

$= (T_p + (EA/L)\delta_3(t))/L$ (9.4)

A_{wp} = Water plane area

g = Accln. due to gravity

ρ_w = Mass density of water

A = Cross sectional area of the cable

L = Length of the cable

δ_3, δ_2 = Heave and sway motions, respectively

$\dot{}$ = Denotes derivation with respect to time

$F_3(t)$ = Wave excited heave force

It is the inclusion of the time dependent stiffness coefficient $(EA/L)\delta_3(t)$ in equation (9.4) that results in the well known Mathieu type dynamic instability causing subharmonic resonances in sway. (See for example Rainey (1977), Patel and Jefferys (1981), Conceicao et al. (1983) etc.) Whenever the forcing frequency (wave excitation frequency) is about twice the natural frequency in sway, ω_s, (equal to $(T_p/M_2L)^{1/2}$ in this case). Here, the non-conservative restoring force resulting from heave motion inputs energy into the otherwise undisturbed sway mode and whenever the rate of energy input is higher than the

dissipation by the damping force, instability occurs. In this case, therefore, if instability exists, a perturbation given to the equilibrium solution $\delta_2(0)=0$ and $\dot{\delta}_2(0)=0$ would cause the solution to grow with time (i.e. move outwardly from the origin of the phase plane δ_2-$\dot{\delta}_2$) even though there is no wave excitation in OX_2 direction.

9.3 Evaluation of Stability and Floquet Theory :

Having formulated the equations of motion, a particular method has to be selected to investigate possible unstable regimes for the system, preferably in terms of some of the key parameters pertaining to the external excitation (say wave height and frequency in this case). Various methods have been used to estimate the stability boundaries and unstable motion amplitudes of systems such as equation (9.2) (see Rainey 1977, Richardson 1979, Patel and Jefferys 1981, Paulling 1982, Conceicao et al. 1983 etc.). One method is to reduce the given equation to the standard Mathieu or Hill's form (with proper substitutions to cater to the drag term when drag is considered). The stability boundaries can then be evaluated by comparing the coefficients of the reduced equation and those of the standard form (since the stability boundaries are available for the standard form in mathematics texts). Another way to locate instability is

through the analogy of these systems to 'feed-back' systems (Rainey, 1977). Unstable solutions have also been obtained from energy considerations (Patel and Jefferys, 1981) and from characteristic equations of the motion amplitudes (Yoneya and Yoshida, 1982).

In certain applications, analytical or semi-analytical means for evaluation of stability may appear cumbersome and complicated. To take advantage of the presently available high speed computers, a numerical method is developed here, based on Floquet theory for non-stationary systems describable by 'n' first order differential equations with periodic coefficients (Deb and Booton 1986a, Leipholtz 1970), to estimate the stability boundaries on a 'wave height-frequency' grid. The underlying theory and the working procedures are described as follows.

Let a general system described by 'n' linear first order differential equations be written as :

$$\dot{\underline{y}} = [P(t)]\,\underline{y} \tag{9.5}$$

where,

$[P(t+T)] = [P(t)]$, T is the fundamental period (9.6a)

$\underline{y}(0) = \underline{y}_0$ (9.6b)

Linearity of equation (9.5) allows one to write the general solution in terms of the 'fundamental matrix' $[\Phi]$ as :

$$\underline{y}(t) = [\Phi(t)]\, \underline{y}_0 \tag{9.7}$$

where, $[\dot{\Phi}] = [P(t)][\Phi]$; $[\Phi(0)] = \underline{I}$ (9.8)

$[\Phi(t)]$ is an 'n x n' square matrix containing 'n' linearly independent solutions of equation (9.5) corresponding to 'n' linearly independent initial conditions.

Because of the periodicity of $[P(t)]$, it is sufficient to examine the properties of the solution over one period.

Letting $\underline{M} = [\Phi(t)]$, the stability condition may be stated on the basis of Floquet theory as :

"If the 'n' eigenvalues $\mu_r = \rho_r e^{i\theta}$, r = 1, ..., n of $\underline{M}$ are distinct, let $\bar{\rho} = \max\{\rho_r\}$. Then the origin of the equation (9.5) is (i) asymptotically stable if $\bar{\rho} < 1$; (ii) unstable if $\bar{\rho} > 1$ and critically stable if $\bar{\rho} = 1$."

If the 'n' solutions of $\Phi(t)$ are not available in closed form, the usual procedure would be to solve $[\dot{\Phi}] = [P(t)][\Phi]$, $[\Phi(0)] = [I]$ numerically up to time $t = T$ so that the matrix $\underline{M}$ can be constructed.

Equation (9.2) can be expressed as a system of two first order differential equations. These equations are linearised in order to investigate the stability relative to the equilibrium position corresponding to $\delta_2(0)=0$ and $\dot{\delta}_2(0)=0$. The linearisation of the quadratic drag term is accomplished as follows (ref Paulling, 1985) :

$$C_{d2}|\dot{\delta}_2|\dot{\delta}_2 = C_{d12}\dot{\delta}_2$$

where,

C_{d12} = Linearised drag coefficient

$= 8C_{d2}|\bar{\dot{\delta}}_2|/3\pi$ and $|\bar{\dot{\delta}}_2|$ is the amplitude of $\dot{\delta}_2$.

A flow-chart, shown in Fig. 9.3 may be used to implement the method mentioned above for evaluation of the stability boundaries for the simplified model. Once the boundary is established, the actual motion can then be computed by directly integrating the nonlinear equations of motion for the chosen pair of wave height and frequency. It should be noted that the expression for heave motion, in

this case, is based on steady state conditions i.e. $\delta_3(t)$ is the particular solution of equation (9.1) assuming that the transient component of the heave motion has essentially decayed to zero.

9.4 Unstable Motion of the Simplified TLP :

In order to illustrate the method discussed in the foregoing, the stability boundaries are evaluated for the simplified TLP shown in Fig. 9.2 (the pertinent data of the platform is also included in the figure) using the algorithm given in Fig. 9.3. The hydrodynamic coefficients and the wave excitaion force are calculated with the program 'FREQ_DOMAIN' described in Chapter 8. Pretension and damping are known to play a significant roles in the occurence of such instabilities (see Rainey 1977, Yoneya and Yoshida 1982, Paulling 1982, Deb and Booton 1986a). To observe these effects, three different pretensions viz. 0.5×10^8 N, 1.0×10^8 N and 1.5×10^8 N are considered while the displacement is maintained constant at 45000 m^3. The resulting stability boundaries are presented in Fig. 9.4. It may be noted that as the pretension is increased the unstable zone moves closer towards wave frequencies. For a pretension of 1.0×10^8 N at 45000 m^3 displacement, damping is varied by varying C_{d2} and the effect on the stability boundary is shown in

Fig. 9.5. It can be seen that increase in damping results in shrinkage of the unstable zone.

Having identified the unstable zones, responses can now be found by directly integrating the nonlinear equations of motion. Fig. 9.6 shows a typical stable state in sway where δ_2, triggered by the initial conditions $\delta_2(0)=0$ and $\dot{\delta}_2(0)=1$ dies out with time while Fig. 9.7 shows the plot of a typical unstable motion for the same initial conditions where the motion grows with time. Fig. 9.8 is δ_2-$\dot{\delta}_2$ phase plane plot corresponding to the case in Fig. 9.6 and signifies asymptotic stability about the origin; Fig. 9.9 presents the phase plane plots for unstable motion for two different damping values (one of which correspond to the case in Fig. 9.7). It can be seen from this plot that eventhough the motion is unstable at the origin, owing to the dissipation of energy by the nonlinear damping term, it attains a 'limit cycle' where the bounds of the motion are heavily dependent on damping.

The effect of tether loss on the unstable zone is also studied by reducing the stiffness. Up to 25% loss of total stiffness is considered (corresponding to complete tether loss at any one corner), but no significant variation is noticed in the boundaries in the practical range of wave

height and frequencies. This may be attributed to the fact that while EA/L decreases, the heave motion $\delta_3(t)$ also increases thus keeping the product $(EA/L)\delta_3(t)$ more or less unaltered.

9.5 Unstable Motion of a Tension Leg Platform :

In the previous example only two degrees of freedom (viz. heave and sway) are considered. In general, a TLP would have more than one tension leg where the motion of the top of tether would alter the lateral stiffnesses rather than just the heave motion. If δ_i $(i = 1,2,\ldots,6)$ denote the translations and rotations about the OX_1, OX_2 and OX_3 axes respectively, then the motion of any jth tether top $z_j(t)$ can be described, under the first-order approximation, as a function of δ_3, δ_4 and δ_5 and the tether top coordinates. Furthermore, more than one lateral motion may exhibit insatbility and these degrees of freedom may be coupled. For example, in a particular case where the wave is progressing in the positive OX_1 direction and the unstable zone has to be investigated in sway and yaw, the procedure to be followed may be outlined as follows :

1. Choose the starting combination of wave frequency and wave height.

2. Form the general equations of motions as :-

$$[M]\{\ddot{\delta}\} + [C]\{\dot{\delta}\} + [K]\{\delta\} = \{F\} \qquad (9.9)$$

where,

[M] = Virtual mass matrix

[C] = Damping matrix

[K] = Hydrostatic + Mooring stiffness matrix with constant coefficients

$\{F\}$ = Wave excitation force vector

$\{\delta\}$ = Displacement vector $(\delta_1, \delta_2, \ldots, \delta_6)^T$

3. Solve eqution (9.9) to obtain steady state solution for $\{\delta\}$.

4. Construct the functions $z_j(t)$, $j = 1,2,\ldots,m$ where 'm' is the total number of tethers :

$$z_j(t) = \delta_3(t) - (r_{1j}-r_{G1})\delta_5(t) + (r_{2j}-r_{G2})\delta_4(t) \qquad (9.10)$$

where,

$\delta_i(t)$ = instantaneous displacement of CG in the ith degree of freedom

r_{1j}, r_{2j} = OX_1 and OX_2 coordinates of the jth tether top

r_{G1}, r_{G2} = OX_1 and OX_2 coordinates of CG

5. Construct the time dependent stiffness terms in sway and yaw as :

$$K_{sway}(t) = \sum_j [(EA/L^2)z_j(t)]_j \quad (9.11a)$$

$$K_{yaw}(t) = \sum_j [(EA/L^2)z_j(t)R^2]_j \quad (9.11b)$$

where, $R^2_j = (r_{1j}-r_{G1})^2 + (r_{2j}-r_{G2})^2$

6. Extract the corresponding rows and columns for sway and yaw from equations of motion in sway and yaw as :

$$[M]'\{\ddot{\delta}\}' + [C]'\{\dot{\delta}\}' + [[K]'+[K(t)]]\{\delta\}' = \{F\}' \quad (9.12)$$

where, [M]', [C]', [K]', {F}' are reduced matrices, $\{\delta\}' = (\delta_2, \delta_6)^T$ and [K(t)] is :-

$$\begin{bmatrix} K_{sway}(t) & 0 \\ 0 & K_{yaw}(t) \end{bmatrix}$$

Also note that $\{F\}' = (0, 0)^T$ in this case.

7. Rewrite equation (9.12) in the form of equation (9.5).

8. Check for instability of this system according to the method already described in section 9.3.

9. Choose next wave frequency and wave height combination.

10. Go back to step 2.

The stability boundary in sway and yaw for the example TLP (pertinent details given in Table 5.3) is computed and the unstable zone is shown in Fig. 9.10. It may be noted that in the example under consideration, because of symmetry, stability boundaries in surge and sway would be identical. For evaluation of the response, any nonlinear time domain analysis may be employed for a given combination of wave frequency, wave height and initial conditions.

9.6 Experimental Verification of Unstable Motion :

The occurrence of unstable motion for the example TLP is verified during the model scale experiment. The model, under the excitation of a regular planar wave 'critical frequency and height' (i.e. as may be found in the unstable zone indicated in Fig. 9.10), is given an initial perturbation in the likely unstable degree of freedom. If

the motion amplitude grows with time , the motion is regarded as unstable. With the available wave tank facility, only yaw instability could be verified. The combinations for which unstable yaw has been observed are indicated in Fig. 9.10. Difficulties existed in observing the unstable motion for a considerable length of time owing to contamination of the incident wave by the reflected waves.

Chapter 10

DISCUSSION AND CONCLUDING REMARKS

10.1 General :

The work completed in the course of the present study may be briefly summarised as follows :

(i) Review of statical stability concepts for floating bodies.

(ii) Review of theoretical and experimental work relating to TLP dynamics in intact and tether damage conditions.

(iii) Review of theoretical and experimental work relating to Mathieu type instability of TLPs.

(iv) Formulation and calculation of equilibrium tensions for a TLP with unequal stiffness of the tethers.

(v) Development of software for hydrostatic calculations.

(vi) Evaluation of statical stability of TLP in intact and damaged cases with the application of a new concept in stability assessment of floating structures.

(vii) Development of computer software for frequency

domain and nonlinear, large displacement time domain analysis of TLPs.

(viii) Deterministic and spectral analysis of TLP in frequency domain for intact and damaged configurations.

(ix) Deterministic time domain analysis of TLP in intact and damaged configurations to find steady state and transient responses.

(x) Development of algorithm based on Floquet theory for Mathieu type instability analysis and application of the same for TLPs.

(xi) Design and fabrication of a 1:100 scale model of an example TLP.

(xii) Experimental verification of the various responses predicted by the above theoretical models.

Under the prevailing constraints of time, facility and availabilty of input data, the effect of tether loss on the static and dynamic behaviour of a TLP has been studied. Eventhough the combinations of input parameters chosen for various analysis and experiments may at times appear hypothetical from the view point of a regular design procedure, an understanding of the following aspects has been substantiated :

(i) Capability and reliability of some of the popular

methods of static and dynamic analysis applicable to TLPs.

(ii) General trend of variations in static and dynamic behaviour of a TLP between intact and tether damage cases.

10.2 Observations :

The major observations that evolve out of the study conducted here may be identified as follows :

(i) The loss of tether at one corner decreases the static equilibrium tensions at the affected corner and the corner diagonally opposite to this corner while the tensions at the remaining corners increase. Even though the tension as a whole decreases at the affected corner, the tension per unit tether increases because after a certain amount of loss, a proportional number of tethers is considered to be inactive. It is seen that when a corner suffers 100% tether loss, the tethers in the opposite corner becomes slack, if no change in the buoyancy force and moments are considered. Even if the effects due to a change in buoyancy force and moments are included, the opposite tether would have such low static tension that it may be considered to be slack for all practical purposes.

(ii) Classical approaches of evaluation of statical stability are found inadequate in certain respects when

applied to unconventional structures such as TLPs. A new approach is therefore used to measure and compare the statical stability of the example TLP in various configurations. Absence of any guidance by the regulatory authorities regarding such calculations with particular application to TLPs is also noted.

(iii) Complete loss of tether at one corner causes drastic reduction in statical stability of TLP rendering its stability characteristics comparable to its free-floating configurations. An 'emergency disconnect' situation, which may be viewed as complete loss of tether at all corners is found to have a very low measure of statical stability. These analyses indicate that any manipulation of on-board weight distribution should be made with great caution after a substantial tether loss. Also, at large angles of heel, additional increase in tension are caused in the intact tethers due to increase in buoyancy.

(iv) Frequency domain analysis, even though inoapable of handling nonlinear effects and predicting the trend of responses correctly over the entire practical range of wave frequencies (note similar observations by Lyons et al., 1983), is found to be very convenient from the view point of parametric studies and spectral analysis.

(v) Time domain simulation, in spite of remarkably high consumption time, seems to model the TLP behaviour in a

better fashion. The formulations used to calculate hydrodynamic loadings, however, must be more accurate in order to better predict the responses.

(vi) In general, loss of tether at any corner causes both the motion and tension responses to increase. Surge motion is found to be rather insensitive to tether loss when the total pretension remains more or less constant. The increases, however, are a function of the amount and location of loss, wave frequency, height and heading. From the limited number of studies conducted here, it is seen that a total loss of tether at any corner is likely to induce snap loads at one or more corners which may be as high as four to five times the normal static pretension in the tethers (note similar observations by Sekita and Sakai, 1984). At smaller levels of tether loss, even though the chances of snap loads are reduced, the tension in the remaining tethers in the affected corner may increase significantly thus increasing the chances of further failure at that corner.

(vii) For the cases studied, a loss of tether at any corner occurring at the peak of tension variation at that corner is seen to cause the highest transient tension responses in the remaining intact tethers. Also, a quartering sea is found to induce higher tension loads as compared to a head sea.

(viii) Cross motions are set up whenever the tether loss introduces asymmetric distribution of stiffness with respect to the direction of wave propagation.

(ix) The regime of Mathieu type instability of TLP is heavily dependent upon the lateral stiffness and damping of the system rather than the axial stiffness of the tethers; even a 25% loss of total axial stiffness does not alter the unstable zones significantly.

Since neither the chosen TLP nor the input parametrs for the various case studies correspond to any particular established design, more precise remarks about the damaged responses of a TLP are not attempted. The need and relevance of such a study, however, is recognised.

8.3 Recommendations :

As a logical consequence of this study, the following may be recommended for future research :

(i) Calculations may be performed with better theoretical models for evaluation of hydrodynamic loadings.

(ii) Similar studies may be conducted with coupled tether dynamics.

(iii) The effect of forces due to wind, current,

second order wave loadings etc. may be investigated.

(iv) Similar analysis and experimentation may be carried out in conjuction with flooding damage in the columns.

(v) Further experimentation may be concducted with more sophisticated instrumentation and calibrated models so that even small variation in responses can be identified more accurately and reliably.

(vi) Research may be conducted to find a better way to present data from analyses such that they can be directly and conveniently used for design purposes.

REFERENCES

Agarwal, V.K. and Spanos, P-T. D., "Significance of wave kinematics in the dynamics of a tension leg platform", Proc. of the 4th Intl. Symp. on Offshore Engineering at COPPE, Brazil, 1983, pp. 154-162.

Albrecht, H.G., Konig, D. and Kokkinowrachos, K., "Nonlinear dynamic analysis of tension leg platforms for medium and greater depths", Offshore Technology Conference, paper # 3044, Houston 1978, pp. 7-12.

Ashford, R.A. and Wood, W.L., "Numerical integration of the motions of a tethered buoyant platform", Intl. J. of Numerical Methods in Engineering, 13, 1978, pp. 165-180.

Bhattacharya, R., "Dynamics of marine vehicles", Willey, New York, 1978.

Bolding, V.E., "Design aspects of tension mooring elements for tension moored platforms", Proc. of the 2nd Intl. OMAE Symp., Houston, 1983, pp. 38-45.

Booton, M., Joglekar, N. and Deb, M.K., "Effect of tether loss on tension leg platform dynamics", Proc of the Intl. OMAE Symp., Tokyo, 1986.

Burke, B.G., "The analysis of motions of semisubmersible drilling vessels in waves", Offshore Technology Conference, paper # 1024, Houston, 1969, pp. 235-245.

Burke, B.G. and Tighe, J.T., "A time series model for dynamic behaviour of offshore structures", Offshore Technology Conference, paper # 1403, Houston, 1971.

Burns, G.E., "Calculating viscous drift of a tension leg platform", Proc. 2nd Intl. OMAE Symp., Houston, 1983, pp. 22-30.

Capanoglu, C., "Tension-leg platform design : Interaction of naval architectural and structural design considerations", Marine Technology, Vol. 16, No. 4, October 1979, pp. 343-352.

Chakraverti, S.K., Tam, W.A. and Wolbert, A.L., "Wave forces on a randomly oriented tube", Offshore Technology Conference, paper # 2190, Houston, 1975, pp. 433-446.

Chou, F.S.F., Ghosh, S. and Kypke, D.A., "Analytical approach to the design of a tension leg platform", Offshore Technology Conference, paper # 3883, Houston, 1980, pp. 287-296.

Chou, F.S.F., Ghosh, S. and Huang, E.W., "Conceptual design process of a tension leg platform", Trans. SNAME, Vol. 91, 1983, pp. 275-305.

Conceicao, C.A.L. and Neves, M.A.S., "Dynamic stability of tension leg platforms in waves", Proc. of the 4th Intl. Symp. on ohhshore engineering held at COPPE, Brazil, 1983, pp. 251-270.

de Boom, W.C., Pinkster, J.A. and Tan, S.G., "Motion and tether force prediction for a deep water tension leg platform", Offshore technology Conference, paper # 4487, Houston, 1983, pp. 377-388.

Deb, M.K. and Booton, M., "On the investigation of dynamic instabilities of compliant floating structures", Pacific Congress on Marine Technology, Honolulu, 1986, OST6/1.

Deb, M.K. and Booton, M., "Unstable motions of a tension leg platform", OSDS, Oregon, 1986, pp. 331-345.

Deb, M.K. and Deb, A., "The matrix method - a powerful technique in dimensional analysis", J. of Franklin Inst., Vol. 321, No. 4, 1986, pp. 233-240.

Denise, J.P.F. and Heaf, N.J., "A comparison between linear and nonlinear response of a proposed tension leg platform", Offshore Technology conference, paper # 3555, Houston, 1979, pp. 1743-1754.

Dillingham, J.T., "Recent experience in model-scale simulation of tension leg platforms", Marine Technology, April 1984, pp. 186-200.

Dunn, F.P., "Outer continental shelf frontier technology", Marine Board, Proc. National Academy of Science Symposium, 1979, pp. 27.

Dunsire, R. and Owen, D.G., "Model testing of TLP systems", Third Intl. OMAE Symp., New Orleans, February 1984, pp. 20-31.

Ellers, F.S., "Advanced offshore oil platforms", Scientific American, Vol. 246, No. 4, April 1982.

Ellis, N., "Hutton tension leg platform structural design and configuration", OSDS, Oregon, 1982, pp. 509-530.

Faltinsen, O.I. and Michelson, F.C., "Motions of large structures in waves at zero Froude No.", Proc. of the Symp. on Dynamics of Marine Vehicles and Structures in Waves, London, 1974, pp. 91-106.

Faltinsen, O.I., Fylling, I.J., Hooff, R.W.V. and Teigen, P.S., "Theoretical and experimental investigations of tension leg platform behaviour", Intl. Conf. on Behaviour of Offshore Structures, 1982, pp. 411-423.

Faulkner, D., Birrell, N.D. and and Stiansen, S.G., "Development of a reliability-based design code for the structure of tension leg platform", Offshore Technology Conference, paper # 4648, Houston, 1983, pp. 575-586.

Garrison, C.J., "Dynamic response of floating bodies", Offfshore Technology Conference, paper # 2067, Houston, 1979.

Garrison, C.J., "Forces on semi-submerged structures", OSDS, Oregon, 1982, pp. 28-64.

Gie, T.S. and de Boom, W.C., "The wave induced motions of a tension leg platform in deep water", Offshore Technology Conference, paper # 4074, Houston, 1981, pp. 89-107.

Godfrey, P.S., "Compliant drilling and production platforms", Proc. of the Conf. on Design and Construction of Offshore Structures, Inst. of Civil engineers, London, 1976, pp. 161-175.

Haritos, N., "Modelling the response of tension-leg platforms to the effects of wind using simulated tracks", Mathematics and Computers in Simulation, Trans. IMACS, April 1985, Vol. 27, No. 2 and 3, pp. 231-240.

Hong, S.T., "Tension in a taut mooring line; frequency domain analysis", Offshore Technology Conference, paper # 2069, Houston, 1974, pp. 389-400.

Hooft, J.P., "A mathematical method of determining hydrodynamically induced forces on a semisubmersible",

Trans., Society of Naval Architects and Marine Engineers, 1971, pp. 28-70.

Hudspeth, R.T. and Leonard, J.W., "Dynamic wave-platform-restraint interaction for tension leg platforms", OSDS, Oregon, 1982, pp. 604-631.

Jefferys, E.R. and Patel, M.H., "Dynamic analysis models of tension leg platforms", J. of Energy Resources Technology, September 1982, Vol. 104, pp. 217-223.

IMSL, "IMSL Reference Manual", Houston, 1984.

Kareem, A. and Dalton, C., "Dynamic effects of wind on tension leg platforms", OSDS, Oregon, 1982, pp. 563-585.

Karsan, D.I. and Manglavacchi, A., "Tension leg platform state of the art and future research and development requirements", OSDS, Oregon, 1982, pp. 547-562.

Kim, C.H. and Chou, F., "Motions of a semisubmersible drilling platform in head seas", Marine Technology, April 1973, pp. 112-123.

Kirk, C.L. and Etok, E.U., "Dynamic response of tethered production platform", BOSS, London, 1979, pp. 139-163.

Leipholtz, H., "Stability Theory", Academic Press, NY, 1970.

Little, L., "Hardware and software modifications to equipment at MUN wave tank", Memorial University of Newfoundland, St. John's, Canada, 1985.

Liu, D., Chen, Y-N, Shin, Y.S. and Chen, P.C., "Integrated computational procedure for hydrodynamic loads and structural response of a tension leg platform", Winter Annual Meeting of ASME, Chicago, November 1980, pp. 87-100.

Lyons, G.J., Patel, M.H. and Sarohia, S., "Theory and model test data for tether forces on tension buoyant platforms", Offshore Technology Conference, paper # 4643, Houston, 1983, pp. 533-550.

Martinovich, W.M. and Praught, M.W., "Stability requirements of semisubmersibles - a designer's viewpoint", Intl. Conf. on Stationing and Stability of Semisubmersibles, Glasgow, U.K., 1986.

McDuff, J.N. and Curreri, J.R., "Vibration Control", McGraw-Hill Book Co., Toronto, 1958.

McIver, D.B., "The static offset in waves of tension leg platforms", Offshore Technology Conference, paper # 4070, Houston, 1981, pp. 33-44.

Mercier, J.A., Leverette, S.J. and Bilault, A.L., "Evaluation of Hutton TLP response to environmental loads", Offshore Technology Conference, paper # 4429, Houston, 1982, pp. 585-601.

Morison, J.R., O'Brien, M.P., Johnson, J.W. and Scharf, S.A., "The force exerted by surface waves on piles", Petroleum Trans., AIME, 189, 1950, pp. 585-601.

Morgan, J.R. and Malaeb, D., "Dynamic Analysis of tension leg platforms", Proc. 2nd Intl. OMAE Symp., Houston, 1983, pp. 31-37.

Muggeridge, D.B. and Murray, J.J., "Calibration of a 58 m wave flume", Canadian J. of Civil Eng., Vol. 8, No. 4, 1981, pp. 449-455.

Natvig, B.J. and Pendered, J.W., "Motion response of floating structures to regular waves", Proc. of the Intl. Symp. on Offshore Structures held at COPPE, Brazil, October 1979, pp. 2.151-2.173.

Patel, M.H. and Jefferys, E.R., "Dynamics of the tensioned buoyant platform", Intl. Symp. on Hydrodynamics in Ocean Engineering, The Norwegian Inst. of Technology, 1981, pp. 923-944.

Patel, M.H. and Lynch, E.J., "Coupled dynamics of tensioned buoyant platforms and mooring tethers", Engineering Structures, Vol. 5, October 1983, pp. 299-308.

Patel, M.H. and Witz, J.A., "On improvements to the design of tensioned buoyant platforms", BOSS, Amsterdam, 1985, pp. 563-575.

Perrett, G.R. and Webb, R.M., "Tethered buoyant platform production system", Offshore Technology Conference, paper # 3881, Houston, 1980, pp. 261-273.

Paulling, J.R. and Horton, E.E., "Analysis of the tension leg stable platform", Offshore Technology Conference, paper # 1263, Houston, 1970, pp. 379-390.

Paulling, J.R., "Time domain simulation of semisubmersible platform motion with application to the tension leg platform", Spring Meeting/ STAR Symp., SNAME, San Fransisco, 1977, pp. 303-314.

Paulling, J.R., "The sensitivity of predicted loads and responses of floating platforms to computational methods", Proc. of 2nd Intl. Symp. on Intgrity of Offshore Structures Glasgow, July 1981, pp. 51-69.

Paulling, J.R., "Mathieu instabilities in TLP response", OSDS, Oregon, 1982, pp. 586-603.

Paulling, J.R., "Hydrodynamic Synthesis of Marine Structures", Theoretical and Apllied Mechanics, Elsevier Science Publishers B.V., North-Holland, 1985, pp. 275-291.

Paulling, J.R. and Webster, W.C., "A consistent large amplitude analysis of the coupled response of a TLP and tendon system", OMAE Symp., Tokyo, 1986, pp. 126-133.

Pawlowski, J.S., "Elements of kinematics and dynamics of the rigid body in Cartesian tensor notation", NRC, Canada, Report # MTB 160, January 1985.

Pawlowski, J.S., "A new procedure for assessing stability of floating structures", IMD, NRCC, Report No. MTB-158, January 1985.

Pawlowski, J.S. and Deb, M.K., "A new procedure for assessment of stability of floating structures", Intl. Conf. on Stationing and Stability of Semisubmersibles, Glasgow, U.K., 1986.

Rainey, R.C.T., "The dynamics of tethered platforms", RINA, 1977, pp. 59-80.

Richardson, J.R., "Mathieu instabilities and response of compliant offshore structures", NMI R49, February 1979.

Roren, E.M.Q. and Steinsvik, B., "Deep water resonance problems in the mooring system of the tethered platform", Proc. of the Intl. Conference on Offshore Structures Engineering held at COPPE, Brazil, September 1977, pp. 135-149.

Rowe, S.J., Fletcher, R.H. and Hedley, C., "The model testing of a tethered buoyant platform and its riser system", NMI R47, May 1979.

Rowe, S.J. and Jackson, G.E., "An experimental investigation of Mathieu instabilities on tetherd buoyant platform models", NMI R73, January 1980.

Sarpakaya, T. and Issacson, M., "Mechanics of wave forces and offshore structures", Van Nostrand Reinhold Company, New York, 1981.

Schamaun, P. and Sannum, H., "Tension leg platforms - a state of the art review", The Naval Architect, April 1985, pp. 166-168.

Sebastiani G., Brandy, R. and Tassini, P., "Theoretical-experimental behaviour of TLP for very deep waters", Proc. 2nd Intl. OMAE Symp., Houston, 1983, pp. 1-14.

Sebastini, G., Della Greca, A. and Bucaneve, G., "Characteristics and dynamic behaviour of Tecnomare's tension leg platform", Intl. Symp. on Hydrodynamics in Ocean Engineering, The Norwegian Inst. of Technology, 1981, pp. 947-961.

Sekita, K. and Sakai, M., "Model tests to establish a design method for TLP-tether", Offshore Technology Conference, paper # 4653, Houston, 1984, pp. 51-56.

Sharp, J.J., "Hydraulic modelling", Butterworths, London, 1981.

Spanos, P.D. and Agarwal V.K., "Response of a simple tension leg platform model to wave forces calculated at displaced position", J. of Energy Resources Technology, December 1984, Vol. 106, pp. 437-443.

Sphaier, S.H., Wrobel, L.C., Esparanca, P.T.T., Vasconcellos, J. M.A., Batista, R.C. and Masetti, I.Q., "Hydrodynamic analysis of deep water platforms using the INPLA system", Proc. of the 4th Intl. Symp. on Offshore Engineering held at COPPE, Brazil, September 1983, pp. 348-377.

Standing, R.G., "Use of diffraction theory with Morison's equation to compute wave loads and motions of offshore structures", NMI-R74, National Maritime Institute, U.K., 1979.

Stiansen, S.G. and Chen, H.H., "Computaional methods for predicting motions and dynamic loads of tension-leg

platform", Proc. of the 2nd Intl. Symp. on Integrity of Offshore Structures, Glasgow, July 1981, pp. 1-18.

Stone, B.M., "An experimental study of the motion response in regular waves of a semisubmersible under damage conditions", M. Eng. Thesis, Memorial University, St. John's, Canada, 1986.

Tein, Y., Chianis, J.W., Teymourian J. and Chou, F.S.F., "An integrated motion and structural analysis for tension leg platforms", Offshore Technology Conference, paper # 4072, Houston, 1981, pp. 55-74.

Teigen, P.S., "The response of a TLP in short-crested waves", Offshore Technology Conference, paper # 4642, Houston, 1983, pp. 525-532.

Vandiver, J.K., "Direct wave force measurements on a model tension leg platform", OSDS, Oregon, 1982, pp. 531-546.

Yoneya, T. and Yoshida, K., "The dynamics of tension leg platform in waves", J. of Energy Resources Technology, March 1982, Vol. 104, pp. 20-28.

TABLES

Table 1.1 : Comparison of some key features of Hutton TLP with other alternatives

	STATFJORD B	MAGNUS	HUTTON	BLOCK 330 (MISSISSIPPI CANYON)
LOCATION	NORTH SEA (NORWAY)	NORTH SEA (U.K.)	NORTH SEA (U.K.)	GULF OF MEXICO (U.S.)
STRUCTURE	CONCRETE GRAVITY	STEEL JACKET AND PILING	TENSION LEG	GUYED TOWER
TYPE	FIXED	FIXED	COMPLIANT	COMPLIANT
WATER DEPTH (FEET)	472	611	485	1,000
100-YEAR WAVE (FEET)	100	102	98	72
PRODUCTION (BARRELS PER DAY)	150,000	120,000	110,000	25,000
INITIAL PRODUCTION (YEAR)	1982	1983	1984	1984
MAXIMUM DECK OFFSET (FEET)	<3	4	79	39
APPROXIMATE TOTAL COST (BILLIONS)	$1 8	$2 6	$1 3	$ 8
COST PER BARREL-DAY	$12,000	$21,700	$11,800	$32,000
PROJECT MANAGEMENT	MOBIL	BRITISH PETROLEUM	CONOCO	EXXON

Table 2.1 Key Particulars of Hutton TLP
(ref. Ellis et al., 1982)

LENGTH	:	Between Column Centres	78.00 m
	:	Overall	95.70 m
BREADTH	:	Between Column Centres	74.00 m
	:	Overall	91.70 m
HEIGHT	:	Keel to Main Deck	57.70 m
	:	Main Deck to Weather Deck	11.25 m
DRAUGHT	:	Operating	32.00 m L.A.T.
FREEBOARD	:	To Bottom of Weather Deck	24.50 m L.A.T.
WATERPLANE	:	Area	1324.00 m^2
COLUMNS	:	4 Corners	17.70 m Dia
	:	2 Centres	14.50 m Dia
PONTOONS	:	Height	10.80 m
	:	Width	8.00 m
	:	Corner Radius	1.50 m
DISPLACEMENT	:	Approx.	61500 Tonne
TOTAL WEIGHT	:	With Riser Tension (Approx.)	48500 Tonne

Table 3.1 Key Plan of Major Research Activities

THEORETICAL	EXPERIMENTAL
General :	General :
T.1. Literature review.	E.1. Design and fabricate a 1:100 scale model of TLP. E.2. Determine the mass/inertia properties of the model. E.3. Design and fabricate the mooring system. E.4. Set up test arrangements, instrumentations and data recording systems.
Statics :	Statics :
T.2. Hydrostatics of floating bodies - formulation and development of computer software. T.3. Choose intact and tether damage configurations and evaluate stability characteristics.	E.5. Experimental verification of results obtained through computer software.
Dynamics : a) Frequency domain :	Dynamics : a) Frequency Domain :
T.4. Frequency domain analysis - formulation and development of computer software T.5. Calculate motion and tension RAOs in intact and tether damage cases. T.6. Perform spectral analysis for intact and damage cases.	E.6. Conduct tests in intact and damage conditions in regular waves and irregular waves. E.7. Compute motion and tension RAOs from regular wave tests and compare with T.5. E.8. Compare response spectra in intact and damage cases with T.6.
b) Time domain :	b) Time domain :
T.7. Time domain simulation - formulation and development of computer software. T.8. Evaluate resopnses in intact and damage cases in regular wave. T.9. Note transient responses immediately follwing tether damage	E.9. Compare a few specific time records from regular wave tests with T.8. E.10. Simulate sudden loss of tether - observe the transients and compare with T.9.
Special Study :	Special Study :
T.10. Mathieu type instability - formulate and develop computer software; evaluate unstable zones and study effect of tether loss on such instabilities.	E.11. Observe if unstable motion develops from an initial perturbation at critical combinations of wave height and frequency - compare the observations with T.10.

Table 5.1 List of Relevant Parameters and Dimensionless Numbers

Parameters	Symbols	Dimensions in L,T & M
Hull Subsystem :		
Length	L	L
Characteristic Length	l	L
Lumped Mass	M	M
Lumped Mass Moment of Inertia	I_{jj}	ML^2
Tether Subsystem :		
Axial Stiffness	k	MT^{-2}
Tether length	L_T	L
Wave Subsystem :		
Density	ρ_w	ML^{-3}
Viscosity	μ	$ML^{-1}T^{-1}$
Acceleration due to Gravity	g	LT^{-2}
Water Depth	D	L
Wave Height	H	L
Wave Period	T	T
General :		
Typical Time	t	T
Typical linear displacements	d	L
Typical Angular Displacements	θ	-
Typical Linear Velocity	V	LT^{-1}
Typical Angular Velocity	ω	T^{-1}
Typical Linear Acceleration	a	LT^{-2}
Typical Angular Acceleration	α	T^{-2}
Typical Force or Reaction	F	MLT^{-2}

Note : Acceleration due to gravity is to remain the same in model and prototype.

Dimensionless Numbers
l/L, $M/(\rho_w L^3)$, $I/(\rho_w L^5)$, $k/(\rho_w g L^2)$, L_T/L, $\mu/(\rho_w g^{1/2} L^{3/2})$, D/L, H/L, $(Tg^{1/2})/L^{1/2}$, $(tg^{1/2})/L^{1/2}$, d/L, θ, $V/(g^{1/2}L^{1/2})$, $(\omega g^{1/2})/L^{1/2}$, a/g, $(\alpha L)/g$, $F/(\rho_w g L^3)$

Table 5.2 Some Scaling Relations

Geometric Scale Factor = L_p/L_m = r (say)		
Characteristic Length Scale	l_p/l_m	r
Mass Scale	M_p/M_m	r^3 *
Mass Moment of Inertia Scale	I_p/I_m	r^5 *
Tether Axial Stiffness Scale	k_p/k_p	r^2 *
Tether Length Scale	L_{Tp}/L_{Tm}	r
Water Depth Scale	D_p/D_m	r
Wave Height Scale	H_p/H_m	r
Wave Period Scale	T_p/T_m	$r^{1/2}$
Typical Time Scale	t_p/t_m	$r^{1/2}$
Typical Linear Displacement Scale	d_p/d_m	r
Typical Angular Displacement Scale	θ_p/θ_m	1
Typical Linear Velocity Scale	V_p/V_m	$r^{1/2}$
Typical Angular Velocity Scale	ω_p/ω_m	$r^{1/2}$
Typical Linear Accln. Scale	a_p/a_m	1
Typical Angular Accln. Scale	α_p/α_m	1/r
Typical Force or Reaction Scale	F_p/F_m	r^3 *

Notes :

1. Suffices 'p' and 'm' indicate that of the prototype and that of the model, respectively.

2. '*' indicates that in case prototype and model water densities are different then the scaling ratio has to be multiplied by 'ρ_{wp}/ρ_{wm}'.

Table 5.3 Key Particulars of Example TLP

LENGTH	:	Between Column Centres	70.00 m
BREADTH	:	Between Column Centres	70.00 m
HEIGHT	:	Upto Weather Dk.	65.00 m
COLUMNS	:	4 Corners	15.24 m Dia
	:	4 Centres	10.16 m Dia
PONTOONS	:	4 Numbers	10.16 m Dia
DRAUGHT	:	Operating	35.00 m
VCG	:	Operating	38.00 m
TOTAL DISPL.	:	Operating	49680 Tonnes
TOTAL WEIGHT	:	Operating	35000 Tonnes
TOTAL STATIC PRETENSION	:	Operating	14680 Tonnes
TETHER AXIAL STIFFNESS	:	Per Corner	$7.6 * 10^7$ N/m
RADIUS OF GYRATION	:	R_{11}	36.00 m
	:	R_{22}	36.00 m
	:	R_{33}	41.20 m
NATURAL PERIODS	:	Surge	51.61 sec
	:	Sway	51.61 sec
	:	Heave	2.76 sec
	:	Roll	2.98 sec
	:	Pitch	2.98 sec
	:	Yaw	43.90 sec

Table 7.1 Key Information for Stability Assessment of the Example TLP

Cases	Draft (m)	Displ. (T)	VCG *(m)*	ϕ (°)
Case # 1 : Operational Draught with 100% tether loss at corner # 1	35.0	49680	38.0	31.0
Case # 2 : Emergency disconnect	21.0	35000	38.0	40.0
Case # 3 : Post-mating	29.5	44000	33.0	35.0

* VCGs are measured from the base of the hull upwards.

Note : 1. The force due to wind F_w is calculated as (ref Bureau Veritas, 1975) :

$$F_w = \sum dF_w = \sum C_w \rho_{wind} V^2_{wind} dA_p$$

where, ρ_{wind} = Mass density of air

V_{wind} = Wind velocity

C_w = A coefficient

dA_p = Elemental area perp. to wind

2. Moment due to wind is calculated as :

$M_{wind} = F_{wind} h_{wind}$,

where, h_{wind} is the distance between the point of action of wind force and the point of rotation.

Table 8.1 Comparison of Theoretical and Experimental Significant (1/3 rd Highest) Tension Double Amplitudes

'PM Spectrum : Classical Form' Wind Speed = 20 m/sec				
Wave Heading = 0 Degrees				
Tension in $*10^7$ N :	# 1	# 2	# 3	# 4
Intact Case :				
Theoretical Spectrum	1.079	1.075	1.075	1.079
Experimental Spectrum	1.053	1.267	1.274	1.164
Time Record	1.261	1.275	1.307	1.180
50% Loss at # 1 :				
Theoretical Spectrum	0.808	1.083	1.106	1.325
Experimental Spectrum	1.029	1.320	1.296	1.649
Time Record	1.100	1.432	1.372	1.703
Wave Heading = 45 Degrees				
Intact Case :				
Theoretical Spectrum	1.467	0.649	1.684	0.649
Experimental Spectrum	1.332	0.584	2.101	0.712
Time Record	1.476	0.642	2.121	0.787
50% Loss at # 1 :				
Theoretical Spectrum	1.096	0.764	1.709	0.764
Experimental Spectrum	1.175	0.679	2.355	0.835
Time Record	1.278	0.776	2.581	0.912

Table 8.2a Comparison of Theory and Experiment for Tensions in Intact and Damaged Conditions

Wave Height = 20.0 m, Period = 21.9 sec, Heading = 0°				
Tension $*10^7$ N	# 1	# 2	# 3	# 4
Intact Case :				
A1 :				
'TIME_DOMAIN'	1.936	1.969	1.969	1.936
Experiment	2.352	2.366	2.382	2.502
'FREQ_DOMAIN'	2.270	2.211	2.211	2.270
50% Loss at # 1:				
A2 :				
'TIME_DOMAIN'	4.688	5.678	4.484	5.993
Experiment	4.701	5.998	5.006	6.053
'FREQ_DOMAIN'	-	-	-	-
A3 :				
'TIME_DOMAIN'	1.399	2.770	1.629	2.812
Experiment	0.903	2.195	1.505	2.412
'FREQ_DOMAIN'	-	-	-	-
A4 :				
'TIME_DOMAIN'	1.622	2.639	1.589	2.817
Experiment	1.954	2.807	2.219	3.087
'FREQ_DOMAIN'	1.488	2.272	2.178	2.723
100% Loss at # 1:				
A2 :				
'TIME_DOMAIN'	0.0	10.293	5.534	11.001
Experiment	0.0	10.766	6.136	11.074
'FREQ_DOMAIN'	-	-	-	-
A3 :				
'TIME_DOMAIN'	0.0	2.712	0.0	2.922
Experiment	0.0	3.445	0.0	2.574
'FREQ_DOMAIN'	-	-	-	-
A4 :				
'TIME_DOMAIN'	0.0	5.283	3.231*	5.246
Experiment	0.0	5.469	3.656*	5.437
'FREQ_DOMAIN'	-	-	-	-

'*' : Indicates snap load

Table 8.2b Comparison of Theory and Experiment for Tensions in Intact and Damaged Conditions

Wave Height = 20.0 m, Period = 21.9 sec, Heading = 45°				
Tension $*10^7$ N	# 1	# 2	# 3	# 4
Intact Case :				
A1 :				
'TIME_DOMAIN'	1.819	1.627	1.963	1.627
Experiment	2.289	2.598	2.980	2.662
'FREQ_DOMAIN'	2.778	1.203	2.712	1.203
50% Loss at # 1:				
A2 :				
'TIME_DOMAIN'	4.685	5.987	4.926	5.987
Experiment	4.669	5.184	5.124	6.293
'FREQ_DOMAIN'	-	-	-	-
A3 :				
'TIME_DOMAIN'	1.442	2.641	1.528	2.641
Experiment	1.528	2.203	1.417	2.105
'FREQ_DOMAIN'	-	-	-	-
A4 :				
'TIME_DOMAIN'	1.506	1.976	1.937	1.976
Experiment	1.961	3.269	3.206	3.325
'FREQ_DOMAIN'	1.813	1.569	2.715	1.569
100% Loss at # 1:				
A2 :				
'TIME_DOMAIN'	0.0	10.750	4.912	11.755
Experiment	0.0	11.128	6.889	11.077
'FREQ_DOMAIN'	-	-	-	-
A3 :				
'TIME_DOMAIN'	0.0	2.014	0.0	2.014
Experiment	0.0	2.161	0.0	2.199
'FREQ_DOMAIN'	-	-	-	-
A4 :				
'TIME_DOMAIN'	0.0	5.158	5.199*	5.158
Experiment	0.0	5.973	6.944*	6.319
'FREQ_DOMAIN'	-	-	-	-

'*' : Indicates snap load

Table 8.3 Computed Tension Responses for the Example TLP by 'TIME_DOMAIN'

Wave Height = 20.0 m, Period = 12.0 sec				
100 % Loss at Corner # 1				
Wave Heading = 0 Degrees				
Tension $*10^7$ N	# 1	# 2	# 3	# 4
A1	1.915	2.289	2.289	1.915
A2	0.0	12.355	9.328	13.456
A3	0.0	0.09	0.0	0.568
A4	0.0	6.289*	11.833*	16.431*
Wave Heading = 45 Degrees				
A1	2.097	1.214	2.458	1.214
A2	0.0	18.269	14.928	18.269
A3	0.0	0.0	0.0	0.0
A4	0.0	20.114*	15.182*	20.189*

'*' : Indicates snap load

FIGURES

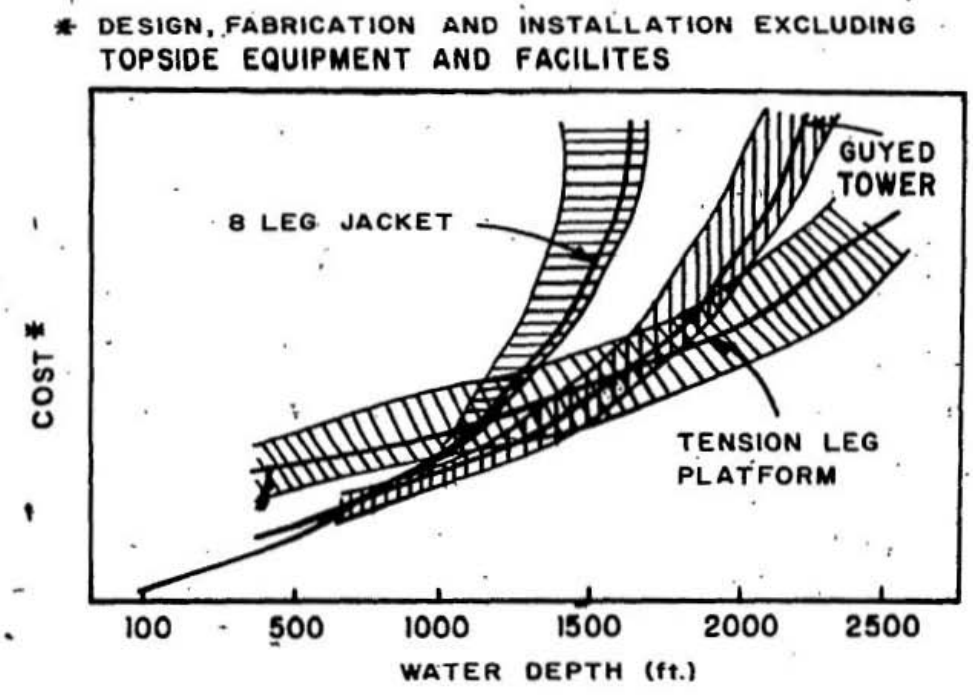

FIG. 1.1 COST COMPARISON OF TLP WITH JACKET STRUCTURES

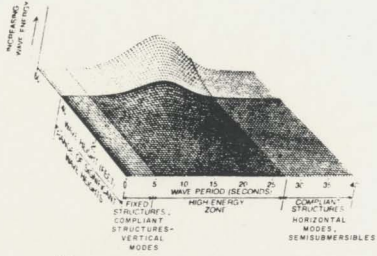

(A)

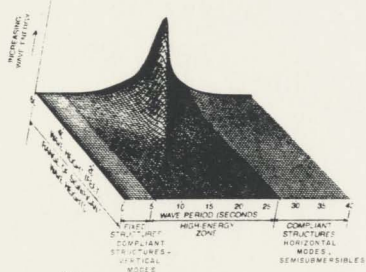

(B)

FIG. 1.2 TYPICAL TLP NATURAL PERIODS AGAINST
(A) GULF OF MEXICO SEA SPECTRUM AND
(B) NORTH SEA SPECTRUM

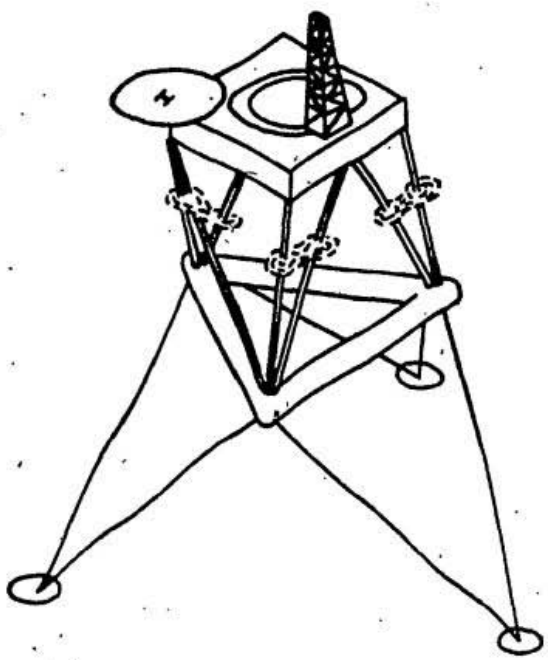

FIG. 1.3 'TRITON' : THE FIRST TLP

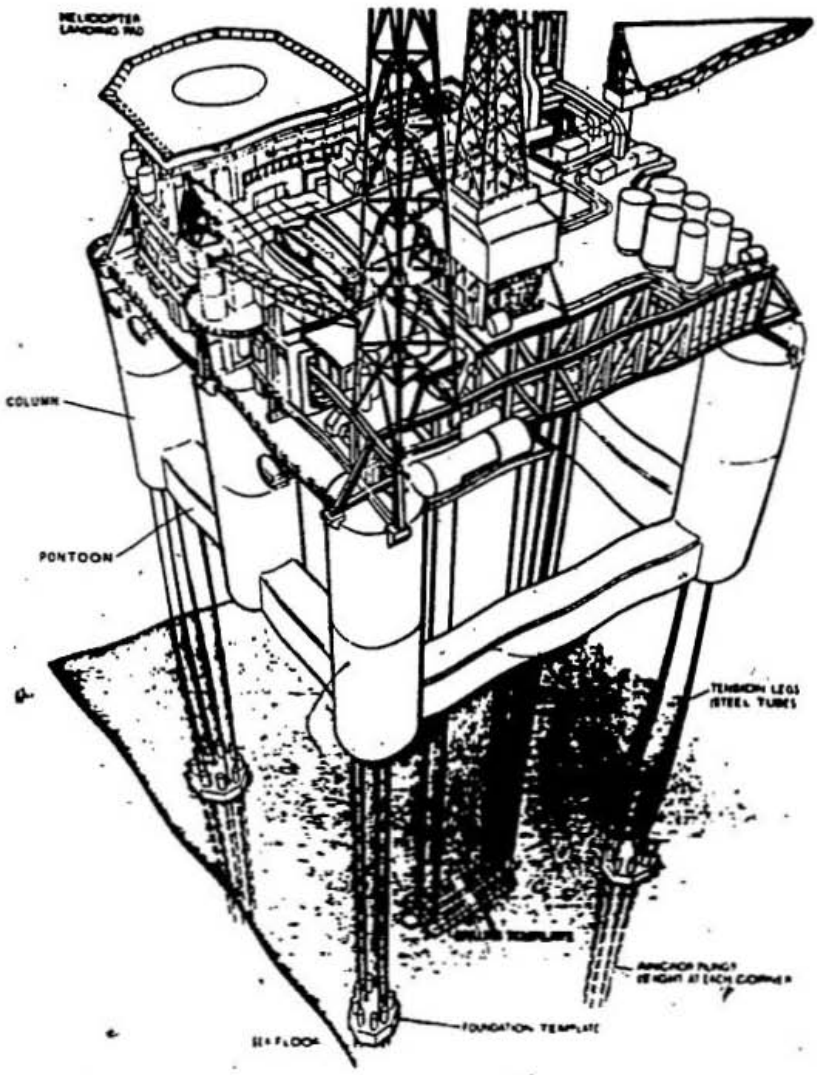

FIG. 2.1 A PERSPECTIVE OF THE HUTTON TLP

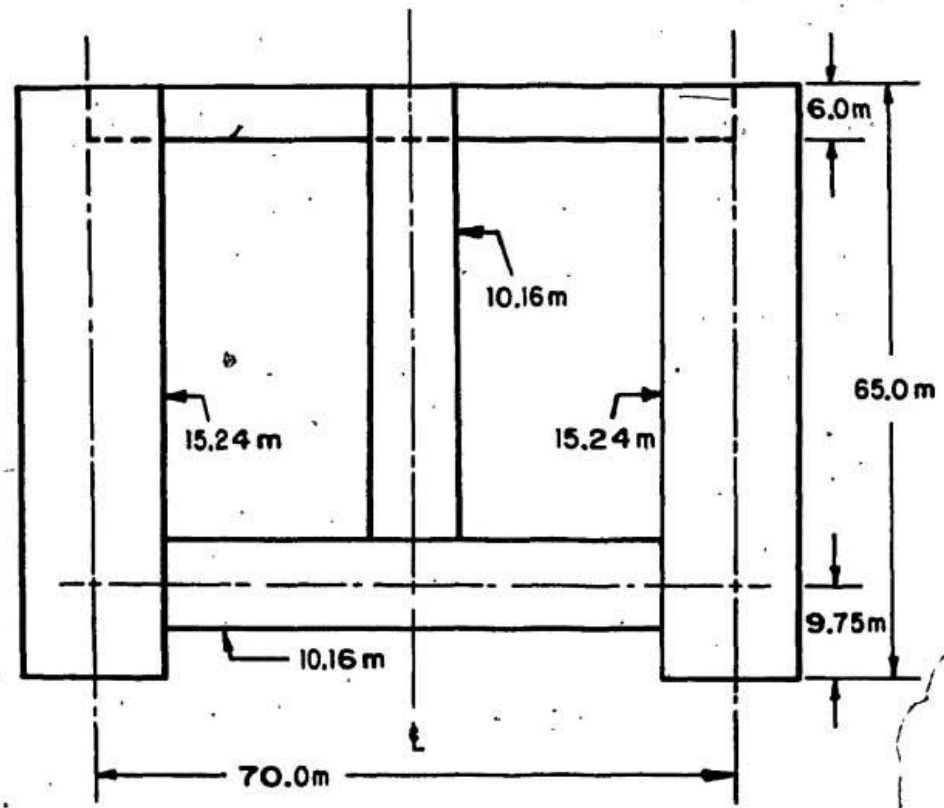

FIG. 5.1A MAIN DIMENSIONS OF THE 'EXAMPLE TLP' : ELEVATION

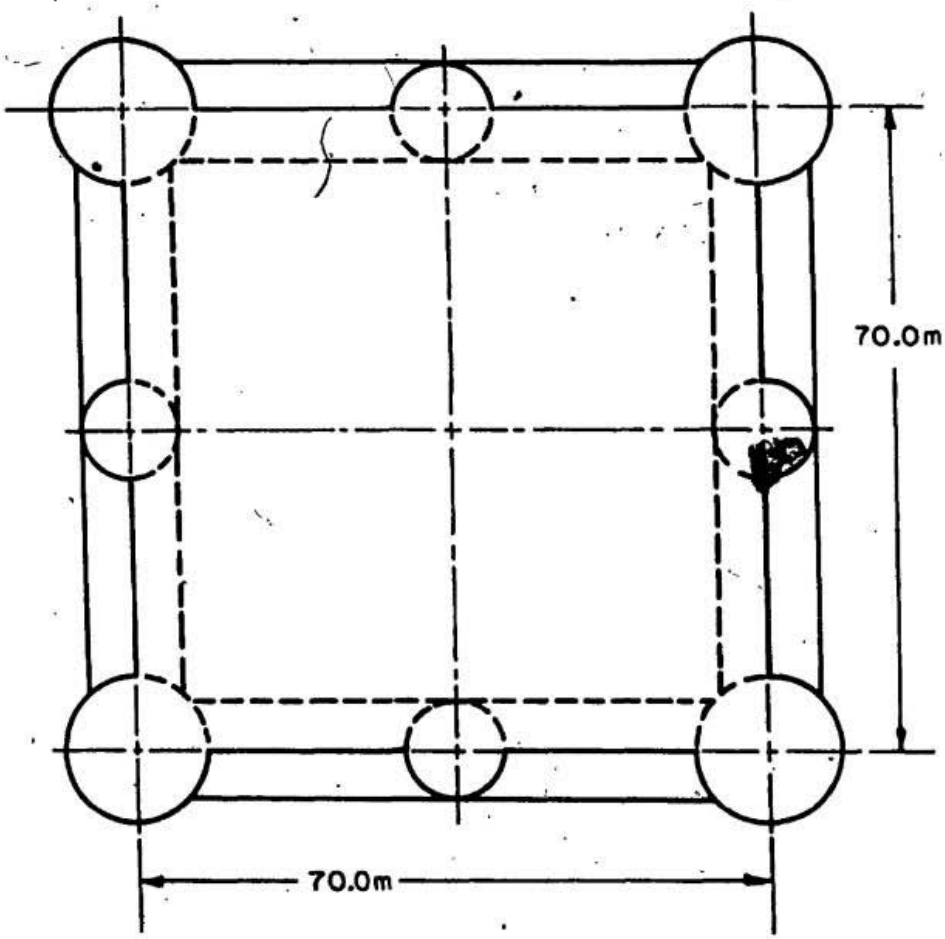

FIG. 5.1B MAIN DIMENSIONS OF THE 'EXAMPLE TLP' : PLAN

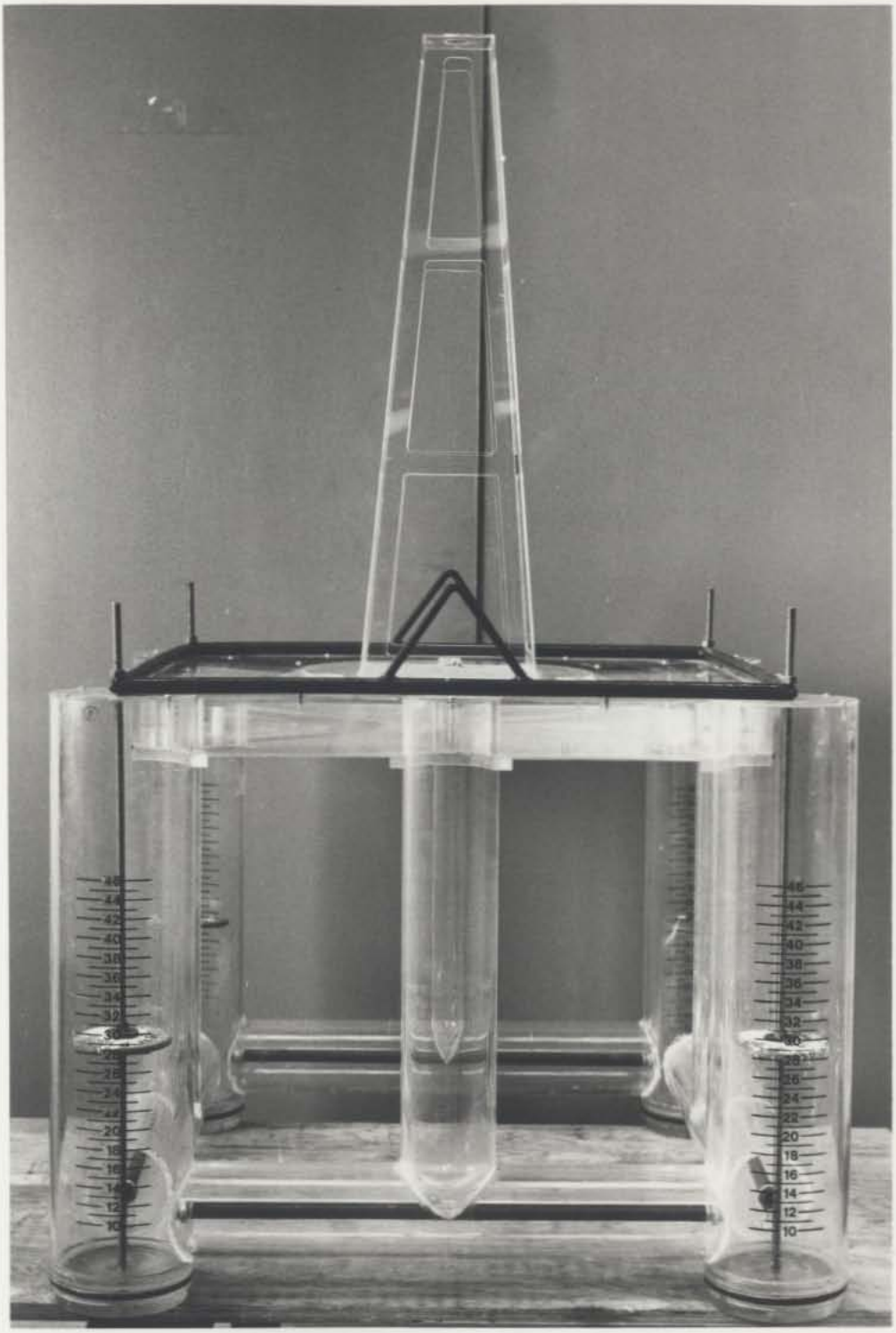

Fig. 5.2 1:100 MODEL OF THE EXAMPLE TLP

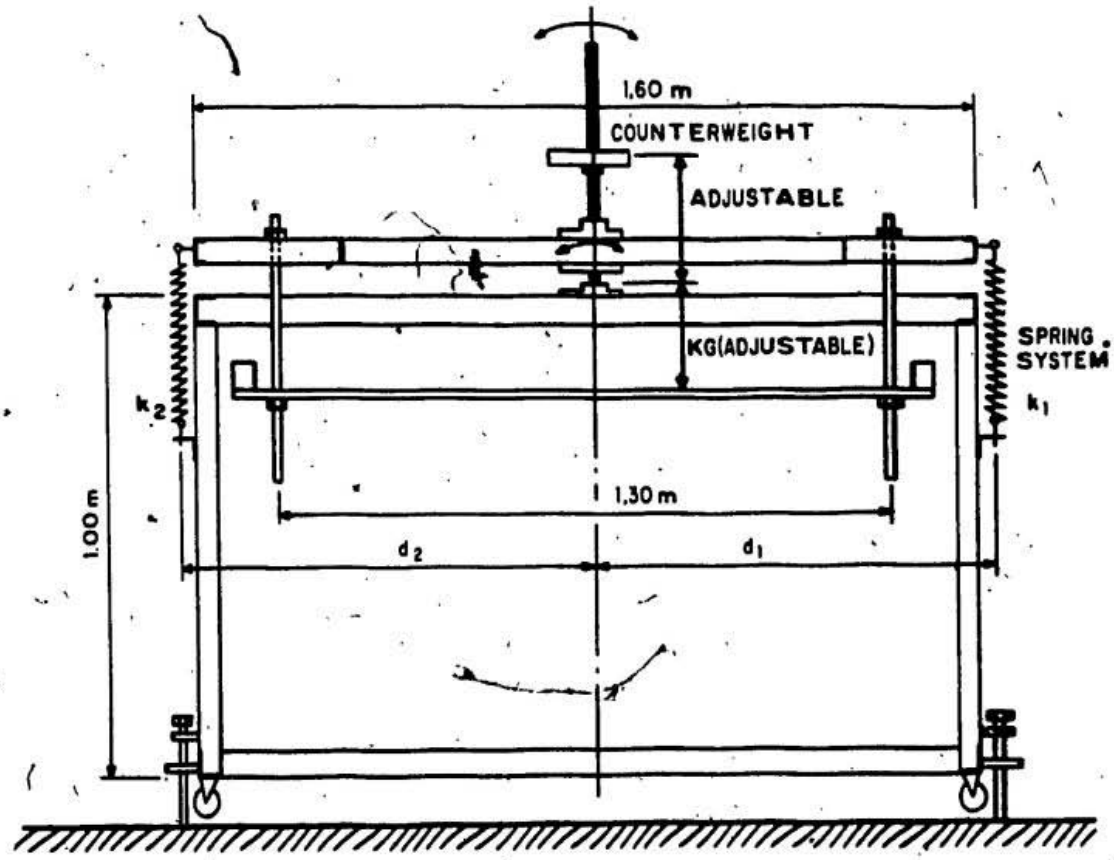

FIG. 5.3 'TILTING PLATFORM'

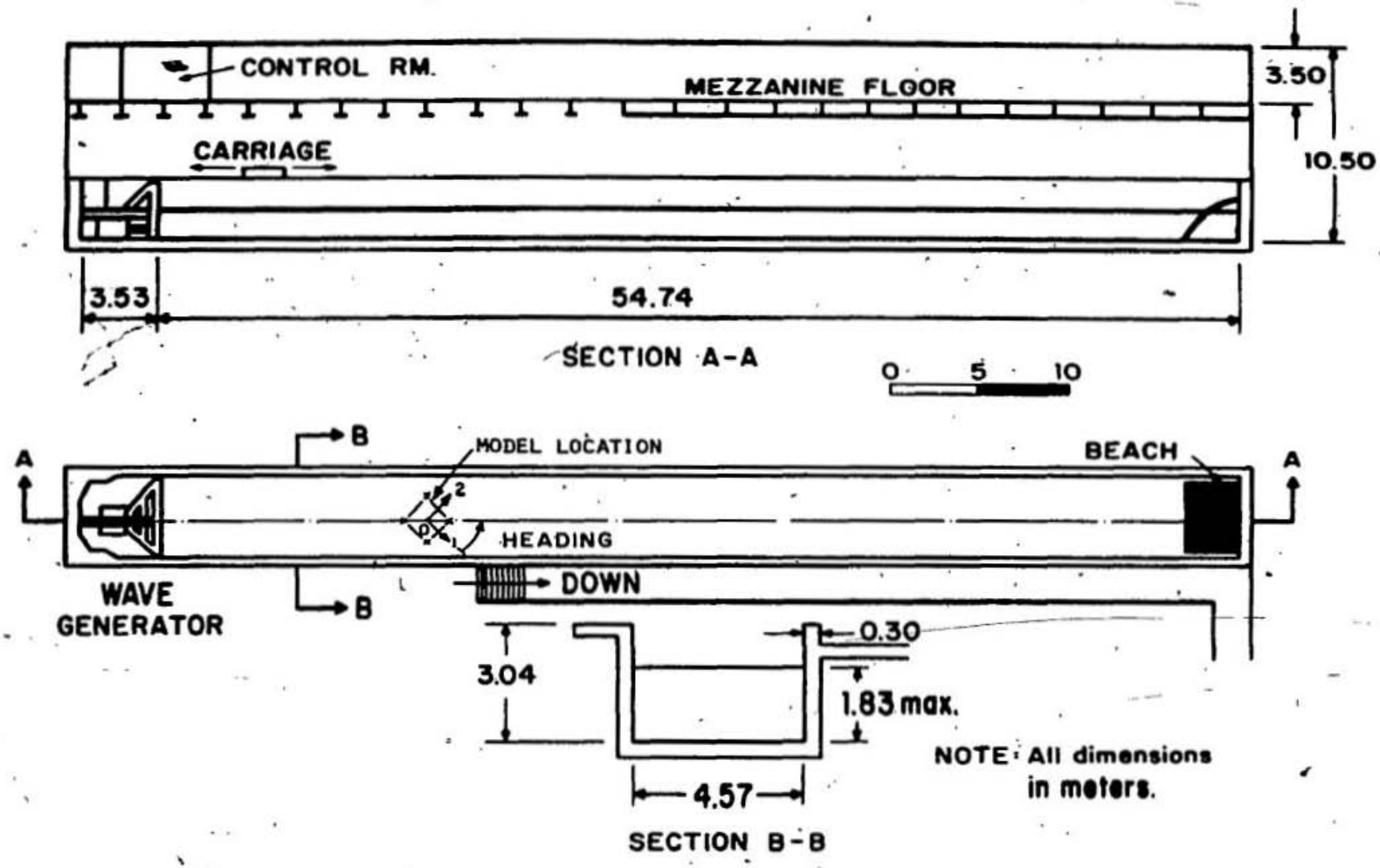

FIG. 5.4 ELEVATION, PLAN AND CROSS-SECTION OF THE WAVE TANK AT MEMORIAL UNIVERSITY.

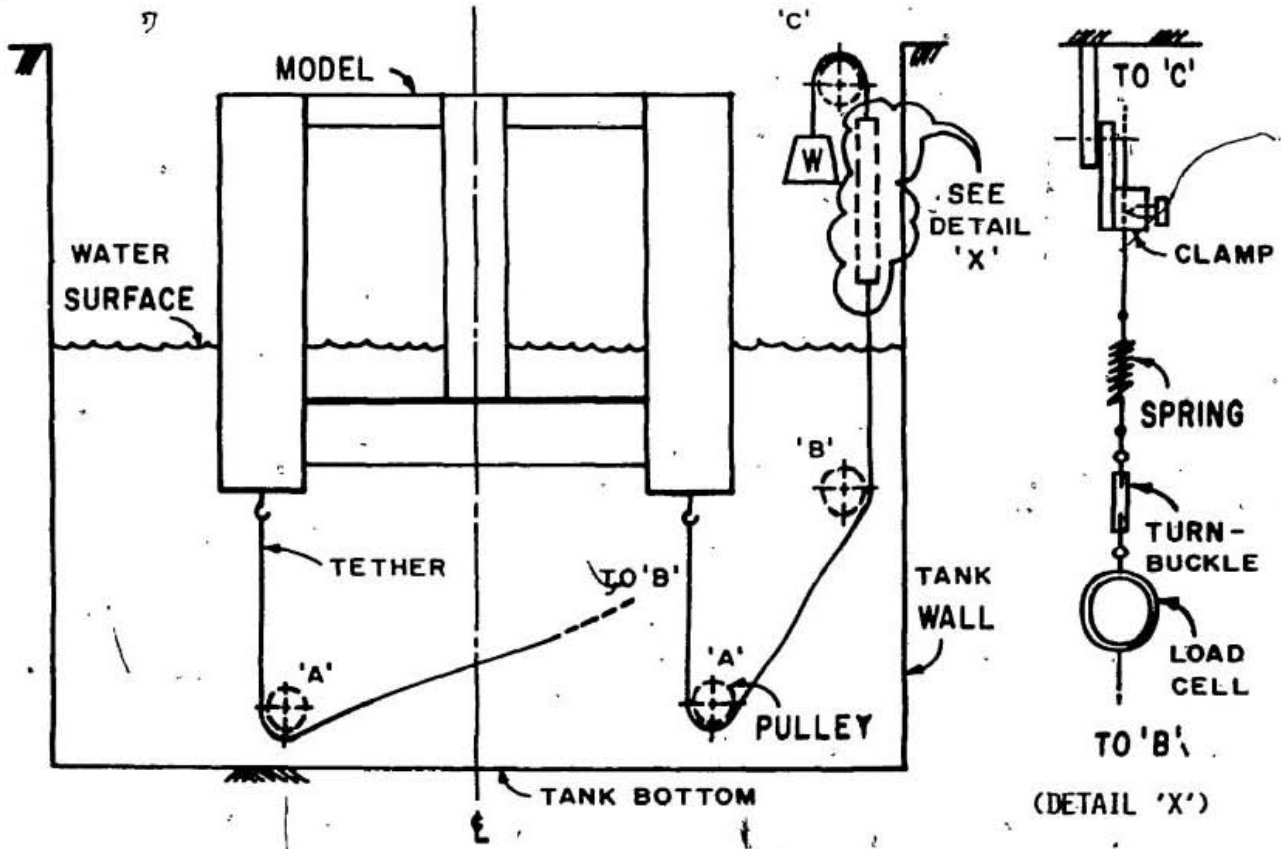

FIG. 5.5 SCHEMATIC OF THE TLP MODEL INSTALLATION IN THE WAVE TANK

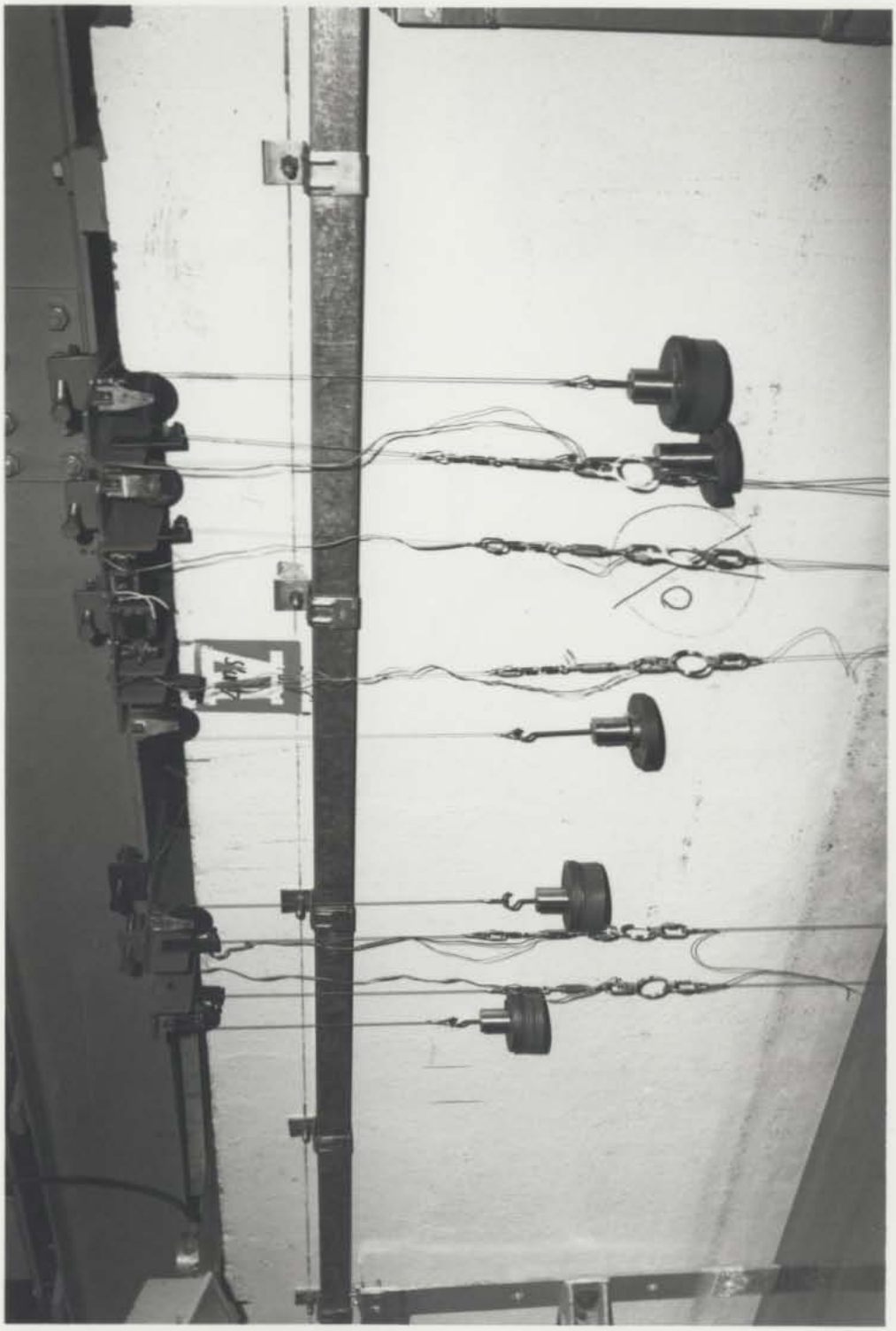

Fig. 5.6 INSTRUMENTATION OF MODEL MOORING SYSTEM

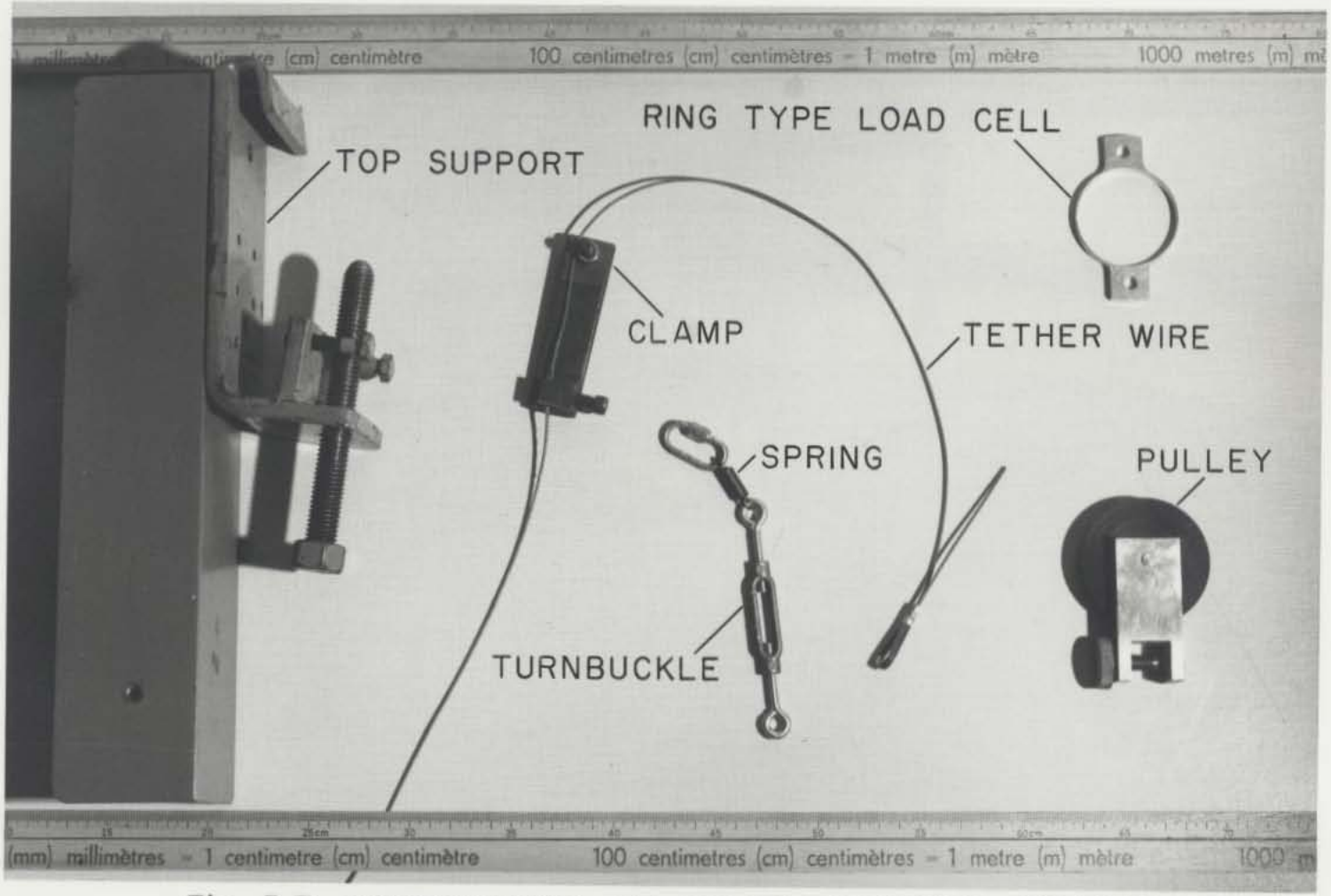

Fig. 5.7 COMPONENTS OF MODEL MOORING SYSTEM

Fig. 5.8 TLP MODEL IN WAVES

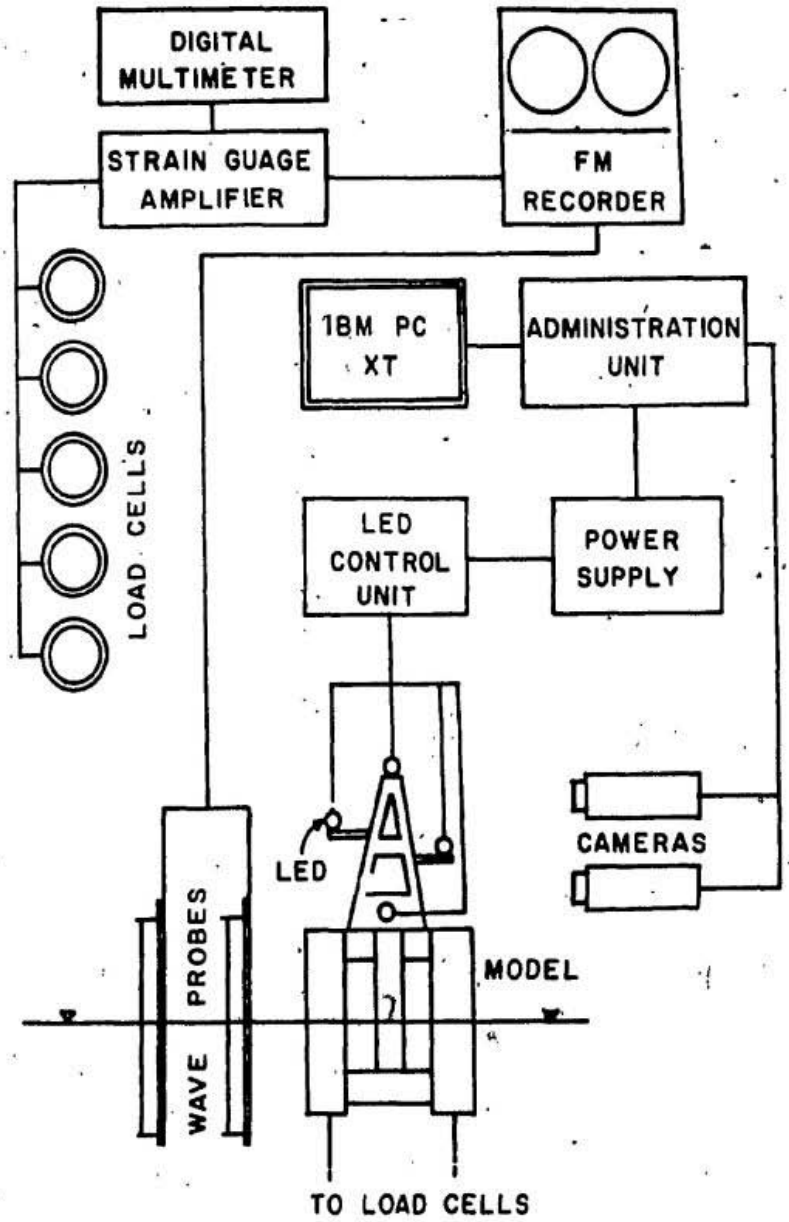

FIG. 5.9 BLOCK DIAGRAM OF TLP MODEL INSTRUMENTATION AND DATA ACQUISITION SYSTEMS

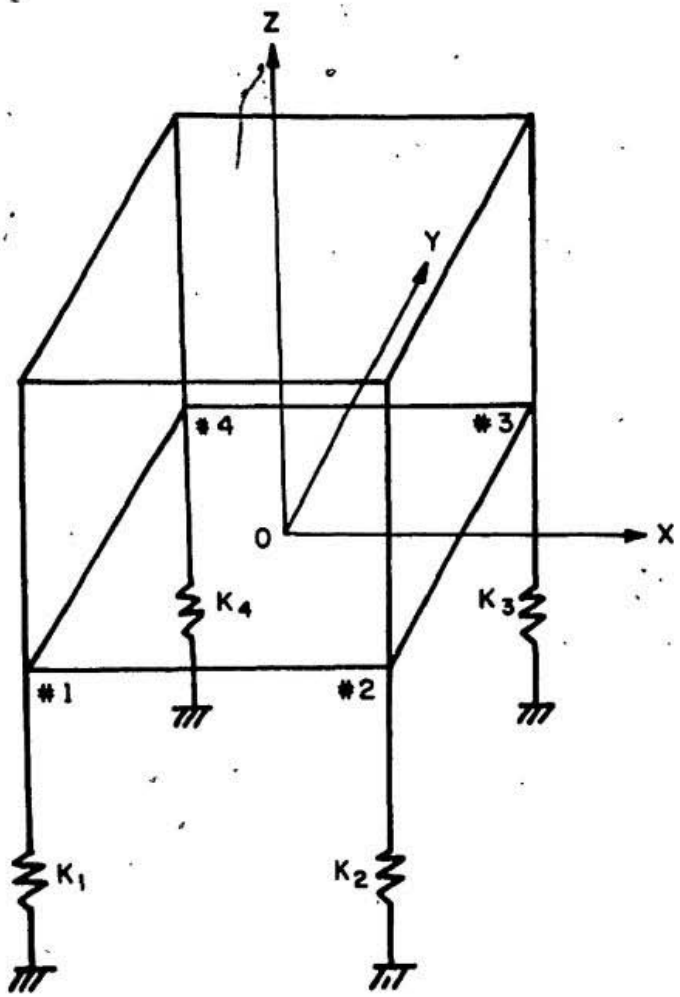

FIG. 6.1 SKELETON DIAGRAM OF TLP SHOWING TETHER STIFFNESS IDEALISATION

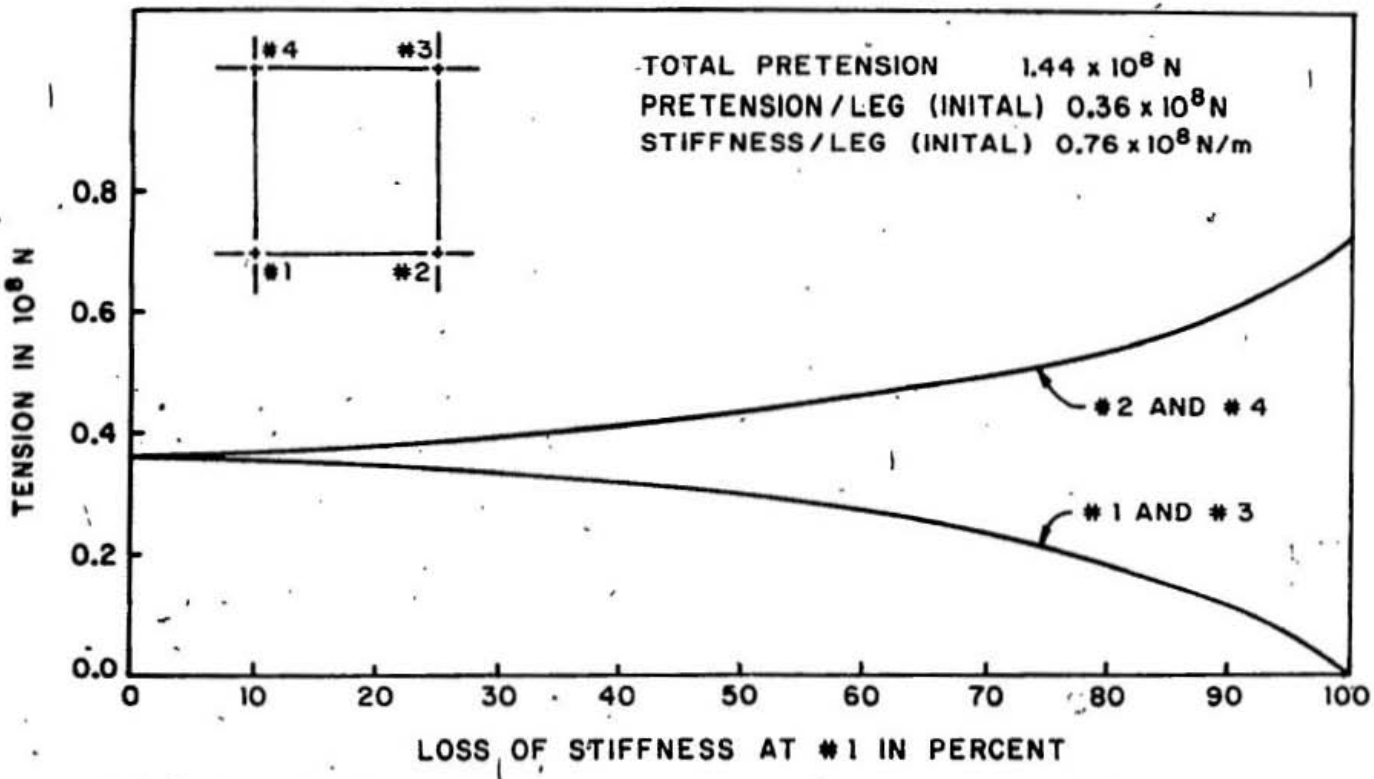

FIG. 6.2 STATIC EQUILIBRIUM TENSIONS AFTER TETHER LOSS AT CORNER # 1

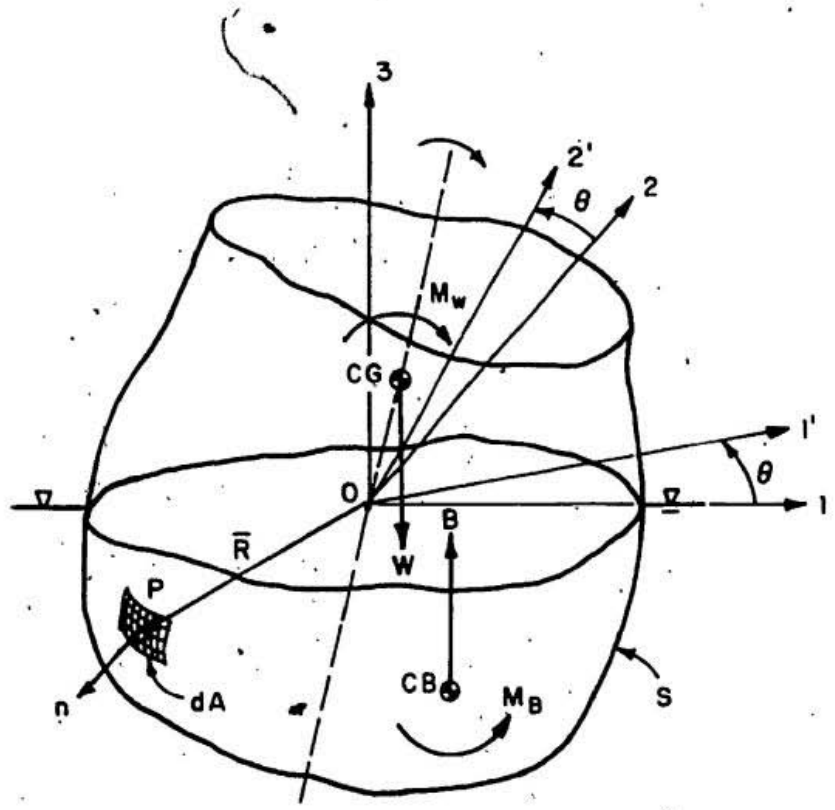

FIG. 7.1 DEFINITION DIAGRAM FOR HYDROSTATICS

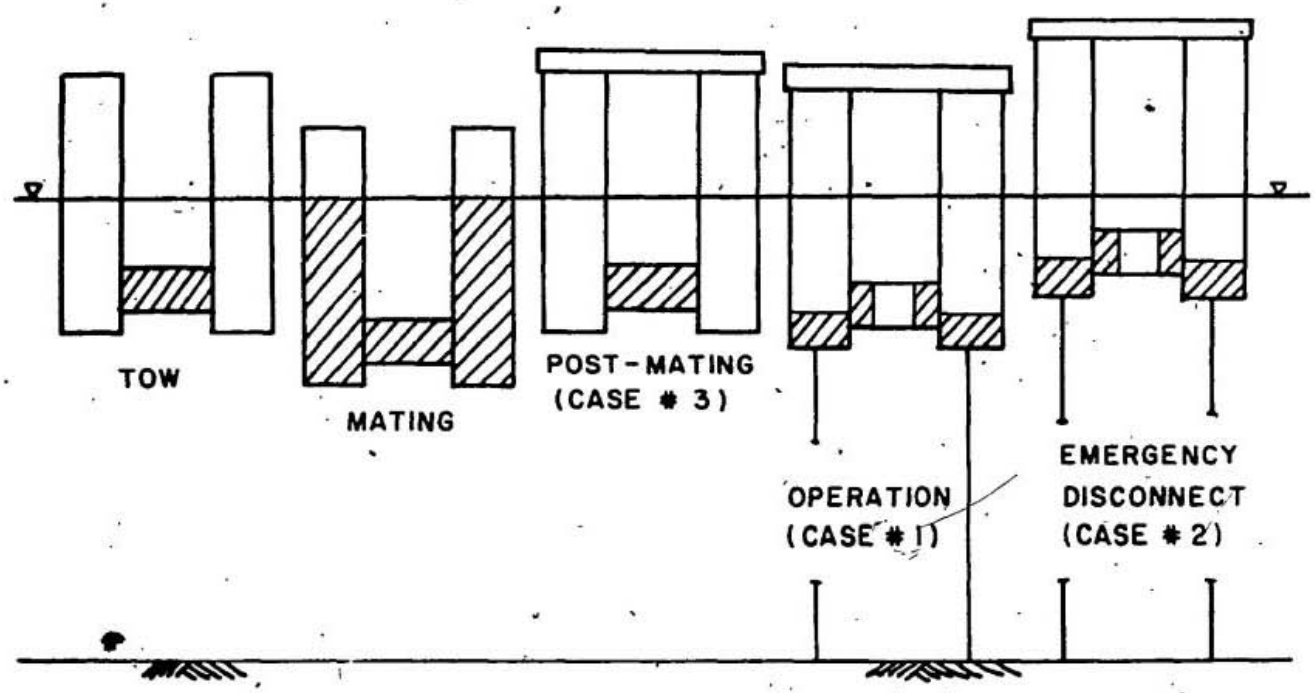

FIG. 7.2 VARIOUS TLP CONFIGURATIONS FOR STATICAL STABILITY ANALYSIS

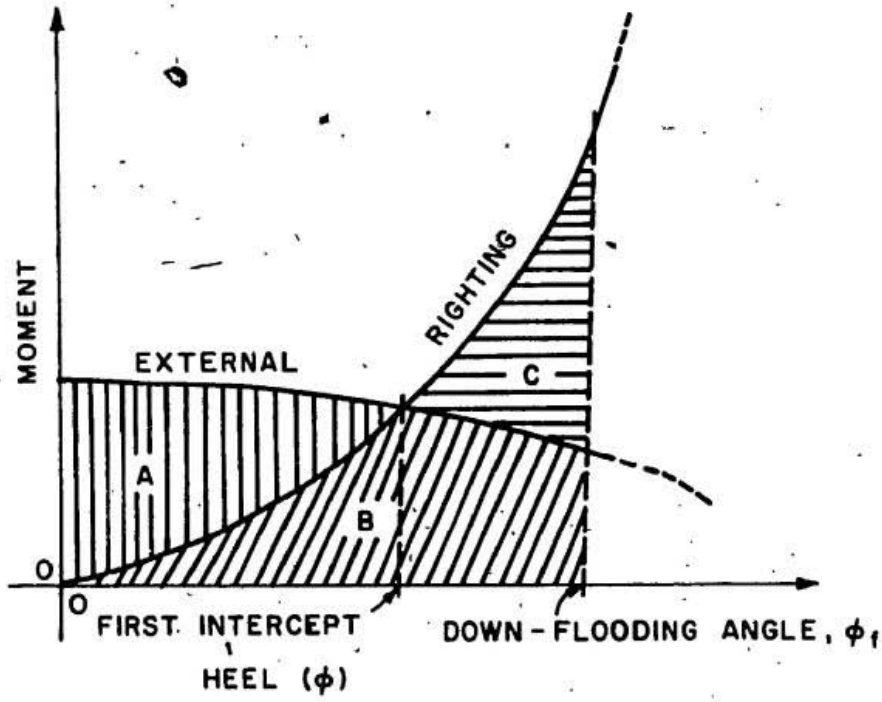

$$\text{AREA RATIO} = \frac{B+C}{A+B} \geq 1.3$$

FIG. 7.3 A STATICAL STABILITY DIAGRAM

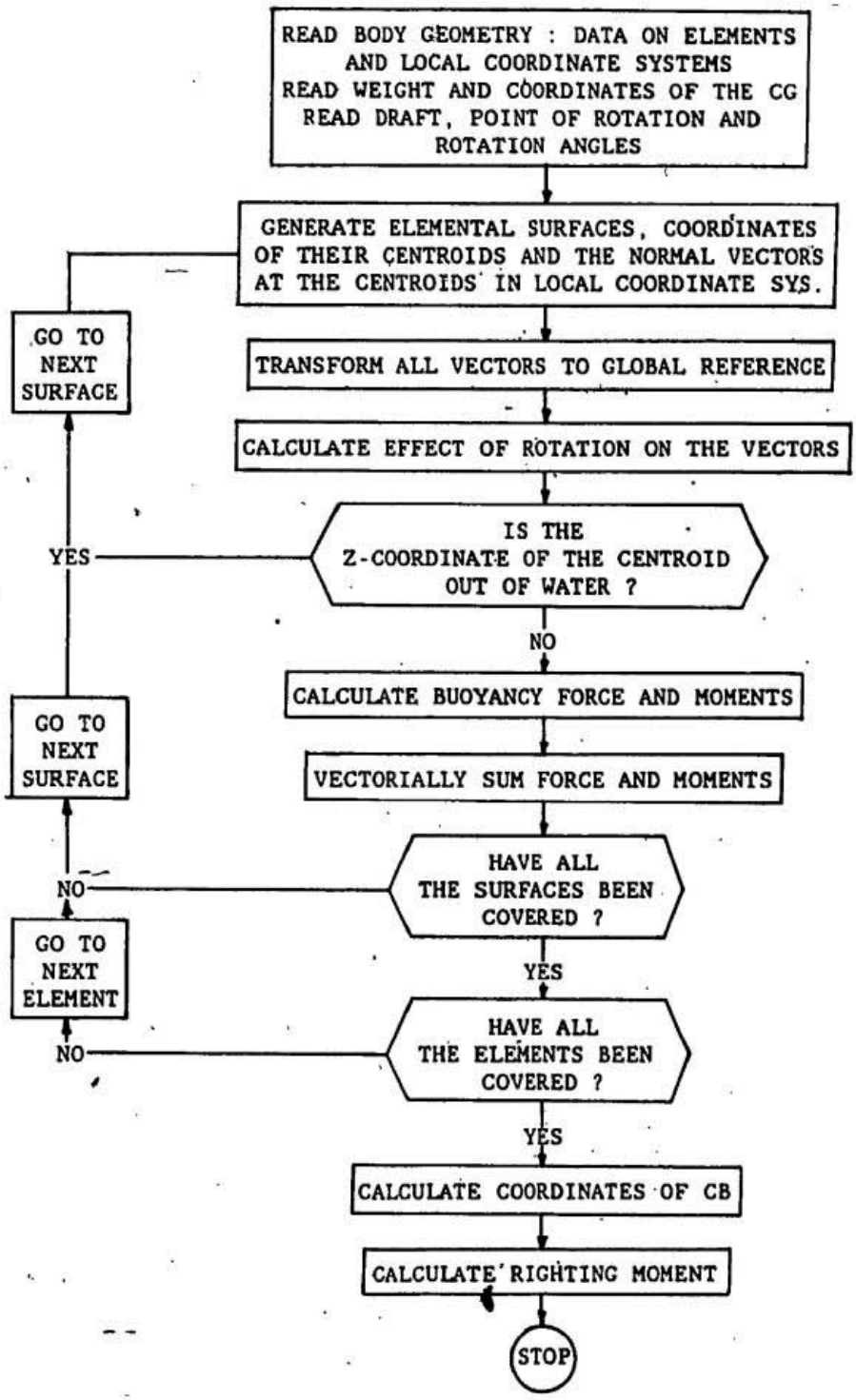

FIG. 7.4 FLOW CHART FOR 'HYDROSTATICS'

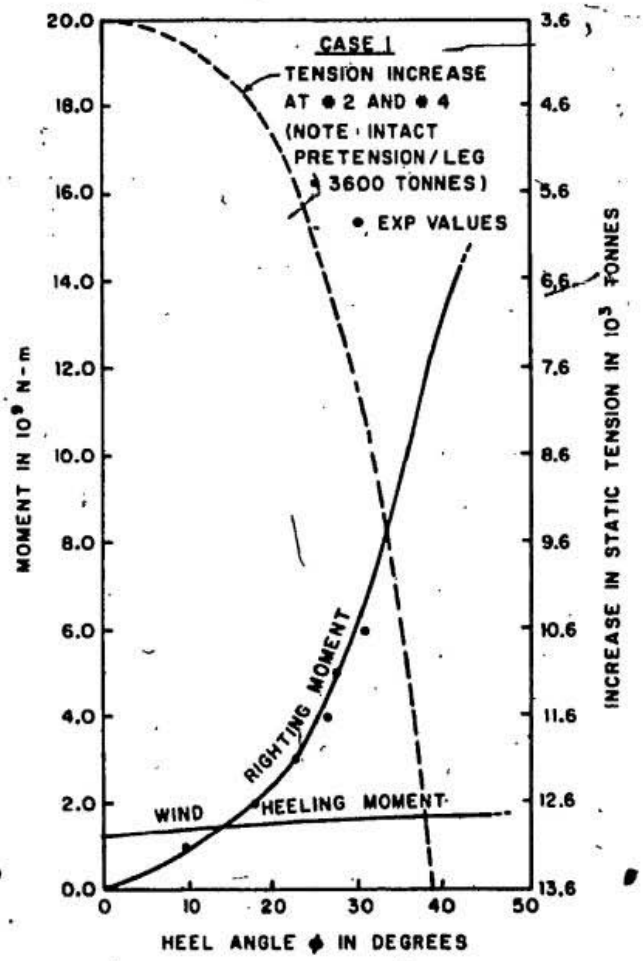

FIG. 7.5 STATICAL STABILITY DIAGRAM : CASE 1

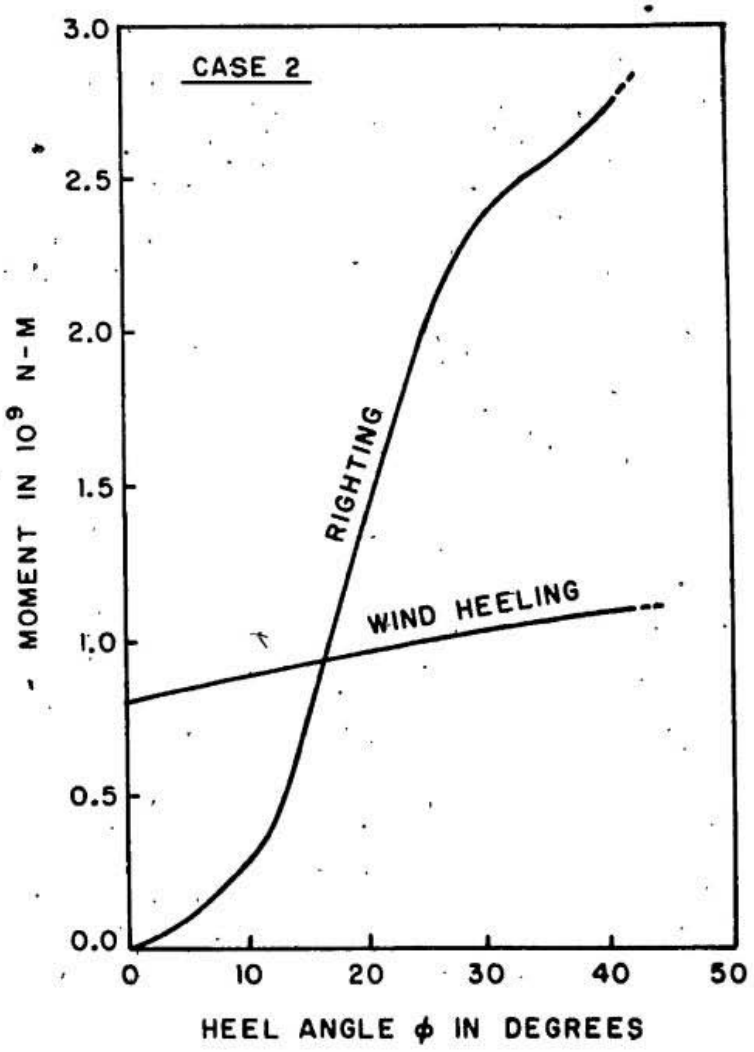

FIG. 7.6 STATICAL STABILITY DIAGRAM : CASE 2

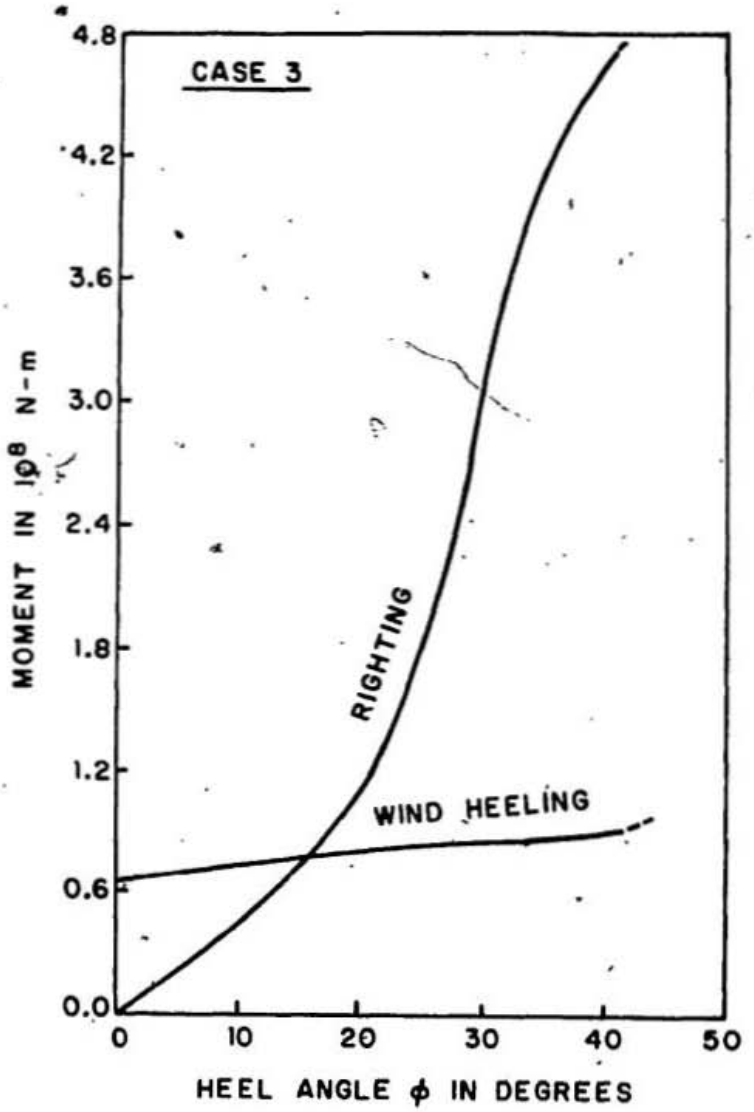

FIG. 7.7 STATICAL STABILITY DIAGRAM : CASE 3

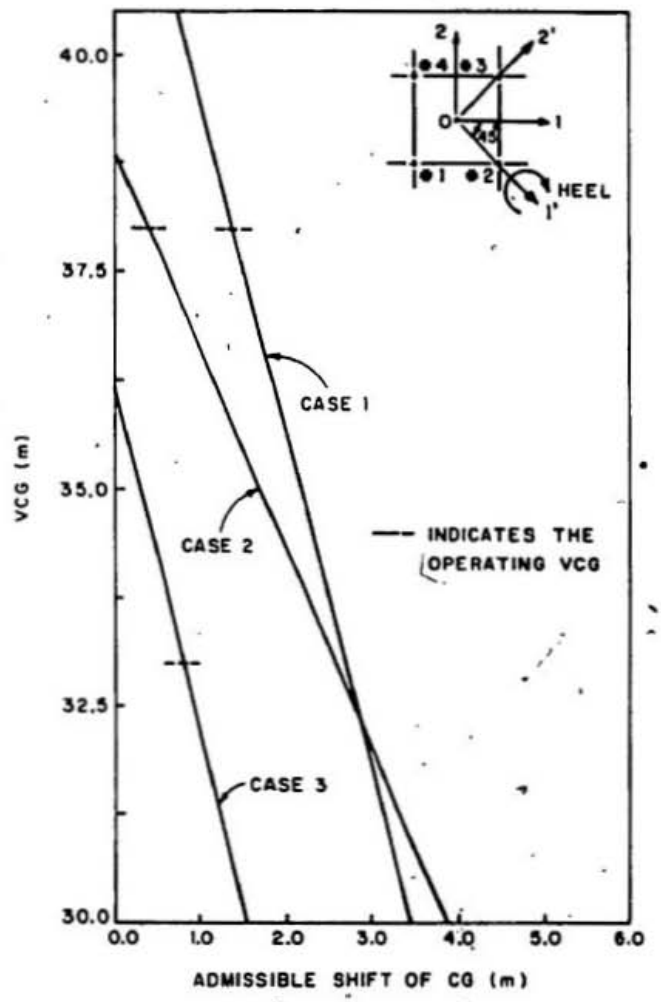

FIG. 7.8 'ADMISSIBLE SHIFTS' OF CG FOR VARIOUS TLP CONFIGURATIONS

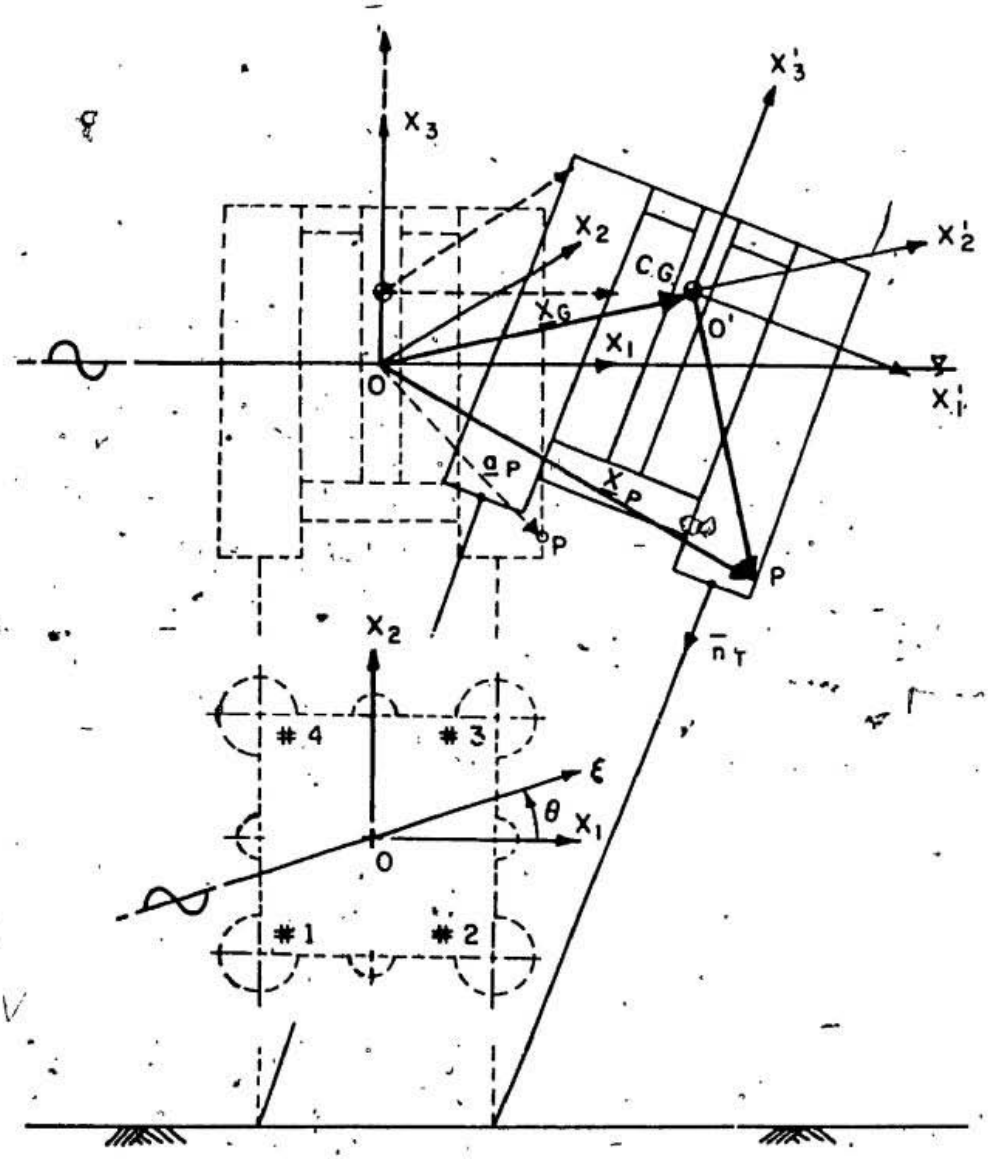

FIG. 8.1A TLP COORDINATE SYSTEMS FOR HYDRODYNAMIC ANALYSIS

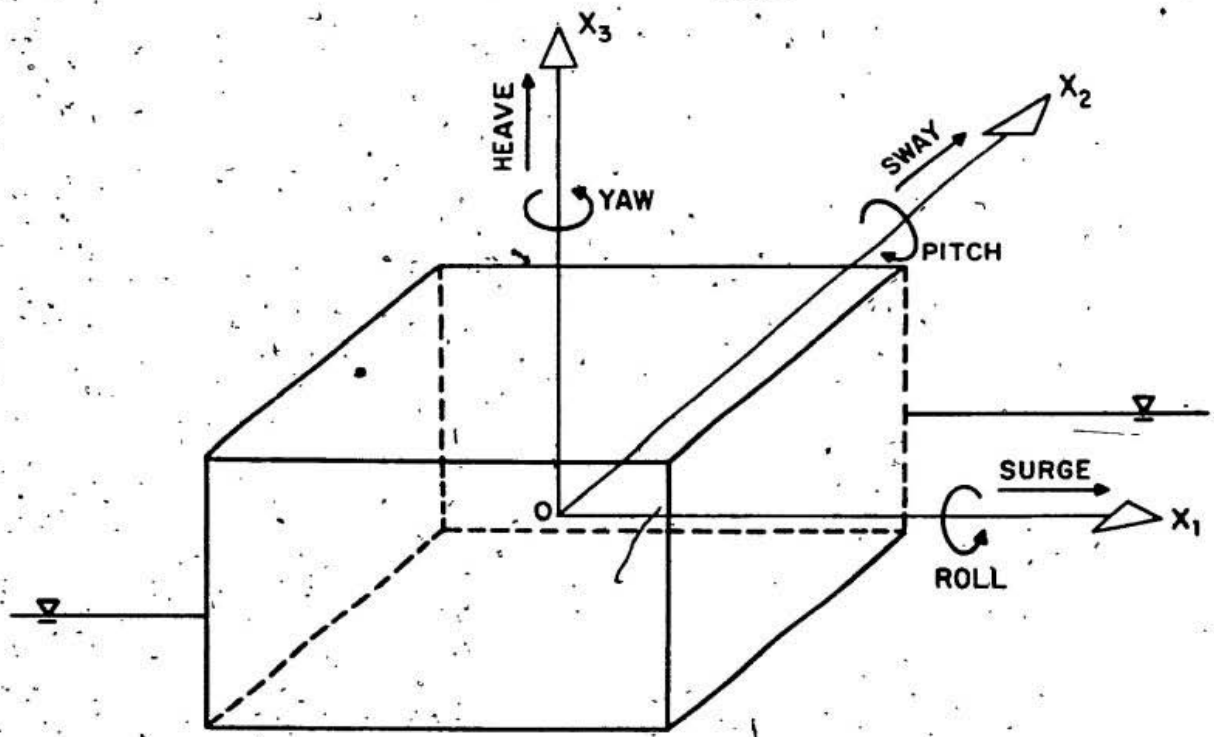

FIG. 8.1B THE SIX DEGREES OF FREEDOM OF A FLOATING BODY

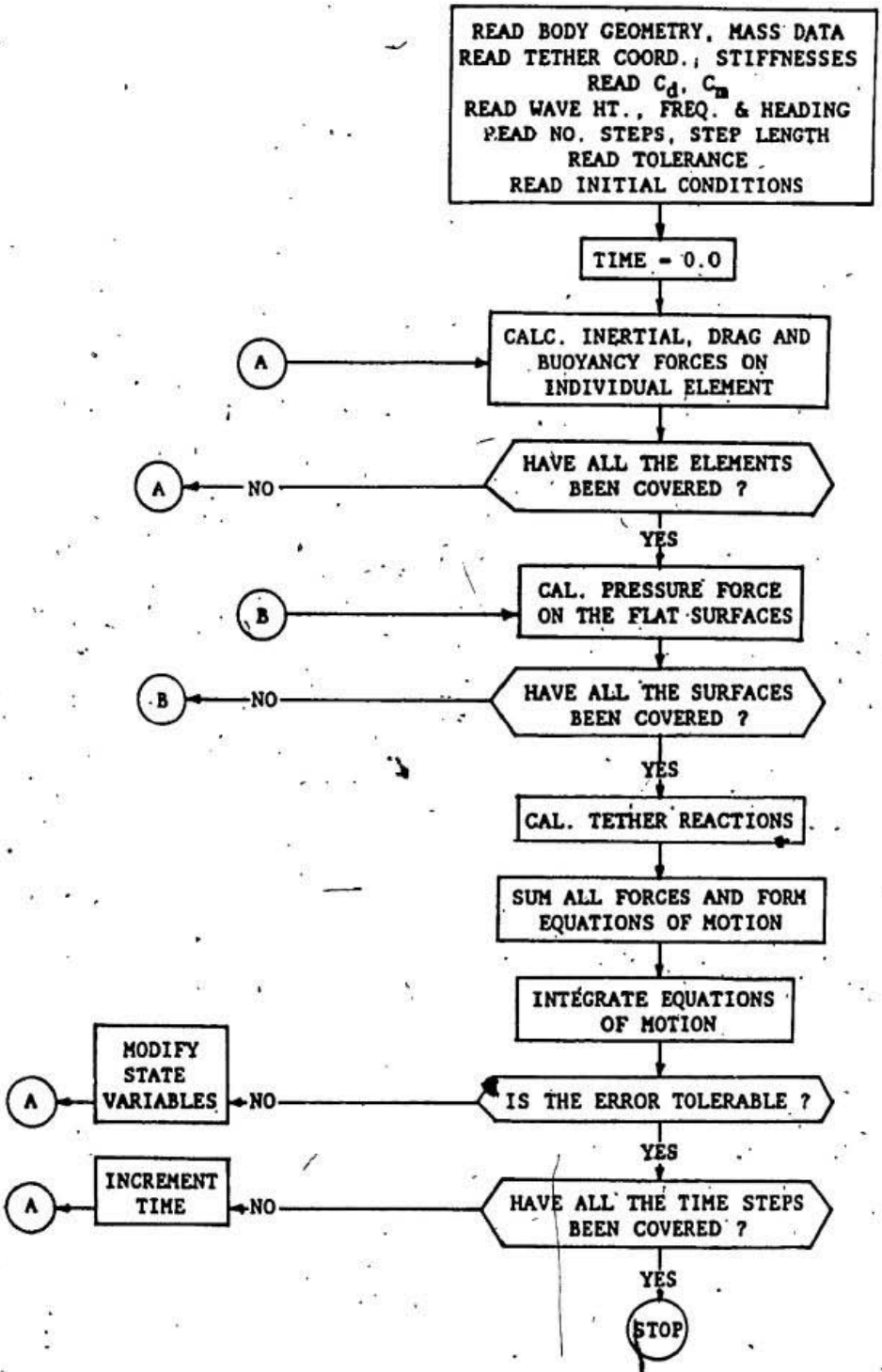

FIG. 8.2 FLOW CHART FOR 'TIME_DOMAIN'

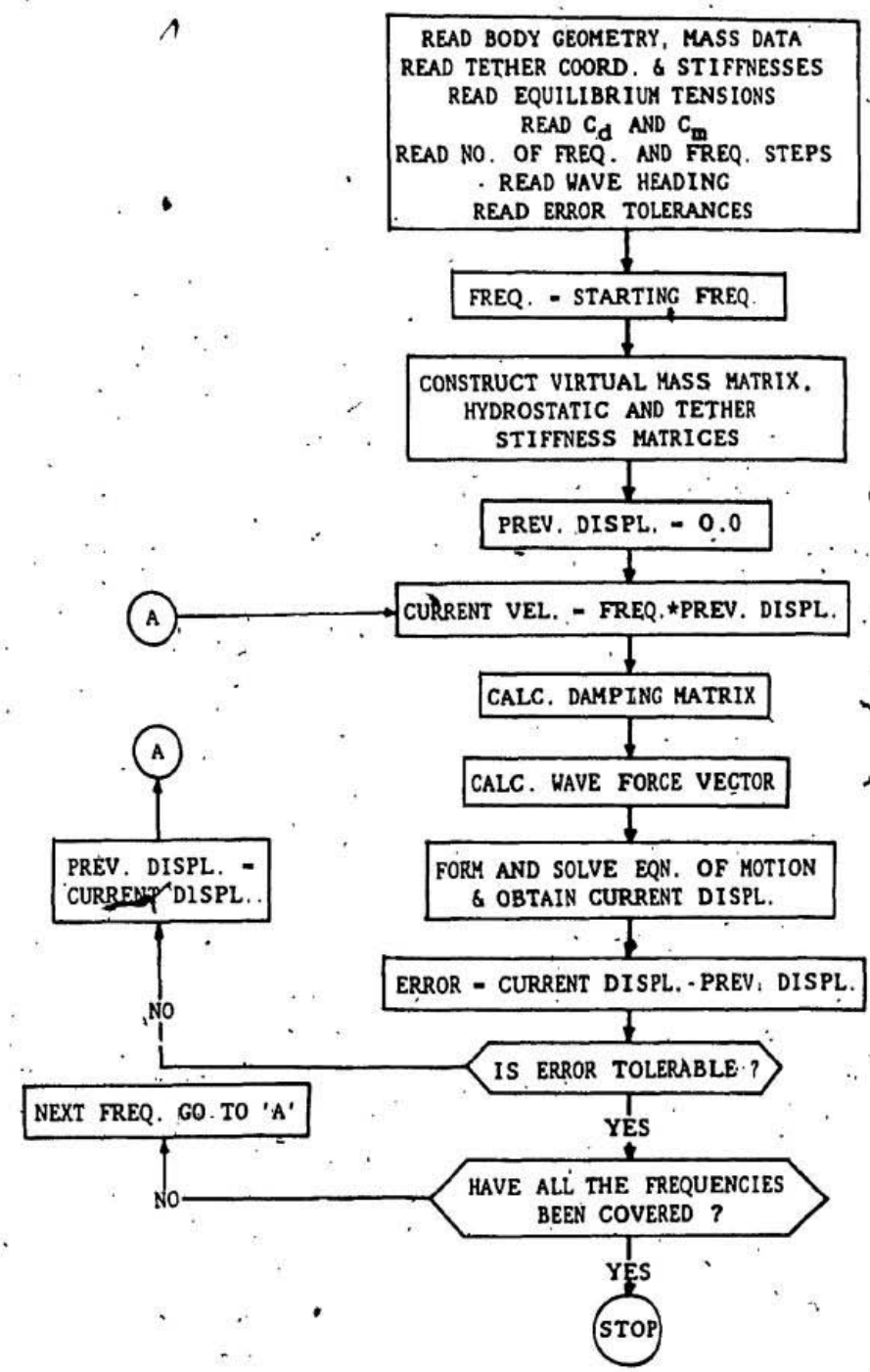

FIG. 8.3 FLOW CHART FOR 'FREQ_DOMAIN'

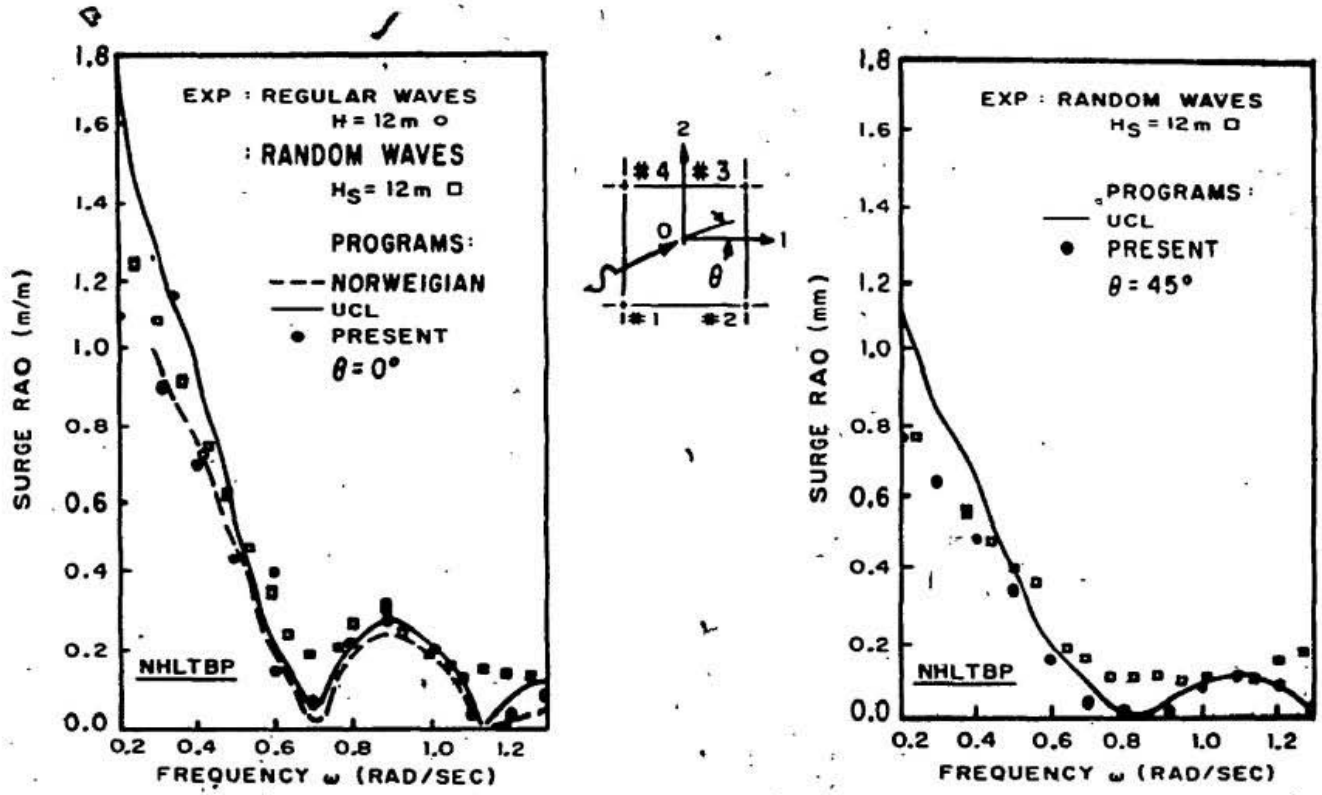

FIG. 8.4A COMPARISON OF SURGE MOTION CALCULATED USING 'FREQ_DOMAIN' AND THE RESULTS FROM LYONS ET AL. (1983)

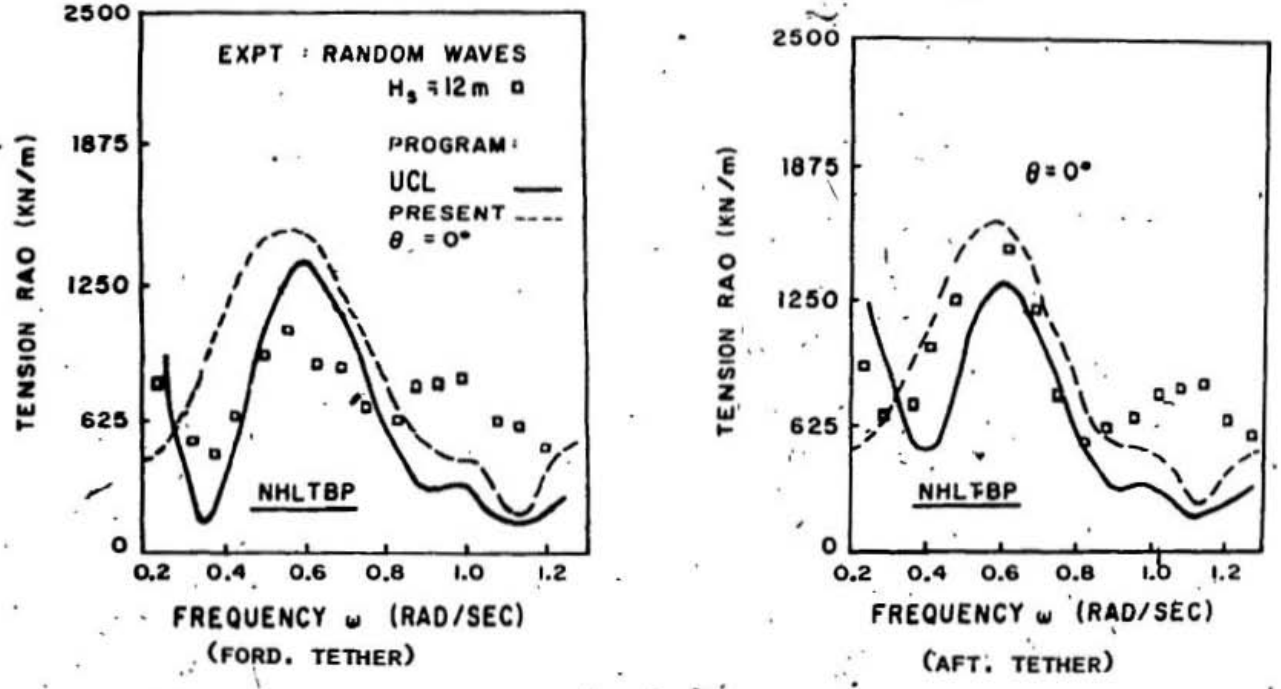

FIG. 8.4B COMPARISON OF TETHER TENSIONS CALCULATED USING 'FREQ_DOMAIN' AND THE RESULTS FROM LYONS ET AL. (1983)

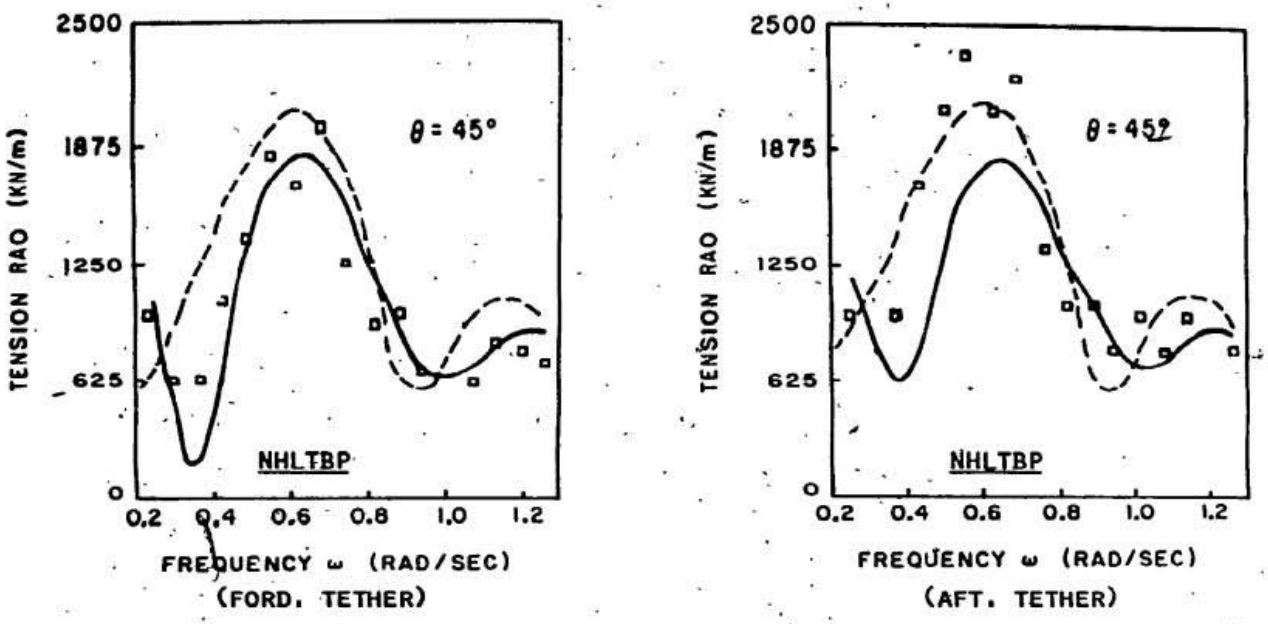

FIG. 8.4B COMPARISON OF TETHER TENSIONS CALCULATED USING 'FREQ_DOMAIN' AND THE RESULTS FROM LYONS ET AL. (1983) (CONTD.)

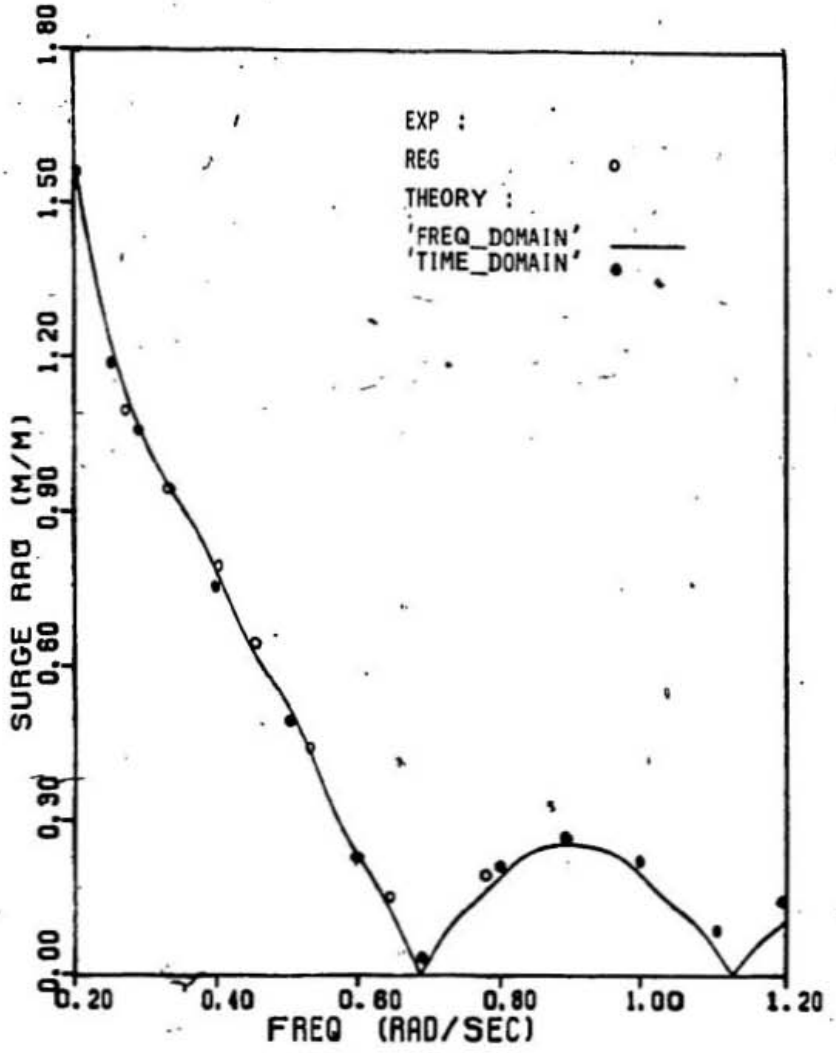

FIG. 8.5 SURGE RAO IN INTACT AND DAMAGE (50% LOSS OF TETHER AT # 1) CASES (0° HEADING)

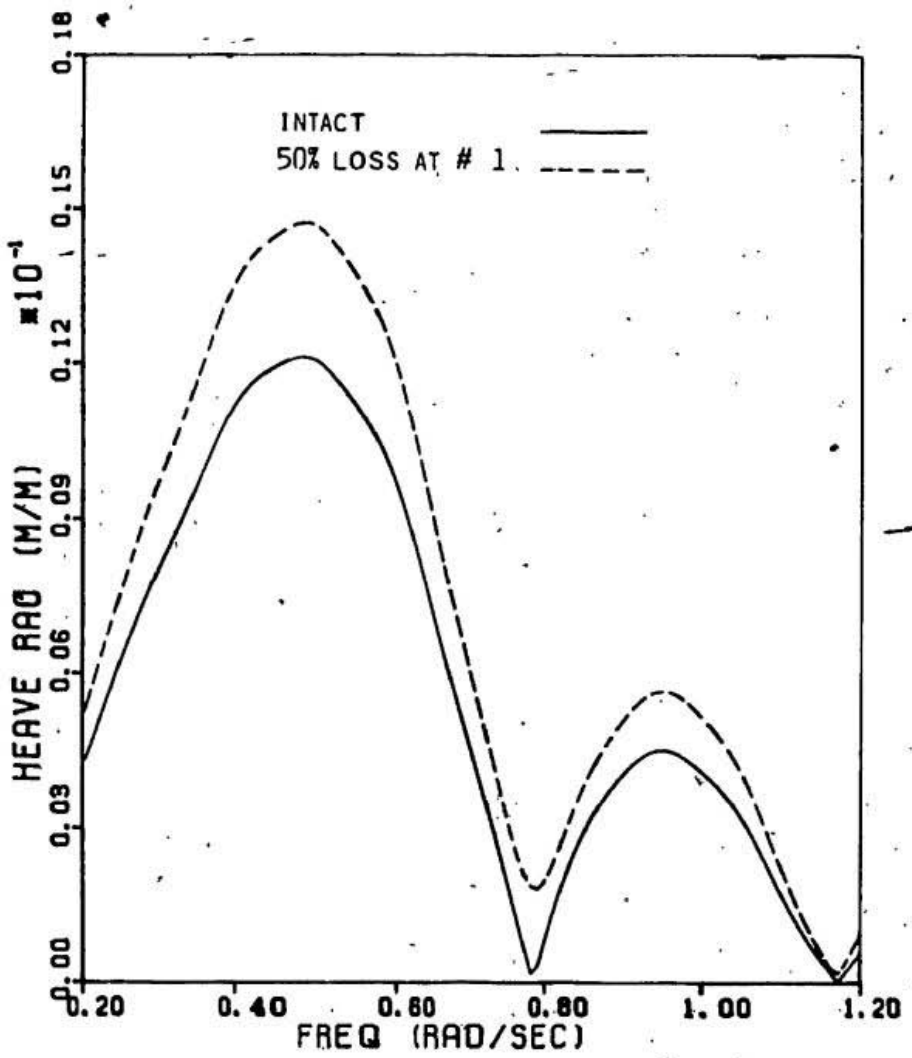

FIG. 8.6 HEAVE RAO IN INTACT AND DAMAGED CASES (0° HEADING)

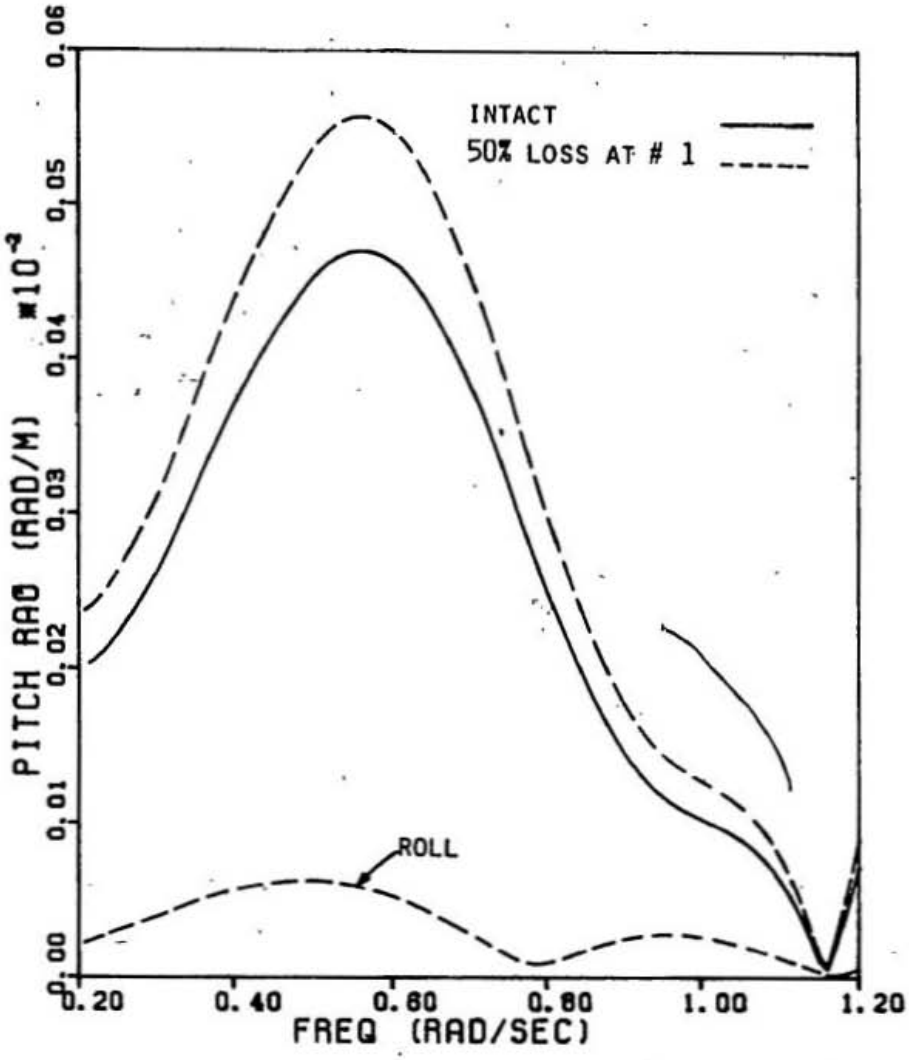

FIG. 8.7 PITCH/ROLL RAO IN INTACT AND DAMAGED CASES (0° HEADING)

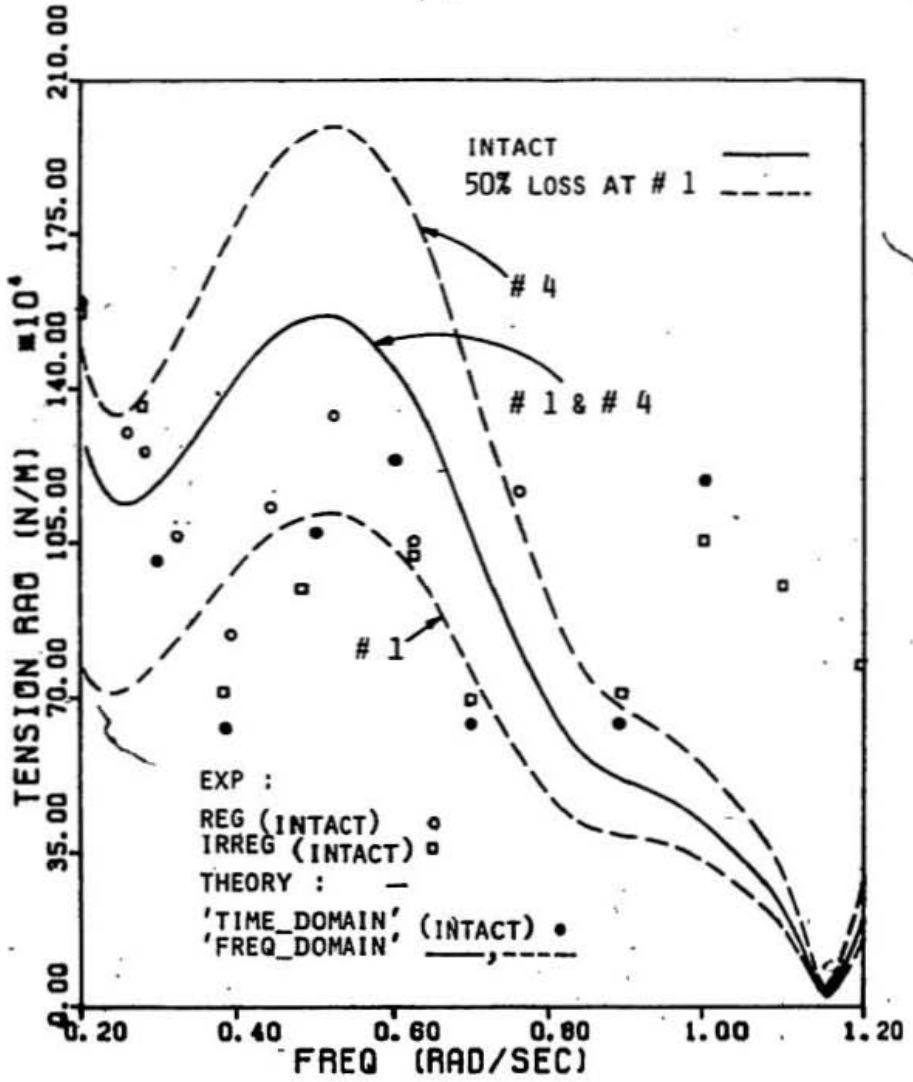

FIG. 8.8 TENSION RAO IN INTACT AND DAMAGED CASES (0° HEADING) : CORNERS # 1 AND # 4

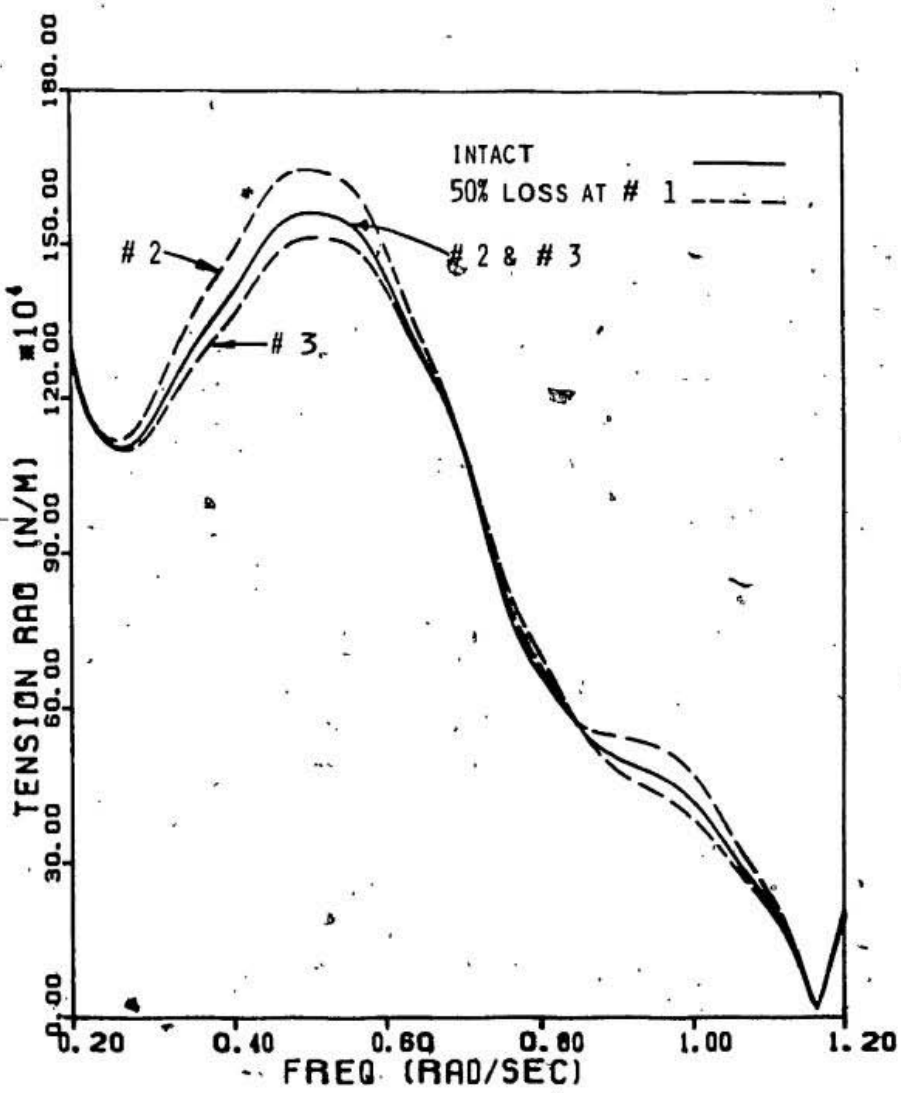

FIG. 8.9 TENSION RAO IN INTACT AND DAMAGED CASES (0° HEADING) : CORNERS # 2 AND # 3

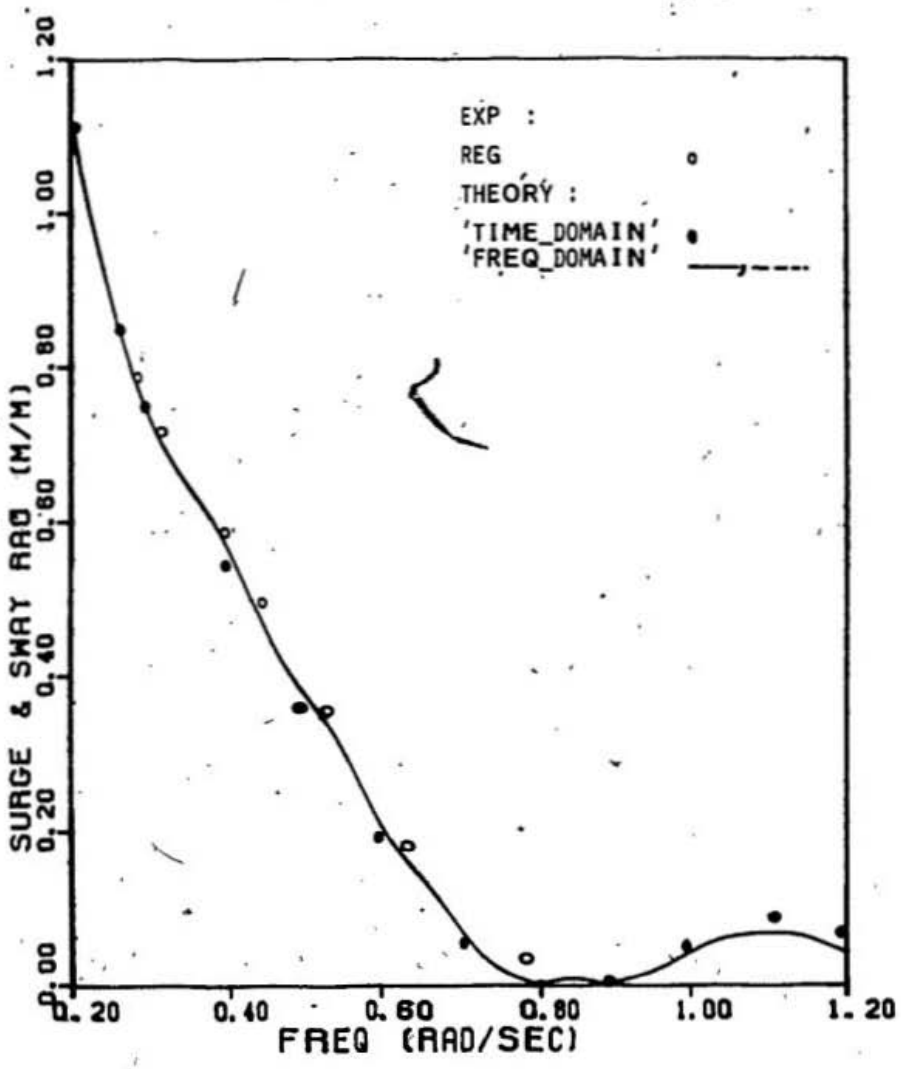

FIG. 8.10 SURGE/SWAY RAO IN INTACT AND DAMAGED (50% LOSS OF TETHER AT # 1) CASES (45° HEADING)

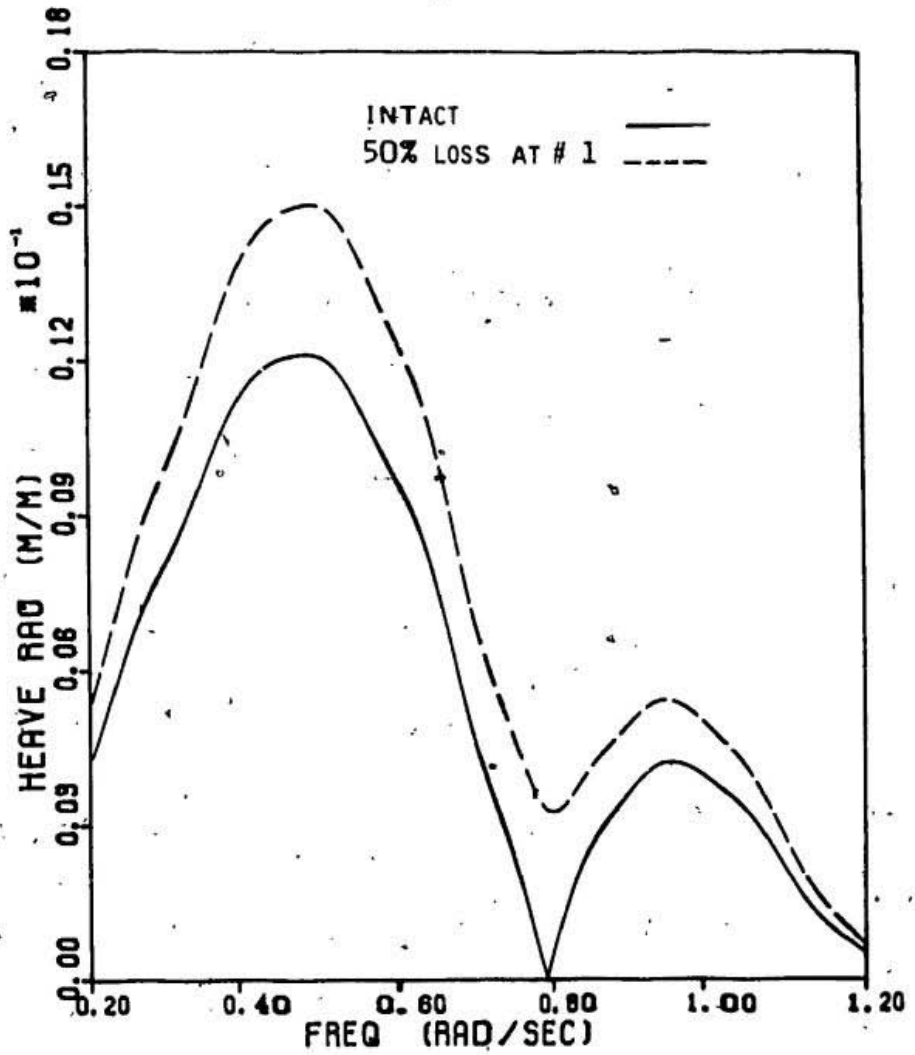

FIG. 8.11 HEAVE RAO IN INTACT AND DAMAGED CASES (45° HEADING)

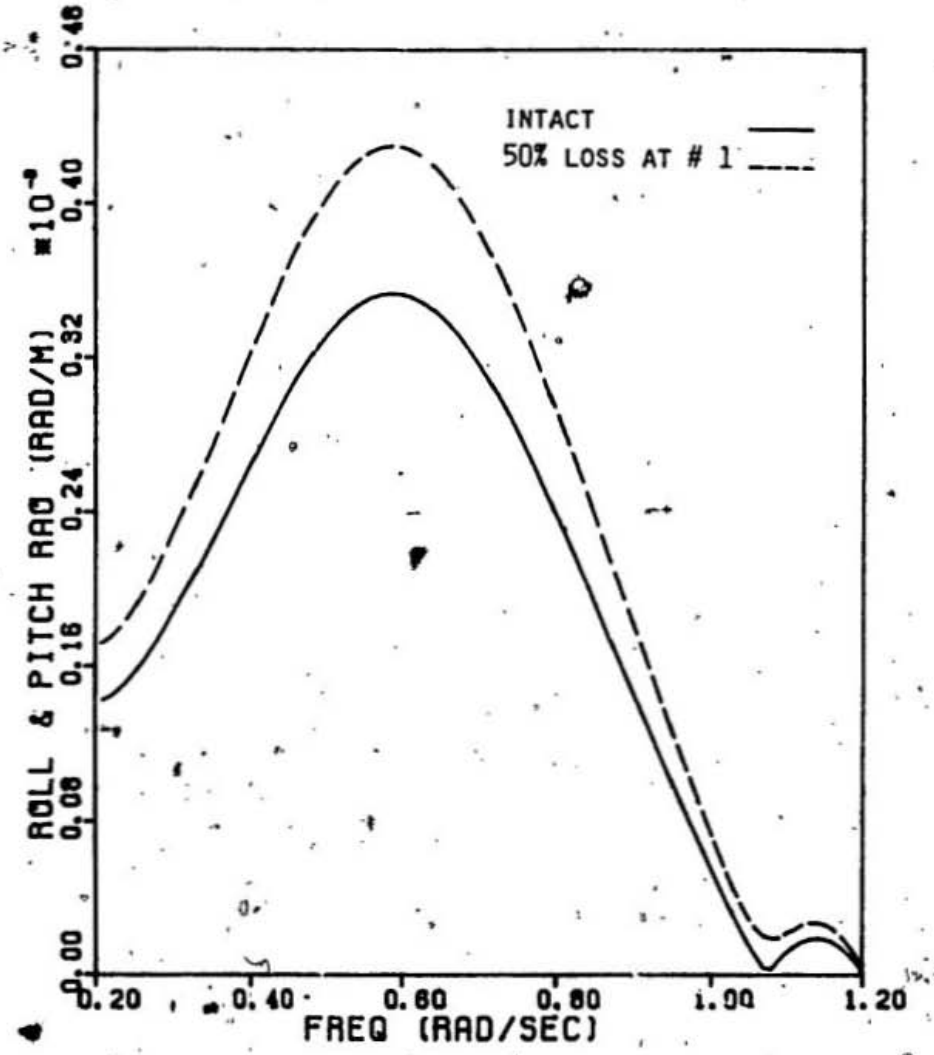

FIG. 8.12 ROLL/PITCH RAO IN INTACT AND DAMAGED CASES (45° HEADING)

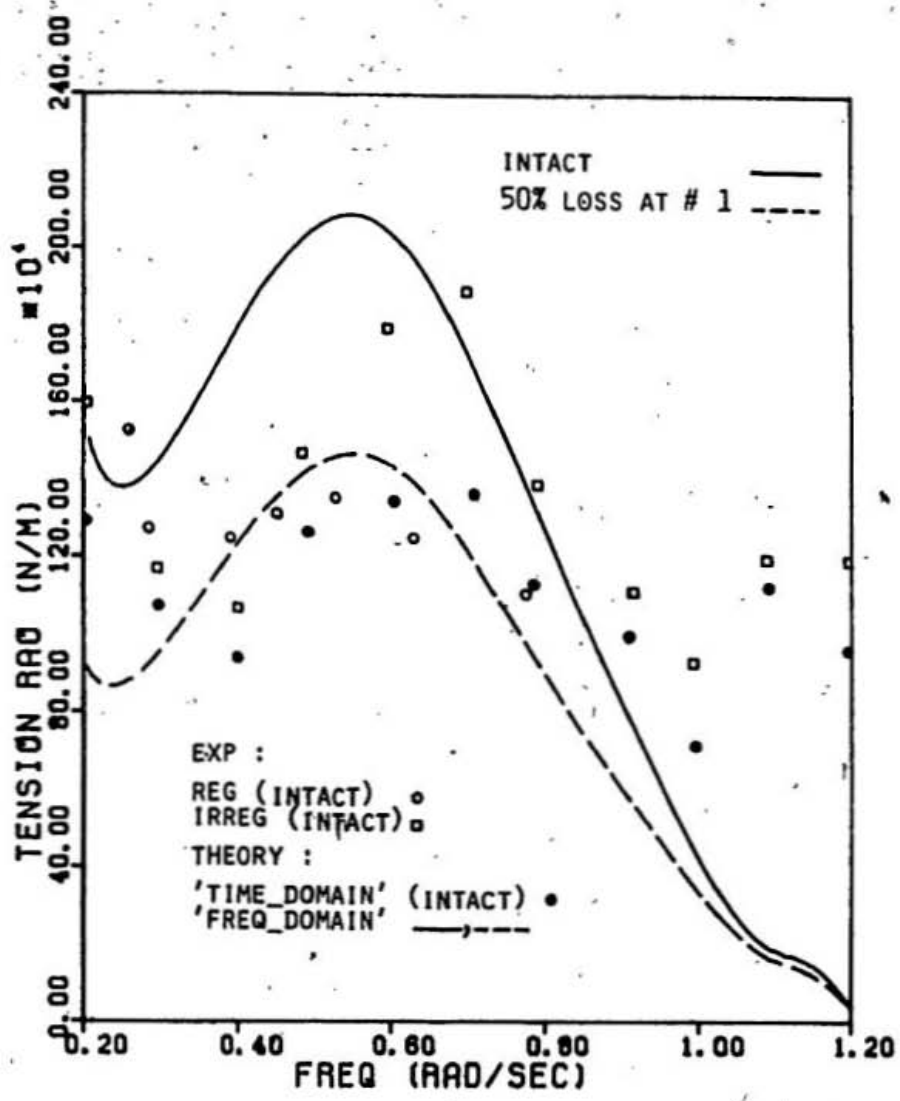

FIG. 8.13 TENSION RAO IN INTACT AND DAMAGED CASES (45° HEADING) : CORNER # 1

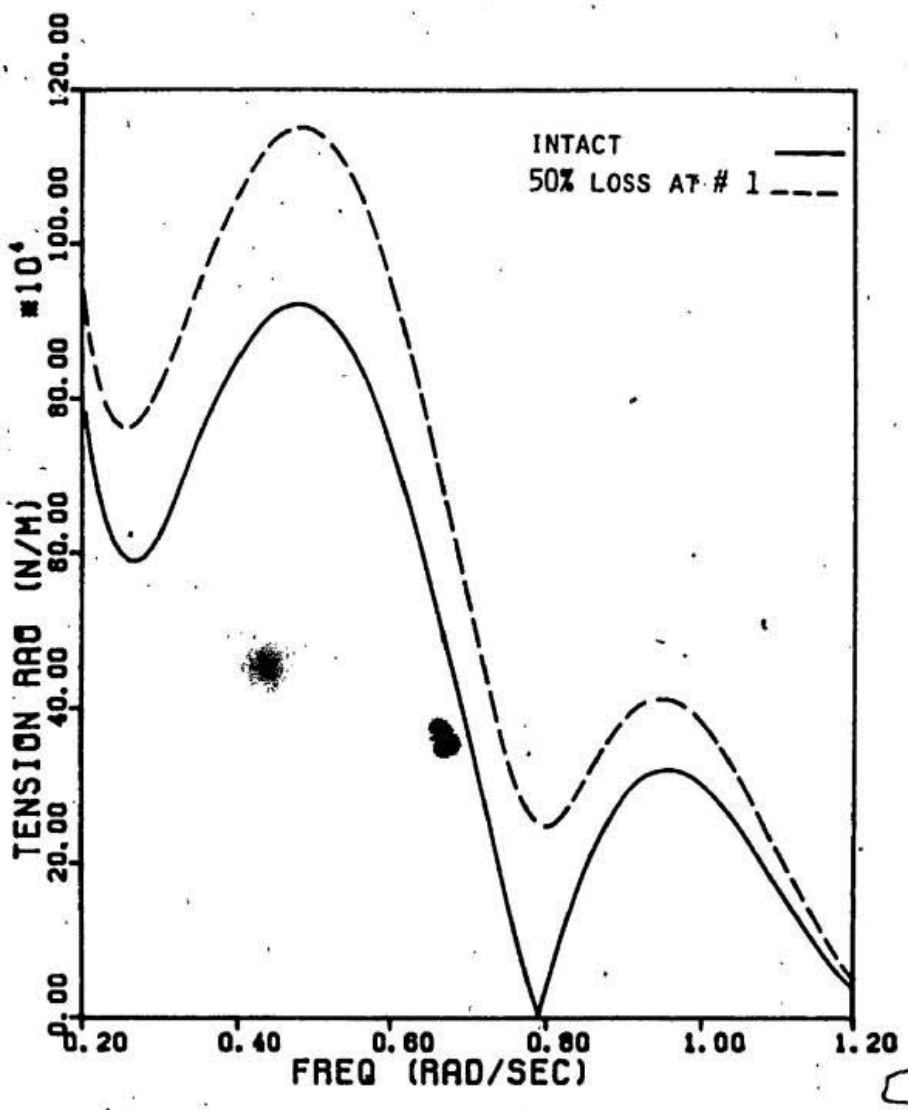

FIG. 8.14 TENSION RAO IN INTACT AND DAMAGED CASES (45° HEADING) : CORNER # 2 AND # 4

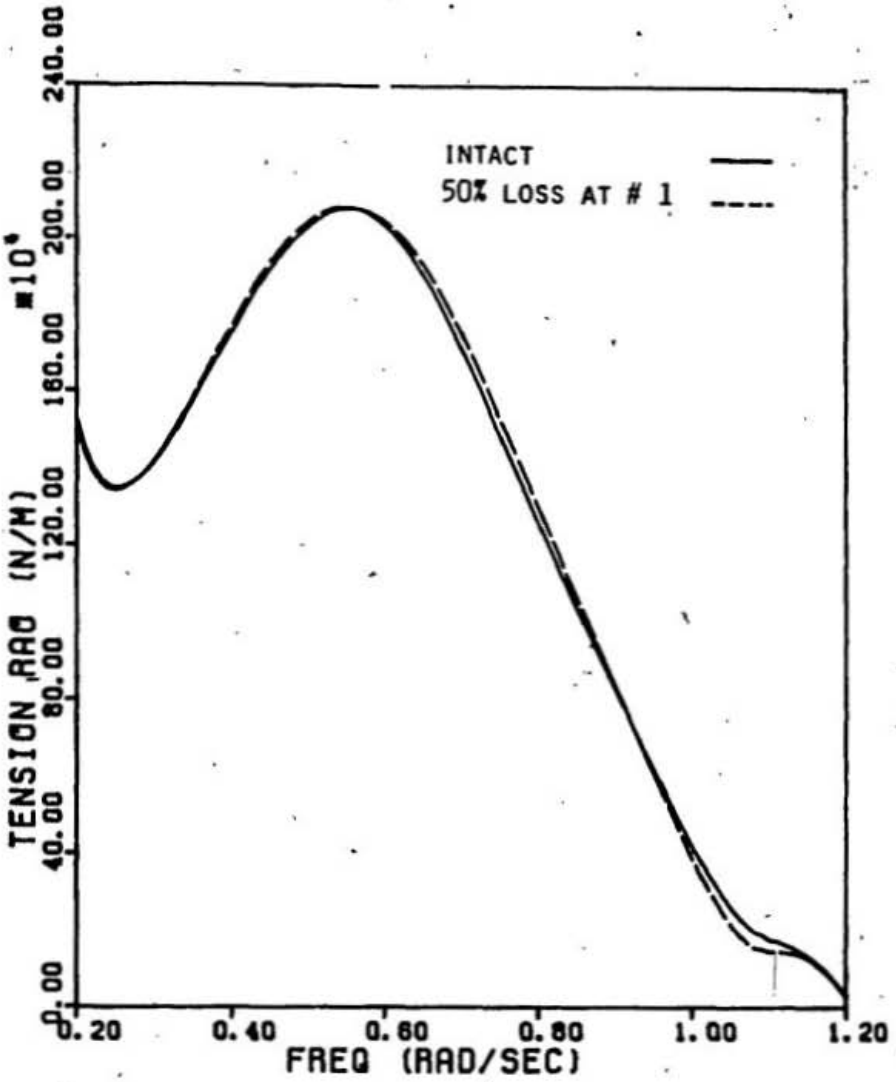

FIG. 8.15 TENSION RAO IN INTACT AND DAMAGED CASES (45° HEADING) : CORNER # 3

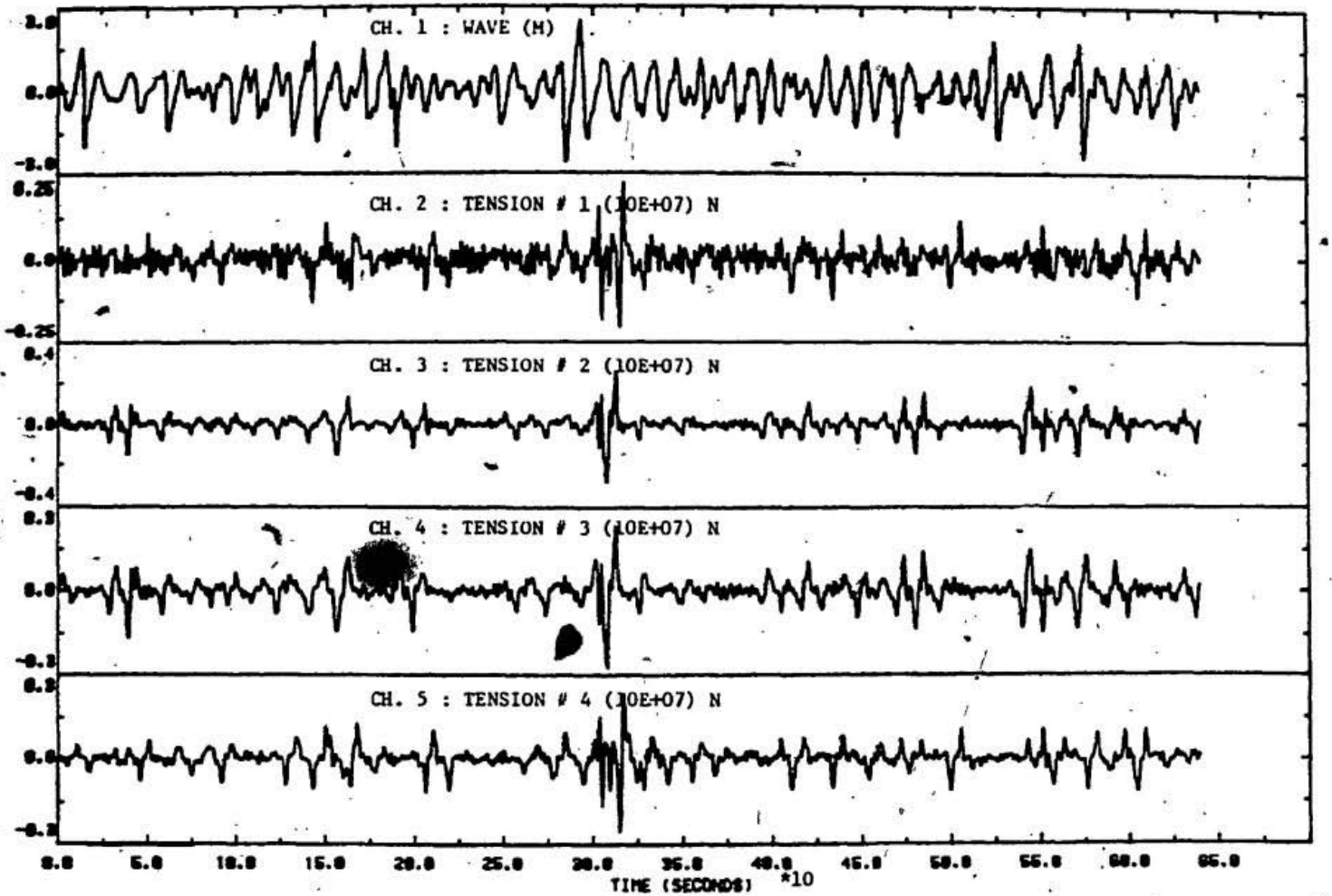

FIG. 8.16 TIME RECORDS FROM IRREG. SEA TEST : INTACT CASE (0° HEADING)

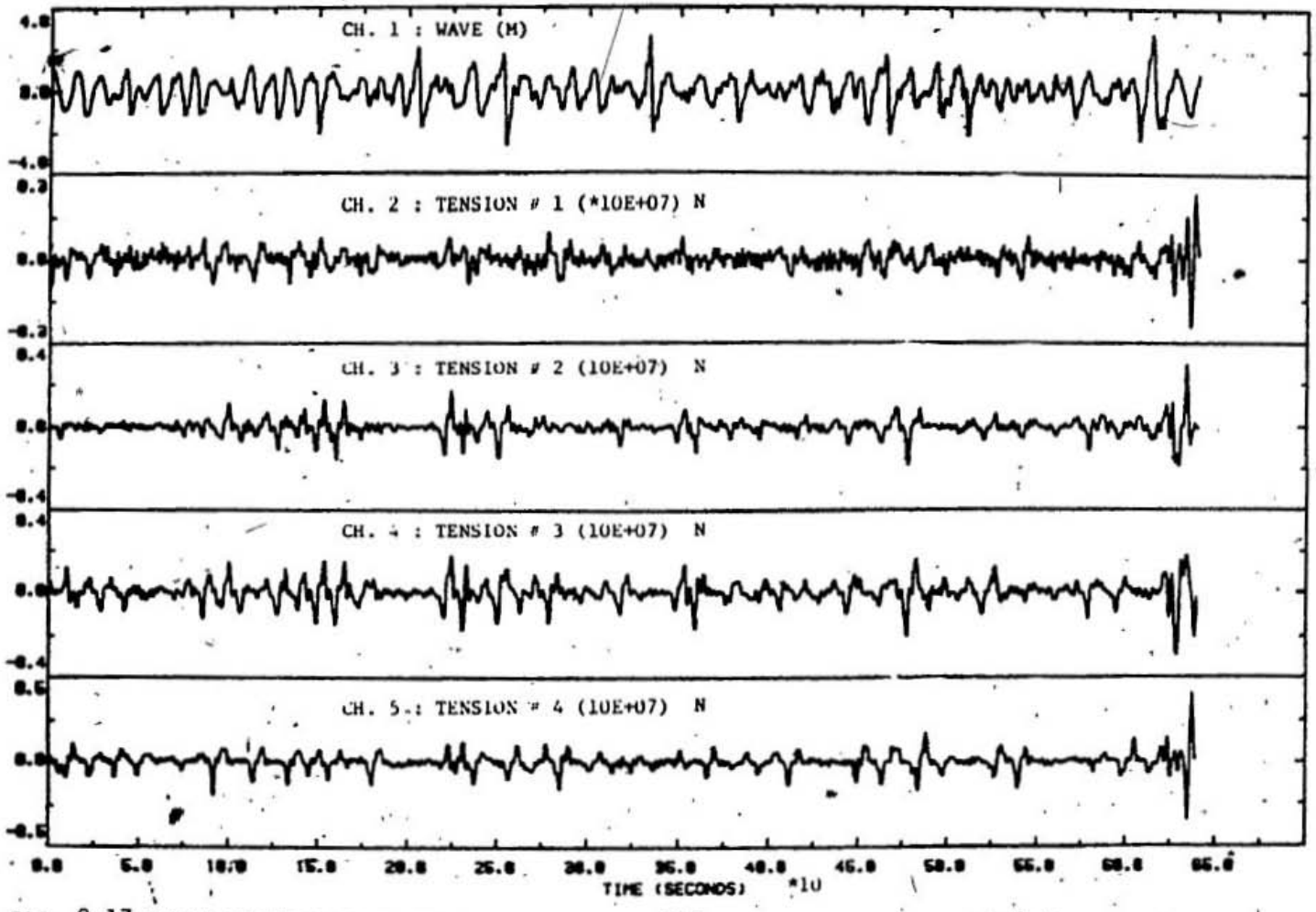

FIG. 8.17 TIME RECORDS FROM IRREG. SEA TEST : 50% LOSS OF TETHER AT # 1 (0° HEADING)

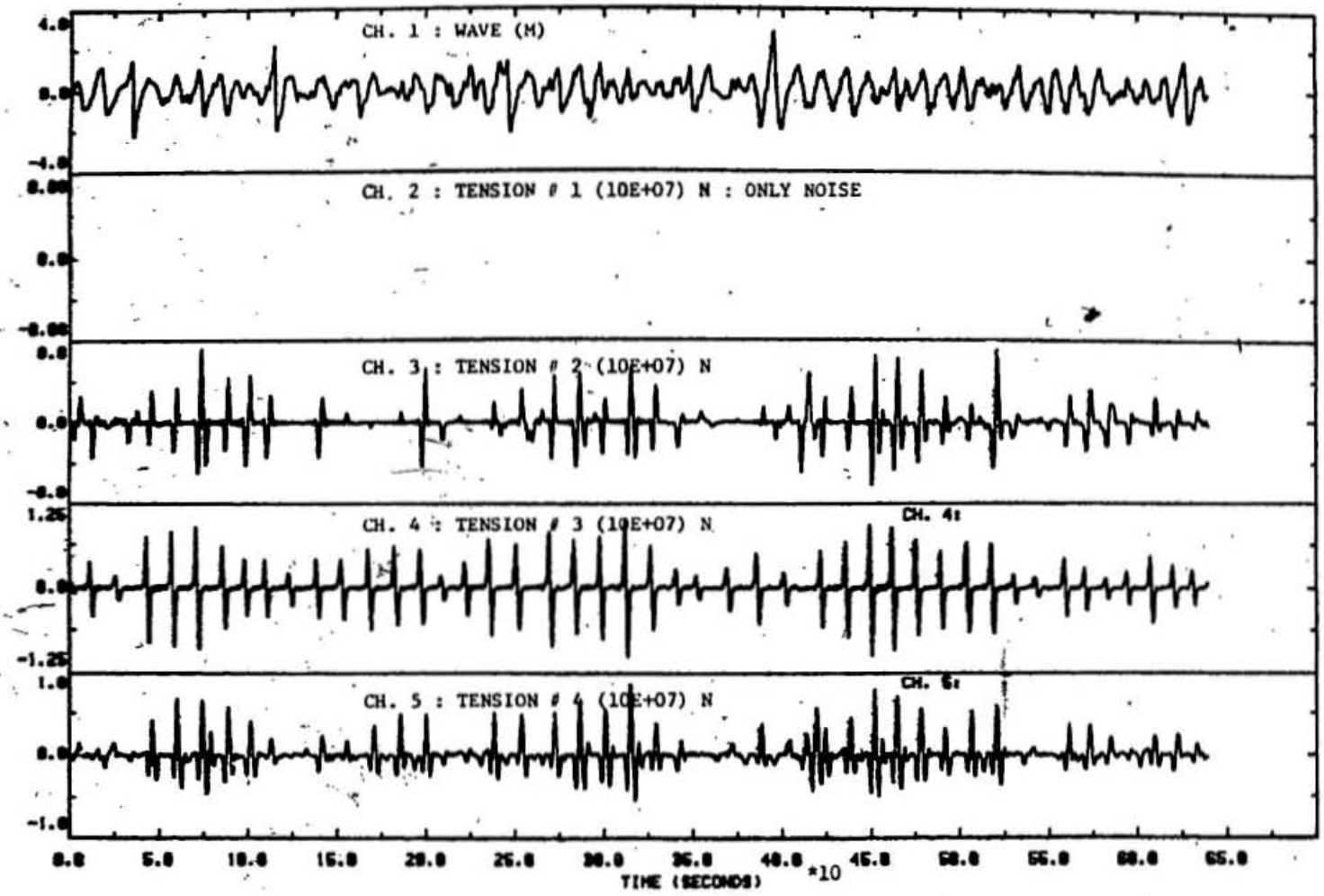

FIG. 8.18 TIME RECORDS FROM IRREG. SEA TEST : 100% LOSS OF TETHER AT # 1 (0° HEADING)

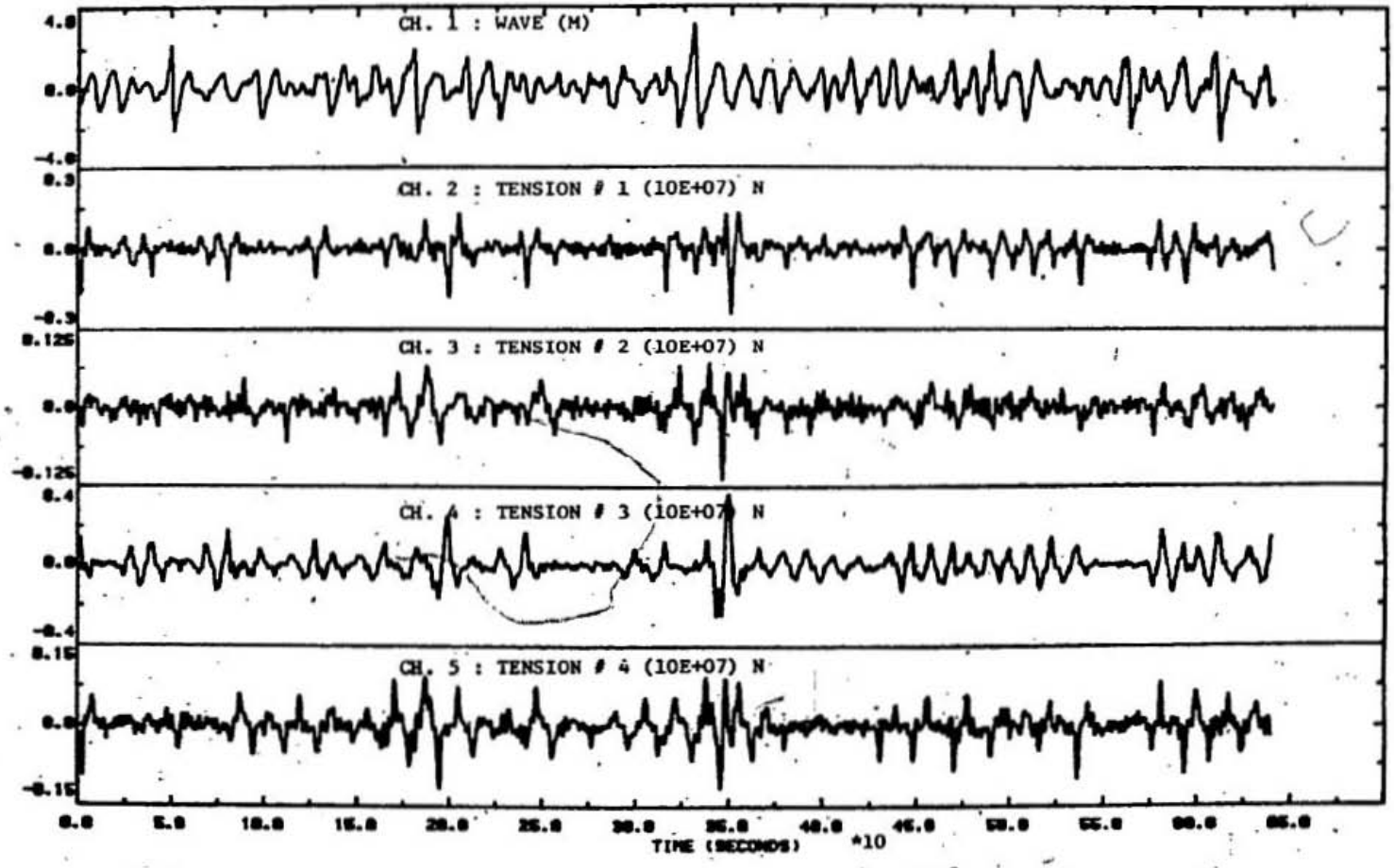

FIG. 8.19 TIME RECORDS FROM IRREG. SEA TEST : INTACT CASE (45° HEADING)

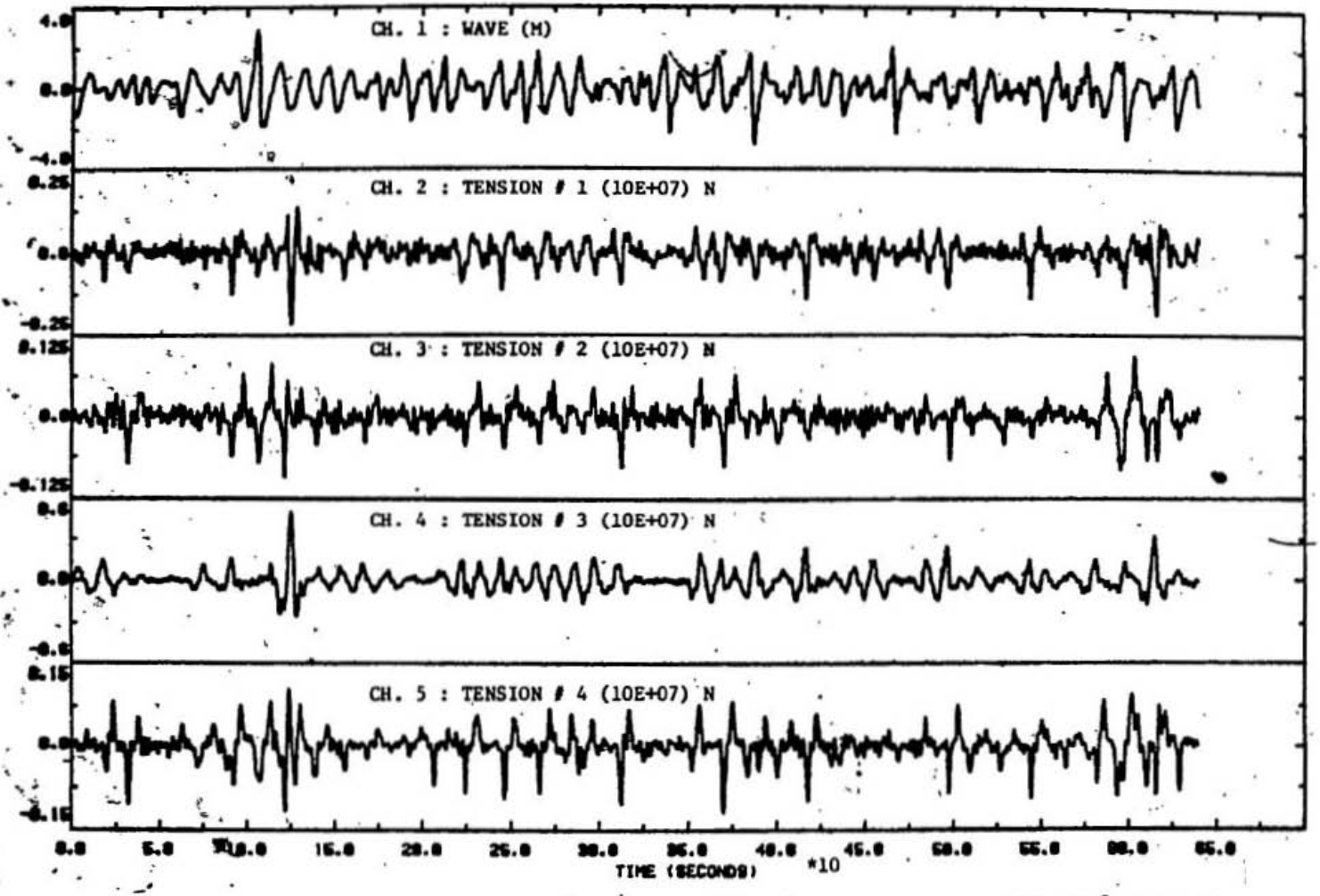

FIG. 8.20 TIME RECORDS FROM IRREG. SEA TEST : 50% LOSS OF TETHER AT # 1 (45° HEADING)

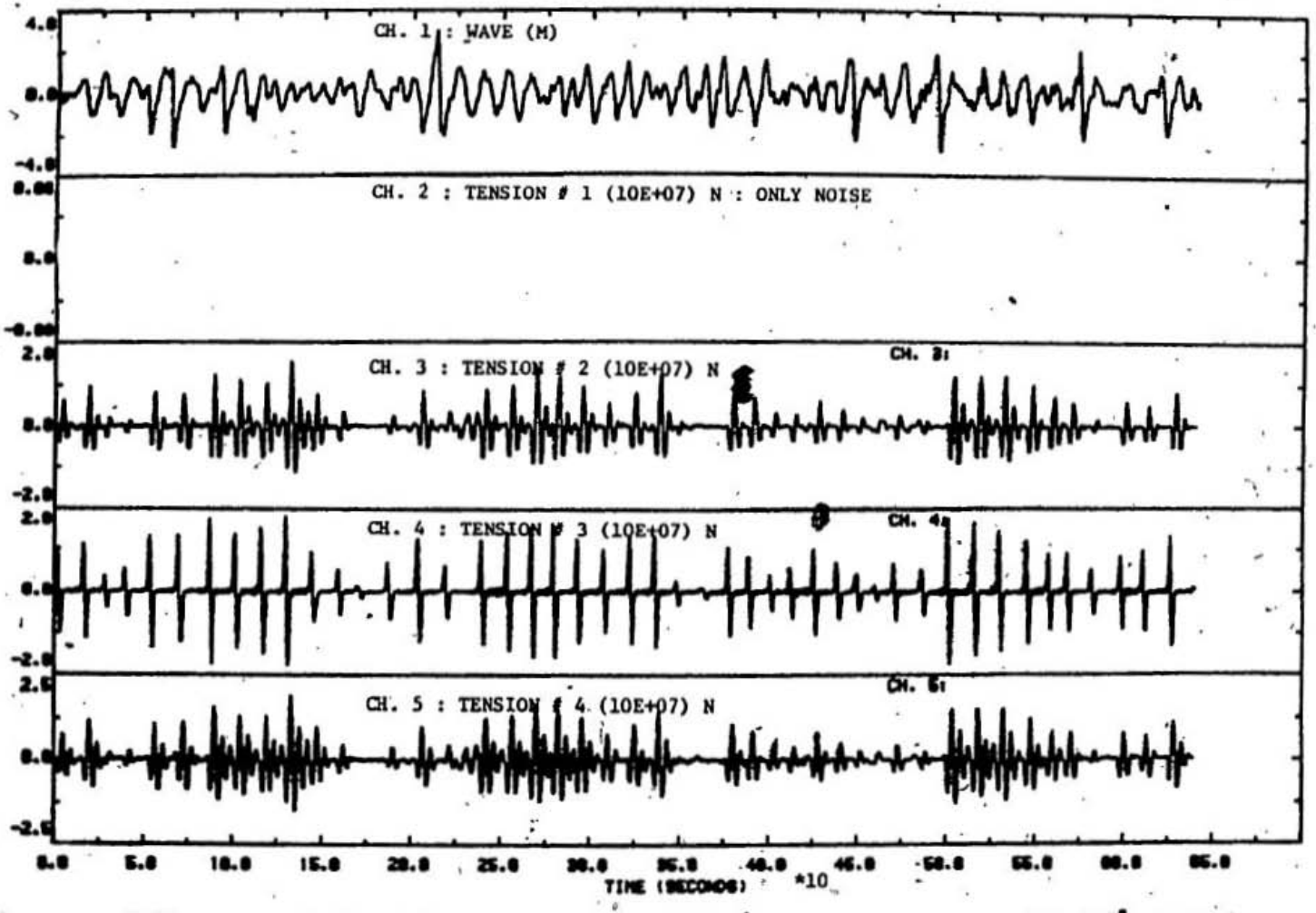

FIG. 8.21 TIME RECORDS FROM IRREG. SEA TEST : 100% LOSS OF TETHER AT # 1 (45° HEADING)

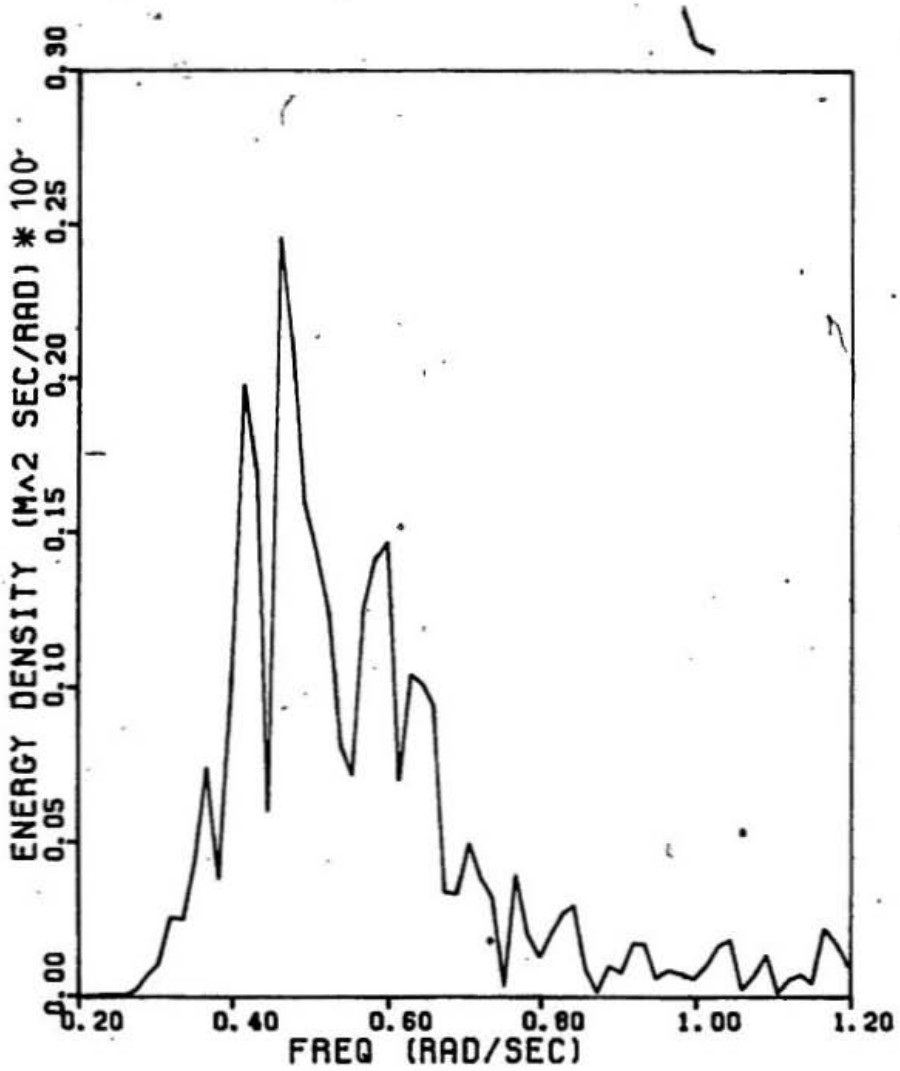

FIG. 8.22 A TYPICAL PIERSON-MOSKOWITZ WAVE ENERGY SPECTRUM (WIND SPEED = 20 M/SEC), DERIVED FROM THE WAVE TIME HISTORY

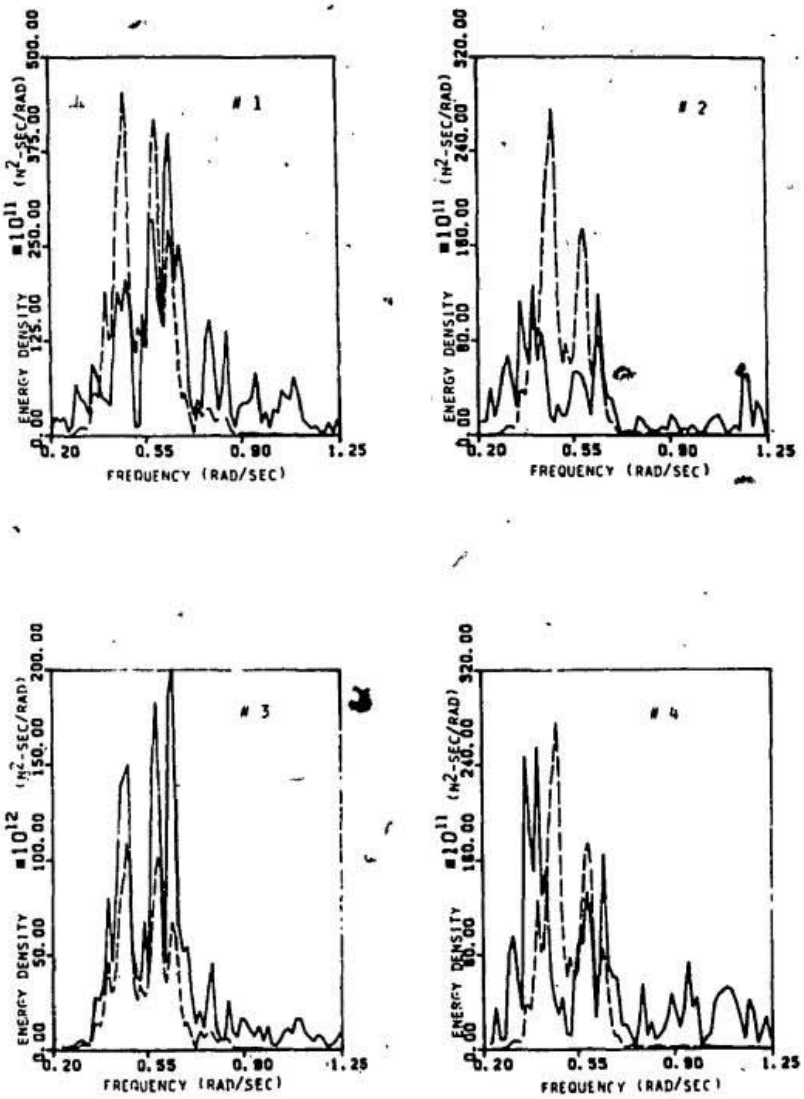

FIG. 8.23 TENSION SPECTRA : INTACT CASE (0° HEADING)

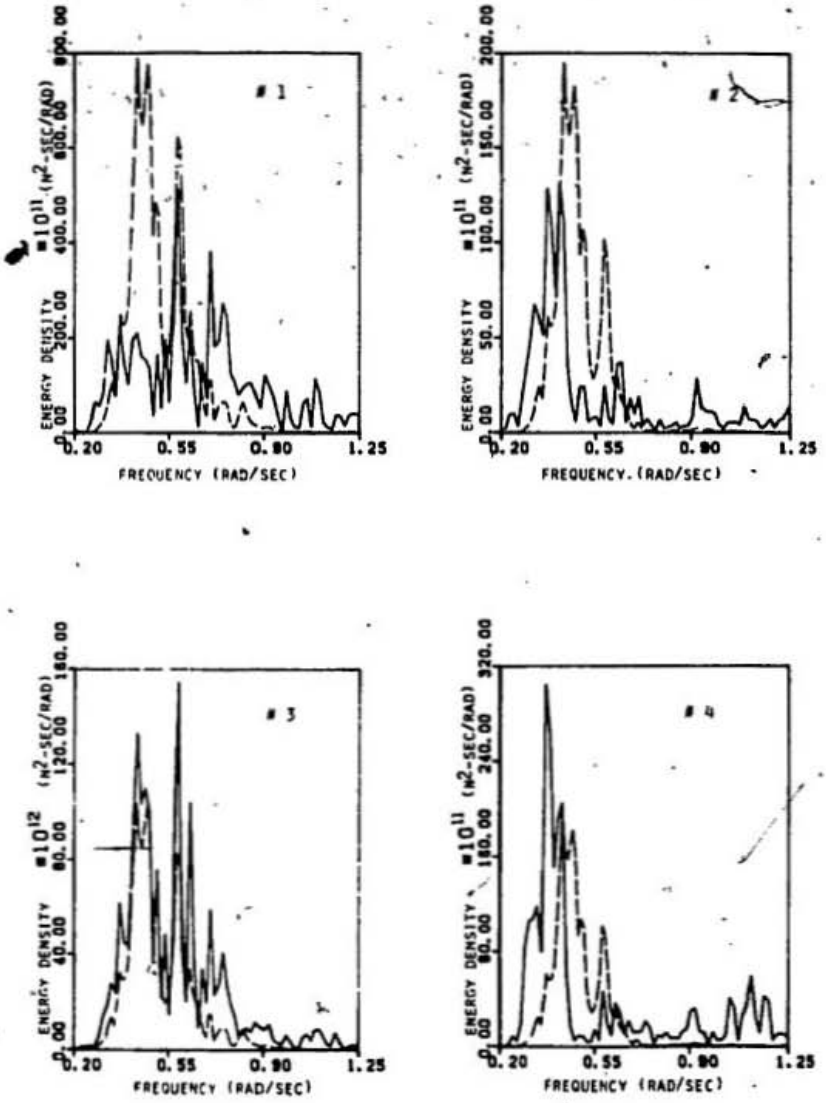

THEORETICAL _____

EXPERIMENTAL ____

FIG. 8.24 TENSION SPECTRA : 50% TETHER LOSS AT # 1 (0° HEADING)

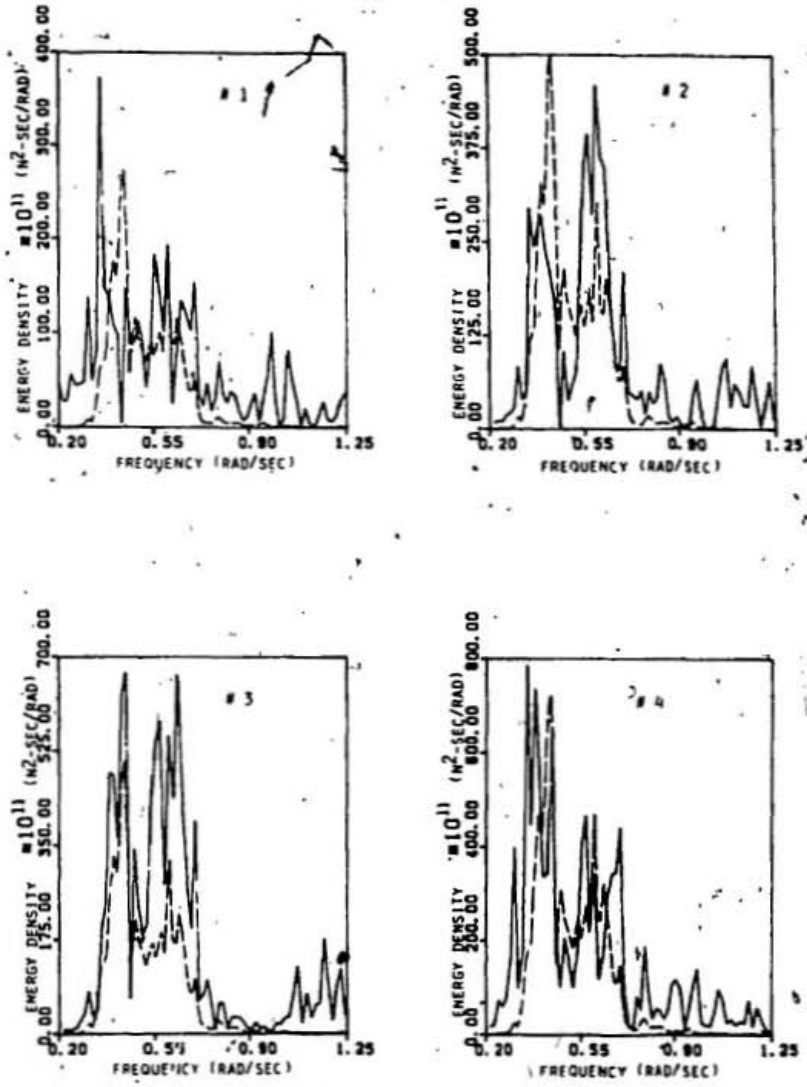

FIG. 8.25 TENSION SPECTRA : INTACT CASE (45° HEADING)

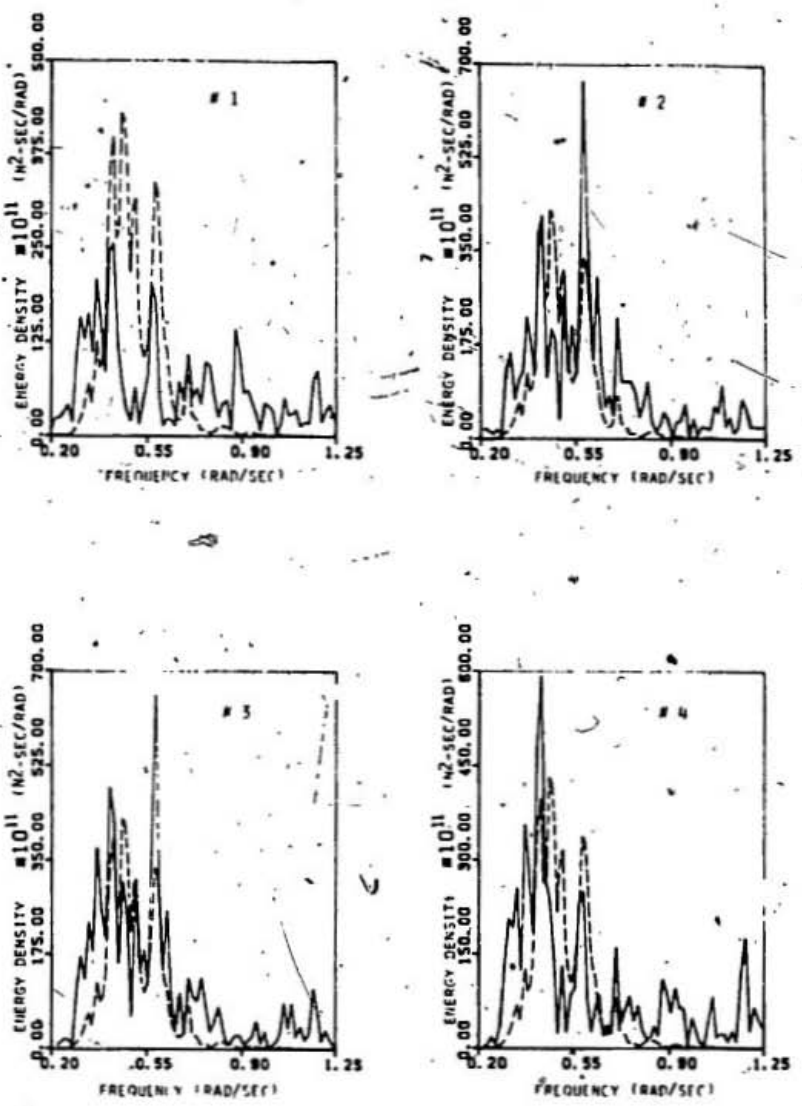

FIG. 8.26 TENSION SPECTRA : 50% TETHER LOSS AT # 1 (45° HEADING)

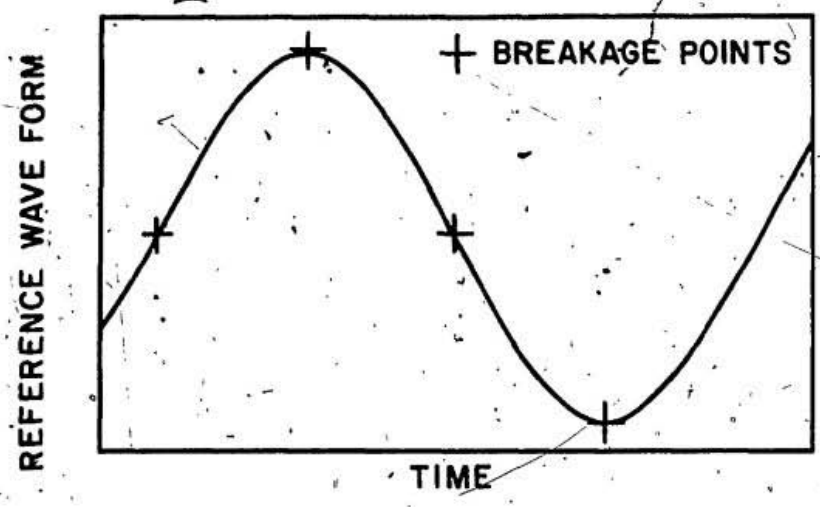

FIG. 8.27A TETHER BREAKAGE INSTANTS

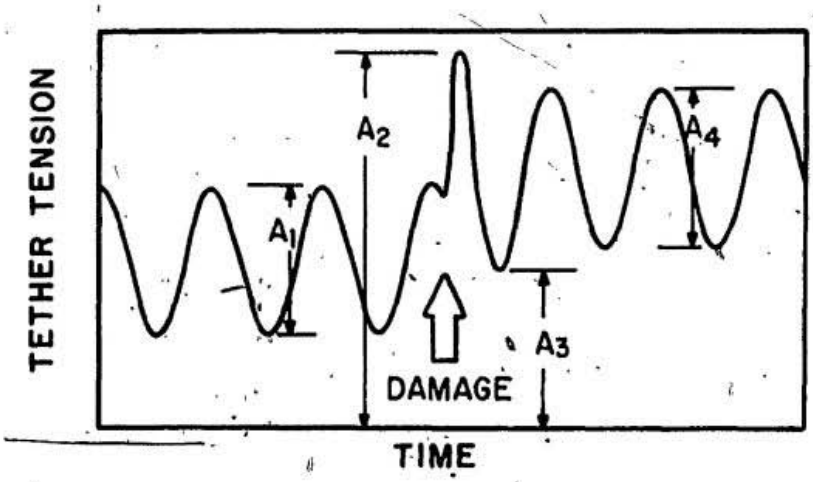

FIG. 8.27B DEFINITION OF RESPONSE PARAMETERS USED FOR COMPARISONS

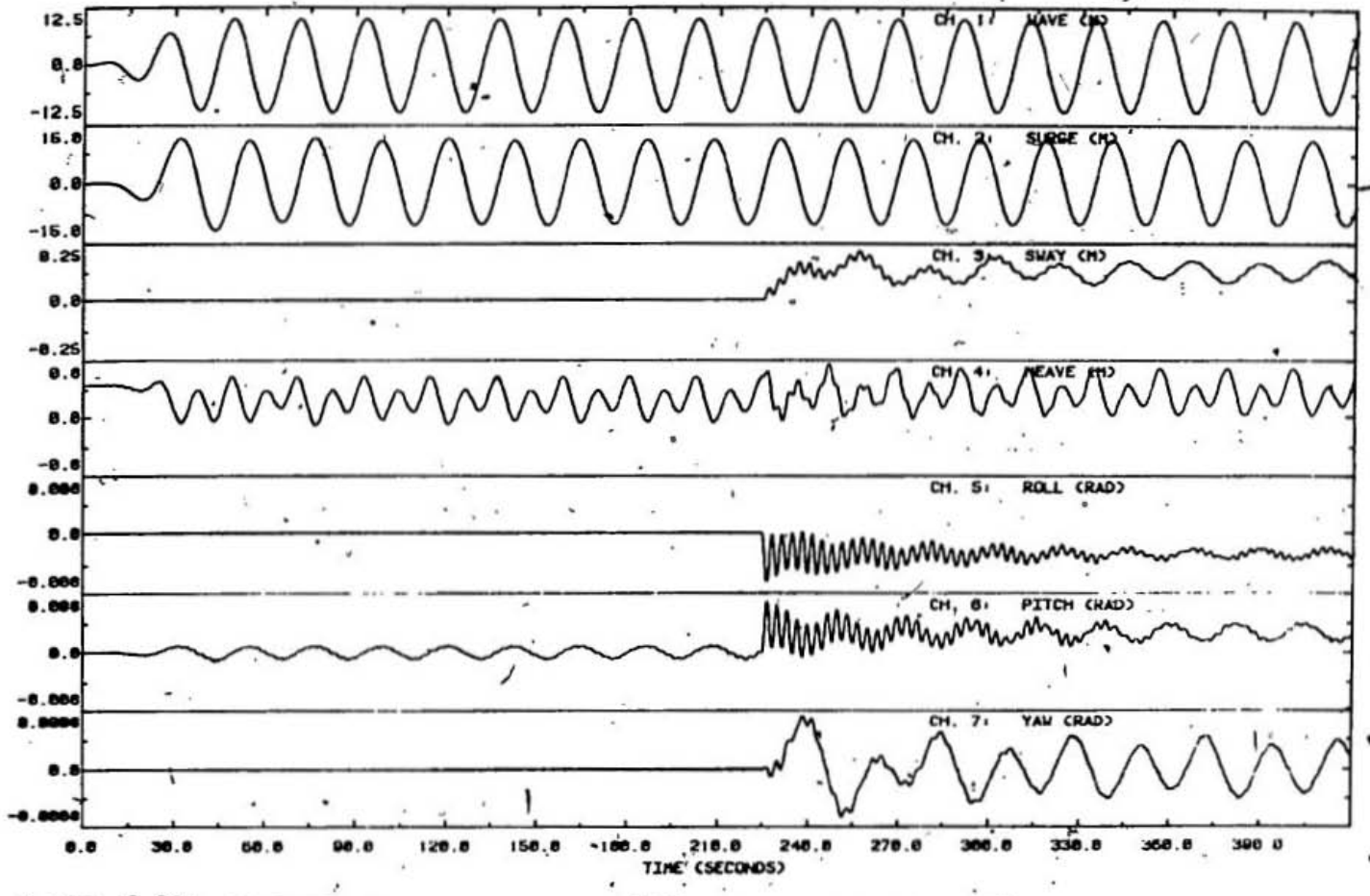

FIG. 8.28A COMPUTED MOTION RESPONSES : 50% TETHER LOSS AT # 1 (0° HEADING)

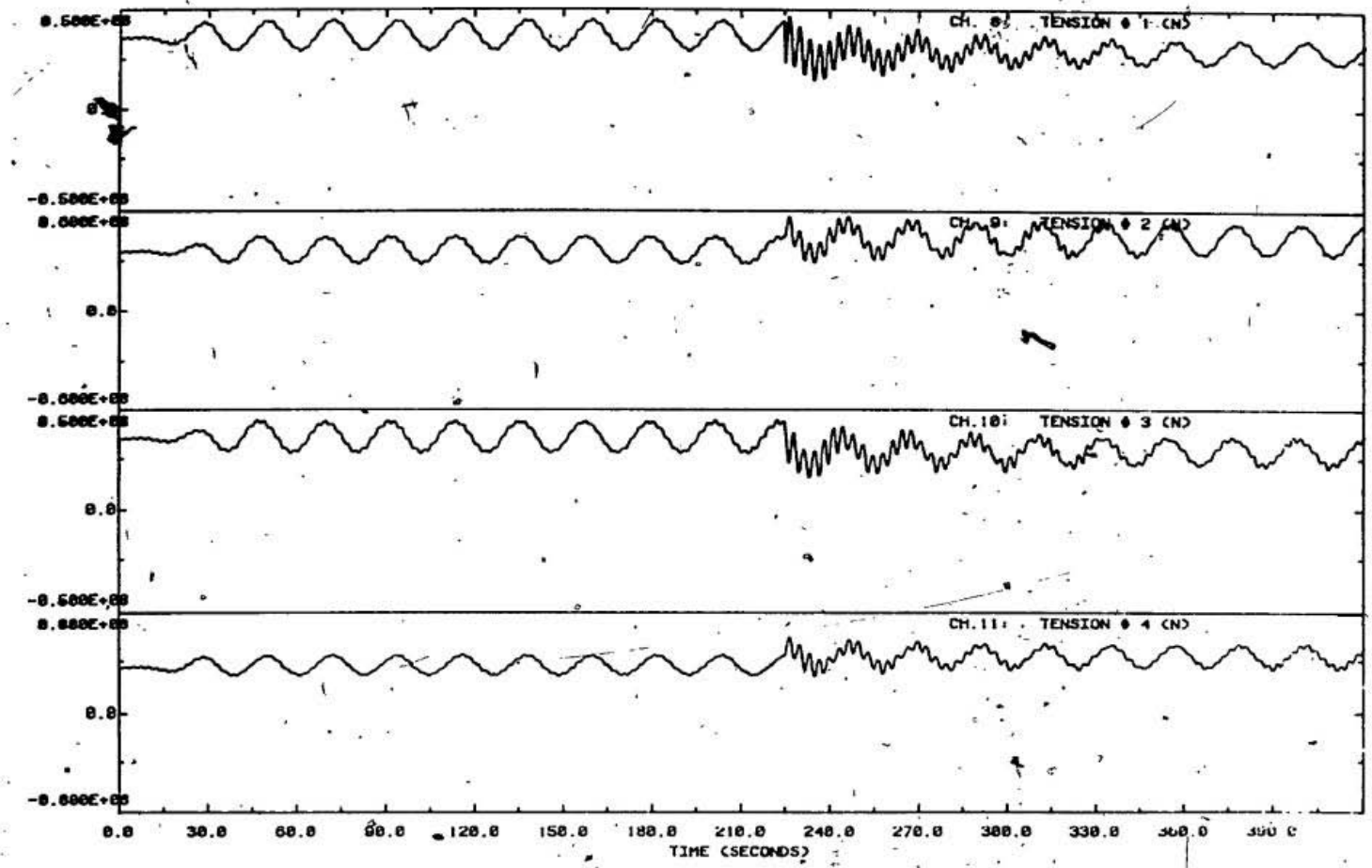

FIG. 8.28B COMPUTED TENSION RESPONSES : 50% TETHER LOSS AT # 1 (0° HEADING)

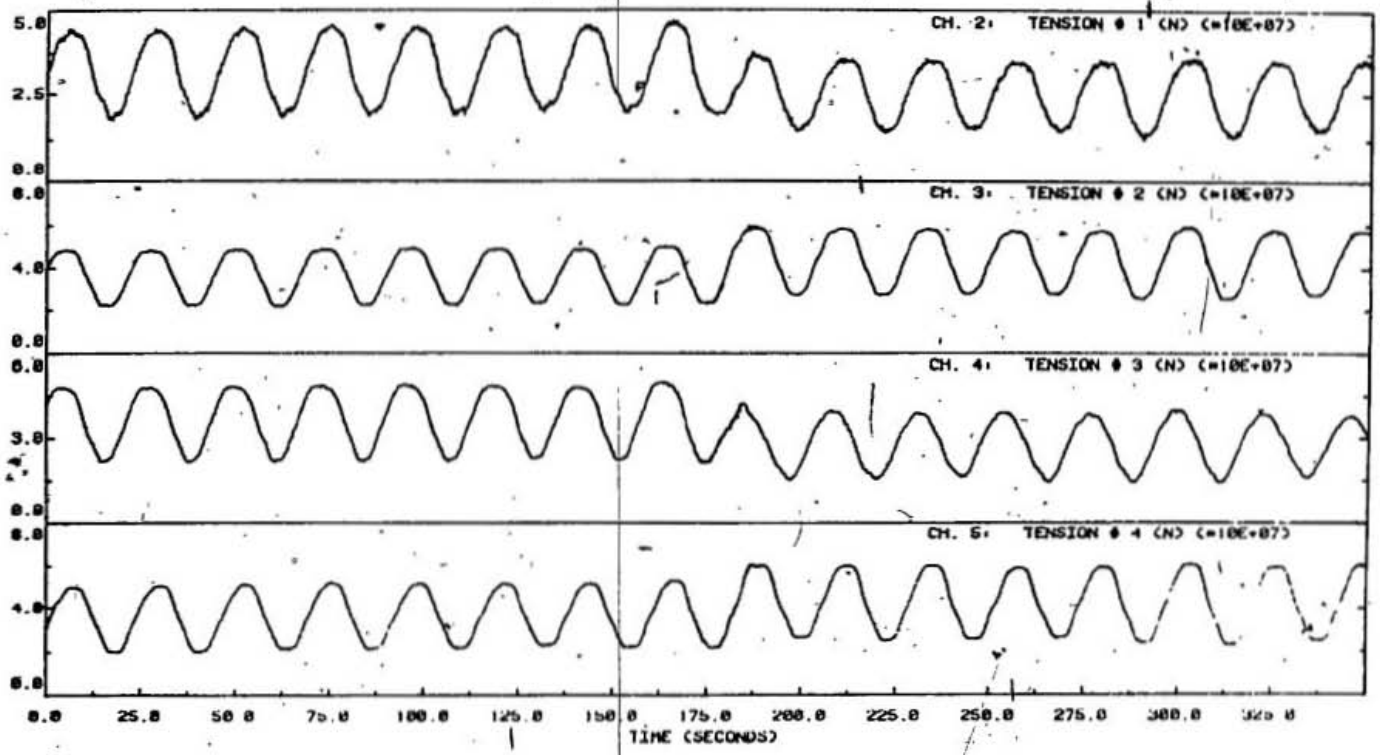

FIG. 8.29 EXPERIMENTAL TENSION RESPONSES : 50% TETHER LOSS AT # 1 (0° HEADING)

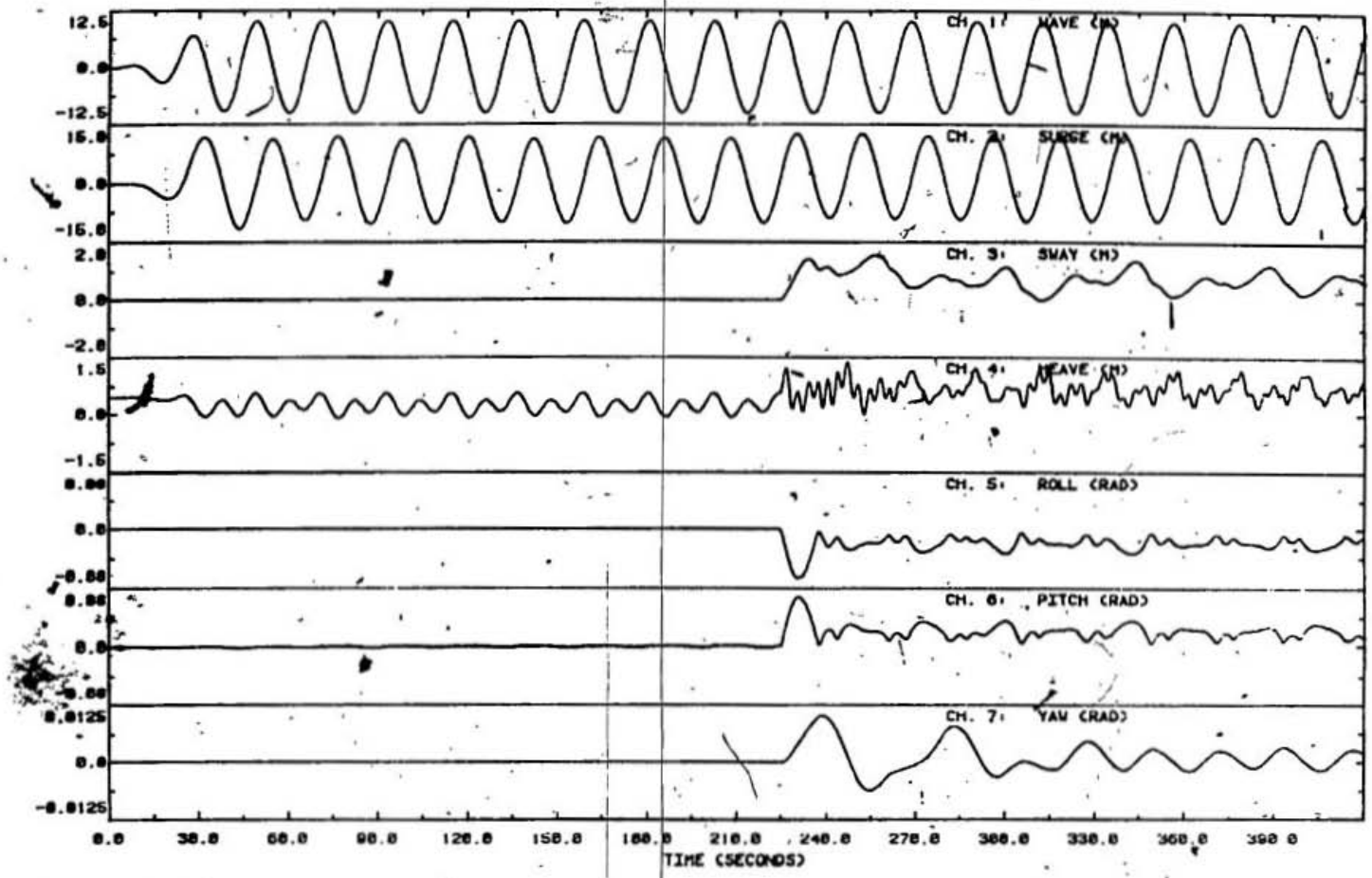

FIG. 8.30A. COMPUTED MOTION RESPONSES : 100% TETHER LOSS AT # 1 (0° HEADING)

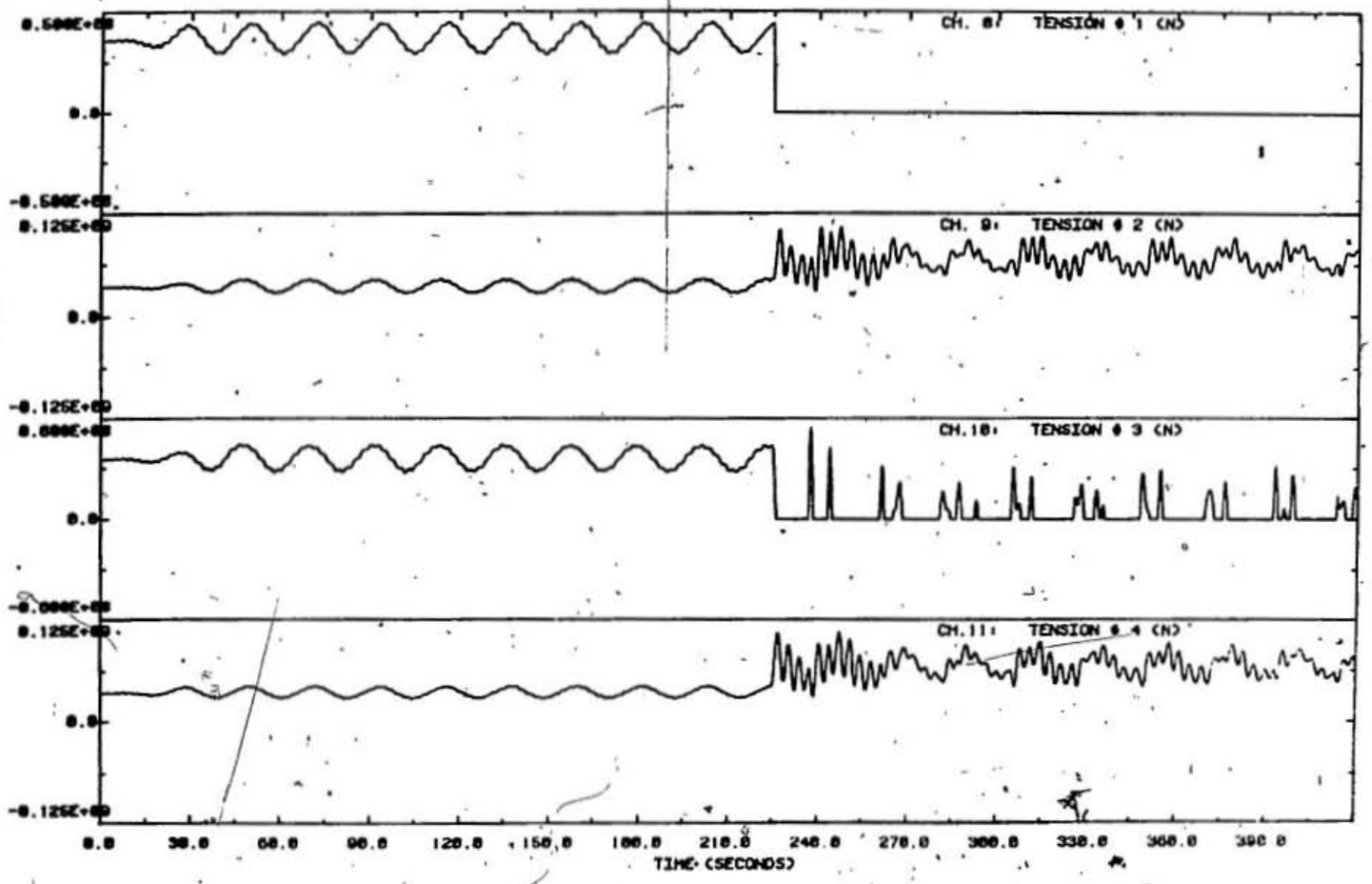

FIG. 8.30B COMPUTED TENSION RESPONSES : 100% TETHER LOSS AT # 1 (0° HEADING)

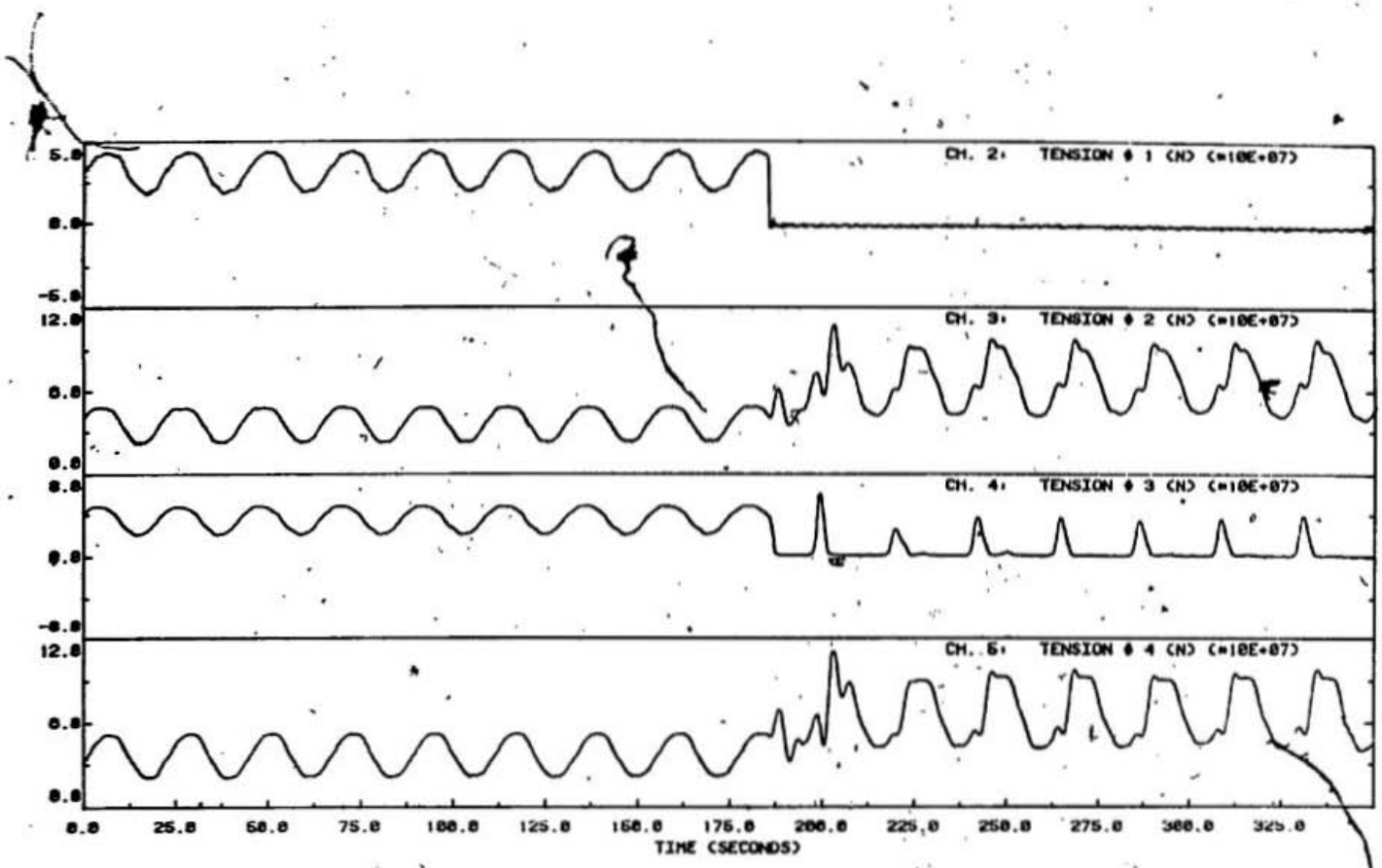

FIG. 8.31 EXPERIMENTAL TENSION RESPONSES : 100% TETHER LOSS AT # 1 (0° HEADING)

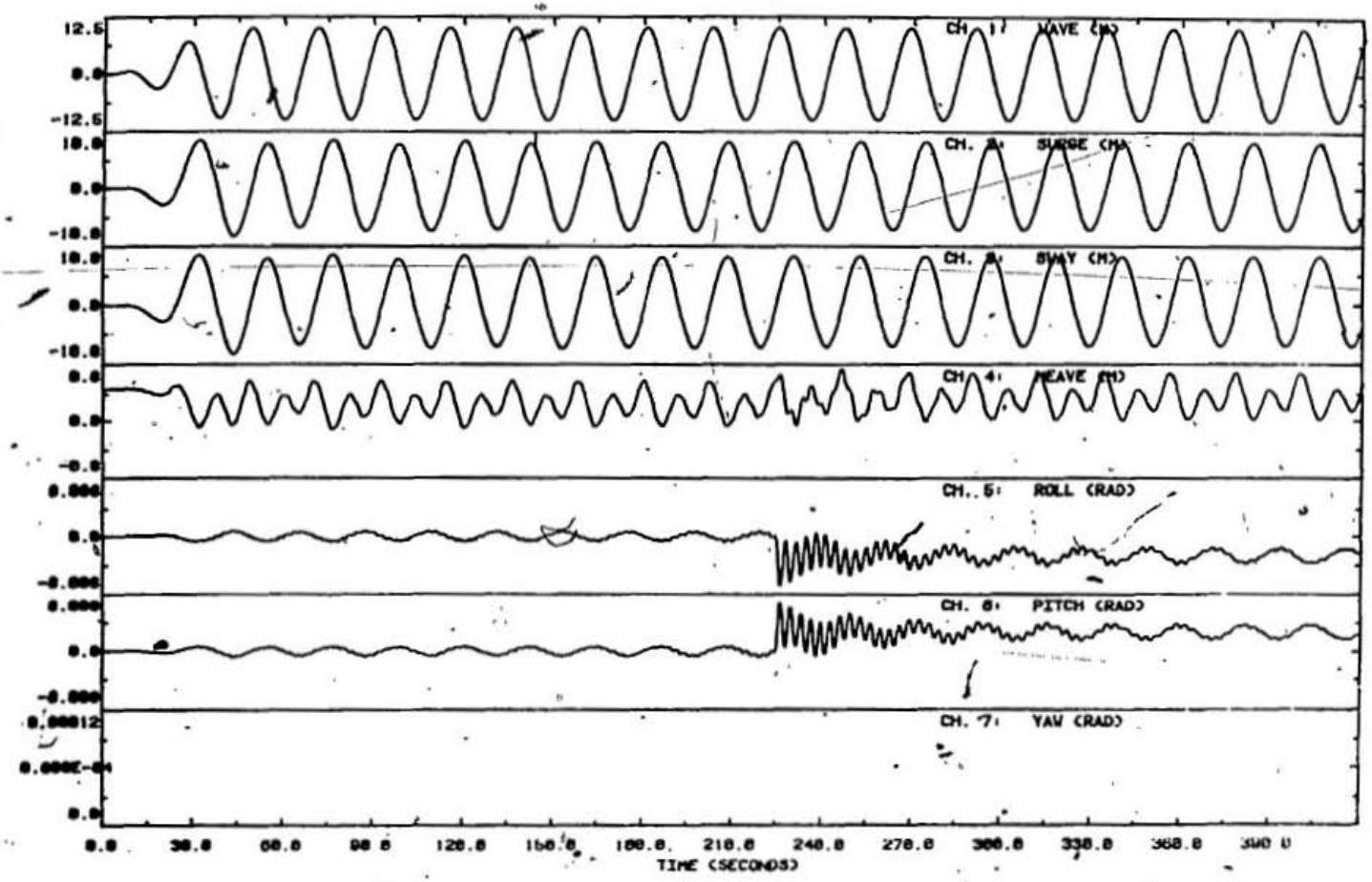

FIG. 8.32A COMPUTED MOTION RESPONSES : 50% TETHER LOSS AT # 1 (45° HEADING)

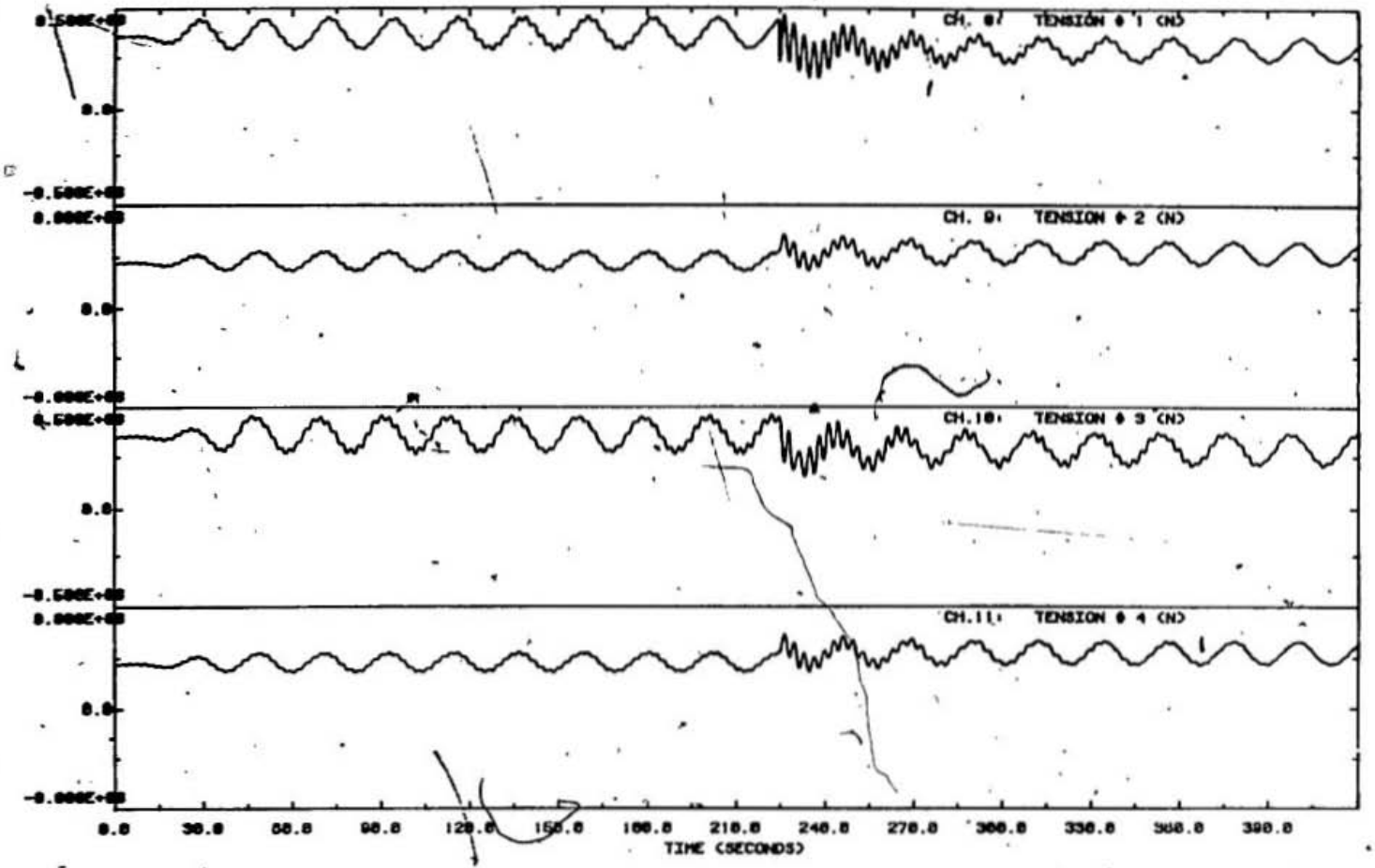

FIG. 8.32B COMPUTED TENSION RESPONSES : 50% TETHER LOSS AT # 1 (45° HEADING)

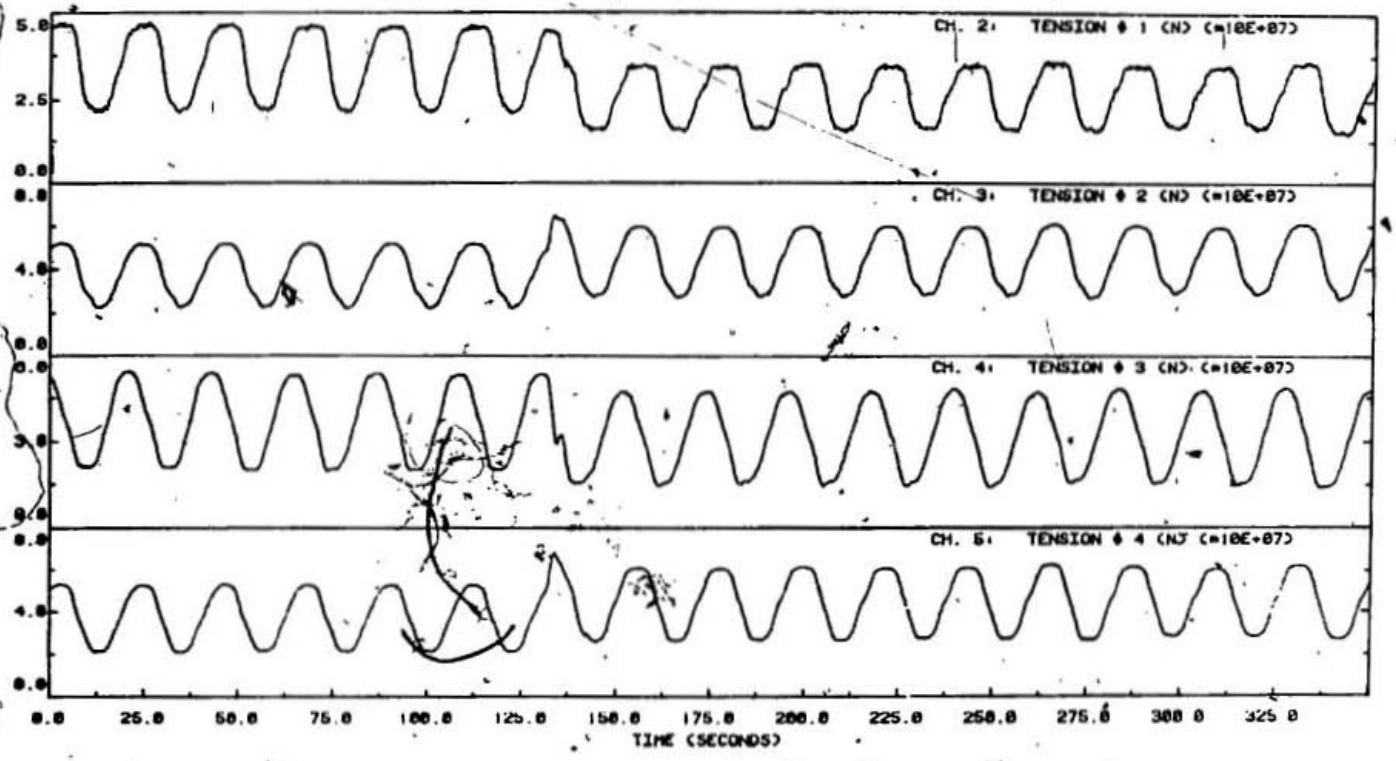

FIG. 8.33 EXPERIMENTAL TENSION RESPONSES : 50% TETHER LOSS AT # 1 (45° HEADING)

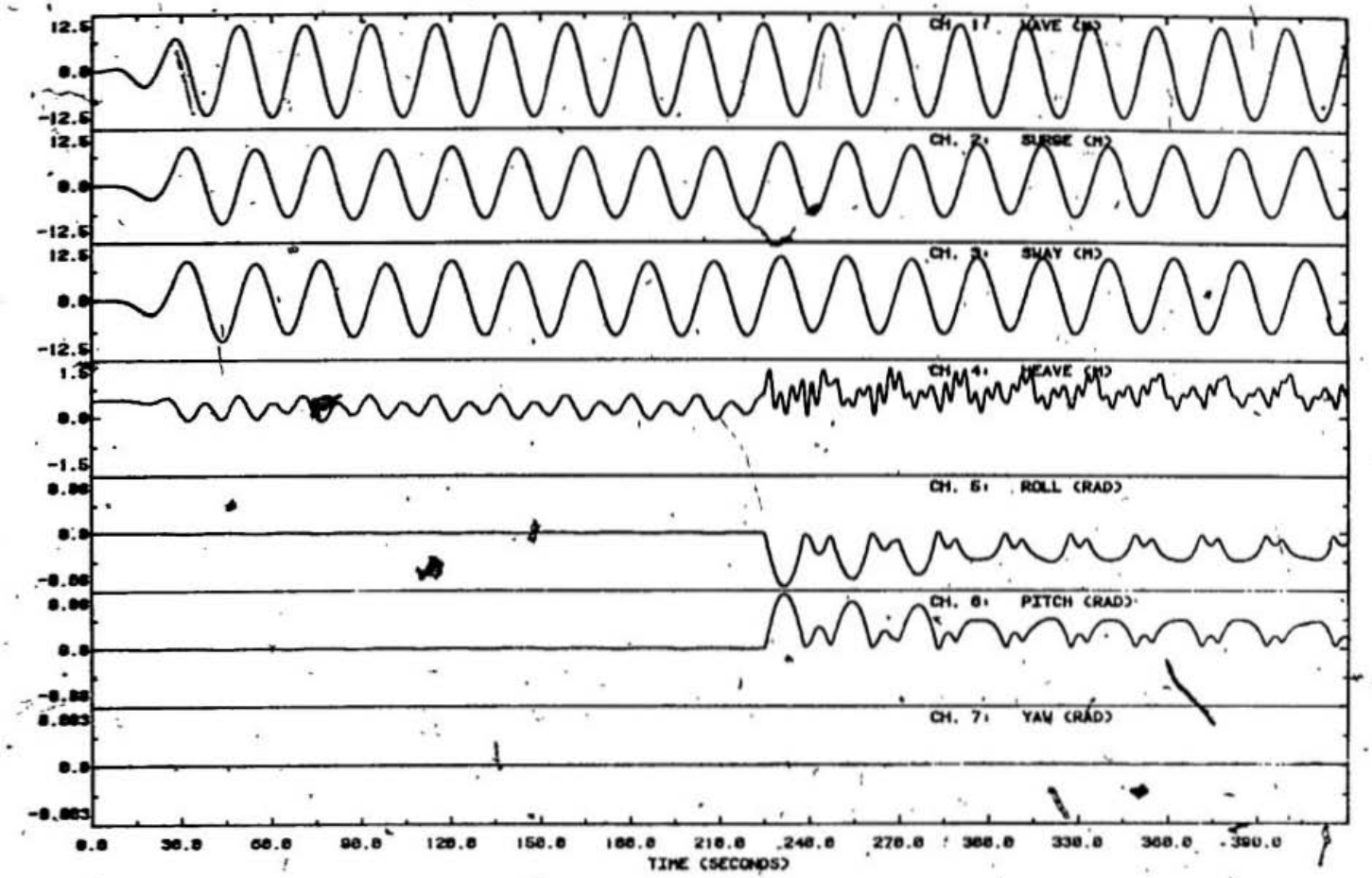

FIG. 8.34A COMPUTED MOTION RESPONSES : 100% TETHER LOSS AT # 1 (45° HEADING)

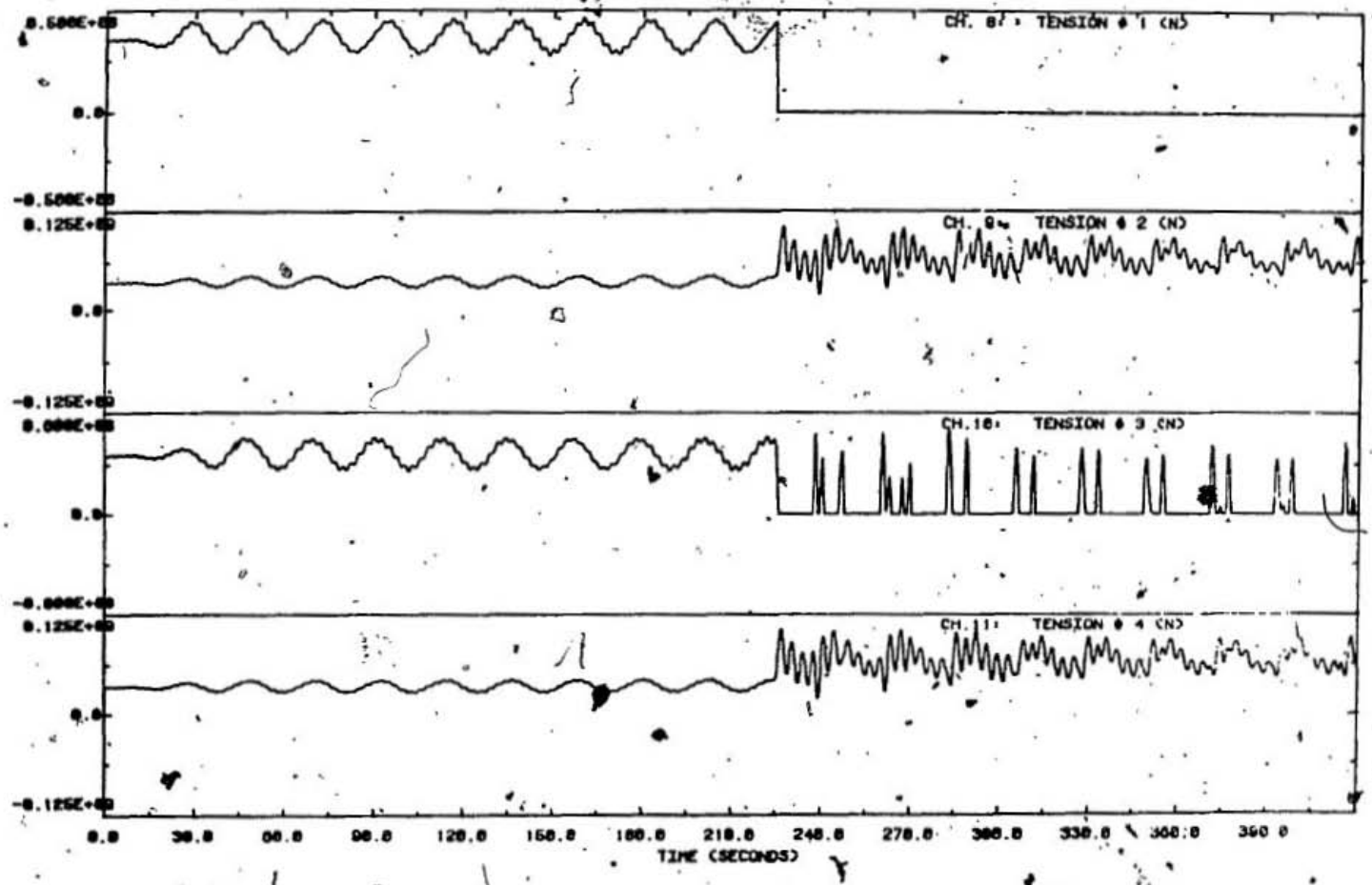

FIG. 8.34B COMPUTED TENSION RESPONSES : 100% TETHER LOSS AT # 1 (45° HEADING)

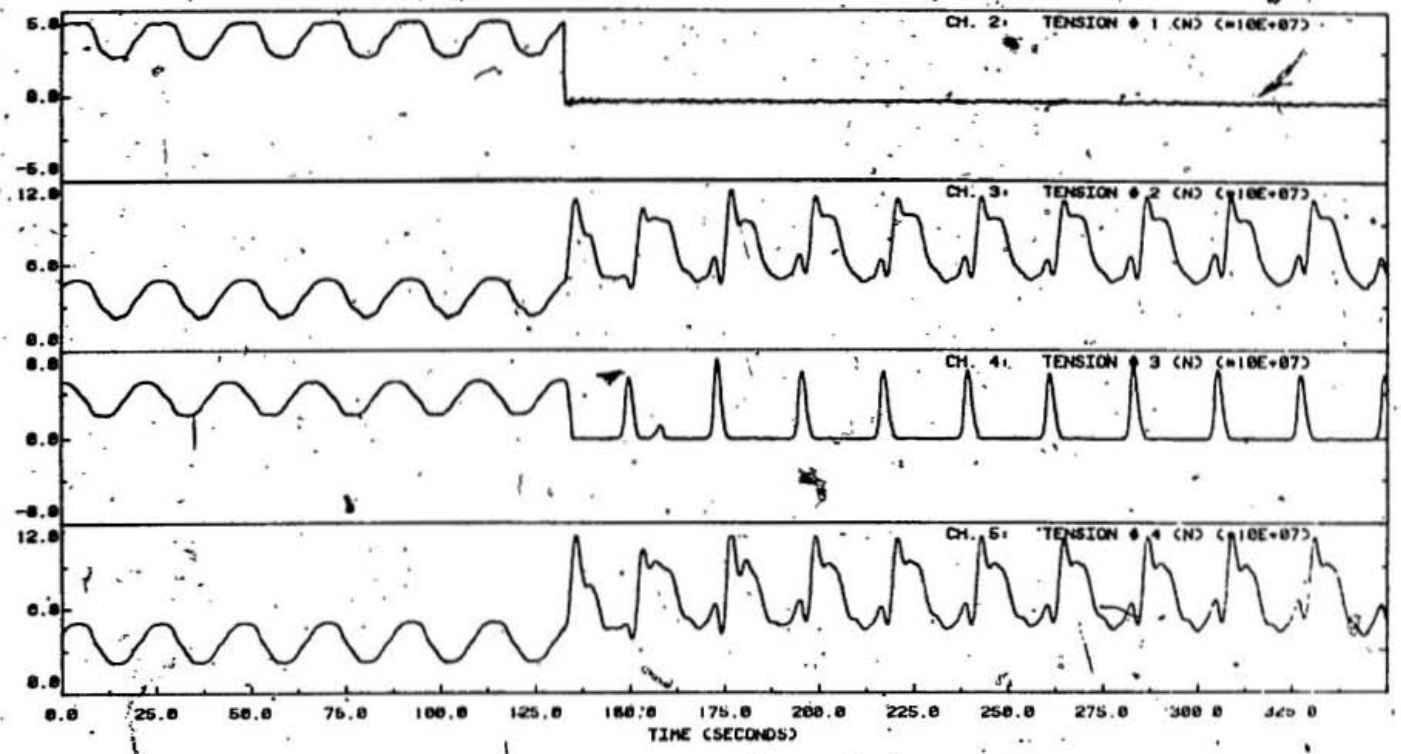

FIG. 8.35 EXPERIMENTAL TENSION RESPONSES : 100% TETHER LOSS AT # 1 (45° HEADING)

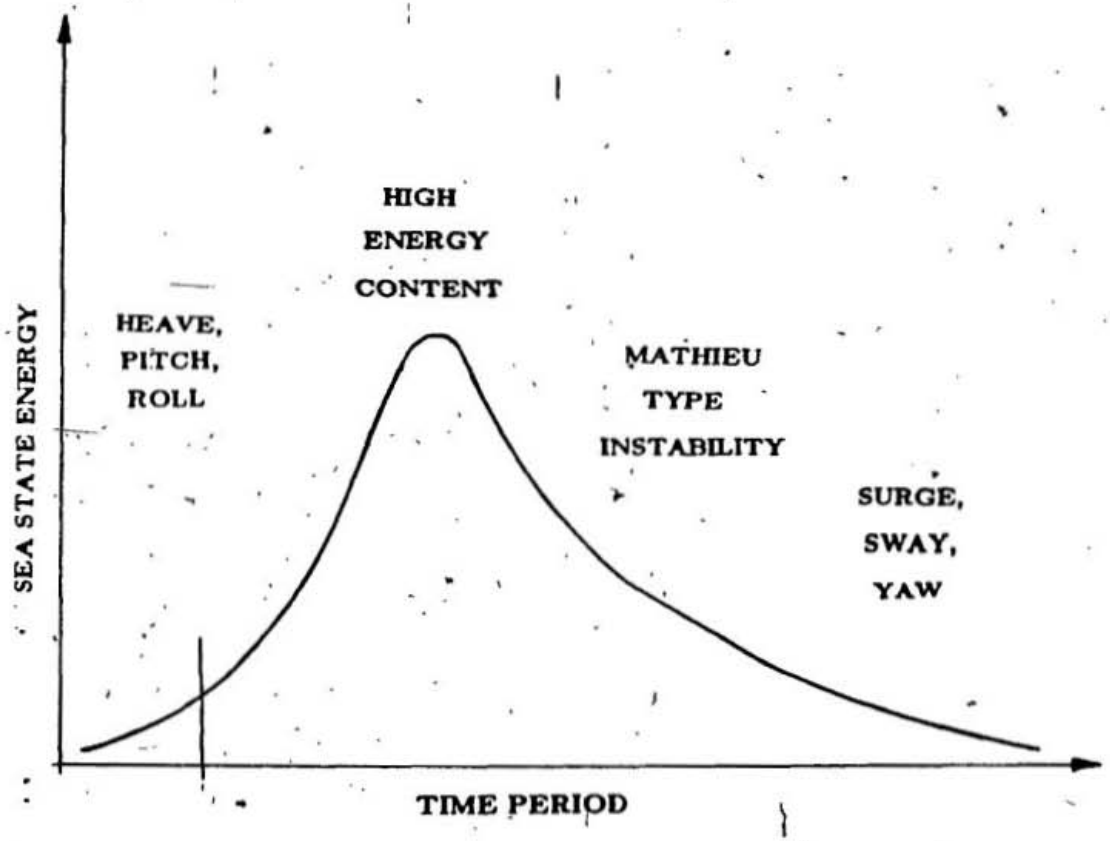

Fig.9.1 TYPICAL UNSTABLE TIME PERIODS

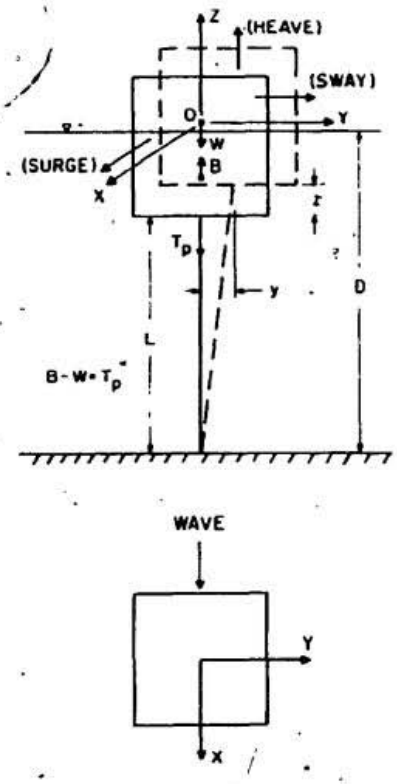

PLATFORM DATA

DISPLACEMENT	45,000 m^3
TOTAL PRETENSION (T_p)	1.5×10^8, 1×10^8, 0.5×10^8 N
WATER DEPTH (D)	160 m
LENGTH OF TETHER (L)	125 m
AXIAL STIFFNESS OF TETHER	30×10^7 N/m

Fig. 9.2 SIMPLIFIED MODEL OF A TENSION LEG STRUCTURE

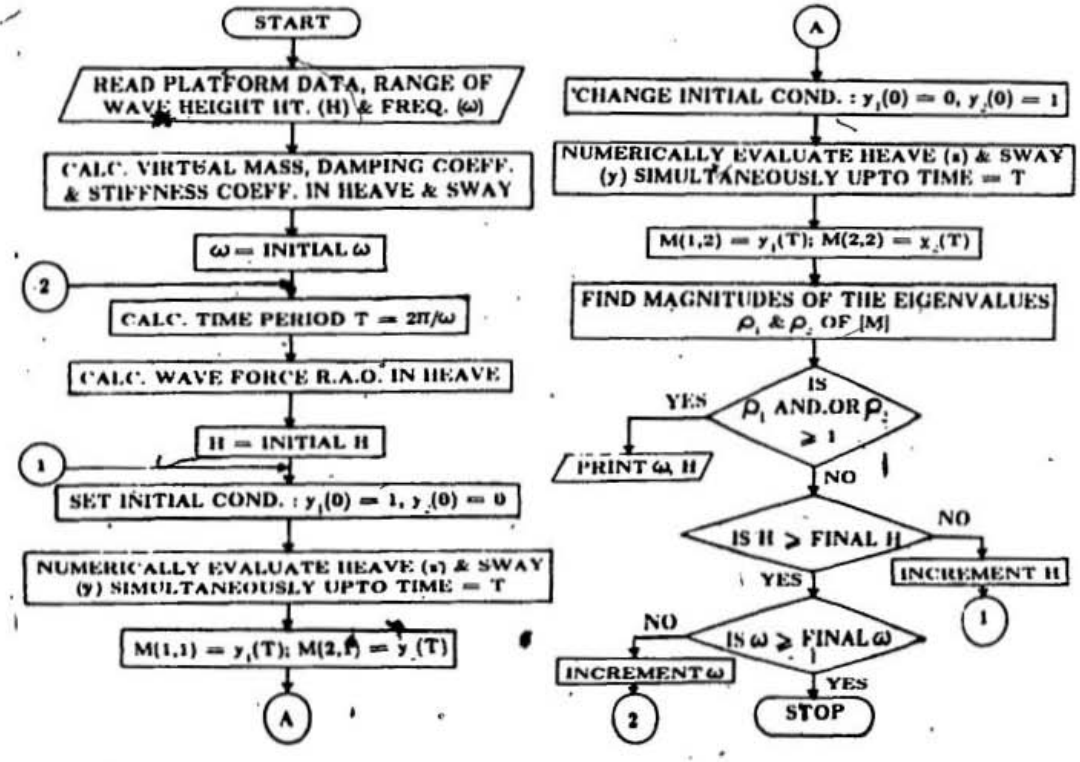

Fig 93 FLOW CHART FOR EVALUATION OF THE STABILITY BOUNDARY

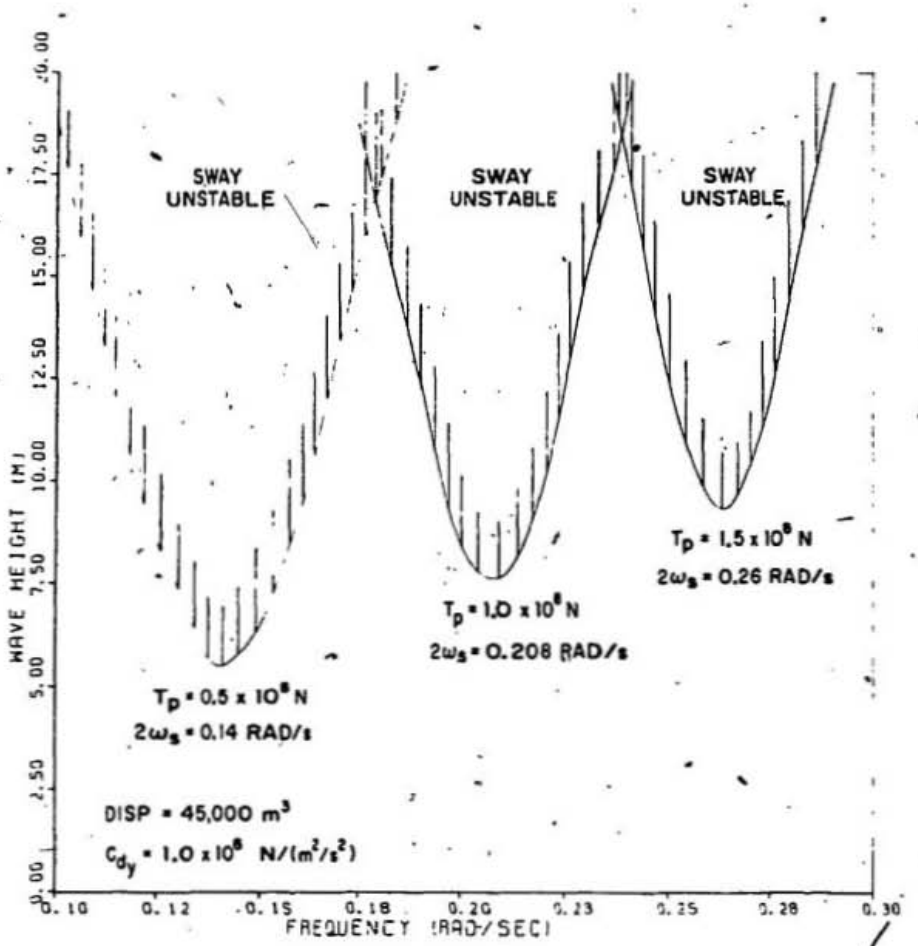

Fig. 9.4 STABILITY BOUNDARIES OF A TLP WITH DIFF. PRETENSIONS

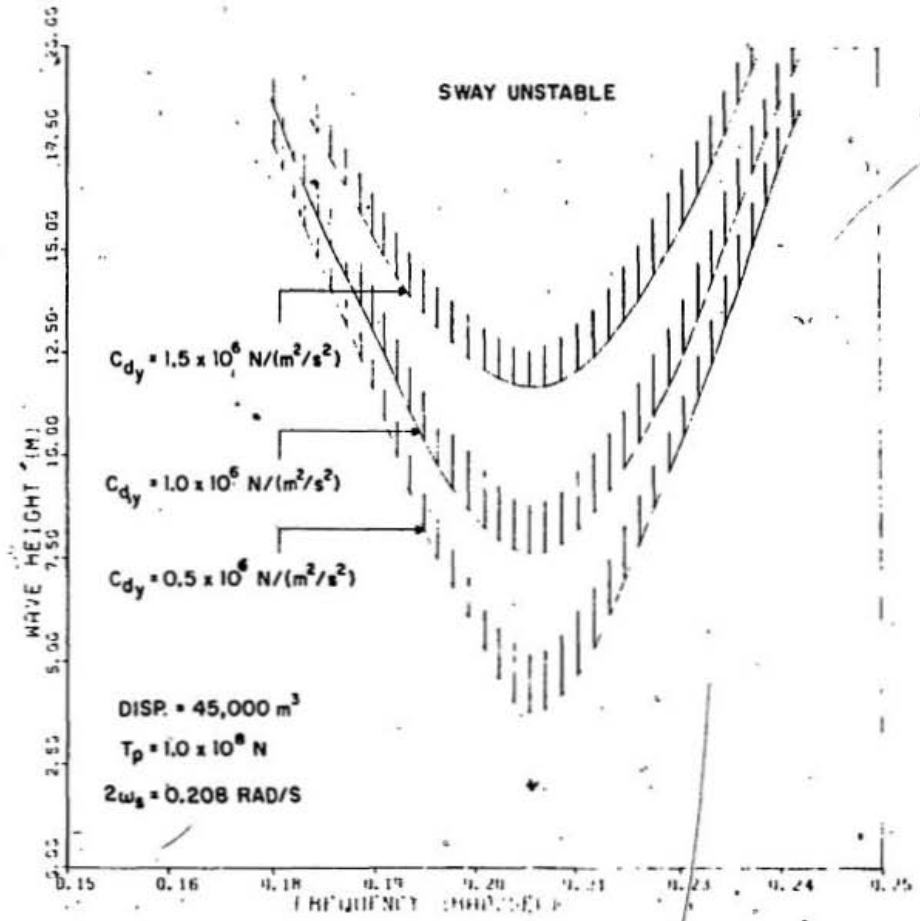

Fig. 9.5 STABILITY BOUNDARIES OF A TLP WITH DIFF. DAMPING COEFF.

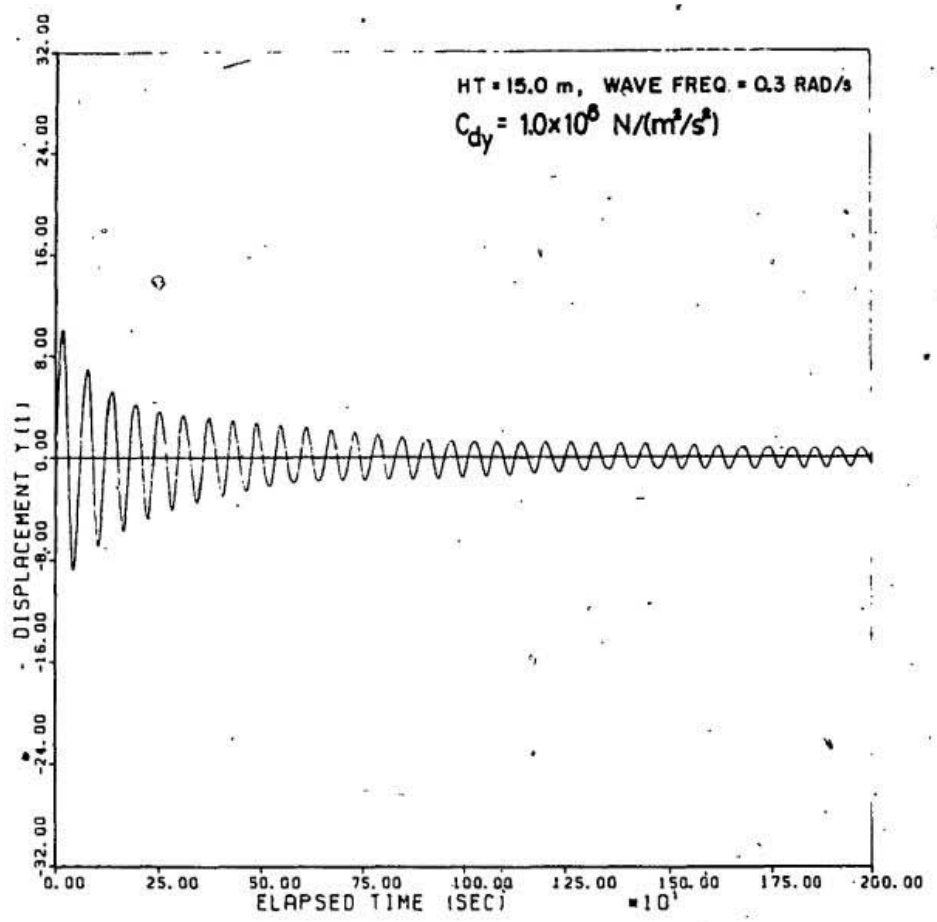

Fig. 9.6 SWAY TIME HISTORY (STABLE CASE)

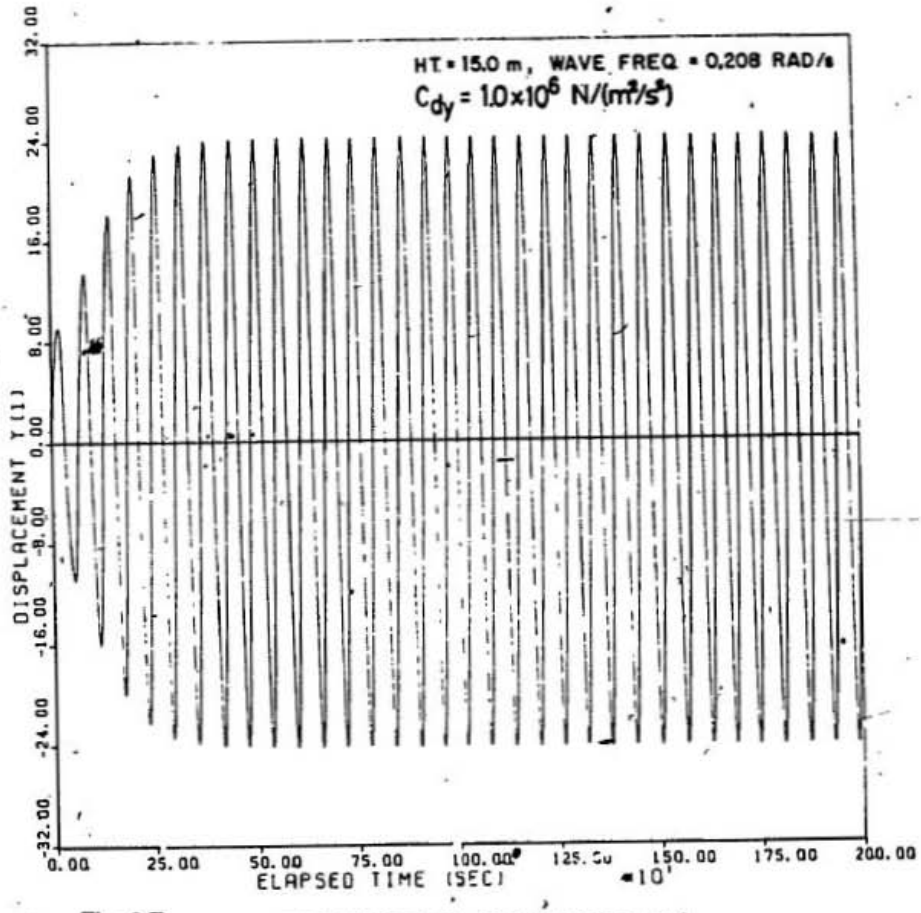

Fig. 9.7 SWAY TIME HISTORY (UNSTABLE CASE)

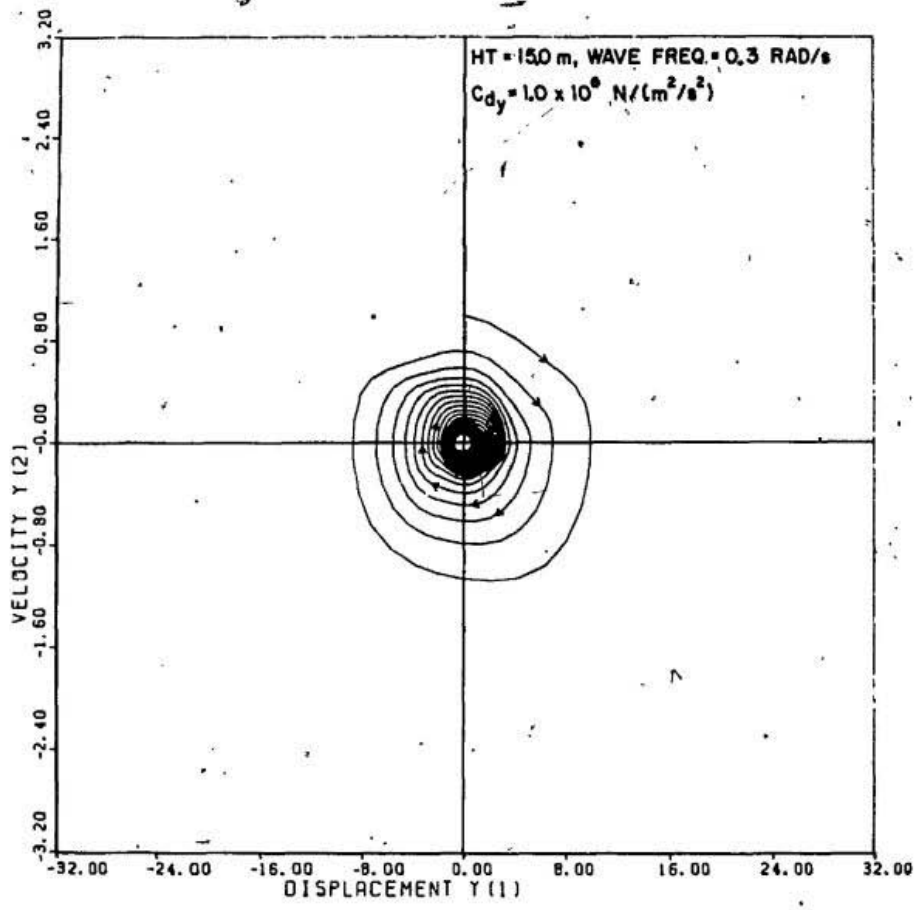

Fig. 9.8 **PHASE PLANE PLOT OF SWAY MOTION (STABLE CASE)**

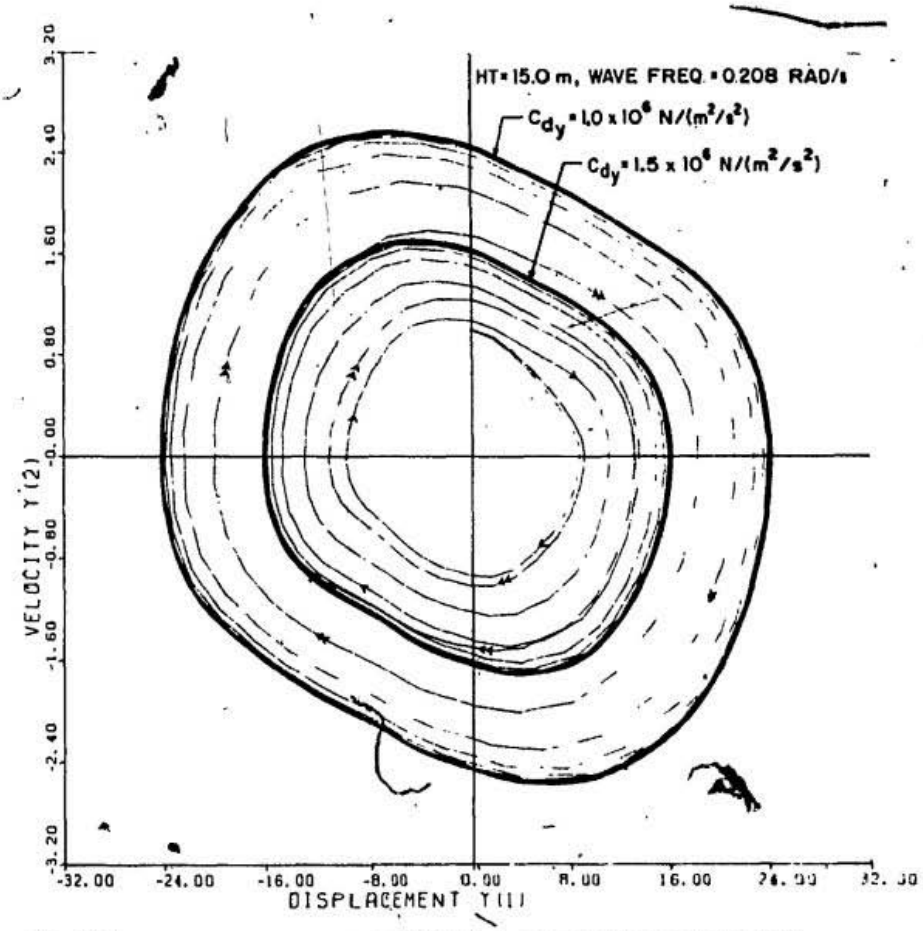

Fig. 9.9 PHASE PLANE PLOT OF SWAY MOTION (UNSTABLE CASE)

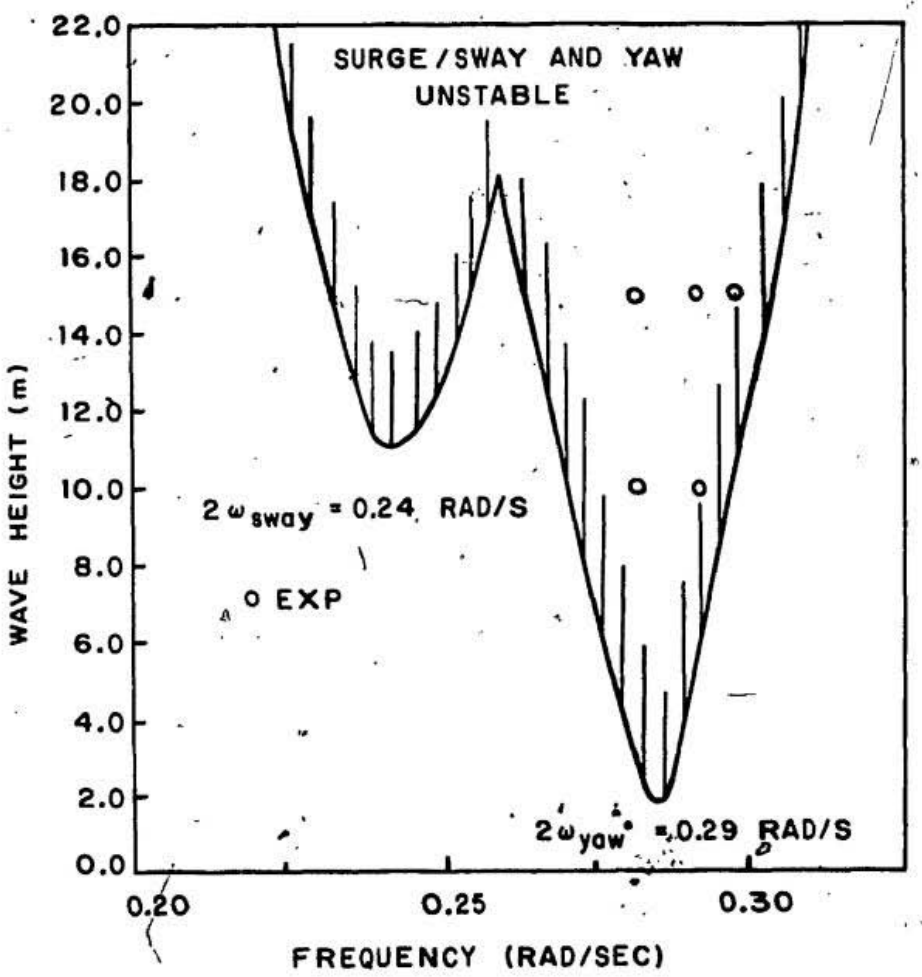

FIG. 9.10 SURGE/SWAY AND YAW STABILITY BOUNDARY FOR THE 'EXAMPLE TLP'

APPENDIX A :

LISTING OF 'EQUILIB'

```
C*****************************************************************
C
C       PROGRAM "EQUILIB" : CALCULATES EQUILIBRIUM POSITION/
C       TENSIONS OF A TLP FOR A GIVEN SET OF TETHER STIFFNESS
C       AND TOTAL PRETENSION
C
C*****************************************************************
C
C       INPUT FILE NAME : 'EQUILIB.DAT'
C
C       INPUT VARIABLES :-
C
C       'PRETEN'
C       PRETEN          = TOTAL STATIC PRETENSION
C       'AK(I),X(I),Y(I)'
C       AK(I)           = AXIAL STIFFNESS AT THE Ith CORNER
C       X(I) & Y(I)     = X & Y COORDINATES OF THE Ith CORNER
C
C       OUTPUT FILE NAME : 'EQUILIB.OUT'
C
C       COMPUTED OUTPUT VARIABLES :-
C
C       DELTA(I)        = EQUILIBRIUM DISPLACEMENT AT THE Ith
C                         CORNER
C       TENS(I)         = EQUILIBRIUM TENSION AT THE Ith CORNER
C
C*****************************************************************
C
C       REQUIRED LIBRARY ROUTINES : IMSL ROUTINE 'LINV2F'
C
C*****************************************************************
C
      IMPLICIT REAL*8(A-H,O-Z)
      DIMENSION STF(3,3),STFINV(3,3),WKAREA(18),F(3)
      DIMENSION AK(4),X(4),Y(4),TENS(4),DELTA(4)
C-----------------------------------------------------------------
C       OPENT I/O FILES
C-----------------------------------------------------------------
      OPEN(UNIT=1,FILE='EQUILIB.DAT',TYPE='OLD')
      OPEN(UNIT=2,FILE='EQUILIB.OUT',TYPE='NEW')
C
      READ(1,*) PRETEN
      DO 10 I=1,4
      READ(1,*) AK(I),X(I),Y(I)
      X(I)=DABS(X(I))
```

```
      Y(I)=DABS(Y(I))
  100 CONTINUE
C
C************************ END OF READ ****************************
C
C     CREATING THE STIFFNESS MATRIX STF(,)
C
      STF(1,1)=AK(1)+AK(4)
      STF(1,2)=AK(2)-AK(4)
      STF(1,3)=AK(3)+AK(4)
      STF(2,1)=AK(1)*Y(1)-AK(4)*Y(4)
      STF(2,2)=AK(2)*Y(2)+AK(4)*Y(4)
      STF(2,3)=-AK(3)*Y(3)-AK(4)*Y(4)
      STF(3,1)=AK(1)*X(1)+AK(4)*X(4)
      STF(3,2)=-AK(2)*X(2)-AK(4)*X(4)
      STF(3,3)=-AK(3)*X(3)+AK(4)*X(4)
C
C     CREATING THE LOAD VECTOR F(,)
C
      F(1)=PRETEN
      F(2)=0.D0
      F(3)=0.D0
C     F(4)=0.D0
C
C     INVERTING STF(,)
C
      N=3
      IA=3
      IDGT=4
      CALL LINV2F(STF,N,IA,STFINV,IDGT,WKAREA,IER)
C
C     SOLVING FOR THE EQUILIBRIUM DISPLACEMENTS AND TENSIONS,
C     "DELTA" AND "TENS" RESPECTIVELY
C
      WRITE(2,1000)
 1000 FORMAT(//10X,'LEG #',6X,'STIFFNESS (N/M)',4X,
     1 'DELTA (M)',4X,'TENSION (N)'/)
      DO 200 I=1,3
C     DO 200 J=1,4
C     DELTA(I)=DELTA(I)+STFINV(I,J)*F(J)
      DELTA(I)=STFINV(I,1)*F(1)
  200 CONTINUE
      DELTA(4)=DELTA(1)-DELTA(2)+DELTA(3)
      DO 300 I=1,4
      TENS(I)=AK(I)*DELTA(I)
```

```
      WRITE(2,2000)I,AK(I),DELTA(I),TENS(I)
2000  FORMAT(10X,I5,5X,E10.4,5X,F10.7,5X,E10.4)
300   CONTINUE
      STOP
      END
```

APPENDIX B :

LISTING OF 'HYDROSTATICS'

```
C*****************************************************************
C
C       PROGRAM "HYDROSTATICS" : HYDROSTATIC PROGRAM INCORPORATING
C       EQUILIBRIUM TRIM CALCULATIONS; COMPUTES BUOYANCY, CENTRE
C       OF BUOYANCY AND THE RIGHTING MOMENT FOR A GIVEN GEOMETRY,
C       DRAFT AND MASS DISTRIBUTION
C
C*****************************************************************
C
C       INPUT FILE NAME : 'HYDROSTATICS.PILOT'
C
C       INPUT VARIABLES :-
C
C       'IDISP,ITRIM,ITRM,TRIMI,IWB'
C       IDISP           = DISPL. ITERATION OPTION (=0 : NO & =1 : YES)
C       ITRIM           = TRIM ITERATION OPTION (=0 : NO & =1 : YES)
C       ITRM            = FIXED TRIM OPTION (=0 : NO & =1 : YES;
C                         IF 'YES' THEN "ITRIM" HAS TO BE 0)
C       TRIMI           = GIVEN FIXED TRIM ANGLE (deg) FOR ITRM=1,
C                         OTHERWISE INPUT 0.0
C       IWB             = 0 IF WEIGHT IS NOT EQUAL TO BUOYANCY AND
C                         1 IF WEIGHT IS EQUAL TO BUOYANCY
C       ** IF (IWB.EQ.0) THEN
C       'WT,RHO'
C       WT              = WEIGHT IN N
C       RHO             = MASS DENSITY OF WATER IN Kg/cu.m
C       'DRAFTI,PTROT,THETA1'
C       DRAFTI          = INITIAL DRAFT IN m
C       PTROT           = DISTANCE OF POINT OF ROTATION ON THE
C                         Z AXIS IN m
C       THETA1          = ROTATION OF 'HEEL AXIS' ON THE
C                         WATERPLANE IN degrees
C       'NLIST,SLIST1,DLIST1'
C       NLIST           = NUMBER OF LIST (OR HEEL) ANGLES
C       SLIST1          = STARTING LIST ANGLE IN degrees.
C       DLIST1          = SPECIFIED LIST INCREMENT IN degrees
C       'DTRIM,DDRAFT,ERRVOL,ERRCB'
C       DTRIM           = SPECIFIED INCREMENTAL TRIM ANGLE (deg)
C       DDRAFT          = SPECIFIED INCREMENTAL DRAFT (m)
C       ERRVOL          = SPECIFIED ERROR TOLERANCE IN VOLUME
C                         CALCULATION (cu.m); REQUIRED FOR EQUILIBRIUM
C                         WATERLINE CALCULATION
C       ERRCB           = SPECIFIED ERROR TOLERANCE ON CENTRE OF
C                         BUOYANCY CALCULATION (m); REQUIRED FOR
C                         EQUILIBRIUM TRIM CALCULATION
```

```
C       '(XCG(I),I=1,3)'
C       XCG             = THREE COORDINATES OF THE CENTRE OF GRAVITY
C                         IN m
C
C       INPUT FILE NAME : 'HYDROSTATIC.DAT'
C
C       INPUT VARIABLES :-
C
C       'NCYL,NRECT'
C       NCYL            = NUMBER OF CYLINDRICAL SURFACES
C       NRECT           = NUMBER OF RECTANGULAR SURFACES
C       ** FOR EVERY CYLINDER PROVIDE :
C       '(XC1(I,J),J=1,3),(XC2(I,J),J=1,3),DIA(I),(NC(I,J),J=1,4)'
C       XC1 & XC2       = COORDINATES OF THE ENDS OF THE CYLINDER (m)
C       DIA             = DIAMETER OF THE CYLINDER (m)
C       NC(,1)          = NUMBER OF VERTICAL DIVISIONS ON THE CYLINDER
C       NC(,2)          = NUMBER OF HORIZONTAL DIVISIONS ON THE
C                         CYLINDER
C       NC(,3)          = NUMBER SECTORS ON THE ENDS OF THE CYLINDER
C       NC(,4)          = NUMBER CIRCULAR DIVISIONS ON THE ENDS OF
C                         THE CYLINDER
C       '(XCLMN(I,J),J=1,3),(YCLMN(I,J),J=1,3),(ZCLMN(I,J),J=1,3)'
C       XCLMN           = DIRECTION COSINES OF LOCAL X AXIS
C       YCLMN           = DIRECTION COSINES OF LOCAL Y AXIS.
C       ZCLMN           = DIRECTION COSINES OF LOCAL Z AXIS
C       ** FOR EVERY RECTANGULAR SURFACE PROVIDE :
C       '(XR(I,J),J=1,3),XLENG(I),YLENG(I),(NR(I,J),J=1,2)'
C       XR              = COORDINATES OF THE CENTROID OF THE
C                         RECTANGULAR SURFACE (m)
C       XLENG & YLENG   = LENGTH OF THE SIDES OF THE RECTANGLE
C                         PARALLEL TO X & Y AXES, RESPECTIVELY
C       NR(,1)          = NUMBER OF DIVISIONS PARALLEL TO X AXIS
C       NR(,2)          = NUMBER OF DIVISIONS PARALLEL TO Y AXIS
C       '(XRLMN(I,J),J=1,3),(YRLMN(I,J),J=1,3),(ZRLMN(I,J),J=1,3)'
C       XRLMN           = DIRECTION COSINES OF LOCAL X AXIS
C       YRLMN           = DIRECTION COSINES OF LOCAL Y AXIS
C       ZRLMN           = DIRECTION COSINES OF LOCAL Z AXIS
C
C       OUTPUT FILE NAME : 'HYDROSTATICS.OUT'
C
C       COMPUTED OUTPUT VARIABLES :-
C
C       REQVOL          = VOLUME CORRESPONDING TO INITIAL DRAFT (cu.m)
C       CB              = COORDINATES OF THE CENTRE OF BUOYANCY IN
C                         FOR THE INITIAL CONFIGURATION (m)
```

```
C       GZ              = RIGHTING ARM (IF IWB=1) IN m OR MOMENT
C                         (IF IWB=0) IN N-m
C       T2              = EQUILIBRIUM TRIM ANGLE (degrees)
C
C*************************************************************************
C
C       REQUIRED LIBRARY ROUTINES : NONE
C
C*************************************************************************
C
C       GENERAL NOTES :
C
C            1. THE ORIGINAL RIG COORDINATE SYSTEM IS ALWAYS
C       CONVERTED TO A PARALLEL ORTHOGONAL SYSTEM WHOSE ORIGIN IS
C       ON THE ORIGINAL RIG SYSTEM Z-AXIS AT DISTANCE "PTROT"
C       FROM THE ORIGIN; THUS IN THE OUTPUT THE 'Z' COORDINATES
C       OF 'CB' & 'CG' ARE EXPRESSED w.r.t. THE SHIFTED SYSTEM
C            2. THE VERTICAL CENTRE OF BUOYANCY 'VCB' i.e.
C       CB(3) IN THIS CASE IS AS SUCH CALCULATED AS THE VERTICAL
C       DISTANCE BELOW THE WATER LINE BUT FINALLY CORRECTED TO
C       THE CURRENT RIG SYSTEM i.e. 'ORIGINAL' OR 'SHIFTED TO
C       "PTROT" POSITION' LATER ON IN THE SUBROUTINE "HYDRO"
C            3. IN CASE THE WEIGHT AND BUOYANCY ARE NOT THE
C       SAME (IN WHICH CASE THE VARIABLE "IWB" HAS A VALUE 0)
C       THEN THE ACTUAL VALUE OF THE WEIGHT (WT) AND THE MASS DENSITY
C       OF WATER (RHO) MUST BE GIVEN IN "N" AND "KG/CU.M" RESPECTIVELY,
C       AND ON THE OUTPUT INSTEAD OF "GZ" THE VALUE OF NET HYDROSTATIC
C       RESTORING MOMENT (RESMOM) WOULD APPEAR.
C
C*************************************************************************
C
      DIMENSION CB(3)
      COMMON/HYD/NCYL,NRECT,XC1(50,3),XC2(50,3),DIA(50),
     *      XCLMN(50,3),YCLMN(50,3),ZCLMN(50,3),NC(50,4),
     *      XR(50,3),XLENG(50),YLENG(50),XRLMN(50,3),
     *      YRLMN(50,3),ZRLMN(50,3),NR(50,2)
      COMMON/EQUAL/DRAFTI,DDRAFT,DTRIM,REQVOL,ERRVOL,ERRCB,IDISP,
     *      ITRIM,R3T(3,3),XCG(3),THETA,TRIMI,ITRM,IWB,WT,RHO
C
C-------------------------------------------------------------
C       OPEN I/O FILES
C-------------------------------------------------------------
C
      OPEN(UNIT=1,FILE='HYDROSTATICS.DAT',TYPE='OLD')
      OPEN(UNIT=10,FILE='HYDROSTATICS.PILOT',TYPE='OLD')
```

```
      OPEN(UNIT=11,FILE='HYDROSTATICS.OUT',TYPE='NEW')
C
      PI=3.1415927
C-----------------------------------------------------------------
C     READ DATA FROM "HYDROSTATICS.PILOT"
C-----------------------------------------------------------------
      READ (10,*) IDISP,ITRIM,ITRM,TRIMI,IWB
      WRITE(11,*)'IS WT EQUAL TO BUOYANCY (=1 : YES & =0 : NO) =',
     *  IWB
      WRITE(11,2030)
      IF (IWB.EQ.0) THEN
      READ (10,*) WT,RHO       ! Weight (N) & Mass Density (Kg/cu.m)
      WRITE(11,*)'GIVEN TOTAL WEIGHT (N) =',WT
      WRITE(11,*)'GIVEN MASS DENSITY OF WATER (KG/CU.M) =',RHO
      WRITE(11,2030)
      ELSE
      END IF
      READ (10,*) DRAFTI,PTROT,THETA1
      READ (10,*) NLIST,SLIST1,DLIST1
      WRITE(11,2010) IDISP,ITRIM,ITRM,TRIMI,DRAFTI,PTROT,THETA1,
     *  NLIST,SLIST1,DLIST1
 2010 FORMAT(////5X,'DISPL ITERATION OPTION (=0 : NO & =1 : YES) =',
     *  I5/5X,'TRIM ITERATION OPTION (=0 : NO & =1 : YES) =',I5/5X,
     *  'FIXED TRIM OPTION (=0 : NO & =1 : YES >"ITRIM" TO BE 0) =',
     *  I5/5X,'GIVEN FIXED TRIM ANGLE (deg) =',F10.5//5X,
     *  'INITIAL DRAFT (m) =',F10.5/5X,
     *  'POINT OF ROTATION ON Z-AXIS ABOVE ORIGIN (m) =',F10.5/5X,
     *  'ROTATION OF X & Y-AXES ON THE WATER PLANE (deg) =',F10.5/5X,
     *  'NO OF LIST ANGLES =',I5/5X,
     *  'STARTING LIST ANGLE (deg) =',F10.5/5X,
     *  'LIST ANGLE INCREMENT (deg) =',F10.5//)
            TRIMI=TRIMI*PI/180.0
            THETA=THETA1*PI/180.0
            SLIST=SLIST1*PI/180.0
            DLIST=DLIST1*PI/180.0
      READ (10,*) DTRIM,DDRAFT,ERRVOL,ERRCB
      WRITE(11,*) 'SPECIFIED "DTRIM" (deg) =',DTRIM
      WRITE(11,*) 'SPECIFIED "DDRAFT" (m) =',DDRAFT
      WRITE(11,*) 'SPECIFIED "ERRVOL" (cu.m) =',ERRVOL
      WRITE(11,*) 'SPECIFIED "ERRCB" (m) =',ERRCB
      WRITE(11,2030)
 2030 FORMAT(/)
      WRITE(11,2030)
            DTRIM=DTRIM*PI/180.0
      READ (10,*) (XCG(I),I=1,3)
```

```
      WRITE(11,*) 'GIVEN CG(X,Y,Z) IN RIG SYS (m) =',(XCG(I),I=1,3)
C
C-----------------------------------------------------------------------
C       READING IN PLATFORM GEOMETRY DATA
C-----------------------------------------------------------------------
C
 1100 FORMAT(/'  COORD OF CYLINDER ENDS  DIA  LOCAL XYZ    DIVN NOS'/)
 1110 FORMAT(F6.2,5(1X,F6.2),1X,F6.2,9(1X,F6.2),1X,4(1X,I3))
 1120 FORMAT(/'  RECT CENTROID  COORD  X,YLENG  LOCAL XYZ  DIVN NOS'/)
 1130 FORMAT(14(F6.2,1X),2(1X,I3))
      READ (1,*) NCYL,NRECT
      WRITE (11,2030)
      WRITE (11,*) '  NO. OF CYLINDERS = ',NCYL
      WRITE (11,*) '  NO. OF RECTANGULAR SURFACES = ',NRECT
      WRITE (11,2030)
      IF (NCYL.EQ.0) GO TO 10
      WRITE (11,1100)
      DO 20 I=1,NCYL
      READ (1,*) (XC1(I,J),J=1,3),(XC2(I,J),J=1,3),DIA(I),
     *          (NC(I,J),J=1,4)
      READ (1,*) (XCLMN(I,J),J=1,3),(YCLMN(I,J),J=1,3),
     *          (ZCLMN(I,J),J=1,3)
 20   WRITE (11,1110) (XC1(I,J),J=1,3),(XC2(I,J),J=1,3),DIA(I),
     *          (XCLMN(I,J),J=1,3),(YCLMN(I,J),J=1,3),
     *          (ZCLMN(I,J),J=1,3),(NC(I,J),J=1,4)
 10   IF (NRECT.EQ.0) GO TO 30
      WRITE (11,1120)
      DO 40 I=1,NRECT
      READ (1,*) (XR(I,J),J=1,3),XLENG(I),YLENG(I),(NR(I,J),J=1,2)
      READ (1,*) (XRLMN(I,J),J=1,3),(YRLMN(I,J),J=1,3),
     *          (ZRLMN(I,J),J=1,3)
 40   WRITE(11,1130) (XR(I,J),J=1,3),XLENG(I),YLENG(I),
     *          (XRLMN(I,J),J=1,3),(YRLMN(I,J),J=1,3),
     *          (ZRLMN(I,J),J=1,3),(NR(I,J),J=1,2)
C
C************************** END OF READ ********************************
C
 30   WRITE (11,2030)
      CALL HYDRO(0.0,0.0,0.0,DRAFTI,REQVOL,CB)
      WRITE(11,*) 'REQUIRED DISPLACEMENT (cu.m) =',REQVOL
      WRITE(11,*) 'CALC CB(X,Y,Z) IN RIG SYS (m) =',(CB(I),I=1,3)
      WRITE (11,2030)
      PRINT*,'     REQUIRED DISPLACEMENT (cu.m) =',REQVOL
      PRINT*,'     CALC CB(X,Y,Z) IN RIG SYS (m) =',(CB(I),I=1,3)
C
```

```
C       SHIFT THE ORIGINAL RIG SYSTEM TO "PTROT"
C
        DO 50 I=1,NCYL
        XC1(I,3)=XC1(I,3)-PTROT
 50     XC2(I,3)=XC2(I,3)-PTROT
        DO 60 I=1,NRECT
 60     XR(I,3)=XR(I,3)-PTROT
        DRAFTI=DRAFTI-PTROT
        XCG(3)=XCG(3)-PTROT
        WRITE (11,2030)
        WRITE (11,*)' $$$$$$$$$$$$$$$$$$$$$$$$$$$$$$$$$$$$$$$$$$$$$$$$$$$$$$$$'
        WRITE (11,2030)
        WRITE (11,*)'     CURRENT RIG SYSTEM IS THE SYSTEM SHIFTED'
        WRITE (11,*)'                    TO "PTROT"'
        WRITE (11,2030)
        WRITE (11,*)' $$$$$$$$$$$$$$$$$$$$$$$$$$$$$$$$$$$$$$$$$$$$$$$$$$$$$$$$'
        WRITE (11,2030)
        CALL ROTATION(R3T,THETA)
              DO 3000 I=1,NLIST
              ALIST=SLIST+(FLOAT(I-1))*DLIST
              T1=ALIST*180.0/PI
        PRINT*,'>>>>>  CALCULATING FOR LIST ANGLE =',T1,'<<<<<'
        CALL EQUIL(ALIST)
 3000   CONTINUE
      STOP
      END
C
C
C*************************************************************************
C       SUBROUTINES
C*************************************************************************
C
C
C
C
C
C
C
        SUBROUTINE MATMUL1 (SA,SB,SC)
        DIMENSION SA(3,3),SB(3),SC(3)
C
              do 5 I=1,3
 5            SC(I)=0.0
              K=0
              do 10 I=1,3
              K=K+1
```

```
                do 10 J=1,3
 10             SC(K)=SC(K)+SA(I,J)*SB(J)
                return
                end
C
C
C
C
      SUBROUTINE MATMUL2 (SA,SB,SC)
      DIMENSION SA(3,3),SB(3,3),SC(3,3)
C
                do 5 I=1,3
                do 5 J=1,3
 5              SC(I,J)=0.0
                do 10 I=1,3
                do 10 J=1,3
                do 10 K=1,3
 10             SC(I,J)=SC(I,J)+SA(I,K)*SB(K,J)
                return
                end
C
C
C
C
      SUBROUTINE HYDRO (THETA,ATRIM,ALIST,DFT,VTOT,CB)
      DIMENSION CB(3),R(3,3),P(3),RP(3),PN(3),RPN(3)
      COMMON/HYD/NCYL,NRECT,XC1(50,3),XC2(50,3),DIA(50),
     *          XCLMN(50,3),YCLMN(50,3),ZCLMN(50,3),NC(50,4),
     *          XR(50,3),XLENG(50),YLENG(50),XRLMN(50,3),
     *          YRLMN(50,3),ZRLMN(50,3),NR(50,2)
C
      PI=3.1415927
C
      CALL RMATRIX (R,THETA,ATRIM,ALIST)
      VTOT=0.0
      XMOM=0.0
      YMOM=0.0
      ZMOM=0.0
C
C     CALCULATING FOR THE CYLINDERS i.e. THEIR WALLS AND ENDS
C
      IF (NCYL.EQ.0) GO TO 100
      DO 10 IC=1,NCYL
      AH=SQRT((XC2(IC,1)-XC1(IC,1))**2+(XC2(IC,2)-XC1(IC,2))**2
     *          +(XC2(IC,3)-XC1(IC,3))**2)
```

```
      DH=AH/FLOAT(NC(IC,2))
      DL=PI*DIA(IC)/FLOAT(NC(IC,1))
      DR=DIA(IC)/(2.0*NC(IC,4))
      DFIC=2.0*PI/FLOAT(NC(IC,1))
      DFI=2.0*PI/FLOAT(NC(IC,3))
      AREAC=DL*DH
C
      DO 20 I=1,NC(IC,2)
      PZ=(FLOAT(I)-0.5)*DH
      DO 30 J=1,NC(IC,1)
      ANG=(FLOAT(J)-0.5)*DFIC
C
      PNX=COS(ANG)
      PNY=SIN(ANG)
      PNZ=0.0
      PN(1)=PNX*XCLMN(IC,1)+PNY*YCLMN(IC,1)+PNZ*ZCLMN(IC,1)
      PN(2)=PNX*XCLMN(IC,2)+PNY*YCLMN(IC,2)+PNZ*ZCLMN(IC,2)
      PN(3)=PNX*XCLMN(IC,3)+PNY*YCLMN(IC,3)+PNZ*ZCLMN(IC,3)
C
      PX=DIA(IC)*COS(ANG)/2.0
      PY=DIA(IC)*SIN(ANG)/2.0
C
      XC=XC1(IC,1)+ZCLMN(IC,1)*PZ
      YC=XC1(IC,2)+ZCLMN(IC,2)*PZ
      ZC=XC1(IC,3)+ZCLMN(IC,3)*PZ
C
      P(1)=XC+PX*XCLMN(IC,1)+PY*YCLMN(IC,1)
      P(2)=YC+PX*XCLMN(IC,2)+PY*YCLMN(IC,2)
      P(3)=ZC+PX*XCLMN(IC,3)+PY*YCLMN(IC,3)
C
      CALL MATMUL1 (R,PN,RPN)
      CALL MATMUL1 (R,P,RP)
      IF (RP(3).GT.DFT) GO TO 30
      VTOT=VTOT-RPN(3)*AREAC*(DFT-RP(3))
      XMOM=XMOM-RPN(3)*AREAC*(DFT-RP(3))*RP(1)
      YMOM=YMOM-RPN(3)*AREAC*(DFT-RP(3))*RP(2)
      ZMOM=ZMOM-RPN(3)*AREAC*(DFT-RP(3))*(DFT-RP(3))/2.0
 30   CONTINUE
 20   CONTINUE
C
      X=XC1(IC,1)
      Y=XC1(IC,2)
      Z=XC1(IC,3)
      PN(1)=-ZCLMN(IC,1)
      PN(2)=-ZCLMN(IC,2)
```

```
      PN(3)=-ZCLMN(IC,3)
C
      DO 40 II=1,2     !  CALCULATIONS FOR THE CIRCULAR ENDS
      DO 50 I=1,NC(IC,4)
      RR=(FLOAT(I)-0.5)*DR
      RR1=RR-DR/2.0
      RR2=RR+DR/2.0
      AREA=PI*(RR2**2-RR1**2)/FLOAT(NC(IC,3))
      DO 60 J=1,NC(IC,3)
      ANG=(FLOAT(J)-0.5)*DFI
C
      PX=RR*COS(ANG)
      PY=RR*SIN(ANG)
      P(1)=X+PX*XCLMN(IC,1)+PY*YCLMN(IC,1)
      P(2)=Y+PX*XCLMN(IC,2)+PY*YCLMN(IC,2)
      P(3)=Z+PX*XCLMN(IC,3)+PY*YCLMN(IC,3)
C
      CALL MATMUL1 (R,PN,RPN)
      CALL MATMUL1 (R,P,RP)
      IF (RP(3).GT.DFT) GO TO 60
      VTOT=VTOT-RPN(3)*AREA*(DFT-RP(3))
      XMOM=XMOM-RPN(3)*AREA*(DFT-RP(3))*RP(1)
      YMOM=YMOM-RPN(3)*AREA*(DFT-RP(3))*RP(2)
      ZMOM=ZMOM-RPN(3)*AREA*(DFT-RP(3))*(DFT-RP(3))/2.0
 60   CONTINUE
 50   CONTINUE
C
      X=XC2(IC,1)
      Y=XC2(IC,2)
      Z=XC2(IC,3)
      PN(1)=ZCLMN(IC,1)
      PN(2)=ZCLMN(IC,2)
      PN(3)=ZCLMN(IC,3)
 40   CONTINUE
 10   CONTINUE
C
C     CALCULATING FOR THE RECTANGULAR SURFACES
C
 100  IF (NRECT.EQ.0) GO TO 110
      DO 70 IR=1,NRECT
      DX=XLENG(IR)/FLOAT(NR(IR,1))
      DY=YLENG(IR)/FLOAT(NR(IR,2))
      DA=DX*DY
C
      DO 80 I=1,NR(IR,1)
```

```
      XX=(FLOAT(I)-0.5)*DX-XLENG(IR)/2.0
      DO 90 J=1,NR(IR,2)
      YY=(FLOAT(J)-0.5)*DY-YLENG(IR)/2.0
C
      P(1)=XR(IR,1)+XX*XRLMN(IR,1)+YY*YRLMN(IR,1)
      P(2)=XR(IR,2)+XX*XRLMN(IR,2)+YY*YRLMN(IR,2)
      P(3)=XR(IR,3)+XX*XRLMN(IR,3)+YY*YRLMN(IR,3)
      PN(1)=ZRLMN(IR,1)
      PN(2)=ZRLMN(IR,2)
      PN(3)=ZRLMN(IR,3)
C
      CALL MATMUL1 (R,PN,RPN)
      CALL MATMUL1 (R,P,RP)
      IF (RP(3).GT.DFT) GO TO 90
      VTOT=VTOT-RPN(3)*DA*(DFT-RP(3))
      XMOM=XMOM-RPN(3)*DA*(DFT-RP(3))*RP(1)
      YMOM=YMOM-RPN(3)*DA*(DFT-RP(3))*RP(2)
      ZMOM=ZMOM-RPN(3)*DA*(DFT-RP(3))*(DFT-RP(3))/2.0
 90   CONTINUE
 80   CONTINUE
 70   CONTINUE
C
C     CALCULATE THE CENTRE OF BUOYANCY
C
 110  CB(1)=XMOM/VTOT
      CB(2)=YMOM/VTOT
      CB(3)=ZMOM/VTOT
C
C     CALCULATE CB(3) w.r.t. THE CURRENT RIG COORD SYSTEM
C
      CB(3)=DFT-CB(3)
      RETURN
      END

C
C
C
C
      SUBROUTINE EQUIL (ALIST)
      DIMENSION CB(3),ROT(3,3),B(3),G(3),CG(3),ROT1(3,3)
      COMMON/EQUAL/DRAFTI,DDRAFT,DTRIM,REQVOL,ERRVOL,ERRCB,IDISP,
     *          ITRIM,R3T(3,3),XCG(3),THETA,TRIMI,ITRM,IWB,WT,RHO
C
C
      PAI=3.1415927
```

```
      GRAV=9.81        ! Accln. due to Gravity in m/sec/sec
      DO 5 I=1,3
      DO 5 J=1,3
5     ROT1(I,J)=0.0
      ROT1(1,1)=1.0
      ROT1(2,2)=1.0
      ROT1(3,3)=1.0
      ITER=0
      INDX1=0
      INDX2=0
      INDX3=0
      INDX4=0
C
      DTRM=DTRIM
      DT=DDRAFT
      D=DRAFTI
      ATRIM=0.0
      IF(ITRM.EQ.1) ATRIM=TRIMI
C
10    ITER=ITER+1
      PRINT*,'>>> ITER =',ITER
      CALL RMATRIX (ROT,THETA,ATRIM,ALIST)
      CALL HYDRO (THETA,ATRIM,ALIST,D,VOL,CB)
      ERR1=REQVOL-VOL
      IF(IDISP.EQ.0) ERR1=0.0
      IF(IDISP.EQ.0) PRINT*,'  *** IDISP = 0 ***'
      PRINT*,'ERR1 =',ERR1
      IF(ERRVOL.LE.0.0) PRINT*,'  *** ERRVOL .LE. 0.0 ***'
      IF(ABS(ERR1).LE.ERRVOL) GO TO 40
      IF(ERR1.GT.0.0) GO TO 20
      IF(INDX1.EQ.1) GO TO 30
      D=D-DT*2.
      GO TO 10
20    D=D+DT
      INDX1=1
      GO TO 10
30    D=D-DT
      DT=DT/2.
      GO TO 10
40    CONTINUE  ! end of const. displ. check
C
      PRINT*,'DISPL. SATISFACTORY : PROCEED FOR EQUILIB TRIM'
      DT=DDRAFT
      INDX1=0
C
```

```
            CG(1)=XCG(1)
            CG(2)=XCG(2)
            CG(3)=XCG(3)
          CALL MATMUL1 (ROT,CG,G)
          CALL MATMUL1 (R3T,G,CG)
          CALL MATMUL1 (ROT1,CB,B)
          CALL MATMUL1 (R3T,B,CB)
C
          ERR2=CG(1)-CB(1)   ! ERR2=CGX-CBX in the yawed coordinate
          IF(ITRIM.EQ.0) ERR2=0.0
          IF(ITRIM.EQ.0) PRINT*,'  *** ITRIM = 0 ***'
          PRINT*,'ERR2 =',ERR2
          IF(ERRCB.LE.0.0) PRINT*,'  *** ERRCB .LE. 0.0 ***'
          IF(ABS(ERR2).LE.ERRCB) GO TO 70
          IF(ERR2.GT.0.0) GO TO 50
          IF(INDX2.EQ.1) GO TO 60
          ATRIM=ATRIM-DTRM*2.0
          GO TO 10
 50       ATRIM=ATRIM+DTRM
          INDX2=1
          GO TO 10
 60       ATRIM=ATRIM-DTRM
          DTRM=DTRM/2.0
          GO TO 10
 70       CONTINUE  ! end of trim iterations for the given list angle
C
          PRINT*,'TRIM ADJUSTMENT SATISFACTORY : PROCEED TO NEXT LIST'
          WRITE(11,2020)
          WRITE(11,2020)
 2020     FORMAT(/)
          T1=ALIST*180./PAI
          T2=ATRIM*180./PAI
          WRITE(11,*)'>>>> LIST ANGLE (DEG) =',T1
          WRITE(11,*)'  ADJUSTED DRAFT (m) =',D
          WRITE(11,*)'  ADJUSTED DISPLACEMENT (cu.m) =',VOL
          WRITE(11,*)'RESULTANT EQUILIBRIUM TRIM ANGLE (DEG) =',T2
          WRITE(11,2020)
          WRITE(11,*)'CG(X,Y,Z) =',CG(1),CG(2),CG(3)   !'in the yawed
          WRITE(11,*)'CB(X,Y,Z) =',CB(1),CB(2),CB(3)   ! coordinate system
          WRITE(11,2020)
          GZ=CG(2)-CB(2)
          RESMOM=CG(2)*WT-CB(2)*VOL*RHO*GRAV
          IF (ALIST.LT.0.0) GZ=-GZ
          IF (ALIST.LT.0.0) RESMOM=-RESMOM
          IF (IWB.EQ.0) THEN
```

```
      WRITE(11,*)' ** HYDROSTATIC RESTORING MOMENT (N-M) =',RESMOM
      ELSE
      WRITE(11,*)' ** RIGHTING ARM GZ (m) =',GZ
      END IF
      WRITE(11,2020)
      WRITE(11,*)'VOL ERROR (cu.m) =',ERR1,'  CB ERROR (m) =',ERR2
      WRITE(11,*)'NO. OF ITERATIONS USED =',ITER
      PRINT*,'LIST ANGLE =',T1,'  TRIM ANGLE =',T2
      PRINT*,'VOL ERROR =',ERR1,'  CB ERROR =',ERR2
      RETURN
      END
C
C
C
C
      SUBROUTINE RMATRIX (R,THETA,ATRIM,ALIST)
      DIMENSION R1(3,3),R2(3,3),R(3,3)
      PAI=3.1415927
C
      E1=COS(THETA)
      E2=SIN(THETA)
      C=COS(ALIST)
      S=SIN(ALIST)
      R1(1,1)=E1*E1+(1.0-E1*E1)*C
      R1(1,2)=E1*E2-E1*E2*C
      R1(1,3)=E2*S
      R1(2,1)=E2*E1-E2*E1*C
      R1(2,2)=E2*E2+(1.0-E2*E2)*C
      R1(2,3)=-E1*S
      R1(3,1)=-E2*S
      R1(3,2)=E1*S
      R1(3,3)=C
C
      E1=COS(PAI/2.0+THETA)
      E2=SIN(PAI/2.0+THETA)
      C=COS(ATRIM)
      S=SIN(ATRIM)
      R2(1,1)=E1*E1+(1.0-E1*E1)*C
      R2(1,2)=E1*E2-E1*E2*C
      R2(1,3)=E2*S
      R2(2,1)=E2*E1-E2*E1*C
      R2(2,2)=E2*E2+(1.0-E2*E2)*C
      R2(2,3)=-E1*S
      R2(3,1)=-E2*S
      R2(3,2)=E1*S
```

```
      R2(3,3)=C
C
      CALL MATMUL2 (R2,R1,R)
C
      RETURN
      END
C
C
C
C
C
C     SUBROUTINE "ROTATION" : CALCULATES THE [R3] TRANSPOSE
C     THE GIVEN ROATION OF THE ARBITARY VECTOR ON THE WATER
C     PLANE ABOUT WHICH "LIST" IS APPLIED. THE MATRIX [R3T]
C     IN THE MAIN$ AND SUBROUTINE "HYDRO" IS USED TO PROJECT
C     THE "CB" AND "CG" VECTORS CALCULATED IN THE CURRENT
C     RIG SYSTEM ONTO THE SYSTEM YAWED w.r.t. X-AXIS OF THE
C     CURRENT RIG SYSTEM BY THE AMOUNT "THETA". THE CALCULATION
C     OF THE RIGHTING ARM "GZ" AND CHECKS MADE FOR EQUILIBRIUM
C     TRIM ARE DONE COMPARING THESE PROJECTIONS.
C
      SUBROUTINE ROTATION(R,THETA)
      DIMENSION R(3,3)
C
      C=COS(THETA)
      S=SIN(THETA)
      R(1,1)=C
      R(1,2)=S
      R(1,3)=0.0
      R(2,1)=-S
      R(2,2)=C
      R(2,3)=0.0
      R(3,1)=0.0
      R(3,2)=0.0
      R(3,3)=1.0
      RETURN
      END
```

APPENDIX C :

LISTING OF 'TIME_DOMAIN'

```
C*****************************************************************
C
C       PROGRAM 'TIME_DOMAIN' : PERFORMS TIME DOMAIN SIMULATION
C       OF A TLP FOR INTACT AND TETHER DAMAGE CONDITIONS
C
C*****************************************************************
C
C     , INPUT FILE NAME : 'TIME_DOMAIN.PILOT'
C
C       INPUT VARIABLES :-
C
C       'METH,MITER,INDEX1'
C       METH,MITER        = IMSL ROUTINE 'DGEAR' PARAMETERS
C       INDEX1            = CORRESPONDS TO 'INDEX' IN 'DGEAR (=1)
C       'NCOND'
C       NCOND             = NUMBER OF NONZERO INITIAL CONDITIONS
C       ** FOR EVERY NONZERO INTIAL CONDITION PROVIDE :
C       'J,Y(J)'
C       Y(J)              = INTIAL VALUE OF THE Jth STATE
C                           VARIABLE Y(J)
C       'DRAFT,WT'
C       DRAFT             = DRAFT OF THE PLATFORM (m)
C       WT                = WEIGHT OF THE PLATFORM (N)
C       '(CG(I),I=1,3)'
C       CG                = COORDINATES OF THE CENTRE OF GRAVITY (m)
C       'RXX,RYY,RZZ'
C       RXX               = RADIUS OF GYRATION ABOUT X-AXIS (m)
C       RYY               = RADIUS OF GYRATION ABOUT Y-AXIS (m)
C       RZZ               = RADIUS OF GYRATION ABOUT Z-AXIS (m)
C       'CD1,CM'
C       CD1               = NONLINEAR DRAG COEFFICIENT
C       CM                = VIRTUAL MASS COEFFICIENT
C       'NSTEP,STEP1,TOL'
C       NSTEP             = NUMBER OF TIME STEPS
C       STEP1             = TIME INTERVAL (sec) FOR RESPONSE OUTPUT
C       TOL               = ERROR TOLERANCE FOR 'DGEAR'
C       'NTRANS,EXPI'
C       NTRANS            = NUMBER OF TIME STEPS IN THE BEGINING
C                           OVER WHICH DRAG MAY ARTIFICALLY INCREASED,
C                           IF DESIRED, TO DAMP THE SYSTEM IN ORDER
C                           TO AVOID INITIAL TRANSIENT
C       EXPI              = INDEX FOR AN EXPONENTIAL MULTIPLIER
C                           USED TO INCREASE DRAG TO DAMP THE
C                           SYSTEM INITIALLY (=0 IF THIS OPTION
C                           IS NOT DESIRED
```

```
C       'TO'
C       TO              = TIME LENGTH OVER WHICH THE 'HALF COSINE
C                         FUNCTION IS APPLIED (sec)
C       'FI,W,AMP1'
C       FI              = WAVE HEADING (degrees)
C       W               = WAVE FREQUENCY (rad/sec)
C       AMP1            = WAVE AMPLITUDE (m)
C       'IZETA,IROT'
C       IZETA           = 0 IF INTEGRATION IS TO BE CARRIED OUT
C                         ONLY UPTO THE MEAN WATERLINE AND
C                         = 1, OTHERWISE
C       IROT            = IF EQUAL TO 0 THEN THE ANGLES ARE TAKEN
C                         AS VECTORS, 1 OTHERWISE
C       'NTRIG,NT,FACTOR'
C       NTRIG           = TIME STEP NUMBER AT WHICH TETHER LOSS
C                         HAS TO OCCUR
C       NT              = TENSION LEG NUMBER AT WHICH TETHER LOSS
C                         HAS TO OCCUR
C       FACTOR          = FACTOR BY WHICH THE STIFFNESS OF THE
C                         AFFECTED TENSION LEG HAS TO BE
C                         MULTIPLIED AFTER TETHER LOSS
C
C       INPUT FILE NAME : 'TIME_DOMAIN.DAT'
C
C       'NCYL'
C       NCYL            = NUMBER OF CYLINDERS
C       ** FOR EVERY CYLINDER PROVIDE :
C       '(X1(I,J),J=1,3),(X2(I,J),J=1,3),D(I),NDIV(I)'
C       X1,X2           = COORDINATES OF THE CYLINDER ENDS (m)
C       D               = DIAMETER OF THE CYLINDER (m)
C       NDIV            = NUMBER OF HORIZONTAL SLICES THE CYLINDER
C                         WOULD HAVE TO BE DIVIDED
C       'NSURF'         = NUMBER CIRCULAR FLAT SURFACES
C       ** FOR EVERY SURFACE PROVIDE :
C       '(XS(I,J),J=1,3),(ANS(I,J),J=1,3),DS(I)'
C       XS              = COORDINATES OF THE CENTRE OF THE FLAT
C                         SURFACE
C       ANS             = DIRECTION COSINES OF THE NORMAL TO THE
C                         FLAT SURFACE
C       DS(I)           = DIAMETER (m) OF THE FLAT SURFACE
C       'NTEN'          = NUMBER OF TENSION LEGS
C       ** FOR EVERY TENSION LEG PROVIDE :
C       '(XT1(I,J),J=1,3),(XT2(I,J),J=1,3),AKT(I)'
C       XT1,XT2         = COORDINATES OF THE ENDS OF THE TETHER
C       AKT             = AXIAL STIFFNESS OF THE TETHER
```

```
C       'NWP'
C       NWP             = NUMBER OF CIRCULAR WATERPLANES >0 IF
C                         LINEAR HYDROSTATIC STIFFNESS ARE DESIRED,
C                         =0 OTHERWISE
C       ** FOR EVERY WATERPLANE PROVIDE
C       'XWP(I),YWP(I),DWP(I)'
C       XWP,YWP         = X AND Y COORDINATES OF THE CENTRE OF
C                         THE WATERPLANE
C       DWP             = DIAMETER OF THE WATERPLANE
C
C       OUTPUT FILES :
C
C       'TIME_DOMAIN.OUT' - PRINTS OUT THE INPUT DATA AND
C                           COMPUTED BUOYANCY AND CB
C       'SURGE.DAT,SWAY.DAT,HEAVE.DAT,ROLL.DAT,PITCH.DAT,YAWW.DAT'
C                         - MOTION RESPONSES AGAINST A TIME SCALE
C       'TEN1.DAT,TEN2.DAT,TEN3.DAT,TEN4.DAT'
C                         - TENSION RESPONSES AT THE FOUR
C                           CORNERS AGAINST A TIME SCALE
C
C*************************************************************************
C
C       REQUIRED LIBRARY ROUTINES : IMSL ROUTINES 'DGEAR' AND
C                                   'LINV1F'
C*************************************************************************
C
        IMPLICIT DOUBLE PRECISION (A-H),(O-Z)
        DIMENSION WK(1000)
C
C-------------------------------------------------------------------
C       OPEN I/O FILES
C-------------------------------------------------------------------
C
        OPEN(UNIT=1,FILE='TIME_DOMAIN.DAT',TYPE='OLD')
        OPEN(UNIT=3,FILE='TIME_DOMAIN.PILOT',TYPE='OLD')
        OPEN(UNIT=4,FILE='TIME_DOMAIN.OUT',TYPE='NEW')
        OPEN(UNIT=7,FILE='SURGE.DAT',TYPE='NEW')
        OPEN(UNIT=8,FILE='SWAY.DAT',TYPE='NEW')
        OPEN(UNIT=9,FILE='HEAVE.DAT',TYPE='NEW')
        OPEN(UNIT=10,FILE='ROLL.DAT',TYPE='NEW')
        OPEN(UNIT=11,FILE='PITCH.DAT',TYPE='NEW')
        OPEN(UNIT=12,FILE='YAW.DAT',TYPE='NEW')
        OPEN(UNIT=13,FILE='TEN1.DAT',TYPE='NEW')
        OPEN(UNIT=14,FILE='TEN2.DAT',TYPE='NEW')
        OPEN(UNIT=15,FILE='TEN3.DAT',TYPE='NEW')
```

```
      OPEN(UNIT=16,FILE='TEN4.DAT',TYPE='NEW')
C
      READ (3,*) METH,MITER,INDEX1
      N = 21
      IF (METH.EQ.1) NMETH = N*13
      IF (METH.EQ.2) NMETH = N*6
      IF (MITER.EQ.0) NMITER =1
      IF (MITER.EQ.2) NMITER = N*(N+1)
      IF (MITER.EQ.3) NMITER = N
      NWK = 4*N+NMETH+NMITER
      PRINT*,'         NWK =',NWK
      CALL SIMUL (WK,NWK)
      STOP
      END
C
C
C
C
      SUBROUTINE SIMUL (WK,NWK)
      IMPLICIT DOUBLE PRECISION (A-H),(O-Z)
      INTEGER*2 M(50000)
      DIMENSION WK(NWK),IWK(21),Y(21)
      COMMON/SUBFCN1/CM,CD,ISTEP,NCYL,NSURF,NTEN,WT,FI,W,AK,
     *         PI,RHO,G,BF,XB,YB,ZB,AMP,IFCN,NWP,BF1,XB1,YB1,ZB1,
     *         IZETA,IROT,NTRIG,NT,FACTOR
      COMMON/SUBFCN2/CG(3),X1(50,3),X2(50,3),D(50),NDIV(50),
     *         AL(50),XS(50,3),ANS(50,3),DS(50),AREA(50),TL(50),
     *         XT1(50,3),XT2(50,3),AKT(50),AKT1(50),AMASS(6),TEN(50),
     *         XWP(50),YWP(50),DWP(50),WPA(50),WPI(50),FTOT(6)
      COMMON/SUBTSD/NSTEP,STEP1
      EXTERNAL FCN,FCNJ,MATMUL1,MATMUL2,MATMUL3,CROSS
C
      PI=3.1415927D0
      G=9.81D0
      RHO=1025.0D0
C
      REWIND 3
      READ (3,*) METH,MITER,INDEX1
      WRITE (4,4005) METH,MITER,INDEX1
 4005 FORMAT (/' **   DGEAR PARAMETERS    ** '/
     * 5X,'METH = ',I2,5X,'MITER = ',I2,5X,'INDEX1 = ',I2/)
      PRINT*,'METH =',METH,'     MITER =',MITER
      PRINT*,'INDEX1 =',INDEX1
      READ (3,*) NCOND  ! NCOND = 0 if all initial cond. are zero
      WRITE (4,*)'    NCOND = ',NCOND
```

```
      IF (NCOND.EQ.0) GO TO 10
      WRITE (4,*)'     J       Y(J) '
      DO 20 I=1,NCOND
      READ (3,*) J,Y(J)
20    WRITE (4,*) J,Y(J)
10    READ (3,*) DRAFT,WT
      WRITE (4,4000)
4000  FORMAT(/)
      WRITE (4,*)'     DRAFT (m) =',DRAFT
      WRITE (4,*)'     WEIGHT (N) =',WT
      WRITE (4,4000)
      READ (3,*) (CG(I),I=1,3)
      WRITE (4,4010) (CG(I),I=1,3)
4010  FORMAT ('       CG(X,Y,Z) IN BODY COORD :  ',3(F10.3,2X))
      READ (1,*) NCYL    !  NCYL = No of cylinders
      WRITE (4,*)'     NO. OF CYLINDERS =',NCYL
      WRITE (4,4020)
4020  FORMAT (/' ** CYL COORD ETC. IN SYS FIXED WITH CG **'/
     *  4X,'X1',8X,'Y1',8X,'Z1',8X,'X2',8X,'Y2',8X,'Z2',11X,'LENGTH',
     *  10X,'DIA',10X,'NDIV'/)
4030  FORMAT (6(F8.3,2X),3X,F10.3,5X,F10.3,5X,I5)
      DO 30 I=1,NCYL
      READ (1,*) (X1(I,J),J=1,3),(X2(I,J),J=1,3),D(I),NDIV(I)
      DO 35 J=1,3
      X1(I,J) = X1(I,J)-CG(J)
35    X2(I,J) = X2(I,J)-CG(J)
      AL(I) = DSQRT((X2(I,1)-X1(I,1))**2+(X2(I,2)-X1(I,2))**2+
     *        (X2(I,3)-X1(I,3))**2)
30    WRITE (4,4030) (X1(I,J),J=1,3),(X2(I,J),J=1,3),AL(I),D(I),
     *        NDIV(I)
      WRITE (4,4000)
      READ (1,*) NSURF
      WRITE (4,*)'     NO. OF CIRCULAR SURFACES =',NSURF
      IF (NSURF.EQ.0) GO TO 41
      WRITE (4,4040)
4040  FORMAT (/' ** SURFACE COORD ETC. IN SYS FIXED WITH CG **'/
     *  4X,'X',9X,'Y',9X,'Z',14X,'NX',8X,'NY',8X,'NZ',10X,'DIA',
     *  10X,'AREA')
4050  FORMAT (3(F8.3,2X),3X,3(F8.5,2X),3X,F10.3,5X,F10.3)
      DO 40 I=1,NSURF
      READ (1,*) (XS(I,J),J=1,3),(ANS(I,J),J=1,3),DS(I)
      DO 45 J=1,3
45    XS(I,J) = XS(I,J)-CG(J)
      AREA(I) = PI*DS(I)**2/4.0D0
40    WRITE (4,4050) (XS(I,J),J=1,3),(ANS(I,J),J=1,3),DS(I),AREA(I)
```

```
      WRITE (4,4000)
41    READ (1,*) NTEN
      WRITE (4,*)'    NO. OF TENSION LEGS =',NTEN
      WRITE (4,4060)
4060  FORMAT (' ** TETHER COORD ETC. IN SYS FIXED WITH CG **'/
     *  4X,'X1',8X,'Y1',8X,'Z1',8X,'X2',8X,'Y2',8X,'Z2',11X,'LENGTH',
     *  3X,'STIFFNESS (N/m)'/)
4070  FORMAT (6(F8.3,2X),3X,F10.3,5X,E12.5)
      DO 50 I=1,NTEN
      READ (1,*) (XT1(I,J),J=1,3),(XT2(I,J),J=1,3),AKT1(I)
      TL(I) = DSQRT((XT2(I,1)-XT1(I,1))**2+(XT2(I,2)-XT1(I,2))**2+
     *        (XT2(I,3)-XT1(I,3))**2)
      AKT(I) = AKT1(I)
      DO 55 J=1,3
55    XT1(I,J) = XT1(I,J)-CG(J)
      XT2(I,3) = XT2(I,3)-DRAFT
50    WRITE (4,4070) (XT1(I,J),J=1,3),(XT2(I,J),J=1,3),TL(I),AKT1(I)
      READ (1,*) NWP  !  NWP = No. of waterplanes for linear
      WRITE (4,4000)  !       hydrstatic calculation
      WRITE (4,*)'    NO. OF WATER PLANES = ',NWP
      IF (NWP.EQ.0) GO TO 56
      WRITE (4,4071)
4071  FORMAT ('  ** WATER PLANE COORDINATES ETC IN RIG SYS ** '/
     *  '  XWP          YWP          DWP          AWP          IWP'/)
4072  FORMAT (5(F12.3,2X))
      DO 57 I = 1,NWP
      READ (1,*) XWP(I),YWP(I),DWP(I)
      WPA(I) = PI*DWP(I)**2/4.0D0
      WPI(I) = PI*DWP(I)**4/64.0D0
57    WRITE (4,4072) XWP(I),YWP(I),DWP(I),WPA(I),WPI(I)
56    READ (3,*) RXX,RYY,RZZ
      WRITE (4,*)'    RXX,RYY,RZZ (m) =',RXX,RYY,RZZ
      WRITE (4,4000)
      READ (3,*) CD1,CM
      WRITE (4,*)'    CD =',CD1,'   CM =',CM
      WRITE (4,4000)
      READ (3,*) NSTEP,STEP1,TOL
      READ (3,*) NTRANS,EXPI   !  NTRANS = NO. OF STEP TILL
C
C     THE EXPONENTIAL DECAY FUNCTION SHOULD BE ACTIVE; EXPI : INDEX
C
      READ (3,*) TO
      WRITE (4,*)'    NO. OF STEPS =',NSTEP
      WRITE (4,*)'    STEP LENGTH (sec) =',STEP1
      WRITE (4,*)'    PRESCRIBED TOLERANCE =',TOL
```

```
      WRITE (4,*)'    NTRANS =',NTRANS,'   EXPI =',EXPI
      WRITE (4,*)'    TO (FOR THE RAMP FUNCTION) =',TO
      READ (3,*) FI,W,AMP1
      READ (3,*) IZETA,IROT     !       If IZETA = 0, then
C               integration is done only upto mean water line
      WRITE (4,4080) FI,W,AMP1,IZETA,IROT
 4080 FORMAT (/5X,'WAVE HEADING (deg) =',F8.4/
     * 5X,'WAVE FREQUENCY (rad/sec) =',F8.5/
     * 5X,'WAVE AMPLITUDE (m) =',F8.4/
     * 5x,'IZETA = ',I5,'  IROT = ',I5)
      READ (3,*) NTRIG,NT,FACTOR
C
C     NTRIG = NUMBER OF STEP WHERE THE TETHER WILL BE DAMAGED
C     NT = TETHER NUMBER THAT WILL SUFFER DAMAGE
C     FRACT = FACTOR BY WHICH STIFFNESS AT 'NT' WILL BE MULTIPLIED
C
C************************* END OF READ ******************************
C
      WRITE (4,4000)
      WRITE (4,*)' NTRIG = ',NTRIG
      WRITE (4,*)' NT = ',NT
      WRITE (4,*)' FACTOR = ',FACTOR
      PHASE = PHASE*PI/180.0D0
      FI = FI*PI/180.D0
      AK=W*W/G          !  AK : Wave No.
C
C     CONSTRUCT THE PHYSICAL MASS-INERTIA ARRAY "AMASS(6)"
C
      AMASS(1)=WT/G
      AMASS(2)=AMASS(1)
      AMASS(3)=AMASS(1)
      AMASS(4)=AMASS(1)*RXX*RXX
      AMASS(5)=AMASS(1)*RYY*RYY
      AMASS(6)=AMASS(1)*RZZ*RZZ
C
C     CONVERT "CG()" FROM BODY COORD TO WL COORD FOR LATER USE
C
      CG(3) = CG(3)-DRAFT
C     GO TO 782
      WRITE (7,*) NSTEP
      WRITE (8,*) NSTEP
      WRITE (9,*) NSTEP
      WRITE (10,*) NSTEP
      WRITE (11,*) NSTEP
      WRITE (12,*) NSTEP
```

```
      WRITE (13,*) NSTEP
      WRITE (14,*) NSTEP
      WRITE (15,*) NSTEP
      WRITE (16,*) NSTEP
C
 782  N = 21
      T = 0.D0
      INDEX = INDEX1
      STEP = STEP1
      DO 1000 ISTEP=1,NSTEP
C
C     INCREASE CD TO ARTIFICIALLY DAMP THE SYSTEM TO
C     AVOID UNDUE INITIAL TRANSIENTS
C
      ECD = 1.0-DFLOAT(ISTEP)/DFLOAT(NTRANS)
      IF (ECD.LT.0.0) ECD = 0.0
      CD = CD1*DEXP(EXPI*ECD)
C
C     INTRODUCE "RAMP" FUNCTION : COSINE TYPE
C
      IF (T0.EQ.0.0) GO TO 60
      RAMP = 0.5*(1.0-DCOS(PI*T/T0))
 60   IF (T.GT.T0) RAMP = 1.0
      AMP = AMP1*RAMP
C
      IFCN = 0
      TEND = T+STEP1
C
      WRITE (7,*) T,Y(1)
      WRITE (8,*) T,Y(2)
      WRITE (9,*) T,Y(3)
      WRITE (10,*) T,Y(19)
      WRITE (11,*) T,Y(20)
      WRITE (12,*) T,Y(21)
      WRITE (13,*) T,TEN(1)
      WRITE (14,*) T,TEN(2)
      WRITE (15,*) T,TEN(3)
      WRITE (16,*) T,TEN(4)
C
      CALL DGEAR (N,FCN,FCNJ,T,STEP,Y,TEND,TOL,METH,MITER,INDEX,
     *          IWK,WK,IER)
      IF (ISTEP.EQ.1) WRITE (4,*)'TOTAL BUOYANCY AFTER STEP # 1 (N) =',
     *  BF,'   CB(X,Y,Z) IN CG COORD :',XB,YB,ZB
      PRINT*,' ISTEP =',ISTEP,'      IFCN =',IFCN
      IF (IER.GT.128) GO TO 500
```

```
      GO TO 501
500   WRITE (2,*)' N =',N,'  T =',T,'   TEND =',TEND,'   TOL =',TOL,
     *  '  METH =',METH,' MITER =',MITER,' ISTEP =',ISTEP,
     *  ' IFCN =',IFCN
      PRINT*,'IER =',IER,' N =',N,'  T =',T,'   TEND =',TEND,
     *  '  TOL =',TOL,'  METH =',METH,' MITER =',MITER
501   CONTINUE
1000  CONTINUE
      RETURN
      END
C
C*****************************************************************************
C
C             SUBROUTINES
C
C*****************************************************************************
C
      SUBROUTINE FCN (N,T,Y,YP)
      IMPLICIT DOUBLE PRECISION  (A-H), (O-Z)
C
      DIMENSION YP(21),DUMMY1(3,3),DUMMY2(3),R(3,3),TR(3,3),XX1(3),
     *          XX2(3),GN(3),ANG(3,3),RNG(3,3),ADMAE(3,3),ADMA1(3,3),
     *          ADJJ(3,3),ANGTR(3,3),XPG(3),XPO(3),AGBAR1(3,3),
     *          AGBAR(3,3),ADJ1E(3,3),ADJ1(3,3),OMEGA(3),WCAG(3),
     *          WCWCAG(3),VW(3),AW(3),VWNG(3),FN1(3),FN2(3),VELG(3),
     *          VRELG(3),AMDG(3),FD(3),AMN1(3),ADMA2(3,3),ADJ2E(3,3),
     *          ADJ2(3,3),AMN2(3),TM(6,6),TMINV(6,6),
     *          WKARTM(6),XSG(3),ANSG(3),ANSO(3),XSO(3),FP(3),AMPG(3),
     *          XT1G(3),Y(21),
     *          XT1O(3),FT(3),AMTG(3),B(3,3),GFOR(6),RWCI(3,3),
     *          BINVW(3),WKARB(3)
C
      COMMON/SUBFCN1/CM,CD,ISTEP,NCYL,NSURF,NTEN,WT,FI,W,AK,
     *          PI,RHO,G,BF,XB,YB,ZB,AMP,IFCN,NWP,BF1,XB1,YB1,ZB1,
     *          IZETA,IROT,NTRIG,NT,FACTOR
      COMMON/SUBFCN2/CG(3),X1(50,3),X2(50,3),D(50),NDIV(50),
     *          AL(50),XS(50,3),ANS(50,3),DS(50),AREA(50),TL(50),
     *          XT1(50,3),XT2(50,3),AKT(50),AKT1(50),AMASS(6),TEN(50),
     *          XWP(50),YWP(50),DWP(50),WPA(50),WPI(50),FTOT(6)
C
      IFCN = IFCN+1
4000  FORMAT(/)
C
C     INITIALIZE
C
```

```
      DO 5 I=1,3
      DO 5 J=1,3
      ADMA1(I,J) = 0.DO
      ADJ1(I,J) = 0.DO
      ADMA2(I,J) = 0.DO
 5    ADJ2(I,J) = 0.DO
      DO 10 I=1,6
      FTOT(I) = 0.DO
      DO 10 J=1,6
 10   TM(I,J) = 0.DO
      BF = 0.DO
      XMOM = 0.DO
      YMOM = 0.DO
      ZMOM = 0.DO
C
C     CONSTRUCT ROTATION MATRIX 'R(3,3)' & ITS TRANSPOSE 'TR(3,3)'
C
      IF (IROT.GT.0) THEN
      II = 0
      DO 11 I=1,3
      DO 11 J=1,3
      II = II+1
      R(I,J) = Y(9+II)
 11   TR(J,I) = Y(9+II)
      ELSE
      DO 12 I=1,3
      DO 12 J=1,3
      R(I,I) = 1.0DO
 12   TR(J,J) = 1.0DO
      END IF
C
C     CONSTRUCT ANGULAR VELOCITY VECTOR 'OMEGA(3)'
C
      DO 50 I=1,3
 50   OMEGA(I) = Y(6+I)
C
      DO 1000 IC=1,NCYL        ! Member Loop Begins
      DO 20 I=1,3
      XX1(I) = X1(IC,I)
 20   XX2(I) = X2(IC,I)
C
C     CALCULATE DIRECTION COSINES 'GN(3)' OF THE MEMBER IN GXYZ
C
      DO 25 I=1,3
 25   GN(I) = (XX2(I)-XX1(I))/AL(IC)
```

```
      DL = AL(IC)/DFLOAT(NDIV(IC))
      DVOL = PI*D(IC)**2*DL/4.0D0
      CM1 = RHO*DVOL*CM
      CM2 = RHO*DVOL*(CM-1.0D0)
C
C     CONSTRUCT [N'] MATRIX : ANG(3,3)
C
      ANG(1,1) = GN(2)**2+GN(3)**2
      ANG(1,2) = -GN(1)*GN(2)
      ANG(1,3) = -GN(1)*GN(3)
      ANG(2,1) = ANG(1,2)
      ANG(2,2) = GN(3)**2+GN(1)**2
      ANG(2,3) = -GN(2)*GN(3)
      ANG(3,1) = ANG(1,3)
      ANG(3,2) = ANG(2,3)
      ANG(3,3) = GN(1)**2+GN(2)**2
C
C     CONSTRUCT MATRICES [ma1] : ADMA1(3,3), [ma] : ADMAE(3,3)
C     [JJ] : ADJJ(3,3)
C
      CALL MATMUL2 (R,ANG,RNG)
      CALL MATMUL2 (RNG,TR,ADMAE)
      DO 30 I=1,3
      DO 30 J=1,3
 30   ADJJ(I,J) = RNG(I,J)*CM2
      CALL MATMUL2 (ANG,TR,ANGTR)
C
      DO 1500 ID=1,NDIV(IC)   ! Slice by slice computation
C
C     CALCULATE "XPG(3)" & "XP0(3)" IN GXYZ & OXYZ
C
      DO 35 I=1,3
 35   XPG(I) = XX1(I)+(DFLOAT(ID)-0.5D0)*DL*GN(I)
      CALL MATMUL1 (R,XPG,XP0)
      DO 40 I=1,3
 40   XP0(I) = XP0(I)+Y(I)+CG(I)
C
C     CALC WAVE ELEVATION "ZETA" W.R.T. WL
C
      XBAR = XP0(1)*DCOS(FI)+XP0(2)*DSIN(FI)
      ARG = -W*T+AK*XBAR
      ZETA = AMP*DCOS(ARG)
      IF (IZETA.EQ.0) ZETA = 0.0
      IF (XP0(3).GT.ZETA) GO TO 1500  !  i.e. go to next slice
C
```

```
C       CALC BUOYANCY FORCE "B" AND ITS X & Y MOMENTS
C
        BF = BF+DVOL*RHO*G
        XMOM = XMOM+DVOL*RHO*G*XPG(1)
        YMOM = YMOM+DVOL*RHO*G*XPG(2)
        ZMOM = ZMOM+DVOL*RHO*G*XPG(3)
C
C       CONSTRUCT MATRICES "AGBAR1(3,3)" & "AGBAR(3,3)"
C
        AGBAR1(1,2) = XPG(3)
        AGBAR1(1,3) = -XPG(2)
        AGBAR1(2,1) = -XPG(3)
        AGBAR1(2,3) = XPG(1)
        AGBAR1(3,1) = XPG(2)
        AGBAR1(3,2) = -XPG(1)
        DO 41 I=1,3
        DO 41 J=1,3
 41     AGBAR(I,J) = -AGBAR1(I,J)
        CALL MATMUL2 (ADJJ,AGBAR1,ADJ1E)
        CALL CROSS (OMEGA,XPG,WCAG)
        CALL CROSS (OMEGA,WCAG,WCWCAG)
C
C       CALC WAVE VEL & ACCLN IN OXYZ
C
        A = AMP*DEXP(AK*XPO(3))
C
        VW(1) = W*A*DCOS(ARG)*DCOS(FI)
        VW(2) = W*A*DCOS(ARG)*DSIN(FI)
        VW(3) = W*A*DSIN(ARG)
        AW(1) = W*W*A*DSIN(ARG)*DCOS(FI)
        AW(2) = W*W*A*DSIN(ARG)*DSIN(FI)
        AW(3) = -W*W*A*DCOS(ARG)
C
        CALL MATMUL1 (TR,VW,DUMMY2)
        CALL MATMUL1 (ANG,DUMMY2,VWNG)
C
C       CALC "FN1(3)" & "FN2(3)"
C
        CALL MATMUL1 (ADMAE,AW,FN1)
        DO 51 I=1,3
 51     FN1(I) = FN1(I)*CM1
        CALL MATMUL1 (ADJJ,WCWCAG,FN2)
C
C       CALC RELATIVE VEL "VRELG(3)" IN GXYZ
C
```

```
      DO 55 I=1,3
55    VELG(I) = Y(3+I)
      CALL MATMUL1 (ANGTR,VELG,VRELG)
      CALL MATMUL1 (ANG,WCAG,DUMMY2)
      DO 60 I=1,3
60    VRELG(I) = VWNG(I)-VRELG(I)-DUMMY2(I)
      AVRELG = DSQRT(VRELG(1)**2+VRELG(2)**2+VRELG(3)**2)
C
C     CALC DRAG FORCE "FD'" AND ITS MOMENT "AMDG(3)"
C
      DO 65 I=1,3
65    DUMMY2(I) = 0.5D0*RHO*CD*D(IC)*DL*AVRELG*VRELG(I)
      CALL CROSS (XPG,DUMMY2,AMDG)
      CALL MATMUL1 (R,DUMMY2,FD)
C
C     CALC MOMENTS "AMN1(3)" & "AMN2(3)"
C
      CALL MATMUL2 (AGBAR,ANGTR,DUMMY1)
      CALL MATMUL1 (DUMMY1,AW,AMN1)
      DO 70 I=1,3
      AMN1(I) = AMN1(I)*CM1
      DO 70 J=1,3
      ADMA1(I,J) = ADMA1(I,J)+ADMAE(I,J)*CM2
70    ADMA2(I,J) = ADMA2(I,J)+DUMMY1(I,J)*CM2
      CALL MATMUL2 (AGBAR,ANG,DUMMY1)
      CALL MATMUL2 (DUMMY1,AGBAR1,ADJ2E)
      DO 75 I=1,3
      DO 75 J=1,3
      ADJ1(I,J) = ADJ1(I,J)+ADJ1E(I,J)
75    ADJ2(I,J) = ADJ2(I,J)+ADJ2E(I,J)*CM2
      CALL MATMUL1 (DUMMY1,WCWCAG,AMN2)
      DO 80 I=1,3
80    AMN2(I) = AMN2(I)*CM2
      DO 85 I=1,3
      FTOT(I) = FTOT(I)+FN1(I)-FN2(I)+FD(I)
85    FTOT(I+3) = FTOT(I+3)+AMN1(I)-AMN2(I)+AMDG(I)
1500  CONTINUE          !  Slice Loop Ends
1000  CONTINUE          !  Member Loop Ends
C
C     CALC CETNRE OF BUOYANCY
C
      IF ((ISTEP+IFCN).EQ.2) THEN
      BF1 = BF
      WRITE(4,*)' ** BUOYANCY (N) =',BF1
      XB1 = XMOM/BF1
```

```
      YB1 = YMOM/BF1
      ZB1 = ZMOM/BF1
      WRITE (4,*)' ** XB1,YB1,ZB1 (m) W.R.T. CG =',XB1,YB1,ZB1
      ELSE
      XB = XMOM/BF
      YB = YMOM/BF
      ZB = ZMOM/BF
      END IF
      IF (BF.LT.WT) PRINT*,' %%% B LESS THAN WT; B =',BF
      IF (BF.LT.WT) WRITE(4,*)' %%% B LESS THAN WT; B =',BF
C
C     CONSTRUCT THE TOTAL MASS-INERTIA MATRIX "TM(6,6)"
C
      DO 90 I=1,3
      TM(I,I) = AMASS(I)
      DO 90 J=1,3
      TM(I,J) = TM(I,J)+ADMA1(I,J)
90    TM(I,J+3) = ADJ1(I,J)
      DO 95 I=1,3
      TM(I+3,I+3) = AMASS(I+3)
      DO 95 J=1,3
      TM(I+3,J) = ADMA2(I,J)
95    TM(I+3,J+3) = TM(I+3,J+3)+ADJ2(I,J)
      IF ((ISTEP+IFCN).EQ.2) THEN
4096  FORMAT (6(E12.5,1X))
      WRITE (4,4000)
      WRITE (4,4000)
      WRITE (4,*)'    TOTAL MASS-INERTIA MATRIX '
      WRITE (4,4000)
      DO 96 I=1,6
96    WRITE (4,4096) (TM(I,J),J=1,6)
      WRITE (4,4000)
      WRITE (4,4000)
      ELSE
      END IF
C
C     INVERT "TM(6,6)" TO "TMINV(6,6)"
C
      NTM = 6
      ITM = 6
      IDGT = 0
      CALL LINV1F (TM,NTM,ITM,TMINV,IDGT,WKARTM,IERTM)
C
C     CALC PRESSURE FOECE "FP(8)" AND MOMENT "AMPG(3)"
C
```

```
      DO 2000 IS=1,NSURF        !  Loop for surfaces begins
      DO 100 I=1,3
      XSG(I) = XS(IS,I)         !  These are in GXYZ
100   ANSG(I) = ANS(IS,I)
      CALL MATMUL1 (R,XSG,XSO)
      CALL MATMUL1 (R,ANSG,ANSO)
      DO 105 I=1,3
105   XSO(I) = XSO(I)+Y(I)*CG(I)
      XBAR = XSO(1)*DCOS(FI)+XSO(2)*DSIN(FI)
      ARG = -W*T+AK*XBAR
      ZETA = AMP*DCOS(ARG)
      IF (IZETA.EQ.0) ZETA = 0.0
      IF (XSO(3).GT.ZETA) GO TO 2000  !  i.e. to next surface
      DO 110 I=1,3
110   FP(I) = AREA(IS)*RHO*G*AMP*DEXP(AK*XSO(3))*DCOS(ARG)*ANSO(I)
      CALL MATMUL1 (TR,FP,DUMMY2)
      CALL CROSS (XSG,DUMMY2,AMPG)
      DO 115 I=1,3
      FTOT(I) = FTOT(I)+FP(I)
      FTOT(I+3) = FTOT(I+3)+AMPG(I)
115   CONTINUE
2000  CONTINUE          !  Surface Loop Ends
C
C     CALCULATE FORCE & MOMENT DUE TO TETHER "FT(3)" & "AMTG(3)"
C
      DO 2500 IT=1,NTEN         !  Tether Loop Begins
C
C     TRIGGERING LOSS OF STIFFNESS
C
      IF(ISTEP.GE.NTRIG) THEN
      IF(IT.EQ.NT) AKT(IT) = AKT1(IT)*FACTOR
      ELSE
      END IF
      DO 120 I=1,3
120   XT1G(I) = XT1(IT,I)
      CALL MATMUL1 (R,XT1G,XT10)
      DO 125 I=1,3
125   XT10(I) = XT10(I)+Y(I)+CG(I)
      TLNEW = DSQRT((XT2(IT,1)-XT10(1))**2+(XT2(IT,2)-XT10(2))**2+
     *          (XT2(IT,3)-XT10(3))**2)
      DTL = TLNEW-TL(IT)
      IF (DTL.LT.0.D0) DTL = 0.D0
      TEN(IT) = AKT(IT)*DTL
      DO 130 I=1,3
130   FT(I) = TEN(IT)*(XT2(IT,I)-XT10(I))/TLNEW
```

```
C
      CALL MATMUL1 (TR,FT,DUMMY2)
      CALL CROSS (XT1G,DUMMY2,AMTG)
      DO 135 I=1,3
      FTOT(I) = FTOT(I)+FT(I)
 135  FTOT(I+3) = FTOT(I+3)+AMTG(I)
 2500 CONTINUE        !   Tether Loop Ends
C
C     INCLUDE HYDORSTATIC FORCES AND MOMENTS IN "FTOT(6)"
C
      IF (NWP.GT.0) THEN
      H33 = 0.0D0
      H44 = 0.0D0
      H55 = 0.0D0
      DO 136 I = 1,NWP
      H33 = H33 + RHO*G*WPA(I)
      H44 = H44 + RHO*G*(WPA(I)*YWP(I)**2 + WPI(I))
 136  H55 = H55 + RHO*G*(WPA(I)*XWP(I)**2 + WPI(I))
      H44 = H44 + ZB1*BF1
      H55 = H55 + ZB1*BF1
      IF ((ISTEP+IFCN).EQ.2) THEN
      WRITE (4,*)'    H33 (N/M) = ',H33
      WRITE (4,*)'    H44 (N-M) = ',H44
      WRITE (4,*)'    H55 (N-M) = ',H55
      WRITE (4,4000)
      ELSE
      END IF
      FTOT(3) = FTOT(3) + BF1 - WT - H33*Y(3)
      FTOT(4) = FTOT(4) - H44*Y(19)
      FTOT(5) = FTOT(5) - H55*Y(20)
      ELSE
      FTOT(3) = FTOT(3)+BF-WT
      FTOT(4) = FTOT(4)+YMOM
      FTOT(5) = FTOT(5)-XMOM
      END IF
C
C     CREATE THE R.H.S. ACCLN VECTOR "GFOR(6)"
C
      CALL MATMUL3 (TMINV,FTOT,GFOR)
C
C     CONSTRUCT  [R][WxI] : RWCI(3,3)
C
      DUMMY1(1,2) = -Y(9)
      DUMMY1(1,3) = Y(8)
      DUMMY1(2,1) = Y(9)
```

```
      DUMMY1(2,3) = -Y(7)
      DUMMY1(3,1) = -Y(8)
      DUMMY1(3,2) = Y(7)
      CALL MATMUL2 (R,DUMMY1,RWCI)
C
C     CONSTRUCT MATRIX "B(3,3)" & OBTAIN "BINVW(3)"
C
      B(1,1) = DCOS(Y(20))
      B(1,3) = -DCOS(Y(19))*DSIN(Y(20))
      B(2,2) = 1.0D0
      B(2,3) = DSIN(Y(19))
      B(3,1) = DSIN(Y(20))
      B(3,3) = DCOS(Y(19))*DCOS(Y(20))
C
      NB = 3
      IB = 3
      IDGT = 0
      CALL LINV1F (B,NB,IB,DUMMY1,IDGT,WKARB,IERB)
      CALL MATMUL1 (DUMMY1,OMEGA,BINVW)
C
C     WRITE THE SYSTEM 21 ORDY. DIFF. EQNS. FOR "DGEAR"
C
      DO 140 I=1,3
      YP(I) = Y(I+3)
      YP(I+3) = GFOR(I)
 140  YP(I+6) = GFOR(I+3)
C
      YP(10) = RWCI(1,1)
      YP(11) = RWCI(1,2)
      YP(12) = RWCI(1,3)
      YP(13) = RWCI(2,1)
      YP(14) = RWCI(2,2)
      YP(15) = RWCI(2,3)
      YP(16) = RWCI(3,1)
      YP(17) = RWCI(3,2)
      YP(18) = RWCI(3,3)
C
      DO 145 I=1,3
 145  YP(I+18) = BINVW(I)
      RETURN
      END
C
C
C
C
```

```
      SUBROUTINE FCNJ (N,T,Y,PD)
      IMPLICIT DOUBLE PRECISION (A-H),(O-Z)
      DIMENSION Y(N),PD(N,N)
      RETURN
      END
C
C
C
C
C
      SUBROUTINE MATMUL1 (A,B,C)
      IMPLICIT DOUBLE PRECISION (A-H),(O-Z)
      DIMENSION A(3,3),B(3),C(3)
C
      DO 5 I=1,3
 5    C(I)=0.0D0
      K=0
      DO 10 I=1,3
      K=K+1
      DO 10 J=1,3
 10   C(K)=C(K)+A(I,J)*B(J)
      RETURN
      END
C
C
C
C
      SUBROUTINE MATMUL2 (A1,B1,C1)
      IMPLICIT DOUBLE PRECISION (A-H),(O-Z)
      DIMENSION A1(3,3),B1(3,3),C1(3,3)
C
      DO 5 I1=1,3
      DO 5 J1=1,3
 5    C1(I1,J1)=0.0D0
      DO 10 I1=1,3
      DO 10 J1=1,3
      DO 10 K1=1,3
 10   C1(I1,J1)=C1(I1,J1)+A1(I1,K1)*B1(K1,J1)
      RETURN
      END
C
C
C
C
      SUBROUTINE MATMUL3 (A2,B2,C2)
```

```
      IMPLICIT DOUBLE PRECISION (A-H),(O-Z)
      DIMENSION A2(6,6),B2(6),C2(6)
C
      K2=0
      DO 5 I2=1,6
 5    C2(I2)=0.000
      DO 10 I2=1,6
      K2=K2+1
      DO 10 J2=1,6
 10   C2(K2)=C2(K2)+A2(I2,J2)*B2(J2)
      RETURN
      END
C
C
C
C
C
      SUBROUTINE CROSS (A,B,C)
      IMPLICIT DOUBLE PRECISION (A-H),(O-Z)
      DIMENSION A(3),B(3),C(3)
C
      C(1)=A(2)*B(3)-A(3)*B(2)
      C(2)=A(3)*B(1)-A(1)*B(3)
      C(3)=A(1)*B(2)-A(2)*B(1)
      RETURN
      END
```

APPENDIX D :

LISTING OF 'FREQ_DOMAIN'

```
C*************************************************************************
C
C       PROGRAM "FREQ_DOMAIN" : PERFORMS FREQUENCY DOMAIN ANALYSIS
C       FOR A TENSION LEG PLATFORM
C
C*************************************************************************
C
C       INPUT FILE NAME : 'FREQ.PILOT'
C
C       INPUT VARIABLES :-
C
C       '(CG(I),I=1,3),RHO'
C       CG              = COORDINATES OF THE CENTRE OF GRAVITY (m)
C       RHO             = MASS DENSITY OF WATER (Kg/cu.m)
C       'DRAFT,WT'
C       DRAFT           = DRAFT OF THE PLATFORM (m)
C       WT              = WEIGHT OF THE PLATFORM (N)
C       'RXX,RYY,RZZ'
C       RXX             = RADIUS OF GYRATION ABOUT X-AXIS (m)
C       RYY             = RADIUS OF GYRATION ABOUT Y-AXIS (m)
C       RZZ             = RADIUS OF GYRATION ABOUT Z-AXIS (m)
C       'CD,CM'
C       CD              = NONLINEAR DRAG COEFFICIENT
C       CM              = VIRTUAL MASS COEFFICIENT
C       'HED,SW,EW,NW'
C       HED             = WAVE HEADING ANGLE (deg)
C       SW              = STARTING FREQUENCY (rad/sec)
C       EW              = LAST FREQUENCY (rad/sec)
C       NW              = NUMBER OF FREQUENCY STEPS
C       ** FOR EVERY TENSION LEG PROVIDE :
C       'TP(I)'
C       TP              = EQUILIBRIUM STATIC PRETENSION AT THE
C                         Ith TENSION LEG (N)
C       '(ERROR(I),I=1,6)'
C       ERROR(I)        = ERROR TOLERANCE FOR THE Ith D.O.F.;
C                         REQUIRED FOR ITERATIONS
C       IERR            = IF EQUAL TO 0, THEN NO ITERATION,
C                         1 OTHERWISE
C
C       INPUT FILE NAME : 'FREQ.DAT'
C
C       'NCYL'
C       NCYL            = NUMBER OF CYLINDERS
C       ** FOR EVERY CYLINDER PROVIDE :
C       '(X1(I,J),J=1,3),(X2(I,J),J=1,3),D(I),NDIV(I)'
```

```
C       X1,X2           = COORDINATES OF THE CYLINDER ENDS (m)
C       D               = DIAMETER OF THE CYLINDER (m)
C       NDIV            = NUMBER OF HORIZONTAL SLICES THE CYLINDER
C                         WUOLD HAVE TO BE DIVIDED
C       'NSURF'         = NUMBER CIRCULAR FLAT SURFACES
C       ** FOR EVERY SURFACE PROVIDE :
C       '(XS(I,J),J=1,3),(ANS(I,J),J=1,3),DS(I)'
C       XS              = COORDINATES OF THE CENTRE OF THE FLAT
C                         SURFACE
C       ANS             = DIRECTION COSINES OF THE NORMAL TO THE
C                         FLAT SURFACE
C       DS              = DIAMETER (m) OF THE FLAT SURFACE
C       'NTEN'          = NUMBER OF TENSION LEGS
C       ** FOR EVERY TENSION LEG PROVIDE):
C       '(XT1(I,J),J=1,3),(XT2(I,J),J=1,3),AKT(I)'
C       XT1,XT2         = COORDINATES OF THE ENDS OF THE TETHER
C       AKT             = AXIAL STIFFNESS OF THE TETHER
C       'NWP'
C       NWP             = NUMBER OF CIRCULAR WATERPLANES
C       ** FOR EVERY WATERPLANE PROVIDE
C       'XWP(I),YWP(I),DWP(I)'
C       XWP,YWP         = X AND Y COORDINATES OF THE CENTRE OF
C                         THE WATERPLANE
C       DWP             = DIAMETER OF THE WATERPLANE
C
C       NAME OF OUTPUT FILE : 'FREQ.DAT'
C
C       COMPUTED OUTPUT VARIABLES
C
C       AMA             = PHYSICAL MASS/INERTA MATRIX
C       ADMA            = ADDED MASS/INERTA MATRIX
C       AM              = VIRTUAL MASS/INERTA MATRIX
C       HK              = HYDROSTATIC STIFFNESS MATRIX
C       TK              = TETHER STIFFNESS MATRIX
C       STF             = TOTAL STIFFNESS MATRIX
C       FREQR           = NATURAL FREQUENCIES (rad/sec)
C       FREQHZ          = NATURAL FREQUENCIES (Hz)
C       TSEC            = NATURAL TIME PERIODS (sec)
C       ** FOR EVERY FREQUENCY THE FOLLOWING ARE COMPUTED
C       BV              = DAMPING MATRIX
C       FORCE1          = WAVE EXCITATION FORCE RAOs
C       DISP            = MOTION RAOs
C       FASE            = PHASE OF MOTIONS IN DIFF. D.O.F.
C       TENRAO          = TENSION RAOs
C
```

```
C*********************************************************************
C
C       REQIURED LIBRARY ROUTINES : IMSL ROUTINE 'LEQ2C'
C
C*********************************************************************
C
        IMPLICIT DOUBLE PRECISION (A-H,O-Z)
C
        DIMENSION CG(3),X1(50,3),X2(50,3),D(50),NDIV(50),
     *          AL(50),XS(50,3),ANS(50,3),DS(50),AREA(50),
     *          XT1(50,3),XT2(50,3),AKT(50),TL(50),TP(50),
     *          DWP(50),XWP(50),YWP(50),WPA(50),WPI(50),XXS(3),
     *          AMA(6,6),ADMA(6,6),AM(6,6),XX1(3),XX2(3),
     *          GN(3),AN(3,3),XP(3),ABAR(3,3),ABAR1(3,3),
     *          AM11(3,3),AM12(3,3),AM21(3,3),AM22(3,3),
     *          HK(6,6),TK(6,6),STF(6,6),FREQR(6),FREQHZ(6),
     *          TSEC(6),VELR(6),VELI(6),DFI1(3),DFI2(3),
     *          DFIN1(3),DFIN2(3),FI1(3),FI2(3),DMIN1(3),
     *          DMIN2(3),FMI1(3),FMI2(3),OMEGAR(3),OMEGAI(3),
     *          VBR(3),VBI(3),VWR(3),VWI(3),VBRN(3),VBIN(3),
     *          VWRN(3),VWIN(3),DFD1(3),DFD2(3),DFDN1(3),
     *          DFDN2(3),FD1(3),FD2(3),DMDN1(3),DMDN2(3),
     *          FMD1(3),FMD2(3),BV11(3,3),BV12(3,3),BV21(3,3),
     *          BV22(3,3),BV(6,6),DFP1(3),DFP2(3),FP1(3),
     *          FP2(3),DMP1(3),DMP2(3),FMP1(3),FMP2(3),
     *          DISP(6),PHASE(6),FASE(6),ERROR(6),PREV(6)
C
        COMPLEX *16 WA(48),WK(6)
C
        COMPLEX *16 DTLX,DTLY,DTLZ,DTLPC,COM,FORCE(6),FORCE1(6),
     *          COEF(6,6),CDISP(6)
C
        CAB(COM) = DSQRT((DREAL(COM))**2 + (DIMAG(COM))**2)
C
C-------------------------------------------------------------------
C       OPEN I/O FILES
C-------------------------------------------------------------------
C
        OPEN (UNIT=1,FILE='FREQ.DAT',TYPE='OLD')
        OPEN (UNIT=3,FILE='FREQ.PILOT',TYPE='OLD')
        OPEN (UNIT=4,FILE='FREQ.OUT',TYPE='NEW')
C
        PI = 3.1415927D0
        G = 9.81D0
C
```

```
      READ (3,*) (CG(I),I=1,3),RHO
      READ (3,*) DRAFT,WT
      WRITE (4,4000)
4000  FORMAT(/)
4001  FORMAT(//)
      WRITE (4,*)'  CGX,Y,Z (m) =',(CG(I),I=1,3)
      WRITE (4,*)' MASS DENSITY OF WATER (Kg/cu.m) = ',RHO
      WRITE (4,*)'  DRAFT (m) =',DRAFT
      WRITE (4,*)'  WEIGHT (N) =',WT
      DRAFT = DRAFT - CG(3)
      WRITE (4,4000)
      READ (1,*) NCYL
      WRITE (4,*)'  NO. OF CYLINDERS =',NCYL
      WRITE (4,4020)
4020  FORMAT (/' ** CYLINDER COORD. ETC IN RIG SYSTEM **'/
     *  4X,'X1',8X,'Y1',8X,'Z1',8X,'X2',8X,'Y2',8X,'Z2',11X,'LENGTH',
     *  10X,'DIA',10X,'NDIV'/)
4030  FORMAT (6(F8.3,2X),3X,F10.3,5X,F10.3,5X,I5)
      DO 30 I = 1,NCYL
      READ (1,*) (X1(I,J),J=1,3),(X2(I,J),J=1,3),D(I),NDIV(I)
      AL(I) = DSQRT((X2(I,1)-X1(I,1))**2 + (X2(I,2)-X1(I,2))**2 +
     *        (X2(I,3)-X1(I,3))**2)
      WRITE (4,4030) (X1(I,J),J=1,3),(X2(I,J),J=1,3),AL(I),D(I),
     *       NDIV(I)
      DO 30 J = 1,3
      X1(I,J) = X1(I,J) - CG(J)
30    X2(I,J) = X2(I,J) - CG(J)
      WRITE (4,4001)
      READ (1,*) NSURF
      WRITE (4,*)'  NO. OF CIRCULAR SURFACES =',NSURF
      WRITE (4,4040)
4040  FORMAT (/'  ** PLANE SURFACE COORD. ETC IN RIG SYSTEM **'/
     *  4X,'X',9X,'Y',9X,'Z',14X,'NX',8X,'NY',8X,'NZ',10X,'DIA',
     *  10X,'AREA'/)
4050  FORMAT (3(F8.3,2X),3X,3(F8.5,2X),3X,F10.3,5X,F10.3)
      DO 40 I = 1,NSURF
      READ (1,*) (XS(I,J),J=1,3),(ANS(I,J),J=1,3),DS(I)
      AREA(I) = PI*DS(I)**2/4.0D0
      WRITE (4,4050) (XS(I,J),J=1,3),(ANS(I,J),J=1,3),DS(I),
     *       AREA(I)
      DO 40 J = 1,3
40    XS(I,J) = XS(I,J) - CG(J)
      WRITE (4,4001)
      READ (1,*) NTEN
      WRITE (4,*)'  NO. OF TENSION LEGS =',NTEN
```

```
      WRITE (4,4060)
4060  FORMAT ('  ** TETHER COORD. ETC IN RIG SYSTEM **'/
     *  4X,'X1',8X,'Y1',8X,'Z1',8X,'X2',8X,'Y2',8X,'Z2',11X,
     *  'LENGTH',3X,'STIFFNESS (N/m)'/)
4070  FORMAT (6(F8.3,2X),3X,F10.3,5X,E12.5)
      DO 50 I = 1,NTEN
      READ (1,*) (XT1(I,J),J=1,3),(XT2(I,J),J=1,3),AKT(I)
      TL(I) = DSQRT((XT2(I,1)-XT1(I,1))**2 + (XT2(I,2)-
     *        XT1(I,2))**2 + (XT2(I,3)-XT1(I,3))**2)
      WRITE (4,4070) (XT1(I,J),J=1,3),(XT2(I,J),J=1,3),TL(I),
     *        AKT(I)
      DO 50 J = 1,3
      XT1(I,J) = XT1(I,J) - CG(J)
50    XT2(I,J) = XT2(I,J) - CG(J)
      WRITE (4,4001)
      READ (1,*) NWP
      WRITE (4,*)' NO. OF WATER PLANES =',NWP
      WRITE (4,4071)
4071  FORMAT ('  ** WATER PLANE COORD. ETC IN RIG SYS **'/
     *  '   XWP        YWP        DWP        AWP        IWP'/)
4072  FORMAT (5(F12.3,2X))
      DO 55 I = 1,NWP
      READ (1,*) XWP(I),YWP(I),DWP(I)
      WPA(I) = PI*DWP(I)**2/4.0D0
      WPI(I) = PI*DWP(I)**4/64.0D0
55    WRITE (4,4072) XWP(I),YWP(I),DWP(I),WPA(I),WPI(I)
      READ (3,*) RXX,RYY,RZZ
      WRITE (4,4001)
      WRITE (4,*)'  RXX,RYY,RZZ (m) =',RXX,RYY,RZZ
      READ (3,*) CD,CM
      WRITE (4,4000)
      WRITE (4,*)'  CD =',CD,'    CM =',CM
      WRITE (4,4001)
      READ (3,*) HED,SW,EW,NW
      WRITE (4,4080) HED,SW,EW,NW
4080  FORMAT ('  WAVE HEADING (DEG) = ',F10.5/
     *  '  START FREQUENCY (RAD/SEC) = ',F10.5/
     *  '  END FREQUENCY (RAD/SEC) = ',F10.5/
     *  '  NO. OF FREQUENCY STEPS = ',I5//)
      HED = HED*PI/180.0D0
      WRITE (4,*)'  ** EQUILIBRIUM TENSIONS **'
      WRITE (4,4000)
      TPTOT = 0.0D0
      WRITE (4,*)'  LEG #       TENSION (N)'
      DO 60 I = 1,NTEN
```

```
      READ (3,*) TP(I)
      WRITE (4,*) I,TP(I)
60    TPTOT = TPTOT + TP(I)
      WRITE (4,*)'  TOTAL STATIC MEAN PRETENSION (N) =',TPTOT
      WRITE (4,4001)
      READ (3,*) (ERROR(I),I=1,6)
      WRITE (4,*)'  **  SPECIFIED ERROR TOLERANCES, 1 THROUGH 6  **'
      WRITE (4,4081) (ERROR(I),I=1,6)
4081  FORMAT (6(F10.6,5X))
      READ (3,*) IERR
      WRITE (4,4000)
      WRITE (4,*)'  IERR = ',IERR
      WRITE (4,4001)
C
C****************** END OF READ ***********************************************
C
C     CONSTRUCT THE PHYSICAL MASS-INERTIA MATRIX AMA(6,6)
C
      AMA(1,1) = WT/G
      AMA(2,2) = AMA(1,1)
      AMA(3,3) = AMA(1,1)
      AMA(4,4) = AMA(1,1)*RXX*RXX
      AMA(5,5) = AMA(1,1)*RYY*RYY
      AMA(6,6) = AMA(1,1)*RZZ*RZZ
C
      CM1 = CM - 1.0D0
C
C     CONSTRUCT ADDED MASS AND STIFFNESS MATRICES viz.  ADMA(6,6)
C     AND STF(6,6) AND ALSO CALCULATE BUOYANCY & CENTRE OF BUOYANCY
C
      DO 1000 IC = 1,NCYL     !  Member loop begins
      DO 70 I =1,3
      XX1(I) = X1(IC,I)
70    XX2(I) = X2(IC,I)
C
C     CALCULATE DIRECTION COSINES *GN(3)* IN GXYZ
C
      DO 75 I =1,3
75    GN(I) = (XX2(I) - XX1(I)) / AL(IC)
      DL = AL(IC) / DFLOAT(NDIV(IC))
      A = PI*D(IC)**2 / 4.0D0
      DVOL = DL*A
      DM = RHO*DVOL
      DA = RHO*D(IC)*DL*0.5D0
C
```

```
C       CONSTRUCT [N] MATRIX : AN(3,3)
C
        AN(1,1) = GN(2)**2 + GN(3)**2
        AN(1,2) = -GN(1)*GN(2)
        AN(1,3) = -GN(1)*GN(3)
        AN(2,1) = AN(1,2)
        AN(2,2) = GN(3)**2 + GN(1)**2
        AN(2,3) = -GN(2)*GN(3)
        AN(3,1) = AN(1,3)
        AN(3,2) = AN(2,3)
        AN(3,3) = GN(1)**2 + GN(2)**2
C
        DO 1500 ID = 1,NDIV(IC)  !  Slice by slice computaion
C
C       CALCULATE POSITION VECTOR "XP(3)"
C
        DO 80 I = 1,3
 80     XP(I) = XX1(I) + (DFLOAT(ID) - 0.5D0)*DL*GN(I)
        IF (XP(3).GT.DRAFT) GO TO 1500  !  to next slice
        BF = BF + RHO*G*DVOL  !  BF = Buoyancy Force
        BXMOM = BXMOM + RHO*G*DVOL*XP(1)
        BYMOM = BYMOM + RHO*G*DVOL*XP(2)
        BZMOM = BZMOM + RHO*G*DVOL*XP(3)
C
C       CONSTRUCT MATRICES "ABAR1(3,3)" AND "ABAR(3,3)"
C
        ABAR1(1,2) = XP(3)
        ABAR1(1,3) = -XP(2)
        ABAR1(2,1) = -XP(3)
        ABAR1(2,3) = XP(1)
        ABAR1(3,1) = XP(2)
        ABAR1(3,2) = -XP(1)
        DO 90 I = 1,3
        DO 90 J = 1,3
 90     ABAR(I,J) = -ABAR1(I,J)
C
C       CONSTRUCT THE SUBMATRICES FOR THE ADDED MASS MATRIX
C
        CALL MATMUL2 (AN,ABAR1,AM12)
        CALL MATMUL2 (ABAR,AN,AM21)
        CALL MATMUL2 (ABAR,AM12,AM22)
        DO 100 I = 1,3
        DO 100 J = 1,3
        AM11(I,J) = DM*CM1*AN(I,J)
        AM12(I,J) = DM*CM1*AM12(I,J)
```

```
      AM21(I,J) = DM*CM1*AM21(I,J)
 100  AM22(I,J) = DM*CM1*AM22(I,J)
C
C     CONSTRUCT THE ADDED MASS MATRIX
C
      DO 110 I = 1,3
      DO 110 J = 1,3
      ADMA(I,J) = ADMA(I,J) + AM11(I,J)
      ADMA(I+3,J+3) = ADMA(I+3,J+3) + AM22(I,J)
      ADMA(I+3,J) = ADMA(I+3,J) + AM21(I,J)
 110  ADMA(I,J+3) = ADMA(I,J+3) + AM12(I,J)
 1500 CONTINUE          !  Slice loop ends
 1000 CONTINUE          !  Member loop ends
C
C     CONSTRUCT TOTAL MASS-INERTIA MATYRIX "AM(6,6)"
C
      DO 115 I = 1,6
      DO 115 J = 1,6
 115  AM(I,J) = AMA(I,J) + ADMA(I,J)
C
C     CALCULATE CENTRE OF BUOYANCY
C
      XB = BXMOM/BF
      YB = BYMOM/BF
      ZB = BZMOM/BF
      WRITE (4,*)'  TOTAL BUOYANCY (N) =',BF
      WRITE (4,*)'  CENTER OF BUOYANCY COORDINATES IN RIG SYSTEM'
      WRITE (4,*)'  XB (m) =',XB+CG(1)
      WRITE (4,*)'  YB (m) =',YB+CG(2)
      WRITE (4,*)'  ZB (m) =',ZB+CG(3)
      WRITE (4,4001)
C
C     CONSTRUCT THE HYDROSTATIC STIFFNESS MATRIX "HK(6,6)"
C
      DO 120 I = 1,NWP
      HK(3,3) = HK(3,3) + RHO*G*WPA(I)
      HK(3,4) = HK(3,4) + RHO*G*WPA(I)*YWP(I)
      HK(4,3) = HK(3,4)
      HK(3,5) = HK(3,5) + RHO*G*WPA(I)*XWP(I)
      HK(5,3) = HK(3,5)
      HK(4,5) = HK(4,5) + RHO*G*WPA(I)*XWP(I)*YWP(I)
      HK(5,4) = HK(4,5)
      HK(4,4) = HK(4,4) + RHO*G*(WPA(I)*YWP(I)**2 + WPI(I))
 120  HK(5,5) = HK(5,5) + RHO*G*(WPA(I)*XWP(I)**2 + WPI(I))
      HK(4,4) = HK(4,4) + ZB*BF
```

```
      HK(5,5) = HK(5,5) + ZB*BF
C
C     CONSTRUCT THE MOORING STIFFNESS MATRIX 'TK(6,6)'
C
      DO 130 I = 1,NTEN
      TPL = TP(I)/TL(I)
      EAL = AKT(I)
      XT = XT1(I,1)
      YT = XT1(I,2)
      ZT = XT1(I,3)
      TK(1,1) = TK(1,1) + TPL
      TK(1,5) = TK(1,5) + TPL*ZT
      TK(5,1) = TK(1,5)
      TK(1,6) = TK(1,6) + TPL*YT
      TK(6,1) = TK(1,6)
      TK(2,2) = TK(1,1)
      TK(2,4) = TK(2,4) - TPL*ZT
      TK(4,2) = TK(2,4)
      TK(2,6) = TK(2,6) + TPL*XT
      TK(6,2) = TK(2,6)
      TK(3,3) = TK(3,3) + EAL
      TK(3,4) = TK(3,4) + EAL*YT
      TK(4,3) = TK(3,4)
      TK(3,5) = TK(3,5) - EAL*XT
      TK(5,3) = TK(3,5)
      TK(4,4) = TK(4,4) + EAL*YT*YT + TPL*ZT*ZT
      TK(5,5) = TK(5,5) + EAL*XT*XT + TPL*ZT*ZT
  130 TK(6,6) = TK(6,6) + TPL*(XT*XT + YT*YT)
C
C     CONSTRUCT THE TOTAL STIFFNESS MATRIX 'STF(6,6)'
C
      DO 140 I = 1,6
      DO 140 J = 1,6
  140 STF(I,J) = HK(I,J) + TK(I,J)
C
C     WRITE THE CONSTANT COEFFICIENT MATRICES
C
      WRITE (4,4001)
 4100 FORMAT (1X,6(E12.5,2X))
      WRITE (4,*)' **  PHYSICAL MASS-INERTIA MATRIX  **'
      WRITE (4,4000)
      DO 150 I = 1,6
  150 WRITE (4,4100) (AMA(I,J),J=1,6)
      WRITE (4,4001)
      WRITE (4,*)' **  ADDED MASS-INERTA MATRIX  **'
```

```
      WRITE (4,4000)
      DO 155 I = 1,6
155   WRITE (4,4100)  (ADMA(I,J),J=1,6)
      WRITE (4,4001)
      WRITE (4,*)' **  VIRTUAL MASS-INERTIA MATRIX  **'
      WRITE (4,4000)
      DO 160 I = 1,6
160   WRITE (4,4100)  (AM(I,J),J=1,6)
      WRITE (4,4001)
      WRITE (4,*)' **  HYDROSTATIC STIFFNESS MATRIX  **'
      WRITE (4,4000)
      DO 165 I = 1,6
165   WRITE (4,4100)  (HK(I,J),J=1,6)
      WRITE (4,4001)
      WRITE (4,*)' **  TETHER STIFFNESS MATRIX  **'
      WRITE (4,4000)
      DO 170 I = 1,6
170   WRITE (4,4100)  (TK(I,J),J=1,6)
      WRITE (4,4001)
      WRITE (4,*)' **  TOATL STIFFNESS MATRIX  **'
      WRITE (4,4000)
      DO 175 I = 1,6
175   WRITE (4,4100)  (STF(I,J),J=1,6)
      WRITE (4,4001)
C
C     CALCULATE NATURAL FREQUENCIES AND TIME PERIODS
C
      DO 180 I = 1,6
      FREQR(I) = DSQRT(STF(I,I) / AM(I,I))
      FREQHZ(I) = FREQR(I) / (2.0DO*PI)
180   TSEC(I) = 1.0DO / FREQHZ(I)
      WRITE (4,*)' **  NATURAL FREQUENCIES AND TIME PERIODS  **'
      WRITE (4,*)' D.O.F.  FREQ(RAD/SEC)     FREQ(HZ)     PERIOD(SEC)'
4110  FORMAT (2X,I5,5X,3(F10.5,5X))
      DO 190 I = 1,6
190   WRITE (4,4110) I,FREQR(I),FREQHZ(I),TSEC(I)
      WRITE (4,4001)
      WRITE (4,*)' 0  CALCULATIONS FOR VARIOUS FREQUENCIES  0'
      W = SW
      DELW = (EW - SW) / DFLOAT(NW)
C
      DO 2000 IW = 1,NW        ! Frequency loop starts
      WRITE (4,4001)
      WRITE (4,*)' ***********************************************'
      WRITE (4,*)'          FREQUENCY (RAD/SEC) =',W
```

```
      WRITE (4,*)'  ************************************************'
      AK = W*W / G     !  AK = Wave No.
      DO 200 I = 1,6
      VELR(I) = 0.0D0
200   VELI(I) = 0.0D0
      ITER = 0
2100  ITER = ITER + 1
      PRINT*,' W =',W,'   ITER =',ITER
      DO 210 I = 1,3
      FI1(I) = 0.0D0
      FI2(I) = 0.0D0
      FMI1(I) = 0.0D0
      FMI2(I) = 0.0D0
      FD1(I) = 0.0D0
      FD2(I) = 0.0D0
      FMD1(I) = 0.0D0
      FMD2(I) = 0.0D0
      FP1(I) = 0.0D0
210   FP2(I) = 0.0D0
      DO 211 I = 1,6
      DO 211 J = 1,6
211   BV(I,J) = 0.0D0
C
      DO 2500 IC = 1,NCYL      !  Member loop begins
      DO 270 I =1,3
      XX1(I) = X1(IC,I)
270   XX2(I) = X2(IC,I)
C
C     CALCULATE DIRECTION COSINES "GN(3)" IN GXYZ
C
      DO 275 I =1,3
275   GN(I) = (XX2(I) - XX1(I)) / AL(IC)
      DL = AL(IC) / DFLOAT(NDIV(IC))
      A = PI*D(IC)**2 / 4.0D0
      DVOL = DL*A
      DM = RHO*DVOL
      DA = RHO*D(IC)*DL*0.5D0
C
C     CONSTRUCT [N] MATRIX : AN(3,3)
C
      AN(1,1) = GN(2)**2 + GN(3)**2
      AN(1,2) = -GN(1)*GN(2)
      AN(1,3) = -GN(1)*GN(3)
      AN(2,1) = AN(1,2)
      AN(2,2) = GN(3)**2 + GN(1)**2
```

```
      AN(2,3) = -GN(2)*GN(3)
      AN(3,1) = AN(1,3)
      AN(3,2) = AN(2,3)
      AN(3,3) = GN(1)**2 + GN(2)**2
C
      DO 3000 ID = 1,NDIV(IC)   !  Slice by slice computaion
C
C     CALCULATE POSITION VECTOR "XP(3)", COORD "ZETA" & "Z"
C
      DO 280 I = 1,3
280   XP(I) = XX1(I) + (DFLOAT(ID) - 0.5D0)*DL*GN(I)
      IF (XP(3).GT.DRAFT) GO TO 3000   !  to next slice
      CH = DCOS(HED)
      SH = DSIN(HED)
      ZETA = XP(1)*CH + XP(2)*SH
      Z = XP(3) - DRAFT
      CZ = DCOS(AK*ZETA)
      SZ = DSIN(AK*ZETA)
C
C     CALCULATE INERTIAL FORCE "FI1(3)" (PROPORTIONAL TO SINwt) &
C     "FI2(3)" (PROPORTIONAL TO COSwt), AND ALSO THE MOMENTS
C
      FIC = DM*CM*W*W*DEXP(AK*Z)
      DFI1(1) = FIC*SZ*CH
      DFI1(2) = FIC*SZ*SH
      DFI1(3) = -FIC*CZ
      DFI2(1) = FIC*CZ*CH
      DFI2(2) = FIC*CZ*SH
      DFI2(3) = FIC*SZ
C
      CALL MATMUL1 (AN,DFI1,DFIN1)
      CALL MATMUL1 (AN,DFI2,DFIN2)
C
      DO 281 I = 1,3
      FI1(I) = FI1(I) + DFIN1(I)
281   FI2(I) = FI2(I) + DFIN2(I)
C
      CALL CROSS (XP,DFIN1,DMIN1)
      CALL CROSS (XP,DFIN2,DMIN2)
C
      DO 290 I = 1,3
      FMI1(I) = FMI1(I) + DMIN1(I)
290   FMI2(I) = FMI2(I) + DMIN2(I)
C
C     CALCULATE DRAG FORCE
```

```
C
      DO 300 I = 1,3
      OMEGAR(I) = VELR(I+3)
300   OMEGAI(I) = VELI(I+3)
      CALL CROSS (OMEGAR,XP,VBR)
      CALL CROSS (OMEGAI,XP,VBI)
      DO 310 I = 1,3
      VBR(I) = VBR(I) + VELR(I)
310   VBI(I) = VBI(I) + VELI(I)
C
      VWR(1) = - W*DEXP(AK*Z)*SZ*CH
      VWR(2) = - W*DEXP(AK*Z)*SZ*SH
      VWR(3) = W*DEXP(AK*Z)*CZ
      VWI(1) = W*DEXP(AK*Z)*CZ*CH
      VWI(2) = W*DEXP(AK*Z)*CZ*SH
      VWI(3) = W*DEXP(AK*Z)*SZ
C
      CALL MATMUL1 (AN,VBR,VBRN)
      CALL MATMUL1 (AN,VBI,VBIN)
      CALL MATMUL1 (AN,VWR,VWRN)
      CALL MATMUL1 (AN,VWI,VWIN)
C
      VELWRN = DSQRT(VWRN(1)**2 + VWRN(2)**2 + VWRN(3)**2)
      VELWIN = DSQRT(VWIN(1)**2 + VWIN(2)**2 + VWIN(3)**2)
      IF (DABS(VELWRN).LT.0.00001) GO TO 311
      GO TO 312
311   FIW = PI / 2.0D0
      IF (VELWRN.LT.0.0D0) FIW = - FIW
      IF (VELWIN.LT.0.0D0) FIW = - FIW
      GO TO 313
312   FIW = ATAN(VELWIN / VELWRN)
C
313   VELBRN = DSQRT(VBRN(1)**2 + VBRN(2)**2 + VBRN(3)**2)
      VELBIN = DSQRT(VBIN(1)**2 + VBIN(2)**2 + VBIN(3)**2)
      IF (DABS(VELBRN).LT.0.00001D0) GO TO 314
      GO TO 315
314   FIB = PI / 2.0D0
      IF (VELBRN.LT.0.0D0) FIB = - FIB
      IF (VELBIN.LT.0.0D0) FIB = - FIB
      GO TO 316
315   FIB = ATAN(VELBIN / VELBRN)
C
316   FI = FIW - FIB
      VELWN = DSQRT(VELWRN**2 + VELWIN**2)
      VELBN = DSQRT(VELBRN**2 + VELBIN**2)
```

```
C
      RT = 8.0D0*DSQRT(VELWN**2 - 2.0D0*VELWN*VELBN*DCOS(FI)- +
     *          VELBN**2) / (3.0D0*PI)
      IF (ITER.EQ.1) RT = 0.0D0
C
      FDC = W*DEXP(AK*Z)*DA*RT*CD
      DFD1(1) = FDC*CZ*CH
      DFD1(2) = FDC*CZ*SH
      DFD1(3) = FDC*SZ
      DFD2(1) = - FDC*SZ*CH
      DFD2(2) = - FDC*SZ*SH
      DFD2(3) = FDC*CZ
C
      CALL MATMUL1 (AN,DFD1,DFDN1)
      CALL MATMUL1 (AN,DFD2,DFDN2)
C
      DO 340 I = 1,3
      FD1(I) = FD1(I) + DFDN1(I)
 340  FD2(I) = FD2(I) + DFDN2(I)
C
      CALL CROSS (XP,DFDN1,DMDN1)
      CALL CROSS (XP,DFDN2,DMDN2)
C
      DO 350 I = 1,3
      FMD1(I) = FMD1(I) + DMDN1(I)
 350  FMD2(I) = FMD2(I) + DMDN2(I)
C
C     CONSTRUCT DAMPING MATRIX "BV(6,6)"
C
      ABAR1(1,2) = XP(3)
      ABAR1(1,3) = -XP(2)
      ABAR1(2,1) = -XP(3)
      ABAR1(2,3) = XP(1)
      ABAR1(3,1) = XP(2)
      ABAR1(3,2) = -XP(1)
      DO 360 I = 1,3
      DO 360 J = 1,3
 360  ABAR(I,J) = -ABAR1(I,J)
C
      CALL MATMUL2 (AN,ABAR1,BV12)
      CALL MATMUL2 (ABAR,AN,BV21)
      CALL MATMUL2 (ABAR,BV12,BV22)
C
      DO 370 I = 1,3
      DO 370 J = 1,3
```

```
      BV11(I,J) = DA*CD*RT*AN(I,J)
      BV12(I,J) = DA*CD*RT*BV12(I,J)
      BV21(I,J) = DA*CD*RT*BV21(I,J)
 370  BV22(I,J) = DA*CD*RT*BV22(I,J)
      DO 380 I = 1,3
      DO 380 J = 1,3
      BV(I,J) = BV(I,J) + BV11(I,J)
      BV(I+3,J+3) = BV(I+3,J+3) + BV22(I,J)
      BV(I+3,J) = BV(I+3,J) + BV21(I,J)
 380  BV(I,J+3) = BV(I,J+3) + BV12(I,J)
 3000 CONTINUE          !  End of slice loop
 2500 CONTINUE          !  End of member loop
C
C     CALCULATE PRESSURE FORCE "FP(3)" AND ITS MOMENTS
C
      DO 4500 IS = 1,NSURF    !  Surface loop starts
      DO 390 I = 1,3
 390  XXS(I) = XS(IS,I)
C
      ZETA = XXS(1)*DCOS(HED) + XXS(2)*DSIN(HED)
      Z = XXS(3) - DRAFT
C
      P1 = - RHO*G*DEXP(AK*Z)*DCOS(AK*ZETA)
      P2 = RHO*G*DEXP(AK*Z)*DSIN(AK*ZETA)
C
      DO 400 I = 1,3
      DFP1(I) = P1*ANS(IS,I)
 400  DFP2(I) = P2*ANS(IS,I)
C
      CALL CROSS (XXS,DFP1,DMP1)
      CALL CROSS (XXS,DFP2,DMP2)
C
      DO 410 I = 1,3
      FP1(I) = FP1(I) + DFP1(I)
      FP2(I) = FP2(I) + DFP2(I)
      FMP1(I) = FMP1(I) + DMP1(I)
 410  FMP2(I) = FMP2(I) + DMP2(I)
 4500 CONTINUE          !  Surface loop ends
C
C     CONSTRUCT THE COMPLEX FORCE ARRAY "FORCE(6)"
C
      WRITE (4,4001)
      DO 420 I = 1,3
      RF = FI2(I) + FD2(I) + FP2(I)
      CF = FI1(I) + FD1(I) + FP1(I)
```

```
      RM = FMI2(I) + FMD2(I) + FMP2(I)
      CMM = FMI1(I) + FMD1(I) + FMP1(I)
      FORCE(I) = DCMPLX(RF,CF)
      FORCE(I+3) = DCMPLX(RM,CMM)
      FORCE1(I) = FORCE(I)
      FORCE1(I+3) = FORCE(I+3)
 420  CONTINUE
C
C     CONSTRUCT THE COMPLEX COEFF. MATRIX "COEF(6,6)"
C
      DO 430 I = 1,6
      DO 430 J = 1,6
      RC = -W*W*AM(I,J) + STF(I,J)
C     PRINT*,' (I,J) :: ',I,J,'       RC = ',RC
      CC = W*BV(I,J)
 430  COEF(I,J) = DCMPLX(RC,CC)
C
C     SOLVE FOR COPMLEX MOTIONS "CDISP(6)", CALCULATE AMPLITUDES
C     AND PHASES
C
      NN = 6
      IA = 6
      MM = 1
      IJOB = 0
      IB = 6
      CALL LEQ2C (COEF,NN,IA,FORCE,MM,IB,IJOB,WA,WK,IER)
C
      DO 440 I = 1,6
      CDISP(I) = FORCE(I)
      DISP(I) = CAB(CDISP(I))
      IF (DABS(DREAL(CDISP(I))).LT.0.00001D0) GO TO 431
      GO TO 432
 431  PHASE(I) = PI / 2.0D0
      IF (DREAL(CDISP(I)).LT.0.0D0) PHASE(I) = - PHASE(I)
      IF (DIMAG(CDISP(I)).LT.0.0D0) PHASE(I) = - PHASE(I)
      FASE(I) = PHASE(I)*180.0 / PI
      GO TO 440
 432  PHASE(I) = ATAN(DIMAG(CDISP(I)) / DREAL(CDISP(I)))
      FASE(I) = PHASE(I)*180.0 / PI
 440  CONTINUE
C
C     ERROR CHECK LOOP
C
      IF (IERR.EQ.0) GO TO 444
      DO 442 I = 1,6
```

```
      IF (ERROR(I).LE.0.0DO) PRINT*,' %%%% WARNING :  ERR.LE.0.0'
442   IF (DABS(DISP(I) - PREV(I)).GT.ERROR(I)) GO TO 443
      GO TO 444
443   DO 450 I = 1,6
      VELR(I) = W*DREAL(CDISP(I))
450   VELI(I) = W*DIMAG(CDISP(I))
      DO 462 I = 1,6
462   PREV(I) = DISP(I)
      GO TO 2100
C
C     WRITE MOTION RAO's AND PHASES
C
444   WRITE (4,4001)
      WRITE (4,*)'  ** DAMPING MATRIX USED FOR FINAL RESULT  **'
      WRITE (4,4000)
      DO 463 I = 1,6
463   WRITE (4,4100) (BV(I,J),J=1,6)
      WRITE (4,4001)
      WRITE (4,*)'  ** FORCE RAOs  **'
      WRITE (4,4000)
      WRITE (4,4121) W,(2.0*PI/W)
4121  FORMAT (2X,'FREQUENCY (RAD/SEC) = ',F10.5,' PERIOD (SEC) = ',
     * F10.5/)
      WRITE (4,*)' D.O.F.  FI1  FI2  FD1  FD2  FP1  FP2  F'
4120  FORMAT (2X,I5,3X,7(E12.5,5X))
      DO 464 I = 1,3
      WRITE (4,4120) I,FI1(I),FI2(1),FD1(I),FD2(I),
     * FP1(I),FP2(I),CAB(FORCE1(I))
      WRITE (4,4120) I+3,FMI1(I),FMI2(1),FMD1(I),FMD2(I),
     * FMP1(I),FMP2(I),CAB(FORCE1(I+3))
464   CONTINUE
      WRITE (4,4001)
      WRITE (4,*)'  ** MOTION RAOs AND PHASES  **'
      WRITE (4,4000)
      WRITE (4,4121) W,(2.0*PI/W)
      WRITE (4,4200) ((DISP(I),FASE(I)),I=1,6)
4200  FORMAT (10X,'SURGE (M/M) = ',F10.5,5X,'PHASE (DEG) = ',
     * F10.5/10X,'SWAY (M/M) = ',F10.5,5X,'PHASE (DEG) = ',F10.5/
     * 10X,'HEAVE (M/M) = ',F10.5,5X,'PHASE (DEG) = ',F10.5/
     * 10X,'ROLL (RAD/M) = ',F10.5,5X,'PHASE (DEG) = ',F10.5/
     * 10X,'PITCH (RAD/M) = ',F10.5,5X,'PHASE (DEG) = ',F10.5/
     * 10X,'YAW (RAD/M) = ',F10.5,5X,'PHASE (DEG) = ',F10.5//)
C
C     CALCULATE TENSION RAO's 'TEN'
C
```

```
      WRITE (4,*)'  ** TENSION RAOs  **'
      WRITE (4,4000)
      WRITE (4,4121) W,(2.0*PI/W)
 4211 FORMAT ('  LEG # :  ',I5,2X,'TENSION RAO (N/M) = ',E12.5,2X)
C
      DO 460 IT = 1,NTEN
      XT = XT1(IT,1)
      YT = XT1(IT,2)
      ZT = XT1(IT,3)
      DTLX = CDISP(1) + CDISP(5)*ZT - CDISP(6)*YT
      DTLY = CDISP(2) + CDISP(6)*XT - CDISP(4)*ZT
      DTLZ = CDISP(3) + CDISP(4)*YT - CDISP(5)*XT
      DTLXR = DREAL(DTLX)
      DTLYR = DREAL(DTLY)
      DTLZR = DREAL(DTLZ)
      DTLXI = DIMAG(DTLX)
      DTLYI = DIMAG(DTLY)
      DTLZI = DIMAG(DTLZ)
      dtlmax = 0.0d0
      delt = 2.0*pi/(w*1000.0)
      tt = 0.0d0
      do 700 II = 1,1001
      swt = dsin(w*tt)
      cwt = dcos(w*tt)
      tltt = dsqrt((dtlxr*cwt + dtlxi*swt)**2 + (dtlyr*cwt +
     *     dtlyi*swt)**2 + (dtlzr*cwt + dtlzi*swt + tl(it))**2)
      dtlt = tltt - tl(it)
      if (dtlt.lt.0.0d0) dtlt = 0.0d0
      if (dabs(dtlt).gt.dtlmax) dtlmax = dabs(dtlt)
      tt = tt + delt
 700  continue
      tenrao = akt(it)*dtlmax
C
      WRITE (4,4211) IT,TENRAO
 460  CONTINUE
      W = W + DELW
 2000 CONTINUE        !  Frequency loop ends
C
      STOP
      END
C
C
C*************************************************************
C     SUBROUTINES
C*************************************************************
```

```
C
C
      SUBROUTINE MATMUL1 (A,B,C)
      IMPLICIT DOUBLE PRECISION (A-H,O-Z)
      DIMENSION A(3,3),B(3),C(3)
C
      DO 5 I = 1,3
 5    C(I) = 0.0D0
      K = 0
      DO 10 I = 1,3
      K = K + 1
      DO 10 J = 1,3
10    C(K) = C(K) + A(I,J)*B(J)
      RETURN
      END
C
C
C
      SUBROUTINE MATMUL2 (A,B,C)
      IMPLICIT DOUBLE PRECISION (A-H,O-Z)
      DIMENSION A(3,3),B(3,3),C(3,3)
C
      DO 5 I = 1,3
      DO 5 J = 1,3
 5    C(I,J) = 0.0D0
      DO 10 I = 1,3
      DO 10 J = 1,3
      DO 10 K = 1,3
10    C(I,J) = C(I,J) + A(I,K)*B(K,J)
      RETURN
      END
C
C
C
      SUBROUTINE CROSS (A,B,C)
      IMPLICIT DOUBLE PRECISION (A-H,O-Z)
      DIMENSION A(3),B(3),C(3)
C
      C(1) = A(2)*B(3) - A(3)*B(2)
      C(2) = A(3)*B(1) - A(1)*B(3)
      C(3) = A(1)*B(2) - A(2)*B(1)
      RETURN
      END
C
C
```

```
C
      SUBROUTINE SUBFASE (RE,AIM,PHIR,PHID)
      IMPLICIT DOUBLE PRECISION (A-H,O-Z)
C
      PI = 3.1415927D0
      IF (DABS(RE).LT.0.00001D0) GO TO 10
      GO TO 20
 10   PHIR = PI / 2.0D0
      IF (RE.LT.0.0D0) PHIR = - PHIR
      IF (AIM.LT.0.0D0) PHIR = - PHIR
      PHID = PHIR*180.0D0 / PI
      GO TO 30
 20   PHIR = ATAN(AIM / RE)
      PHID = PHIR*180.0D0 / PI
 30   RETURN
      END
```